Rekbare en wasbare elektronica voor textielintegratie

Stretchable and Washable Electronics for Embedding in Textiles

Thomas Vervust

Promotor: prof. dr. ir. J. Vanfleteren
Proefschrift ingediend tot het behalen van de graad van
Doctor in de Ingenieurswetenschappen: Elektrotechniek

Vakgroep Elektronica en Informatiesystemen
Voorzitter: prof. dr. ir. J. Van Campenhout
Faculteit Ingenieurswetenschappen en Architectuur
Academiejaar 2012 - 2013

UNIVERSITEIT
GENT

ISBN 978-90-8578-549-1
NUR 959
Wettelijk depot: D/2012/10.500/75

Universiteit Gent
Faculteit Ingenieurswetenschappen en Architectuur
Vakgroep Elektronica en Infromatiesystemen

Promotor: Prof. dr. ir. Jan Vanfleteren

Universiteit Gent
Faculteit Ingenieurswetenschappen en Architectuur

Vakgroep Elektronica en Informatiesystemen
Centrum voor Microsysteemtechnologie (CMST)
Technologiepark 914-A
B-9052 Gent-Zwijnaarde, België

Tel.: +32-9-264.53.50
Fax.: +32-9-264.53.74

Examencomisie:

Prof. dr. ir. Rik Van de Walle	(UGent - Voorzitter)
Dr. ir. Frederick Bossuyt	(UGent - CMST, Secretaris)
Ir. Johan De Baets	(IMEC - CMST)
Prof. dr. ir. Lieva Van Langenhove	(UGent - Textielkunde)
Prof. dr. ir. Bob Puers	(KU Leuven - ESAT/MICAS)
Dr. ir. Guy Buyle	(Centexbel)
Ir. Koen van Os	(Philips Corporate Technologies)
Dr. ir. Torsten Linz	(Fraunhofer IZM / TU Berlin)

Proefschrift ingediend tot het behalen van de graad van
Doctor in de Ingenieurswetenschappen: Elektrotechniek
Academiejaar 2012-2013

Dankwoord

Iedereen herinnert het zich nog wel: De zoektocht naar een geschikte studie na het behalen van het diploma secundair onderwijs. Wat mij vooral is bijgebleven is het beeld dat ik toen had van doctoraatstudenten. Tijdens de rondleiding op de infodag kwam je ze verschillende malen tegen. Ze zaten achter een PC in een muf bureau in het technicum, gevangen tussen stapels boeken en meetapperatuur. Af en toe was er dan eentje die uitleg mocht geven over 'zijn onderzoek' waar er naar verluid ongeveer vier jaar op gewerkt zou worden. Hoewel het meestal interessant klonk, leek het mij weinig aantrekkelijk om gedurende zo een lange periode in je eentje te zwoegen op een bepaald onderwerp. Het besluit kwam er al snel. Die vijf jaar opleiding tot daar aan toe, maar vervolgens nog eens zo lang als een eenzaat werken? Dat zou niets voor mij zijn!

Ongeveer tien jaar later wordt het tegendeel echter realiteit. De reden dat ik de stap zette om een doctoraat te beginnen heb ik vooral te danken aan mijn promotor Jan Vanfleteren. Na mijn masterproef bij de CMST onderzoeksgroep wist hij me te overtuigen dat een doctoraal onderzoek wel degelijk een interessante ervaring kan zijn op zowel wetenschappelijk als sociaal vlak. En hij heeft gelijk gekregen! Het stelde mij onder andere in staat om te werken op een aantal interessante Europese projecten. Hierdoor kwam ik in contact met tal van mensen, werkzaam in onderzoeksinstellingen en bedrijven wereldwijd. Ook het presenteren van behaalde resultaten op internationale conferenties was een unieke ervaring. Vooral de presentatie in Shanghai was zeer bijzonder aangezien deze simultaan vertaald werd in het chinees. Kortom, bedankt Jan om mij te overtuigen het doctoraat te starten en om mij ook de nodige vrijheid te geven tijdens het onderzoek!

Ook wens ik André Van Calster te bedanken voor het leiden van de CMST onderzoeksgroep. Mede door zijn jarenlange inspanningen is CMST een vooraanstaande onderzoeksgroep geworden die beschikt over een goede infrastructuur. Verder ook bedankt voor de leuke activiteiten zoals dé CMST barbecue en het jaarlijkse etentje. Dergelijke sociale activiteiten hebben zeker bijgedragen aan de goede werksfeer die er is binnen de groep.

Verschillende mensen hebben op de één of andere manier een bijdrage geleverd aan het uiteindelijke resultaat. In het bijzonder wens ik Frederick te bedanken voor de verschillende technische (en andere) discussies die ze-

ker een positieve impact gehad hebben op de resultaten. Sheila wens ik te bedanken voor haar nauwgezette manier van werken tijdens het uitvoeren en rapporteren van een aantal processtappen die ze voor me uitvoerde. Naast Frederick en Sheila bedank ik ook de andere leden van ons stretch team, Michal en Bjorn voor de goede samenwerking. Guy van Centexbel bedank ik voor de vlotte samenwerking rond de wastesten. Bedankt aan Bjorn om me bij te staan bij het manueel plaatsen van de talloze componenten, Steven voor de hulp bij het laserwerk en Filip voor de assistentie bij het tekenen en het uitfrezen van de mallen.

Verder wens ik gans het CMST team te bedanken voor de ongelofelijk toffe sfeer die er altijd heerst zowel tijdens als na de werkuren. In het bijzonder dank aan de harde kern van het CMST minivoetbalteam van vroeger en nu: Bram, David, Dominique, Erwin, Frederick, Geert, Stefaan en Steven. We hebben een aantal echte topmatchen gespeeld de voorbije jaren en de vele momenten in de bar achteraf waren ook in dik orde! Bedankt ook aan de collega's en hun partner voor de schitterende drieweekse reis in India: Eveline, Ann, Alwin, Bram, Elien, Frederick, Adinda, Pritesh en Fabrice. Dit was echt een avonuur om nooit meer te vergeten! Ook dank aan mijn bureaugenoten die er nu nog zitten: Amir, David, Jeroen, Rik, Sandeep, Sanjeev, Sheila, en zij die er niet meer zitten: Benoît, Jindrich en Tom. We zijn een paar keer verhuisd van een tijdelijke bureau naar de volgende tijdelijke bureau, maar dit laat niet weg dat we het altijd goed gehad hebben!

Naast de mensen die ik ken via het werk bedank ik nog mijn familie en vrienden. Jullie zijn voor mij zeer belangrijk en ik bedank jullie voor alle plezante bijeenkomsten. In het bijzonder wens ik mijn ouders Nadine en Marnix te bedanken. Zonder het enthousiasme en steun die ik van jullie kreeg gedurende mijn volledige bestaan was ik nooit de persoon geworden die ik nu ben. Zeker nu als jonge vader besef ik maar al te goed wat jullie vroeger, maar ook nu allemaal voor mij gedaan hebben. Ook mijn zus Heleen en broer Brecht, het is tof dat we zo een goede band hebben en ik hoop dat we samen nog veel leuke momenten mogen beleven!

Ten slotte wil ik nog één persoon vermelden. Een persoon die er altijd is voor mij en waarbij ik mij ongelofelijk goed voel. Mijn allerliefste Eveline, merci voor alle steun en vreugde die je me brengt, en proficiat dat je zo een goede mama bent voor onze schattige Enora! Ik kijk al uit naar alles wat we nog samen zullen beleven...

Gent, november 2012
Thomas Vervust

Table of Contents

List of Figures

List of Tables

List of Acronyms

AC	Alternating Current
A/D	analog-to-digital
ASTM	American Society for Testing and Materials
BGA	Ball Grid Array
CAD	Computer-Added Design
CEA	Commissariat à l'énergie atomique et aux énergies alternatives
Centexbel	Belgian Textile Research Centre
CMST	Centre for Microsystems Technology
CNC	Computer Numerical Control
DC	Direct Current
ECE	Europäische Convention für Echtheitsprüfungen
EMI	Electromagnetic interference
ESD	ElectroStatic Discharge
ESAT-MICAS	Microelectronics and Sensors group at KU Leuven
FCB, FPCB, FPC	Flexible Printed Circuit Board
FR4	Flame Retardant number 4
GPIB	General Purpose Interface Bus
IC	Integrated Circuit
I^2C	Inter-Integrated Circuit
IEC	International Electrotechnical Commission
IMEC	Interuniversity MicroElectronics Centre
I/O	Input/Output
IPEM	Institute for Psychoacoustics and Electronic Music
ISO	International Organization for Standardization
JTAG	Joint Test Action Group
KU Leuven	University of Leuven
LED	Light-Emitting Diode
LDO	Low-dropout regulator
MCU	Microcontroller
MIT	Massachusetts Institute of Technology
MD	Measurement Delay
NMOS FET	n-channel metal oxide semiconductor field effect transistor
OEM	Original Equipment Manufacturer
OSP	Organic Surface Protection

PDMS	Polydimethylsiloxane
PEP	Pôle Européen de Plasturgie
PCB	Printed Circuit Board
PU	Polyurethane
PI	Polyimide
PMMA	Poly methyl methacrylate
PTFE	Polytetrafluoroethylene
PET	Polyethylene terephthalate
PES	Polyethersulfone
PSA	Pressure Sensitive Adhesive
PWM	Pulse Width Modulation
PDA	Personal Digital Assistant
ppm	parts per million
QFN	Quad-Flat No-leads
QFP	Quad Flat Package
RGB	Red Green Blue
RF	Radio Frequency
RX	Receiver
SEM	Scanning Electron Microscope
SMI	Stretchable Molded Interconnect
SMD	Surface-mounted device
SMU	Source-measurement unit
SOT	Small Outline Transistor
SMT	Surface-mount technology
TBM	Time Between Measurements
TCP/IP	Transmission Control Protocol/Internet Protocol
TNO	Netherlands Organisation for Applied Scientific Research
TPU	Thermoplastic Polyurethane
TSSOP	Thin Shrink Small Outline Package
TU Berlin	Technische Universität Berlin
TX	Transmitter
UART	Universal Asynchronous Receiver/Transmitter
UGent	Ghent University
ULP	user language program
USB	Universal Serial Bus
USCI	Universal Serial Communication Interfaces
WET	Water Effect Test
WPC	Wireless Power Consortium
WR	Washing Reliability

Nederlandse samenvatting –Summary in Dutch–

Zoals toegelicht in **Hoofdstuk 1**, is de belangrijkste doelstelling van dit proefschrift het overwinnen van een aantal problemen die geconstateerd werden in de huidige inspanningen om textiel geïntegreerde elektronica te creëren. Daarom worden bestaande en nieuwe technologieën gebruikt en verder ontwikkeld die het mogelijk maken om textiel geïntegreerde elektronica te realiseren op zo'n manier dat de flexibele/rekbare aard van typische textielproducten behouden blijft. Om de kloof tussen de elektronica en textielindustrie te dichten wordt het concept van een technologie toolbox geïntroduceerd.

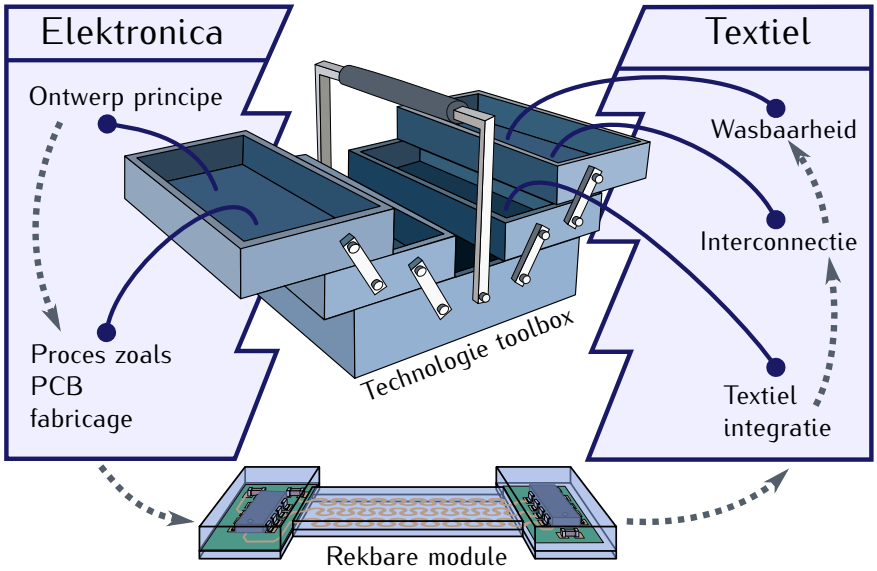

De onderwerpen rond de toolbox geven enkele van de belangrijkste aspecten tijdens het complete productieproces weer, gaande van ontwerp tot realisatie en testen. Dezelfde logische volgorde wordt bewaard in de inhoud van dit proefschrift.

In **hoofdstuk 2** blijven we binnen de wereld van de elektronica. In het eerste deel van het hoofdstuk wordt het ontwerpprincipe van een rekbaar circuit

uitgelegd. Om rekbaarheid te verkrijgen, wordt de schakeling onderverdeeld in verschillende niet-rekbare functionele eilanden die verbonden zijn met rekbare verbindingen (meanders). Dit rekbare circuit wordt geëncapsuleerd in een elastomeer, wat resulteert in een rekbare module die in textiel kan worden geïntegreerd. Het ontwerp van een textielproduct, met uitrekbare elektronische modules, vereist het denken over bepaalde onderwerpen en een goede planning vanaf het begin. Een eenvoudig dertien stappen implementatieproces wordt voorgesteld, dat gebruikt kan worden om geleidelijk aan tot een goed ontworpen demonstrator of product te komen. Ook een meander ontwerptool voor de EAGLE PCB-software wordt gepresenteerd. Deze tool werd ontwikkeld om de routering van de meanderende rekbare verbindingen te vereenvoudigen.

De volgende twee delen van het hoofdstuk behandelen het productieproces van de uitrekbare modules. Deze productie wordt onderverdeeld in een substraatfabricagedeel en een encapsulatiedeel. De ontwikkelde substraat fabricage methode vertrekt van een standaard flexibele printplaat en maakt gebruik van lasersnijden om de rekbare meanders en de functionele eilanden te structureren. Na de substraatfabricage, wordt de ontwikkeling van twee encapsulatiemethodes beschreven: encapsulatie door spuitgieten en door lamineren. Thermohardende PDMS materialen werden gebruikt voor het spuitgieten en thermoplastisch PU in het geval van laminatie. Naast de encapsulatiemethodes wordt ook het belang van openingen in de encapsulatie aangehaald. Dit om het ademend vermogen van de module te verbeteren en om toegang tot contactvlakken te verkrijgen.

Het laatste onderwerp van het hoofdstuk beschrijft de hechting tussen het rekbare circuit en de encapsulatie. Een goede hechting is belangrijk om delaminatie van de encapsulatie tijdens de levensduur van het product te voorkomen.

In **Hoofdstuk 3** komen we terecht in de textielwereld en bespreken we hoe de uitrekbare elektronische modules geïntegreerd kunnen worden in textiel. Om de industrialisatie van de processen te vergemakkelijken, werden integratiemethoden ontwikkeld die makkelijk over te nemen zijn in textielproductie. De twee verschillende encapsulatie materiaal types (thermohardend en thermoplastisch) hebben geleid tot twee verschillende integratiemethoden. De eerste methode maakt gebruik van een gezeefdrukte PDMS lijmlaag om PDMS geëncapsuleerde rekbare modules en stoffen te verlijmen. Er wordt aandacht besteed aan de penetratiediepte van de gedrukte laag. Door de penetratie in de stof zo veel mogelijk te beperken, werd de rekbaarheid van de stof zo goed mogelijk bewaard. De tweede methode maakt gebruik van een laminatiestap om een TPU geëncapsuleerde rekbare module te hechten aan een stof.

Eenmaal de module aan de stof gehecht is, moet deze vast blijven zitten tijdens de levenscyclus. Daarom moet de lijmlaag tussen de stof en de rekbare module betrouwbaar genoeg zijn om fysische vervormingen tijdens gebruik en reiniging te overleven. De hechting tussen Sylgard 186 (PDMS) of PE

Krystalflex 429 (TPU) geëncapsuleerde modules en stoffen bleek voldoende te zijn. Stoffen met dummy geëncapsuleerde modules werden tot 50 keer gewassen zonder delaminatie te vertonen.

Met de nadruk op draagbaarheid, tonen we aan dat de bereikte realisaties van textiel geïntegreerde rekbare elektronica het heel goed doen. Technologische ontwikkelingen hebben geleid tot lichte, rekbare modules die gebruikt kunnen worden in kledij, zonder afbreuk te doen aan het gebruikscomfort. De verandering in rekbaarheid die ze veroorzaken, zijn van dezelfde orde als deze van typische kleurenprints in hedendaagse textielproducten.

Het is mogelijk dat toepassingen vereisen dat verschillende rekbare modules geïntegreerd worden in textiel. Dit is het onderwerp van **Hoofdstuk 4**, waar we kijken naar de interconnectie van rekbare modules. De stroomdistributie is waarschijnlijk de meest voorkomende reden voor het verbinden van een rekbare module. Andere redenen zijn de signaaloverdracht tussen de verschillende modules en de interconnectie van modules met geleidende textiel-elementen (bv. textiel sensor, textiel antenne). In alle gevallen zorgt de interconnectie voor een elektrisch pad tussen verschillende elektrische elementen. Daarom zijn de elektrische eigenschappen van de interconnectie van groot belang. Enkele belangrijke parameters bij de bepaling van de interconnectievereisten worden aan het begin van het hoofdstuk gegeven.

Het aantal verschillende textielgebaseerde interconnectiemethoden die bestaan of die op dit moment het onderwerp van onderzoek zijn, is groot. Om een beter overzicht te krijgen, worden ze ingedeeld naar het niveau waarop ze geïntroduceerd worden tijdens de textiel productie: via het intrinsieke textiel productieproces, via het textielveredelingsproces, via het textiel confectieproces. Voor elk van deze categorieën worden verschillende voorbeelden gegeven en van commentaar voorzien.

Tenslotte wordt de verbinding van rekbare modules met een bepaalde textielgebaseerde interconnectiemethode besproken. Een rekbare module bestaat uit een volledig afgesloten encapsulatie. Daarom is er een manier nodig om toegang te krijgen tot contactvlakken in de module. De eerste manier is de creatie van een opening in de encapsulatie om contact te maken met een contactvlak in de module. In een tweede manier om een contact te voorzien, steken de contacten uit module. Verschillende uitvoeringen van sommige voorgestelde connectie mogelijkheden worden getoond.

In de eerste hoofdstukken word uitgelegd hoe rekbare modules ontworpen kunnen worden, geproduceerd, geïntegreerd in textiel en indien nodig geïnterconnecteerd met andere textiel geïntegreerde modules. Afhankelijk van de uiteindelijke toepassing is het mogelijk dat het textielproduct gereinigd moet worden tijdens zijn levenscyclus. Daarom onderzoekt **Hoofdstuk 5** de wasbaarheid van textiel geïntegreerde rekbare modules. In het algemeen kan gesteld worden dat er twee grote uitdagingen zijn om wasbaarheid van rekbare elektronica te verkrijgen: voldoende waterbestendigheid en een goede

mechanische betrouwbaarheid. In dit doctoraat lag de focus op water gebaseerde reiniging. Voor watergebaseerde reiniging werd de ISO 6330:2000 norm geselecteerd omdat deze representatief is voor huishoudelijke wasomstandigheden.

Het eerste gedeelte van het hoofdstuk behandelt de waterdichtheid van de modules. Tijdens het reinigen, worden de elektronische modules ondergedompeld in een warm water/zeep mengsel. De encapsulatie moet de elektronica beschermen van dit mengsel om kortsluitingen en een elektrisch falen van het apparaat te voorkomen. De Water Effect Test (WET) werd ontworpen om de waterbestendigheid van rekbare modules te evalueren en is gebaseerd op lekstroommetingen tussen geëncapsuleerde koperbanen tijdens de onderdompeling. Zes verschillende WET-staaltypes werden getest: zonder encapsulatie, met PDMS en met TPU encapsulatie, en dezelfde, maar met een extra soldeermasker. Uit testen blijkt dat alle encapsulatie types het potentieel van een goede encapsulatie hebben, met betrekking tot waterbestendigheid. In alle gevallen waren de lekstromen aanzienlijk lager in vergelijking met het referentiestaal zonder encapsulatie. De beste resultaten werden verkregen met de PDMS en TPU encapsulatie in combinatie met het soldeermasker. In beide gevallen bleven de lekstromen stabiel rond de $10^{-9}A$. Dit bewijst een goede waterbestendigheid tijdens de onderdompeling in water, gemeten tot 55 uur.

Naast waterbestendig, moeten de modules robuust genoeg zijn om het mechanische 'misbruik' die ze ondervinden tijdens typische textiel reinigingsprocessen te overleven. Deze wasbetrouwbaarheid is het onderwerp van het tweede gedeelte van het hoofdstuk. Ten eerste wordt de betrouwbaarheid van textielgeïntegreerde knipperende LED-modules geëvalueerd. Elke knipperende LED-module bevat een flexibel eiland met vier LEDs die per twee afwisselend knipperen. Deze modules waren oorspronkelijk bedoeld om de interconnectie van verschillende PDMS geëncapsuleerde modules met een textielgeïntegreerde elektrische draad te illustreren. In een later stadium werden deze knipperende LED-modules ook gebruikt om een eerste aantal wasproeven uit te voeren. Op alle teststalen werd het defect na wassen gevonden aan de interconnectie tussen de knipperende LED-module en de elektrische draad voor het voeden van de modules, terwijl de modules zelf nog steeds functioneel waren. Na de evaluatie van deze verkennende wastesten werd het duidelijk dat er meer specifieke testen nodig waren. De ontwikkelde wasbetrouwbaarheidstest (WR-test) evalueert de soldeercontacten van SMD-componenten op een flexibel eiland, waarbij een geëncapsuleerde module meerdere malen gewassen wordt in een standaard wasmachine. Een WR-test module bevat 50 SMD weerstanden (0402 en 0603 behuizingen) en vier dummy IC's (TSSOP28 en QFN32 behuizingen). Er zijn in totaal 220 contacten die kunnen breken tijdens het wassen. Deze contacten zijn ingedeeld in ketens, wat resulteert in 42 meetpunten bij elke module. Twee verschillende ontwerpen voor de WR-test modules werden gebruikt tijdens de tests. Het doel van de WR2-test was het verbeteren van het WR1 ontwerp. Wijzigingen werden aangebracht

in de 0402 en 0603 contactvlak lay-out en FR4 plaatjes werden gebruikt om de TSSOP-en QFN contacten te versterken. De WR-test modules werden gehecht aan een gebreide of geweven stof om een verschil te maken tussen rekbare (gebreide) en stijve (geweven) stoffen. Er wordt geconcludeerd dat het WR2 ontwerp een grote verbetering is ten opzichte van het WR1 ontwerp. In het geval van het WR1 ontwerp breken het grootste deel van de soldeer contacten na één wascyclus. Uit testen met het WR2 ontwerp bleek dat de WR2-modules die geplaatst werden op een breisel het best presteerden. Er werden geen defecten geïntroduceerd tijdens de 25 wascycli die uitgevoerd werden gedurende de test. Het verlies in geleidbaarheid in enkele van de ketens van de WR2-modules op geweven stoffen werd in verband gebracht met vouwlijnen en scheuren in de flexibele printplaat en waren niet het gevolg van gebroken connecties. Er wordt uitgelegd dat deze defecten ontstaan door spanningen in de module wanneer deze naar binnen gebogen wordt.

Tenslotte worden in **Hoofdstuk 6** verschillende demonstratoren voorgesteld die ontworpen en gerealiseerd werden om het gebruik van de ontwikkelde rekbare elektronica technologie voor textiel integratie te illustreren. Deze succesvolle realisaties zijn: een rekbaar LED-array, een 7x8 LED-display, knipperende LED-modules, een RGB-kleurenscherm, een feest T-shirt en een draadloze oplader. Deze demonstratoren kunnen beschouwd worden als bouwstenen, die mogelijk kunnen leiden tot een aantal eerste echte toepassingen in de toekomst ...

English summary

As explained in **Chapter 1**, the main objective of this PhD thesis is to overcome some of the difficulties observed in today's efforts to create textile integrated electronics. Therefore existing and new technologies are used and further developed to obtain textile integrated electronics in such a way that the typical flexible/stretchable nature of textile products are preserved. In order to bridge the gap between the electronic and textile industries, the concept of a technology toolbox was created.

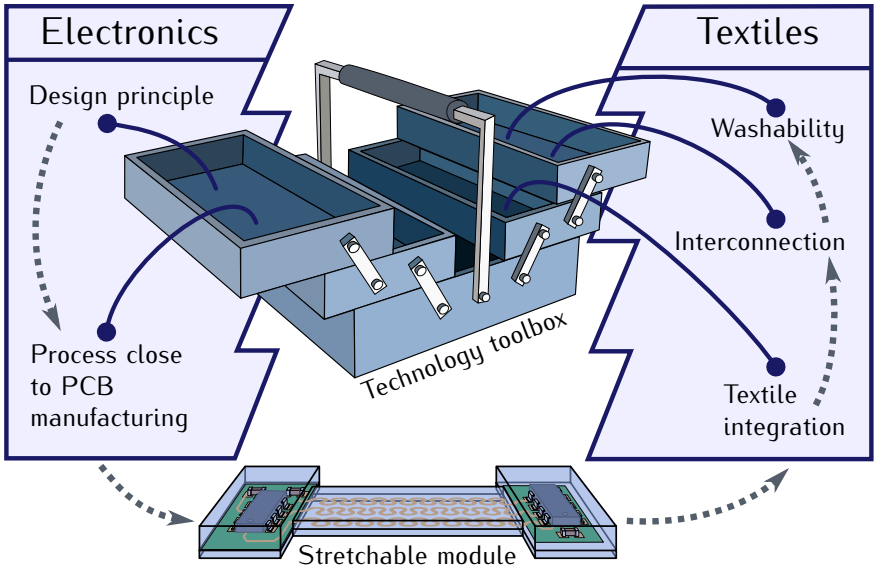

The topics surrounding the toolbox reflect some of the key aspects during the complete manufacturing process, going from design to realization and testing. This same logical order is preserved in the contents of this dissertation.

In **Chapter 2** we stay within the world of electronics. In the first part of the chapter, the design principle of a stretchable circuit is explained. To obtain stretchability, the circuit is subdivided in several non-stretchable functional islands, which are interconnected with stretchable interconnections (meanders). This stretchable circuit is encapsulated in an elastomer, resulting in a stretchable module that can be integrated in textile. The design of a tex-

tile product, containing stretchable electronic modules, requires thinking on certain topics and a good planning from the start. A simple thirteen-step implementation process is proposed, which can be used to gradually come to a well designed demonstrator or product. Also a meander design tool for the EAGLE PCB software is presented. This tool was developed to simplify the routing of the meandering stretchable interconnections.

The next two parts of the chapter deal with the production process of the stretchable modules. This production is subdivided into a substrate fabrication part and an encapsulation part. The developed substrate fabrication method starts from a standard flexible circuit board and uses laser cutting to structure the stretchable meanders and the functional islands. Next to the substrate fabrication, the developments of two encapsulation methods are discussed; encapsulation by injection molding and by lamination. Thermosetting PDMS materials were used for the injection molding and thermoplastic PU in the case of lamination. Besides the encapsulation methods, also the importance of openings in the encapsulation for breathability and contact pad access is addressed.

The last topic of the chapter describes the adhesion between the stretchable circuit and the encapsulation. It is important to have a good adhesion to prevent delamination of the encapsulant during product life.

In **Chapter 3** we enter the world of textiles and we discuss how the stretchable electronic modules can be integrated into textiles. To facilitate industrialization of the processes, the target was to develop integration methods that are easy to adopt in textile manufacturing. The two different encapsulation material types (thermosetting and thermoplastic) have led to two different integration methods. The first method uses the screen printing of a PDMS glue layer to bond PDMS encapsulated stretchable modules and fabrics together. Attention is given to the penetration dept of the printed layer. By limiting the penetration into the fabric as much as possible, the stretchability of the fabric was preserved as well as possible. The second method uses a lamination step to bond a TPU encapsulated stretchable module to a fabric.

Once the module is attached to the fabric it should remain attached during the product life cycle. Therefore, the adhesive layer between the fabric and the stretchable module should be reliable enough to survive physical deformations during use and cleaning. The adhesion between Sylgard 186 (PDMS) or Krystalflex PE 429 (TPU) encapsulated modules and fabrics was found to be adequate. Fabrics containing dummy encapsulated modules were washed up to 50 times without showing delamination.

With a focus on wearability, we show that the achieved realizations of textile integrated stretchable electronics are doing very well. Technological developments have resulted in lightweight stretchable modules that can be used in clothing without compromising user comfort. The change in stretchability they cause, is in the same range of changes introduced by typical color prints in todays textile products.

It is possible that applications require different stretchable modules integrated into the textile. This is the topic of **Chapter 4** where we look at the interconnection of stretchable modules. Probably the most common reason for interconnecting a stretchable module is the power distribution. Other reasons include the signal transmission between different modules and the interconnection of modules with conductive textile elements (e.g. textile sensor, textile antenna). In all cases, the interconnection provides an electrical path between different electrical elements. Therefore, the electrical characteristics of the interconnection are of major importance. Some important parameters for the determination of the interconnection requirements are given at the beginning of the chapter.

The amount of different textile based interconnection methods that exist or are currently the topic of research is large. To get a better overview, they are categorized according to the level at which they are introduced during textile manufacturing: via the intrinsic textile manufacturing process, via the textile finishing process, via the textile confection process. For each of these categories, different examples are given and commented on.

Finally, the connection of stretchable modules with a certain textile based interconnection method is discussed. A stretchable module consists of an entirely enclosed encapsulation. Therefore, a way to access contact pads in the module is needed. The first way is to create an opening in the encapsulation in order to make contact with a contact pad. A second way to provide contact with the module is to let the contacts protrude out of the module. Different realizations of some of the proposed connection possibilities are presented.

The first chapters explain how stretchable modules can be designed, produced, integrated in textile and if required interconnected with other textile integrated modules. Dependent on the final application it might be possible that the textile product needs cleaning during its life cycle. Therefore, **Chapter 5** investigates the washability of textile integrated stretchable modules. In general, it can be stated that there are two major challenges to obtain washability for stretchable electronics: sufficient water resistance and good mechanical reliability. In this PhD the focus was on water-based cleaning. For water-based cleaning the ISO 6330:2000 standard was selected as it is representative for domestic washing conditions.

The first main part of the chapter discuses the water resistance of the modules. During cleaning, the modules are immersed in a hot water/soap mixture. The encapsulant should protect the electronics from this mixture to prevent short circuits and electrical failure of the device. The Water Effect Test (WET) was designed to evaluate the water resistance of stretchable modules and is based on leakage current measurements between encapsulated copper tracks during immersion. Six different WET-sample types were tested: without encapsulation, with PDMS and with TPU encapsulation, and the same but with an additional solder mask. The tests reveal that all encapsulation types have the potential of being a good encapsulant with respect to water resistance.

In all cases, the leakage currents were lowered significantly compared to the reference sample without encapsulation. Best results were obtained with the PDMS and TPU encapsulation in combination with the solder mask. In both cases, the leakage currents remained stable around $10^{-9}A$. This proves good water resistance during water immersion, measured up to 55 hours.

Next to being water resistant, the modules should be robust enough to survive the mechanical 'abuse' they encounter during typical textile cleaning processes. This washing reliability is the topic of the second main part of the chapter. First, the washing reliability of textile integrated blinking LED modules is evaluated. Every LED module is a flexible island with four LEDs that are blinking two by two. These modules were originally designed to illustrate the concept of interconnecting different PDMS encapsulated modules with a textile integrated electric wire. In a later phase these blinking LED modules were also used to conduct a first number of washing tests. On all test samples the failure after washing was found at the interconnection between the module and the electric wire for powering the modules, while the modules itself were still functional. After the evaluation of these exploring washing tests, it became clear that more dedicated tests where needed. The developed washing reliability test (WR test) evaluates the solder contacts of SMD components on a flexible island when an encapsulated module is washed several times in a standard washing machine. One WR test sample contains 50 SMD resistors (0402 and 0603 packages) and four dummy IC's (TSSOP28 and QFN32 packages). In total there are 220 contacts that can cause failure during washing. These contacts were grouped together in daisy chains, resulting in 42 measurement pads on each sample. Two different WR designs were used in the tests. The purpose of the WR2 test was to improve the WR1 test design. Changes were made to the 0402 and 0603 pad layout and FR4 stiffeners were used to reinforce the TSSOP and QFN contacts. The WR test modules were attached to a knitted or woven fabric in order to make a difference between stretchable (knitted) and less stretchable (woven) fabrics. It is concluded that the WR2 design is a major improvement compared to the WR1 design. Most of the solder contacts in the WR1 design fail after one washing cycle. The tests with the WR2 design revealed that the WR2 modules on a knitted fabric are performing the best. No defects were introduced during the 25 washing cycles that were conducted during the test. Conductivity loss in some of the chains of the WR2 samples on woven fabrics were related to folds and cracks in the flexible board and not because of broken contacts. It is explained that these defects arise due to stresses in the module when it is bent inwards.

Finally, **Chapter 6** presents different demonstrators that were designed and realized to illustrate the use of the developed stretchable electronics technology for textile integration. These successful realizations include a stretchable LED array, a 7x8 LED display, blinking LED modules, an RGB color display, a party shirt and a wireless battery charger. These demonstrators can be considered as building blocks, possibly leading to some first real applications in the future...

1 Introduction

1.1 Electronics in textiles

In our ever-changing world, we hardly realize how developments in the field of electronics have created the lives we are so used to. If we think about it, it is hard to imagine what our lives would be like without electronics. There would be no computers, no Internet, no TV, no smart phones, no GPS, no tablets, no... Figure 1.1 shows an example of how electronic circuitry evolves over time.

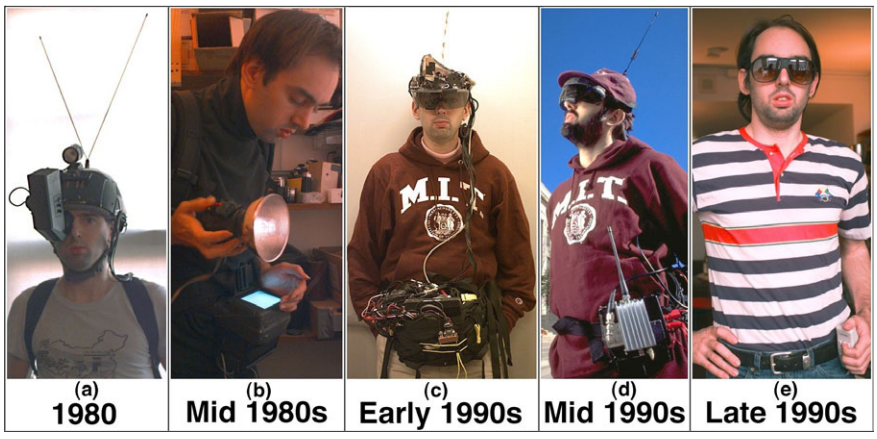

Figure 1.1: Steve Mann's "wearable computer" and "reality mediator" inventions of the 1980s have evolved into what looks like ordinary eyeglasses in the late 1990s. [1]

These pictures show the evolution of wearable computer inventions from the 1980s till the late 1990s, made by Steve Mann who was a pioneer in the field [2]. It is clearly visible how already at that time the electronic circuit technology was getting smaller and smaller, whereas in the mean time the functionality increased. This trend, that is still ongoing today, has led to the very compact and intelligent electronic devices that we use nowadays.

Textile products are another established value in our lives. While we also use them every day, they are totally different compared to electronic products. Clothing and textiles have a much longer history. From ancient times to the present day, methods of textile production have continually evolved, which have led to new types of yarns and fabrics and new applications. Textiles are found in our cloths, cars, interiors, agriculture, constructions,...

The first time the younger electronics sector came in contact with the established textile industry was during new developments in the field of textile machinery. As an example, the publication titled 'The application of electronic techniques to textiles' by Butler back in 1957 reports how 'electronic techniques play an important part in the efficient production of modern textiles' [3]. The electronics were used in electronic control applications and electronic textile testing equipment. The next interesting situation where electronics and textiles found each other, was in the realization of ESD (Electrostatic discharge)-protective clothing. Electric charges that build up on clothing can cause a spark discharge that may completely destroy electronic chip devices in the microelectronics industry. To overcome this problem, conductive threads are woven into garments in order to discharge the static charge, ensuring that the components remain undamaged. The publication by Azoulay in 1988 reports for example 'the electrical conduction properties of an antistatic 2/1 twill fabric textile, containing 10% of a new conductive fiber'[4]. This 'new conductive fiber' had a thin conductive film, containing copper, sulfur and cyanogen, on an acrylic fiber surface.

With further developments of conductive yarns and textile materials and the continuing miniaturization of electronic components, the new field of electronic textiles (E-textiles, smart textiles) was born. An example of early research with the goal of integrating electronic components in textiles was for example the development of E-broidery, published by Post et al. in 2000 [5]. They embroidered conductive stainless steel yarns onto a fabric to create conductive tracks and they attached printed circuit boards (PCBs) to these tracks to realize electronic systems. Over the years, research has led to numerous examples of possible applications of E-textiles. It was found however, that most of these developments make use of rigid electronic modules. This dissertation contributes to the field of smart textiles, by presenting a stretchable technology that allows the integration of electronics in textiles in such a way that the typical flexible/stretchable nature of textile products is preserved.

1.2 Objectives for this PhD study

In order to realize products where electronics are integrated into textiles, two totally different industries should meet each other, namely the textile and the electronics industry. One of the questions that arise around manufacturing smart textiles is: At which point in the production process of the product will the electronics be introduced? The answer will depend on the targeted level of integration of the electronics in the textile.

An option could be to connect small electronic components to conductive filaments to create a yarn with integrated electronics. This yarn could be used for example in a weaving process to make the smart textile. It is clear that this way of working introduces big challenges for electronic and textile industries. At first electronic packages should be designed that are suited for integration in a conductive textile yarn. Secondly this yarn with the integrated electronics should survive the different textile processes (i.e. weaving). In the end there is also a technology needed to interconnect the different conductive yarns if the circuit design has different electronic components. A complete production process like this would create a high level of integration of the electronics into the textile. However this means that industrial textile and electronic processes should be mixed and a lot of know how should be exchanged. It is also not clear if it is possible to create electronic packages for integrated circuits (ICs) with multiple interconnections that are suited for integration in a single textile yarn. If not, this could limit the number of possible applications. An example of the chip in yarn concept is the diabolo chip package developed by CEA [6]. At the moment this package is limited to two component contacts (Figure 1.2).

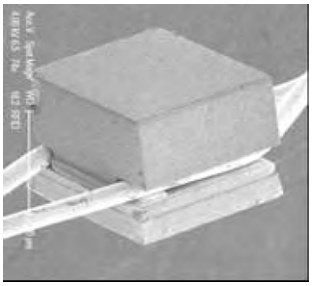

Figure 1.2: SEM (scanning electron microscope) views of a Diabolo Assembly [6].

Another option is to introduce the electronics at the end of the textile process. This makes it possible to maintain more or less the traditional electronic and textile processes. In the most simple form one could think of a rigid box with the electronics that is sewn into a pocket on the textile. Basically this means that an electronic company produces the rigid modules in a traditional

way and that a textile company only needs to know were to put these modules. The circuit complexity can be a lot higher because the different electronic components are interconnected on a traditional printed circuit board. However, in this concept the look and feel of a textile product can be lost if the rigid module becomes to big.

In this PhD it is the objective to overcome some of the difficulties observed in todays efforts to create textile integrated electronics. Therefore, existing and new technologies are used and further developed to obtain textile integrated electronics in such a way that the typical flexible/stretchable nature of textile products is preserved. Manufacturability was considered as an important aspect when developing new technologies. This means it should be straight forward for electronic and textile industries to adopt the new technologies. In order to bridge the gap between the two different industries the concept of a technology toolbox was created (Figure 1.3).

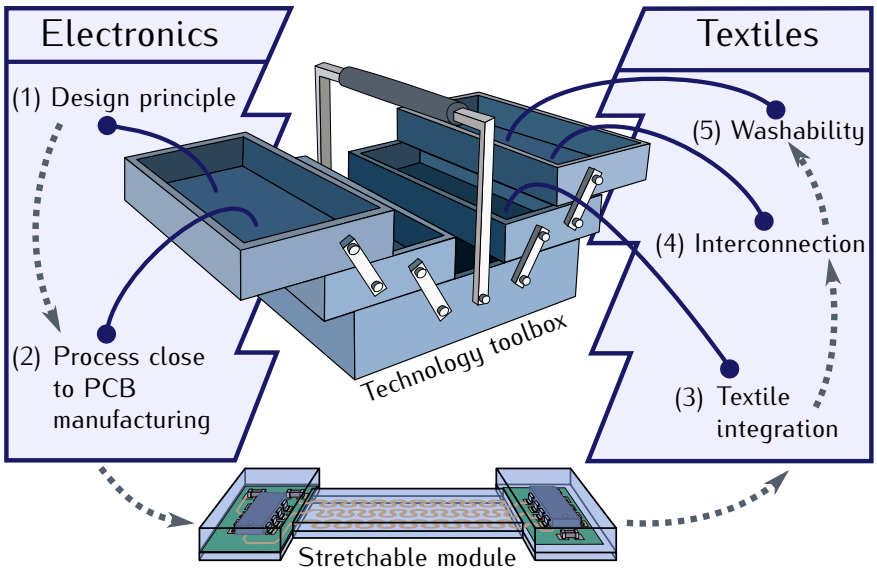

Figure 1.3: Technology toolbox for stretchable and washable electronics in textiles

The topics visible in Figure 1.3 reflect some of the key aspects during the complete manufacturing process, going from design to realization and testing. This same logical order is preserved in the contents of this dissertation:

- Because this work contains stretchable electronics, a general introduction is given in Section 1.3.
- The first two topics in the scheme of Figure 1.3 will be covered in Chapter 2. In this chapter we stay within the world of electronics. We discuss

how a ***design*** is made and focus on the developed technologies used to ***produce a stretchable module*** ready for textile integration.

- In Chapter 3 we enter the world of textiles. We discus how the stretchable module can be ***integrated*** into textiles.
- Some applications could require different stretchable modules integrated into the textile. This is the topic of Chapter 4 were we look to the ***interconnection*** between modules.
- The focus of Chapter 5 is on ***washability*** of electronics in textiles. Indeed one of the main challenges of integrating electronics into fabrics is the cleaning of the product that contains the electronics.
- During the research described in this Phd different ***technology demonstrators*** where designed and realized. Some of them are described in Chapter 6.
- Finally guidelines for further research and development are given in Chapter 7.

1.3 Introduction on stretchable electronics

At the end of 2007, on the commencement of this PhD, different research groups were active in the field of elastic, stretchable electronics. Different concepts and technologies for fabricating stretchable substrates were published. Most of these technologies can be divided into two design types: Out-of-plane and In-plane designs. The difference between the two is illustrated in Figure 1.4.

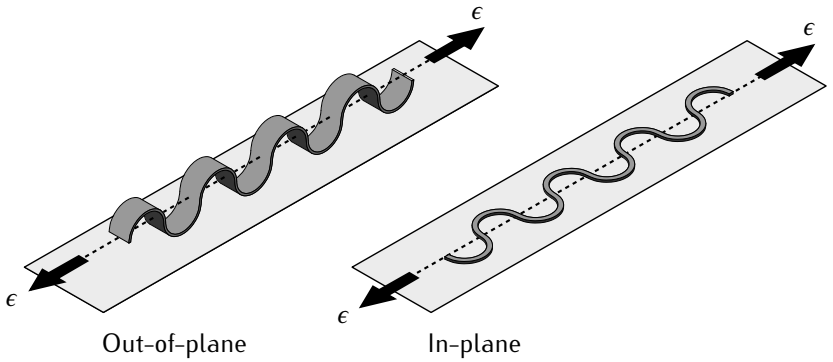

Figure 1.4: Difference between an out-of-plane and in-plane stretchable design.

The first method to make non-stretchable conducting materials stretchable is the use of out-of-plane designs to accommodate the applied strains. This method was used at Princeton University [8]. In their work very thin films of gold were evaporated on pre-stretched or 3D-structured PDMS (Polydimethylsiloxane) membranes to obtain stretchable conductors. Work at the

University of Illinois used inorganic materials (e.g. single-crystal inorganic semiconductor materials) to realize the stretchable out-of-plane structures. In this way a stretchable silicon photodetector array was realized [9].

In a second method the non-stretchable conductors are structured in a planar horseshoe shape to accommodate the applied strains. Initial results on this approach were published by Gray et al. and Brosteaux et al. in 2004 and 2007, respectively [10, 11]. Gold was lithographically patterned to form meander shaped metal tracks. PDMS elastomer had been used to mechanically protect and electrically insulate the interconnections.

Additional examples of stretchable technologies based upon these two design types can be found in chapter one of the dissertation on 'Novel Technologies for Elastic Microsystems', submitted by Bossuyt in 2011 [12]. More recent technologies using the planar horseshoe shape were developed within the framework of the project STELLA (STretchable ELectronics for Large Area applications) [13]. The STELLA project's duration was from 1 February 2006 till 31 January 2010. Focus was on the development of stretchable electronics for large area applications for use in healthcare, wellness and functional clothes, and for integrated electronics in stretchable parts and products. TUB developed a technology using thermoplastic polyurethane (TPU) to support stretchable copper meanders [14]. IMEC-UGent developed a technology where stretchable copper meanders and electronic components are completely embedded in PDMS [15].

The dissertation on 'Novel Technologies for Elastic Microsystems', written by Bossuyt [12], is a good reference where the different IMEC-UGent stretchable technology developments from 2006 till 2010 are described. An overview of the main topics:

- Chapter 1: Literature study on stretchable electronics.
- Chapter 2: Introduction on polymers and mechanical aspects of elastic microsystems.
- Chapters 3,4 and 5: Different technology developments for large area stretchable electronics.
- Chapter 6: Reliability study of the copper meanders in the different technologies.
- Chapter 7: Demonstrators of the different technologies.

The Phd on stretchable and washable electronics for embedding in textiles presented here, was done more or less in parallel with the work described by Bossuyt (PhD) [12] and is therefore closely related. The current Phd will describe the development of stretchable technologies in the context of textile applications. Shortcomings in previous technologies are explained and new solutions are provided.

1.4 Research context

The research which formed the basis of this dissertation was carried out mainly within the framework of the SWEET project. Developments within this project were the integration method by screen printing, the creation of openings to contact pads and first washing experiments (blinking LED modules and WR1 test). The development of the laser based substrate fabrication method was carried out in the framework of the STELLA project. Within the Place-It project, the improvements from the WR1 design to the WR2 design were made and the WR2 tests were conducted and evaluated. The results obtained during this PhD are now used and further developed in the framework of the PASTA project in order to create a stretchable electronic package that can be assembled on fabrics containing conductive yarns. Also the first injection molding tests on an industrial machine were performed within this project.

More information on these projects is given below:

SWEET (Stretchable and Washable Electronics for Embedding in Textiles)

Belgian Science Policy (Belspo)-project

Starting date: March 1, 2007
Finishing date: February 28, 2010
Project coordinator: Prof. Dr. ir. Jan Vanfleteren (IMEC/UGent/CMST, Belgium)
Partners: UGent, Centexbel, KULeuven, UCLouvain.

Innovations from the proposed SWEET project include:

- Technology for stretchable electronic circuits, suitable for textile embedding.
- Technology for surface modification and characterisation of elastic polymer base materials and metals to improve the polymer/polymer and polymer/metal adhesion.
- Encapsulation technology for the electronic substrate and for bonding the electronic substrate to the textile, including washability and typical textile handling tests.
- Technology for connection of the stretchable circuits with textronics elements like for example conducting fibres.

STELLA (Stretchable Electronics for Large Area Applications)

European IST-Project, Framework 6, 4th call

Starting date: February 1, 2006
Finishing date: January 31, 2010
Project coordinator: Dr. Christopher Klatt (Freudenberg, Germany)
Partners: Freudenberg, IMEC, TU Berlin, CEA, Philips, QPI, BESI, Verhaert, Urgo, Fundico, NXP, TNO.

Innovations from the proposed STELLA project include:

- New stretchable substrates with stretchable conductor pattern.
- Assembly technology on stretchable substrates, based on lead-free reflow soldering.
- Integration methods for electronics in stretchable products.

Place-It (Platform for Large Area Conformable Electronics by InTegration)

European IST-Project, Framework 7, 4th call

Starting date: February 1, 2010
Finishing date: January 31, 2013
Project coordinator: ir. Koen van Os (Philips Corporate Technologies, The Netherlands)
Partners: Philips Corporate Technologies, TNO, TU Berlin, Freudenberg, IMEC, Centexbel, TITV Greiz, Philips Lighting, Grupo Antolin, Zentrum für Medizinische Forschung, RWTH Aachen, Ohmatex.

Innovations from the proposed Place-It project include:

- Development of an integration platform of foil, stretch and fabric technologies with opto-electronic functionality.
- Development of foil, stretchable and fabric-based devices for light emission, electronics, sensing and with interfaces to other technology building blocks.

Pasta (Platform for Large Area Conformable Electronics by In-Tegration)

European IST-Project, Framework 7, 5th call

Starting date: October 1, 2010
Finishing date: September 30, 2014
Project coordinator: ir. Johan De Baets (IMEC/UGent/CMST, Belgium)
Partners: IMEC, CEA, Fraunhofer-Gesellschaft, STFI, CSEM, PEP, ETTLIN, Peppermint Holding, SPS, Asyril, Fundico, FOV Fabrics, NikeTech.

Innovations from the proposed Pasta project include:

- Combination of research on electronic packaging and interconnection technology with textile research to realize an innovative approach of smart textile.
- Development of new concepts for electronic packaging and module interconnect to obtain more comfortable and more robust integration of electronics in textile.
- Development of a stretchable interposer serving as a stress relief interface between the rigid component and the elastic fabric.

References

[1] Wearable computer inventions by Steve Mann, as seen on Steve's Wikipedia entry. [Online]. Available: http://en.wikipedia.org/wiki/Steve_Mann

[2] S. Mann, "Humanistic computing: ldquo;wearcomp rdquo; as a new framework and application for intelligent signal processing," *Proceedings of the IEEE*, vol. 86, no. 11, pp. 2123 –2151, nov 1998.

[3] K. Butler, "North-western radio and telecommunication group: Chairman's address. the application of electronic techniques to textiles," *Proceedings of the IEE - Part B: Radio and Electronic Engineering*, vol. 105, no. 20, p. 118, march 1958.

[4] J. Azoulay, "Anisotropy in electric properties of fabrics containing new conductive fibers," *Electrical Insulation, IEEE Transactions on*, vol. 23, no. 3, pp. 383 –386, jun 1988.

[5] E. R. Post, M. Orth, P. R. Russo, and N. Gershenfeld, "E-broidery: Design and fabrication of textile-based computing," *IBM Systems Journal*, vol. 39, no. 3.4, pp. 840 –860, 2000.

[6] J. Brun, D. Vicard, B. Mourey, B. Lepine, and F. Frassati, "Packaging and wired interconnections for insertion of miniaturized chips in smart fabrics." in *Microelectronics and Packaging Conference, EMPC*, june 2009, pp. 1 –5.

[7] (2012) The PASTA project website. [Online]. Available: http://www.pasta-project.eu/

[8] S. Lacour, J. Jones, S. Wagner, T. Li, and Z. Suo, "Stretchable interconnects for elastic electronic surfaces." in *Proceedings of the IEEE*, vol. 93, no. 8, Aug 2005, pp. 1459–1467.

[9] D. Kim and J. Rogers, "Stretchable electronics: materials strategies and devices." *Advanced Materials*, vol. 20, no. 24, pp. 4887–4892, 2008.

[10] D. Gray, J. Tien, and C. Chen, "High conductivity elastomeric electronics." *Advanced Materials*, vol. 16, no. 5, pp. 393–397, 2004.

[11] D. Brosteaux, F. Axisa, M. Gonzalez, and J. Vanfleteren, "Design and fabrication of elastic interconnections for stretchable electronic circuits." *IEEE Electron Device Letters*, vol. 28, no. 7, pp. 552–554, 2007.

[12] F. Bossuyt, *Novel Technologies for Elastic Microsystems: Development, Characterisation and Applications. PhD thesis*. Ghent University, 2011.

[13] (2012) The STELLA project website. [Online]. Available: http://www.stella-project.de/

[14] T. Loher, M. Seckel, and A. Ostmann, "Stretchable electronics manufacturing and application," in *3rd Electronic System-Integration Technology Conference (ESTC)*, Sept 2010.

[15] F. Bossuyt, T. Vervust, F. Axisa, and J. Vanfleteren, "Improved stretchable electronics technology for large area applications," in *MRS Proceedings*, vol. 1271. San Francisco, CA, USA: Materials Research Society (MRS), April 2010, pp. 1–7. [Online]. Available: http://dx.doi.org/10.1557/PROC-1271-JJ08-03

2

Fabrication technologies for stretchable electronics

2.1 Introduction

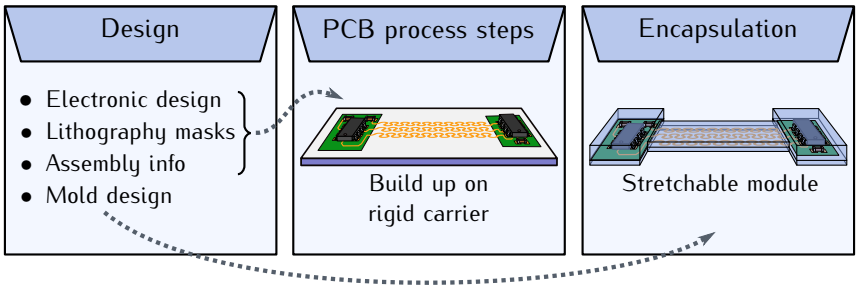

Figure 2.1: Chapter overview.

In this PhD thesis new technologies for textile integrated electronics are presented. They are based on novel technologies for elastic, stretchable electronic circuits. This chapter presents the starting point of the technology developments and how these technologies were further used and improved to fabricate stretchable modules, well suited for textile integration. First we discuss a general implementation process for designing a technology demonstrator or a product that contains textile integrated electronics. The reader

will learn the different steps to follow in order to design a stretchable module and how this design is thereafter translated into a stretchable module ready for textile integration. The actual textile integration of these modules will be covered in the next chapter on integration.

SMI design principle

The general design principle of the type of stretchable circuits that we will use was presented in 2005 in the proposal of the STELLA project [1]. In this project IMEC-UGent worked as a partner to develop a technology that implements the proposed idea of a stretchable circuit. The IMEC-UGent technology was differentiated from the other technology implementations in the STELLA technology platform by naming it Stretchable Molded Interconnect (SMI).

The design principle of the SMI technology is illustrated in Figure 2.2. A traditional flexible printed circuit board (FCB) can bend or fold in one direction. Over the years this property of flexible circuits was used in an uncountable amount of static and dynamic applications. The SMI technology pushes the conformability of the substrate to an even higher level by allowing it to stretch in different directions. To accomplish this, an electronic circuit is subdivided in several non-stretchable functional islands, which are interconnected with stretchable interconnections as illustrated in Figure 2.2.

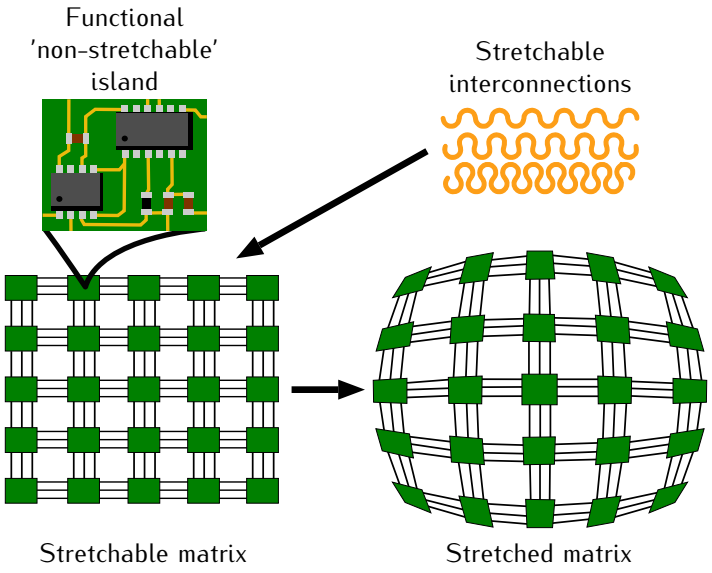

Figure 2.2: Design principle of the SMI technology: functional 'non-stretchable' islands are interconnected via stretchable copper connections.

These islands contain rigid or flexible electronic components. Conventional electronic component types can be used (Bare die, SOT, QFP, flip-chip, BGA, SMD,...). By interconnecting the islands with stretchable interconnections, the circuit becomes stretchable. In the SMI technology, in-plane spring-shaped copper connections are used. The stretchable circuit, which is the combination of islands and stretchable interconnections, is encapsulated in an elastomer, resulting in a stretchable module.

An implementation example of the design principle is shown in the pictures of Figure 2.3. This stretchable module is one of the technology demonstrators designed and realized during this PhD thesis. A description of this demonstrator is given in Chapter 6.

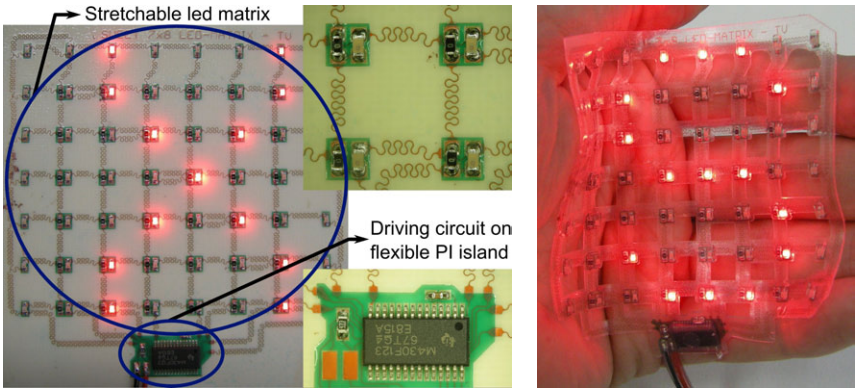

(a) Before encapsulation. (b) After encapsulation.

Figure 2.3: Stretchable 7x8 LED matrix.

2.2 Stretchable electronic design.

2.2.1 Implementing stretchable circuit technologies in textiles.

Before we jump into the technology developments, we take a look at the question 'How to design a textile product that contains stretchable electronics?'. This is an important question because whatever technology has been developed, in the end it is the goal to make something with it. Real product design is far beyond the scope of this PhD. Nevertheless, realizing a technology demonstrator will follow more or less the same design steps. In order to be successful in the end it is important to go through an implementation process which requires thinking on certain topics and a good planning from the start. The implementation process for textile integrated stretchable circuits presented here (Figure 2.4) is based on a simple thirteen-step approach for implementing flexible circuit technology [2]. Flexible circuit technology development faced different pitfalls, but a lot of experience was gained over the years, leading to new and better product generations. Fortunately, the process of implementing flexible circuit technology into a design is not as challenging today as it once was. We can draw a parallel between flexible circuit technology and stretchable circuit technology. The stretchable technologies are now in the early days with a lot of new challenges, and the experiences and lessons learned by flexible circuit technology pioneers can be used as guidelines. Therefore, the implementation process for flexible circuits was changed and mapped to the needs for textile integrated stretchable circuitry.

1) Define end product requirements.

The product, its application and performance expectations should be given as much definition as possible by the end user to ensure that they will get the value and/or features they seek. At this time, it is worthwhile to determine if a stretchable circuit is even the best choice for the product. It is possible that a better or more cost-effective solution can be found when other alternatives are explored. For example, a thin encapsulated flexible module can be integrated into the textile if the module can be made small enough to be unnoticeable for the user. It is also not needed to design a stretchable module which can have a high elongation if the textile itself is not considered as very stretchable. The user should also consider the product's cost targets or requirements, product life expectations, size, etc., to make sure that the decision to use a certain technology is the right one in terms of cost and performance. At the time of writing this PhD, the stretchable technology is applied in a lab environment and not yet on an industrial level. Therefore it is hard to make cost estimations. But even for demonstrators, with a certain product in mind, it is interesting to have a cost target from an end user, to steer for example material selection.

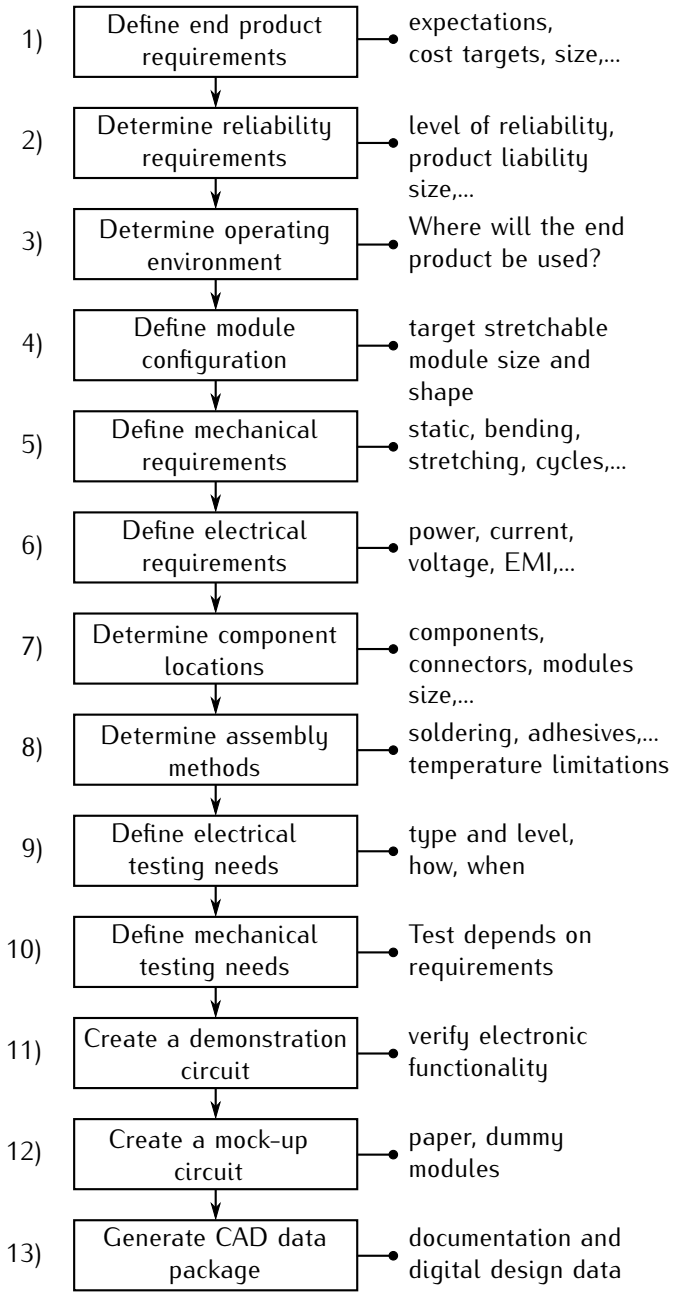

Figure 2.4: Thirteen step implementation process for stretchable circuit implementation.

2) Determine reliability requirements.

Early consideration should be given to the reliability requirements for the product. What level of reliability is needed? IPC, the association connecting electronics industries, uses three general end-product classes depending on the ultimate use, life expectancy and operating environment of the electronic assembly [3]. Those classes are as follows:

- *Class 1 - General Electronic Products*, which includes consumer products and the major requirement is function of the completed assembly.
- *Class 2 - Dedicated Service Electronic Products*, which includes communications equipment, sophisticated business machines, instruments and military equipment where high performance and extended life is required, and for which uninterrupted service is desired but not critical.
- *Class 3 - High Reliability Electronic Products*, which includes the equipment for commercial and military products where continued performance or performance on demand is critical. Equipment downtime cannot be tolerated, and must function when required such as for life support items, or critical weapons systems.

It is also worthwhile to consider product liability. What are the ramifications of product failure due to a stretch circuit-related design problem? While not a necessarily comfortable task, it is very important that liability is consciously addressed. For flexible circuits thermal cycling is considered one of the key determinants of electronic product life (along with flexural durability), and products from different markets must endure very different conditions. As a guide, the IPC provides a chart to assess and approximate thermal cycling conditions for electronic assemblies. It can be found in IPC-SM-785 Guidelines for Accelerated Reliability Test of Surface Mount Solder Attachments [4]. The same tests should be used for stretchable electronics. Additionally, standards for accelerated reliability tests to assess stretch durability under different conditions should be defined.

3) Determine operating environment.

Product operating environment determination is an important factor that will influence later design and manufacturing choices. Where will the end product be used? In an outdoor application? At home? In an automobile? In a medical application? These questions will help to determine the likely operating environment for the product, what temperatures and relative humidity extremes are to be expected over product life and how often they might be thermally cycled. This will also help to define the stretchability needs, what the maximum elongation will be and how many cycles the modules might be stretched.

4) Define module configuration.

The target size and shape of the stretchable module should be established early in the process since it is the foundation from which many other decisions will be made. In addition to size and shape, optimum locations for component islands and stretchable meanders should be considered.

5) Define mechanical requirements.

It is necessary to consider the mechanical requirements that will be placed on the stretchable module. For example, will the application be static, requiring a one time stretch? Or will the application require active bending and/or stretching? If the application requires dynamic stretching, will it require continuous or intermittent operation? Requirements for dynamic stretching vary since an application can require anywhere from hundreds of cycles per year to hundreds of cycles per minute. Also the (maximum) elongation and the stretch rate will depend on the application. Design layout issues (e.g. meander shape) and material choices will be influenced by the answers to these questions.

6) Define electrical requirements.

Like any electronic product, it is necessary to determine what the key electrical requirements will be as early as possible. For example, what are the power requirements? How much current is needed? At what voltage? What is the expected maximum or peak current? Is electromagnetic interference (EMI) a concern and is there a need for shielding? If the circuit is large, is voltage drop a concern? Are common electrical parasitic effects, such as capacitance and inductance, important to the performance for the design or application? Each of these considerations can potentially affect material choice and/or circuit design/layout approach.

7) Determine module locations.

Integrating stretchable electronic modules into textiles requires determination of the total product layout in an early phase. At what positions in or on the textile can the modules be integrated? At what point in the textile product manufacturing process will the integration take place? Is there more than one module and is there an electrical interconnection between them? In general, electrical component and meander locations will define the stretchable module shape. If interconnection between modules is needed, connection position should be defined and taken into account during module design.

8) Define assembly methods.

It is important to give early consideration to which type of component assembly method is to be used. The quantity of the product, the substrate material and the size of the part will all help to determine the assembly method. Choices for electromechanical joining include soldering, using conductive adhesives and even mechanical fastening. With the higher temperatures associated with lead-free solders, the temperature limitations of materials must be fully understood. It is possible to perform assembly by hand or machine. If assembly requires special or individual handling, cost will greatly increase. Costs can be better managed by carefully considering the best layout of the circuit to facilitate the assembly process.

9) Define electrical testing needs.

What type and level of testing will be required? How, when and where will testing be performed? These questions are often ignored or are afterthoughts in the design process. It is important that testing be given due consideration before embarking on a design. Some questions to raise in design are: Will testing of the unencapsulated module be required? Will only the assembled module be tested? Or are both levels of test needed? How will the test contacts be accessed? Design complexity will impact and steer decisions regarding electrical test needs. Since stretchable circuits employ relatively soft and highly flexible substrates, there are special concerns when it comes to electrical test because the test probes can easily damage the circuit's surfaces. On the other hand, because they are flexible, circuit test fixtures can be made smaller than normal when necessary and the stretchable circuit can be shaped to fit the fixture.

10) Define mechanical testing needs.

There are a number of different options for mechanical testing of flexible circuits in dynamic flexure applications [2] (see Chapter 14 - Inspection and Test of Flex Circuits). Most stretchable circuits are also subjected to dynamic flexing, meaning that these flexural endurance tests can be considered. Cyclic stretching is the appropriate test to evaluate stretch requirements. In case of textile products, cleaning needs will define additional mechanical requirements and tests. Given the amount of different test possibilities, it is good to be properly prepared with appropriate equipment.

11) Create a demonstration circuit.

At some point, before committing the circuit to prototyping or production, it is worth taking the time to verify the electronic functionality of the circuit. This

can be accomplished using long-standing empirical methods such as breadboarding, but it is becoming more common to use simulation software. Creating a demonstration circuit avoids wasting the time and expense of tooling for manufacture until the fundamental circuit is proven. While this may not prevent all unforeseen incompatibilities between circuit elements in the final form, it should reduce overall costs over time. Simulation tools are continually improving, so in many cases this step can be satisfied by simulation.

12) Create a mock-up circuit.

A mock-up of the final stretchable module should be used to minimize the potential for easily-avoidable errors and to expose eventual textile integration problems. The mock-up can go from a simple paper model up to an encapsulated dummy FCB. Having a physical model also saves time and money by providing an ergonomic check for circuit access and verifying the ease of final assembly and field service.

13) Generate CAD (Computer-Added Design) data package.

As a final step, it is necessary to generate appropriate documentation and data packages with circuit features and circuit outline information. Today, most manufacturers prefer to receive data in digital form, which allows them to make needed adjustments to compensate for circuit processing. The data package should be double-checked for mechanical and electrical concerns as well as accuracy to avoid a loss of time due to downstream problems.

The thirteen steps described encompass some important considerations for textile integrated stretchable circuit implementation and provide an understanding of the level of detail that must be addressed before entering into a real product design. It is not the intention of this PhD to provide a solution for the large amount of requirements and design questions that are encountered during the implementation process. Nevertheless they were kept in mind during technology development and were applied to some extent during demonstrator design. Eventually, they should be addressed when a real product design is considered. Similar to the evolution FCB technology underwent, stretchable electronics for textiles will be adopted slowly, starting with simple constructions before undertaking more complex designs.

2.2.2 Meander design tool.

One of the differences in a stretchable electronic design compared to rigid or flexible printed circuit (FPC) design is the presence of meander shaped tracks instead of straight tracks. This provides additional requirements for PCB CAD design tools in order to route signals in a certain meander shape. General information on typical design tools used for PCB design can be found in 'Printed circuits handbook - The PCB design process'[5].

Here we present a meander design tool, developed during this PhD research, well suited for routing meanders in the EAGLE PCB design software [6]. The meander program was programmed as an ULP (user language program) and makes also use of EAGLE's scripting possibilities. ULP's are written in a C-like program language that can be executed by EAGLE. A screenshot of the tool is given in Figure 2.5.

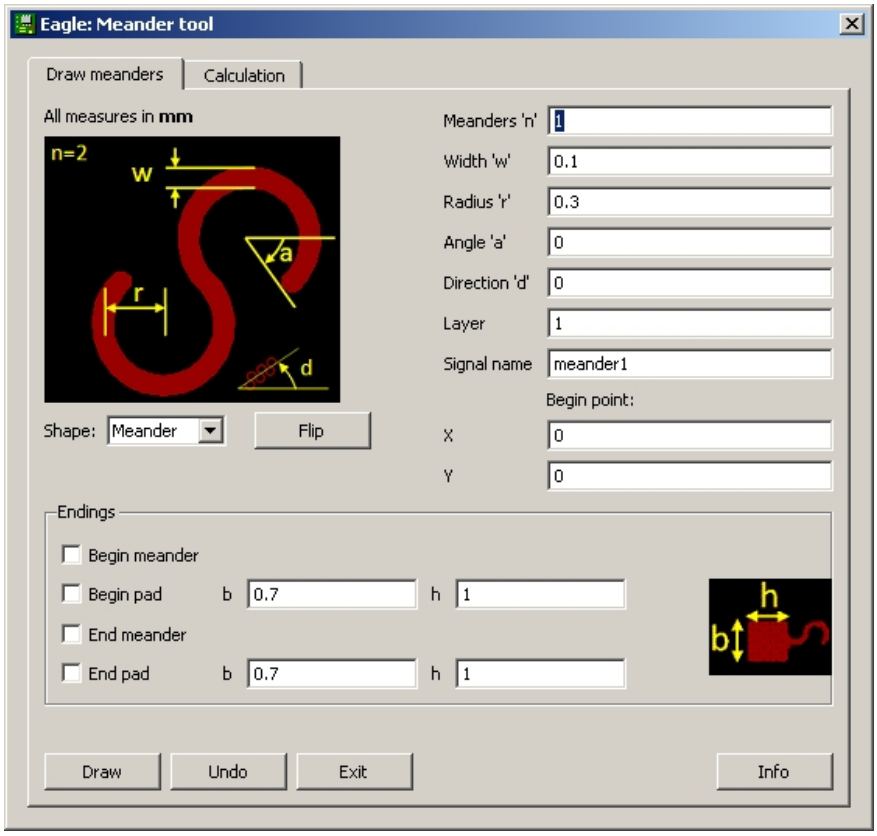

Figure 2.5: Eagle meander tool

This meander design tool can be used to:

- Draw meanders in the PCB design software. The meander shape is based upon a few parameters (e.g. number of meanders, width, radius, angle, direction,...). This simplifies the drawing process for the user and avoids repetition of calculations and thus decreases drawing time.
- Draw the beginning and ending structures of a meander.
- Draw other structures like arcs, corners and splits.
- Calculate the number of turns and meander parameters to draw a meander between two points on the layout.

During this PhD this meander tool was used to design technology demonstrators of which some of them are described in chapter 6. Also this tool was successfully used in student projects and master theses. More information on the features of this tool and the goniometric calculations behind it are found in appendix A.

2.3 Substrate fabrication

Creation of a CAD data package, including circuit features and circuit outline information, finalizes the design process. In a next phase these design files are used in stretchable module production and textile integration. The SMI technology differs itself from other stretchable technologies by separating the stretchable module production in a **substrate fabrication part** and an **encapsulation part**. This way the encapsulating elastomer is introduced at the end of the process, making the substrate fabrication steps independent from the encapsulating material. Other stretchable technologies (e.g. [7]) tend to use an elastomer from the beginning of the process. This can lead to a more limited choice of elastomer and to adaptation of processing steps if the elastomer is changed.

In this section we cover the substrate fabrication part and the encapsulation is described in the next section (Section 2.4). The SMI substrate fabrication can be done in different ways, using different materials, but they all have common properties:

- Standard PCB process steps are used.
- The build up is done on a substrate carrier with an temporary adhesive.
- After encapsulation the substrate carrier is removed.

Two different SMI substrate fabrication methods will be described. The first one uses a photo definable polyimide (PI) as an island and meander support layer. The second one starts form a normal FCB and uses laserstructuring.

2.3.1 Using photo definable polyimide

This SMI substrate fabrication method was described in the PhD dissertation on 'Novel Technologies for Elastic Microsystems: Development, Characterization and Applications' in Chapter 5: Peelable technology with local polyimide support [8]. This method was developed by Bossuyt, a colleague at IMEC-UGent. It looked a good candidate to start from, in order to evaluate the modules produced by this method in terms of textile integration. The reason for that is the presence of the local PI support. In general, the stretchable modules we want to use for textile integration should be robust enough to survive deformations during product life and cleaning processes. The local PI support gives additional strength to the copper meanders and can be used to define the flexible functional islands presented in the introduction (Section 2.1). The process for this method is summarized in Figure 2.6.

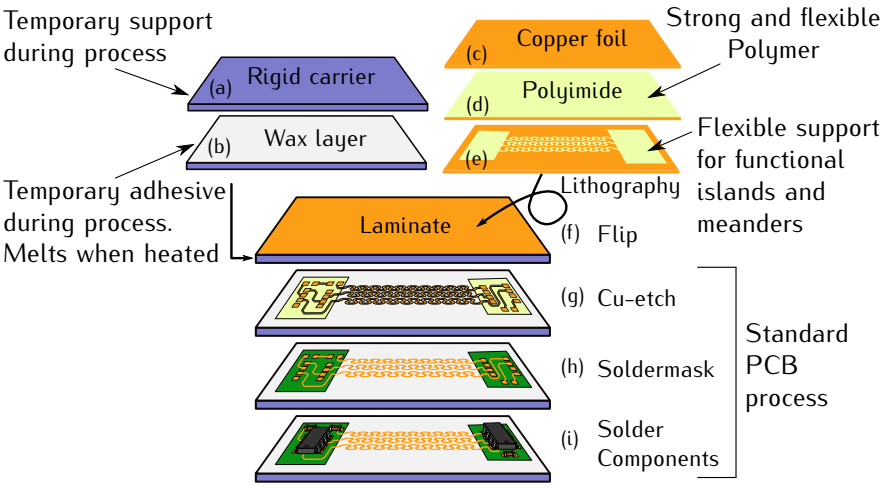

Figure 2.6: Process flow (from top to bottom) for stretchable substrate fabrication in the SMI technology.

During this substrate fabrication process, the circuit is build on a rigid carrier (a) with a wax layer on top (b). First a copper foil (c) is covered with a layer of photo definable PI (d). By lithography the PI is patterned to create non-stretchable, but flexible islands (e). The PI also supports the copper meanders in order to give them additional strength. After patterning, the foil is flipped and laminated onto the carrier (f). The carrier and the wax are temporary and will be removed later on during the encapsulation process. At this stage of the process, the substrate looks like a standard single layer copper clad laminate, used in rigid PCB processing.

The next steps in the process are the same steps used in PCB manufacturing:

- pattern the copper by lithography and spray etching (g)
- screen print the solder mask (h)
- mount electrical components and perform a reflow solder cycle (i)

The Printed Circuits Handbook [5] is a good reference for more information on PCB process steps. At this point in the process the substrate fabrication part is finished. The circuit can be tested and, if necessary (and feasible), repaired before proceeding with the encapsulation part. **Remark:** During reflow soldering the wax melts, but the structures are floating on the wax, making this step possible. However it is possible that their position shifts, which can cause problems in case accurate dimensions are requested. To evaluate the SMI method with PI support, an actual design was made, using the meander tool (see Appendix A). This technology demonstrator has a 7x8 LED display. Information on the design and functionality is described in Chapter 6. Figure 2.7 shows the substrate at different moments in the process.

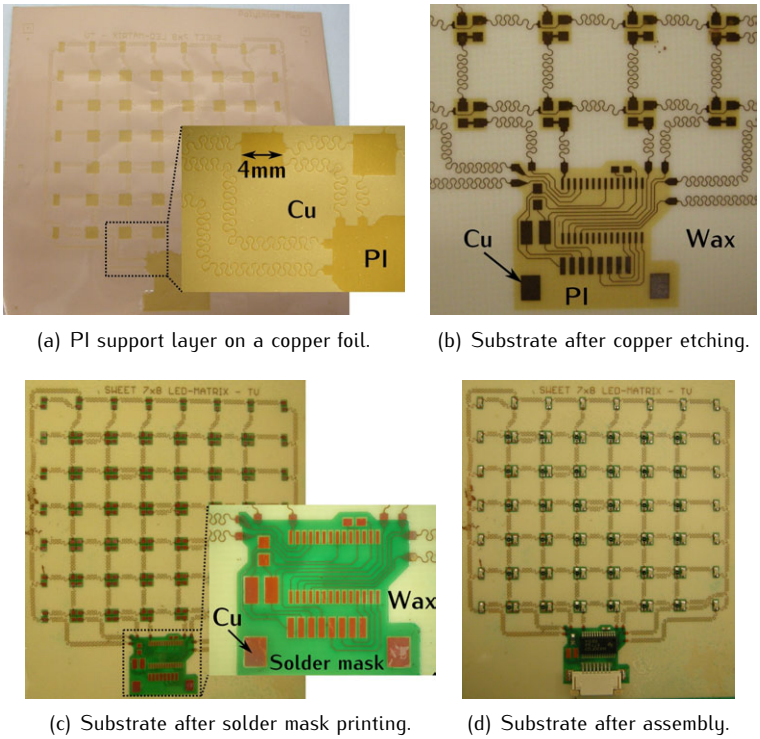

(a) PI support layer on a copper foil.

(b) Substrate after copper etching.

(c) Substrate after solder mask printing.

(d) Substrate after assembly.

Figure 2.7: Snapshots of the substrate during substrate fabrication.

The encapsulation of this technology demonstrator is illustrated in the section on encapsulation (Section 2.4). Besides the fact that it was possible to realize this demonstrator, this substrate fabrication method seemed to be inadequate for our purpose. The PI support was too fragile and brittle, leading to bad reliability of the stretchable module. In other words, the mechanical properties of the PI support were acceptable during processing, but were disappointing when the module was dynamically stressed (bending, stretching, twisting, crumpling,...). Cracking and tearing of the PI support layer resulted in discontinuities in copper tracks on the functional islands, eventually leading to circuit failure. This problem was not reported nor solved in the referred PhD thesis [8]. For textile applications it is necessary to have robust stretchable modules. In order to overcome this reliability problem, another way of producing the substrate was explored. This method is described in the next section (Section 2.3.2).

2.3.2 Using laser structuring

To obtain good reliability, it is important to have a support layer that withstands multiple bending cycles. In fact we want something that acts like an FCB, so why do we not use an FCB? This idea was the starting point of this laser structuring fabrication method. The process flow for this method is illustrated in Figure 2.8.

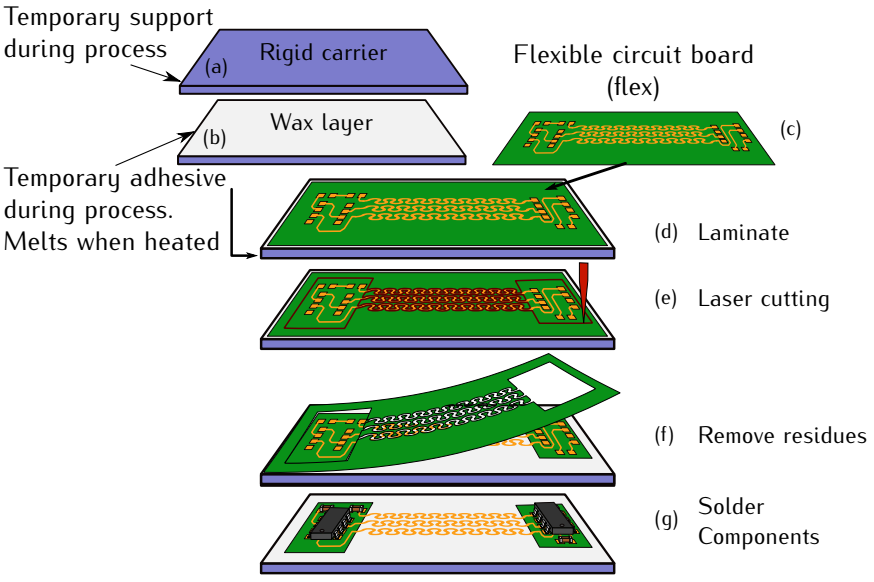

Figure 2.8: Process flow for the laser structuring technology.

The laser structuring method starts from a finished FCB (PI + copper pattern + solder mask + surface finish). This means that this circuit can be produced in any PCB fab, capable of doing FCB manufacturing, which narrows the gap to industrialization. Another benefit is the avoidance of the wax adhesive during the PCB processes. The used wax starts to soften around 70°C. For PCB processes using a higher temperature this can be a problem because the wax loses its adhesion and the structures come off. This makes it, for example, impossible to have a Ni/Au finish, as it requires using baths at 80°C. Also the curing temperatures for solder masks are too high. In the PhD thesis of Bossuyt [8], the temperatures were lowered, but then material properties became questionable because curing was done out of the advised range. So starting from a finished FCB avoids all these problems. In the same way as was done with the PI support method, the FCB (c) is laminated (d) on a temporary rigid carrier (a) with wax adhesive (b). The meanders and PI islands are structured in one step by laser cutting (e). After laser structuring the FCB residues are removed by peeling them off (f). The substrate fabrication part is finalized by assembling the electrical components (g). Figure 2.9 shows some examples of laser structured FCBs.

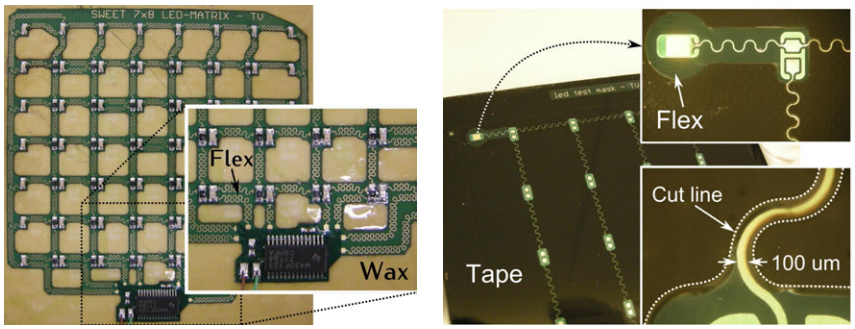

(a) Laser structured 7x8 LED display. (b) Laser structured meanders.

Figure 2.9: Examples of laser structured FCBs.

The meandering tracks of the substrate in Figure 2.9(a) were not laser structured. Instead they remain 'fixed' in the flexible matrix by only laser cutting some openings between the meanders. This was done to show the difference in conformability with a completely stretchable module. In textile applications where little or no stretchability is needed, this approach can be sufficient. In the example shown in Figure 2.9(b), the meander shapes are cut out to allow stretching. Note that the structures are not bonded to the rigid carrier with the transparent wax adhesive, but with a black tape. The use of this tape will be explained in Section 2.4.2 on encapsulation by lamination.

Industrialization

Most of the test samples and demonstrators realized during this PhD were made with this laser structuring method. The FCBs were mainly produced in the lab or were outsourced in some cases. Laser structuring itself was always done at the lab on an automated laser platform, custom built by Optec [9]. A software program sends CAD data of the cutting line to the laser setup. A Nd-Yag laser beam with a wavelength of 355nm follows the path provided by the software program. The 50 μm thick PI layer of the FCBs was cut by using a power of 150 mW. The width of the cut line is around 20 μm. Although this method yielded good results in a lab environment, the question remains whether this is possible on an industrial scale. To do so, the following conditions should be fulfilled:

- The laser cutting should be fast to achieve an acceptable throughput.
- Alignment of the laser beam should be accurate and the laser spot fine enough in order to follow the meander tracks. This will define the smallest features that can be achieved.
- Removal of the FCB residues should be easy, fast enough and preferably automated.

The used laser setup was sufficient for prototyping a few samples, but the cutting speed of 5mm/s might be too slow for production on an industrial scale. Laser structuring a sample without a lot of complexity like the one in Figure 2.9(b) took around 10 minutes (sample on 10cm x 10cm carrier). The main reason for this slow speed is the construction of the laser setup, that was designed to use different laser types. In this setup it is the table, holding the substrate, that moves and these movements are too slow for fast laser cutting. An example of equipment that could meet the needed specs is the MicroLine 6000P from LPKF [10]. This is a UV-laser system for cutting coverlayers, FCBs and PCBs. In this machine it is the laser beam that moves over the substrate, resulting in higher cutting speeds. The remaining industrialization issue is the FCB residue removal. In the lab this was done manually by peeling out the residues with tweezers. Depending on the design this can be an easy or a difficult task. If there are only a few, big parts to remove this can go fast. If the design contains a lot of closely spaced meanders this can be a slow and tedious job. Therefore, it is important to take this into account during the design phase. One should provide easily accessible points to start the peeling. Figure 2.10 shows an example were the four peel points are indicated. The dotted arrow at peel point two illustrates the peel direction.

A technology where similar 'peeling operations' are performed is the technology to produce vinyl stickers and banners in the sign making industry. Letters and other patterns are cut in vinyl with a 'vinyl cutter'. Solid colored

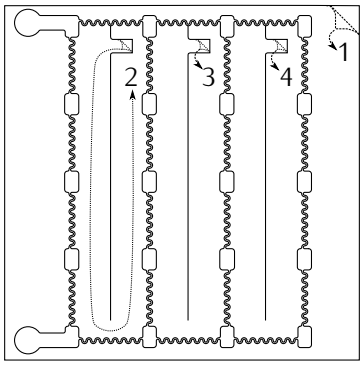

Figure 2.10: Design tip: Provide additional features to facilitate the residue peel out.

rolls of vinyl film are fed into the cutter. These vinyl rolls are composed of two parts - adhesive vinyl on top of a waxy paper 'carrier'. The software program sends the vector image to the knife blade of the cutter. This knife blade follows the artwork 'path' instructions provided by the software program. The blade cuts through the vinyl layer but not through the paper carrier producing the desired graphic shape. The next step is 'weeding' the vinyl and this step is similar to what we called 'peeling'. It is called weeding because it is like weeding a vegetable garden - all of the good stuff stays and all the 'weeds' or bad stuff gets pulled out and is thrown away. Weeding is hand done. There is no such thing as a weeding machine. Each unwanted element is picked out of the roll of vinyl and discarded. The more letters and graphics that are on a sticker or banner, the more time it takes to weed away the unwanted vinyl [11]. Figure 2.11 shows a picture of this weeding process [12].

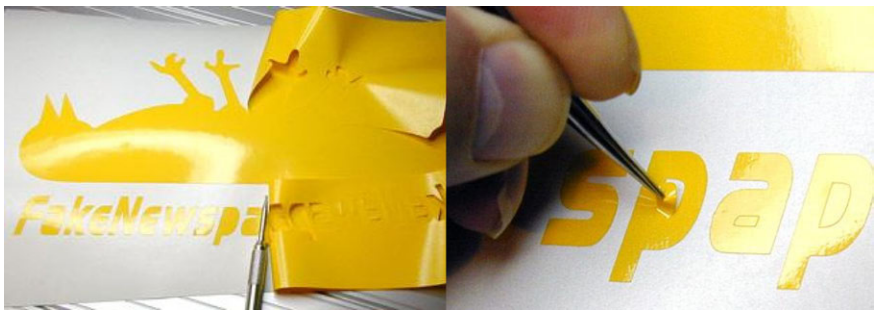

Figure 2.11: Weeding a vinyl sticker. (Pictures obtained form [12])

While cutting with a vinyl cutter is automated, the question remains why the weeding is still done manually. It could be that it is cheaper to perform this step manually than to design and buy a machine suited for the job. Different

hand tools and techniques are used to speed up this weeding process [13] and software tools exist to reduce weeding time by the automatic creation of weed borders [14]. It should be evaluated if the manual peeling in the SMI laser structuring method is also acceptable for production. Of course this will depend on the design (number of residual surfaces to peel out) and product quantities.

One possibility to overcome the peeling step is to laser structure the FCBs, prior to laminating them to the temporary rigid carrier. Then the residues will fall out and no peeling step is needed. However, care should be given to the fact that laser structuring meanders results in a stretchable and thus difficult to handle FCB. Therefore additional features should be foreseen to fix the functional island in a frame, preventing them from moving. Depending on the design this may or may not be possible and maybe some zones in the design would still need peeling. Figure 2.12 gives an example of 'a frame' that fixes the functional islands. After encapsulation the islands can be 'released' by (laser) cutting or punching the additional structures away. Using a punch makes it possible to punch out excess encapsulation material in the same step (see Section 5.4.5.2 for more info on punching).

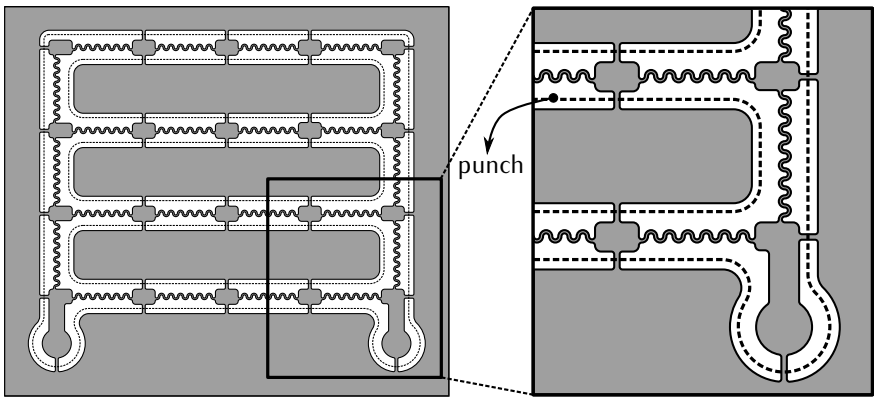

Figure 2.12: Functional islands of a stretchable module fixed in a frame by additional features.

2.4 Encapsulation

In Section 2.3 we described two methods to fabricate a substrate containing a stretchable circuit. This circuit consists of flexible islands, with electrical components, interconnected by stretchable meanders. A temporary carrier with adhesive holds this stretchable circuit (Figure 2.13).

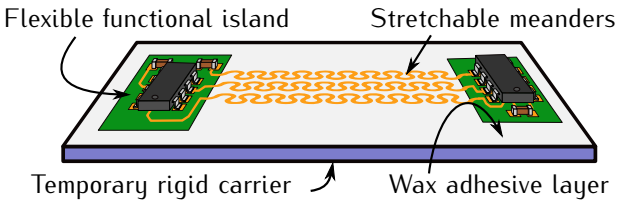

Figure 2.13: Substrate before the encapsulation part in the process.

In the second part of the SMI process, the stretchable circuit is encapsulated in an elastomer, to obtain a stretchable module which will be used for textile integration. We will describe two encapsulation methods that were used and investigated during this PhD study; encapsulation by injection molding and by lamination.

2.4.1 Injection molding

In this method the encapsulation of the stretchable circuit is done by injecting the elastomer in a mold. The encapsulation is split up in two parts; top and bottom encapsulation. The process is illustrated in Figure 2.14.

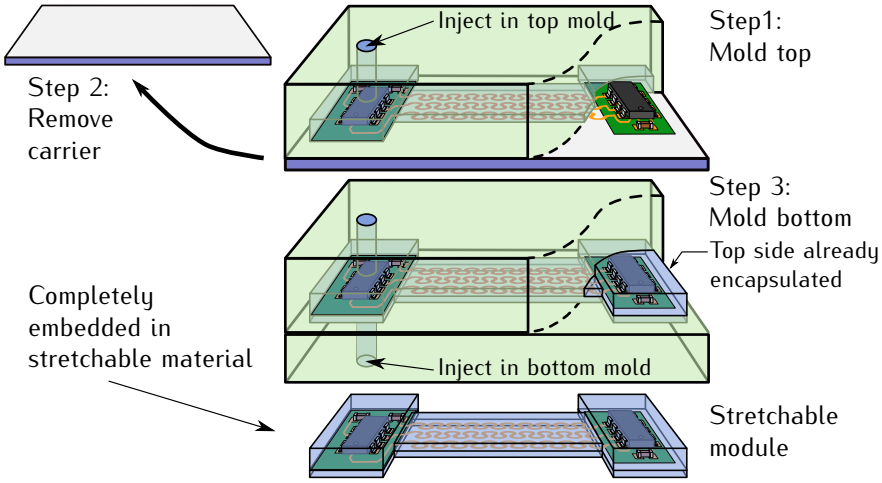

Figure 2.14: Encapsulating the electronics in PDMS by liquid injection molding.

In step one the upper mold is clamped onto the substrate containing the stretchable circuit. The liquid elastomer is injected into the mold and once solid, the upper part of the circuit is encapsulated. In step two the rigid carrier is released from the stretchable circuit. To do this, the wax is heated so that it loses adhesion and the carrier can be removed. The half encapsulated stretchable module remains fixed in the upper mold, so the support is

no longer needed. In the last step the bottom part of the circuit is molded by injection of the material into the bottom mold. This completes the encapsulation process, resulting in a stretchable electronic module. Figure 2.14 shows only a simple scheme of the molding process to illustrate the principle. The actual implementation of this scheme, to produce a stretchable module, can be challenging and versatile depending on the design and user specifications. Some of the most important factors that will influence the molding process are listed below:

- Choice of encapsulation material and its properties (thermoplastic or thermoset, melting or curing temperature, viscosity during injection,...).
- Stretchable module dimensions (size, thickness, shape).
- Production targets (quantities, cycle time, cost).

By using a temporary carrier during the substrate fabrication part, it is possible to introduce the encapsulating material at the end of the process. This causes a great choice of encapsulation materials. On the other hand the material choice can have a big impact on the molding process. Injection molding of thermoset materials is totally different compared to molding thermoplastic materials, resulting in different molding equipment needs. When injection molding a **thermoplastic** material, the melted material is pushed into a cold mold. The mold holds the shape of the material as it cools and solidifies. In some cases active cooling of the mold is needed. Injection molding of **thermoset** materials is generally more difficult than the injection molding of thermoplastic materials. Thermoset materials irreversibly chemically react during the molding process. The material is injected cold into the mold and this mold is heated to start the chemical reaction in order to cure the material.

For both, thermoplastic and thermoset, **elevated temperatures** are present. The melting temperature of the thermoplastic material or the needed curing temperature in case of a thermoset material will determine if the material can be used in the presented SMI process. The reason for that is the use of the wax adhesive that holds the stretchable circuit and the rigid carrier together. The Quickstick T135 wax [15] used in the SMI technology has a softening point of 71°C and starts to loose its adhesion at temperatures above that temperature [8]. This means that the cold injection of a thermoset is no problem, but the curing temperature should be limited to about 60°C. For thermoplastic materials the temperature limitation of the wax can be a bigger problem, as these materials are injected at higher temperatures. We will see further that in this case the wax melts during injection, causing delamination of the stretchable circuit from the carrier. This problem was solved during this PhD work, for some materials, by the use of a different type of temporary adhesive. Another important material property is the materials **viscosity** at injection.

Viscosity describes a fluid's internal resistance to flow. As an example, water has a lower viscosity than honey. The less viscous the fluid is, the greater its ease of movement. This implies that injecting a material with a higher viscosity requires higher injection pressure. If this injection pressure becomes too high, the electrical components can shear off the rigid carrier.

Besides the material choice, also the dimensions of the stretchable module are important to allow injection molding. Large modules will take a longer time to fill the mold, generally using higher injection pressures. Thin modules will also require a higher injection pressure compared to thicker ones.

Lastly, the production targets will also influence injection molding choices. The injection cycle time will determine the number of modules that can be produced per time unit. Therefore the cool down time for thermoplastics or the curing time for thermosets should be as short as possible.

Injection molding is a well established manufacturing process in the industry, but is beyond the capabilities and knowledge of our research lab. However, two strategies were followed during this PhD in order to realize stretchable modules for textile integration. We will describe how the manual injection molding of a silicone material was done at the lab and how later on also injection molding tests were done in an industrial environment.

Injection molding in a lab environment

Most of the stretchable modules realized during this PhD were manually encapsulated with Sylgard 186 from Dow Corning [16]. Sylgard 186 is a silicone rubber which was found to be easy to handle in the lab because of the following properties:

- The material is provided in two components; a base and a curing agent.
- After mixing, the pot life is around 2 hours at room temperature. This gives sufficient time to use the silicone for manual injection molding.
- The viscosity of 66700 cP is low enough to make manual injection possible, but at low injection speeds.
- The cured silicone is transparent, making visual inspection of the encapsulated circuit possible.
- Mechanical properties are appropriate for the use in textile integrated electronic systems; high tear strength, elongation till break of $\sim$400%.

In most cases molds are made from metal, usually either steel or aluminum. In our lab however, we use molds that are milled out of PMMA. PMMA (Poly methyl methacrylate) is a transparent thermoplastic and is sometimes called

acrylic glass. Its transparency makes visual inspection possible while the mold is closed. The PDMS is cured inside the mold at a temperature of 60°C, preventing the wax from melting and mixing with uncured PDMS. At this temperature we stay well below 109°C, the heat distortion temperature under load of the used PMMA [17]. A limitation of the PMMA, used as mold material in the SMI process, is that it dissolves in acetone. Step two as illustrated in Figure 2.14 shows the release of the rigid carrier from the stretchable circuit after molding the top. This is done by heating up the wax above 135°C (shortly to prevent mold deformation) and peeling off the carrier. After this step some wax residues remain on the top mold and on the PDMS of the top encapsulation. Removing these wax residues is done by dissolving them in acetone, which consequently attacks the PMMA mold and creates cracks on the PMMA surface. Dependent on the amount of acetone used during wax removal, the PMMA mold can be used 5 to 10 times. An alternative, amber-to-transparent material with good chemical resistance to acetone is ULTEM (polyetherimide). ULTEM has also a higher heat resistance and high mechanical strength, but is more expensive compared to PMMA. ULTEM molds were used in cases were damage to the mold by the acetone was not allowed.

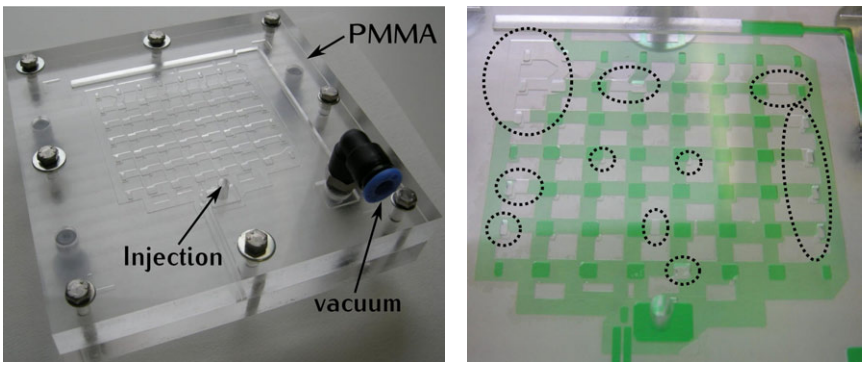

(a) PMMA mold for the 7x8 LED matrix demonstrator.

(b) Mold filled with colored water without using vacuum, showing air entrapment.

Figure 2.15: PMMA molds were used for PDMS encapsulation in the lab.

Figure 2.15(a) shows the PMMA mold for the 7x8 LED matrix demonstrator (info on demonstrator in chapter 6). The PDMS injection was done through an injection hole in the mold, using a hand gun. In some cases, like this one, an additional connection for vacuum was necessary to prevent air entrapment during molding. The occurrence of this problem is illustrated in the picture of Figure 2.15(b). Green pigmented water was injected into the mold to show how air can be entrapped. By creating slight underpressure in the mold during injection, air bubbles can escape.

Eventually we want to integrate the stretchable electronic modules into a textile product. These modules add additional weight to the fabric and decrease its breathability. To keep these changes to a minimum, the volume of the PDMS encapsulation needs to be minimized. This is done by keeping zones without meanders or functional islands free from encapsulation (see Figure 2.16). This will also improve the overall module stretchability.

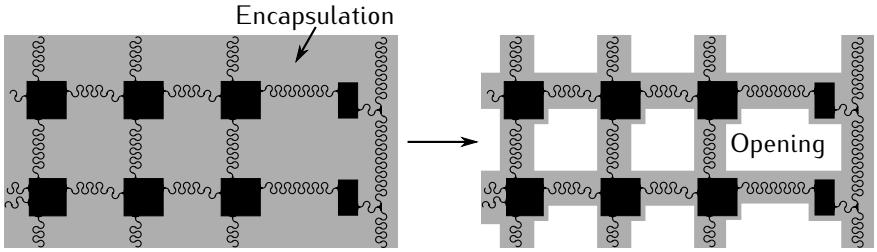

Figure 2.16: Open zones in the encapsulation lower the module weight and enhance the breathability.

In order to create the openings, the upper mold half should close properly onto the temporary rigid carrier with wax during the molding of the upper part. This is to avoid a thin layer of excess material exceeding normal part geometry. Also during encapsulation of the bottom part of the module, the upper mold should close properly, but now onto the bottom mold. Figure 2.17 shows the difference between a badly molded dummy module and a good molded module.

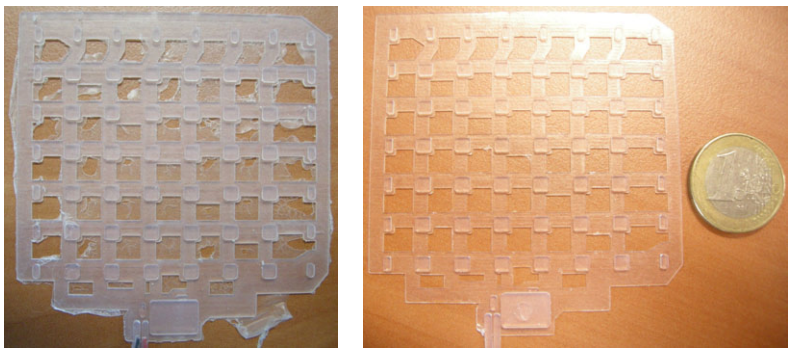

(a) Badly molded dummy module with excess material in the open zones.

(b) Good molded dummy module.

Figure 2.17: Pictures of a good and a bad dummy molded LED module.

To close the mold properly, the mold surface should be smooth. Therefore the PMMA mold surface was polished after CNC (Computer Numerical Control) milling. The mold polishing showed improved molding results but was

not sufficient to eliminate excess PDMS in the openings. This was due to the wax surface on the carrier not being smooth and uniform enough to allow a perfect sealing of the mold. In order to solve this, the wax was melted slightly by heating it to $\sim 80°C$. Then the top mold was pushed into the soft wax and was cooled down until the wax was solid again. This way, a tight sealing was obtained, resulting in good molding results as depicted in Figure 2.17(b). A schematic representation of this principle is shown in Figure 2.18.

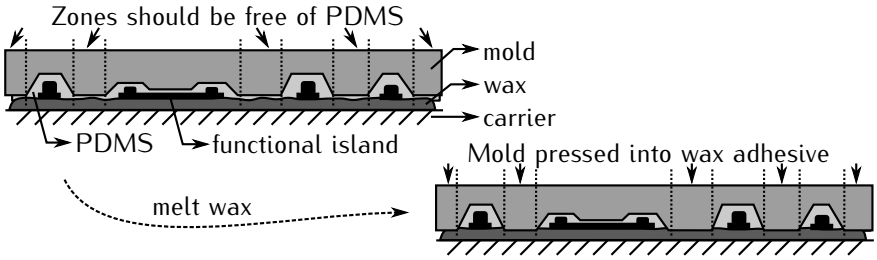

Figure 2.18: Pushing the mold in the molten wax to obtain a perfect seal. Drawing dimensions are not to scale.

Next to openings in the PDMS for breathability, openings to access contact pads on the functional islands were needed in some designs. This was especially the case for the WR samples, which were used in washing reliability tests (Section 5.4.3). These samples had 43 contact pads requiring openings in the encapsulation. In this case the trick to obtain a good mold closure, by pushing the mold into the wax, could not be used. To create a contact opening, the mold should close onto the contact pad. Figure 2.19 illustrates this.

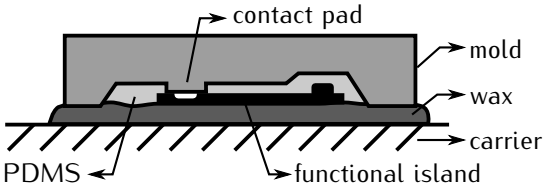

Figure 2.19: Closing of the mold onto the contact pad to create an opening in the PDMS encapsulation. Drawing dimensions are not to scale.

For small 10cm x 10cm samples, using 13cm x 13cm molds, best results were obtained by additional clamping in the center of the mold. This gives a more uniform clamping force, compared to just clamping the edge with bolts. Figure 2.20 shows an example of the used clamps onto an ULTEM mold, which was used for the 7x8 LED demonstrator. For larger samples these clamps could not be used because they did not reach far enough. As a result, a thin film of PDMS covered the pads in come cases (see Section 5.4.5.4 for an example). This layer was manually removed with a scalpel to free up the pad.

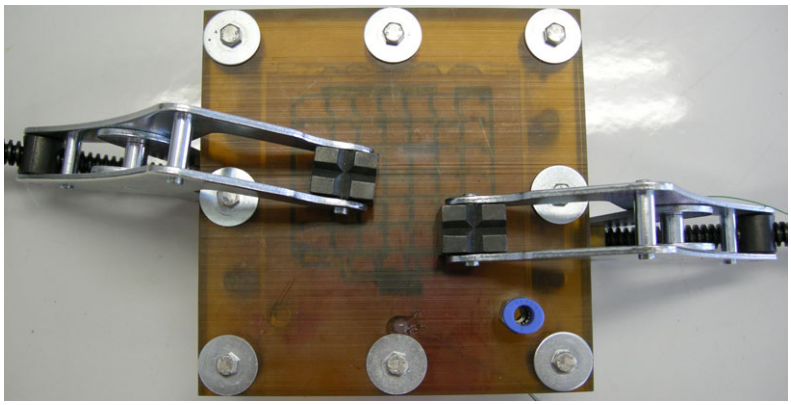

Figure 2.20: A more uniform clamping force by using additional clamps.

Industrial injection molding

The PDMS techniques developed in the lab were sufficient for the successful realization of stretchable test modules and demonstrators. To obtain faster molding cycles and higher clamping forces onto the mold, one should use dedicated industrial molding equipment. This also allows better control of molding parameters like injection pressure, injection speed, mold temperature and clamping force. First tests with industrial injection molding equipment were performed at Pôle Européen de Plasturgie (PEP) [18] in the frame of the PASTA project [19]. PEP is a private technical center dedicated to injection molding of thermoplastics. It was mentioned before that molding a thermoplastic material is different compared to a thermoset material. A general drawing of a machine for thermoplastic injection molding is given in Figure 2.21.

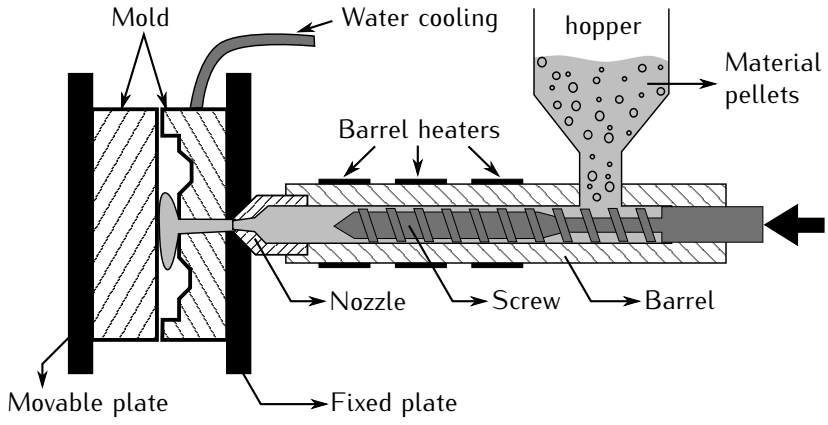

Figure 2.21: Drawing of an injection molding machine for thermoplastic materials.

The thermoplastic material used in the plastic injection molding process is supplied in the form of small pellets. These pellets are loaded into the hopper, then gravity-fed into the barrel and the screw assembly. The barrel is the chamber in which the reciprocating screw is located. This barrel is heated by electric heater bands. The screw compresses and melts the plastic material. It also moves the material toward the mold. The flights of the screw compress the material against the inside of the barrel. This motion creates viscous (shear) heat. Although there are heater bands on the barrel, this shear heat is the primary heat that melts the plastic. The main function of the heater bands is to maintain the temperature of the molten material. The nozzle forms a sealed connection between the barrel and the mold. The temperature of the nozzle is usually set near the plastic's melt temperature [20].

Two thermoplastic elastomers from BASF [21] were selected for the injection molding tests. Their mechanical properties are listed in Table 2.1 [22].

Property	Unit	Test method	value for 35A	value for 45A
Hardness	Shore A	DIN 53505	37	46
Density	g/cm^3	DIN EN ISO 1183-1-A	1,18	1,18
Tensile strength	MPa	DIN 53504-S2	12	34
Elongation at break	%	DIN 53504-S2	1150	950
tear strength	N/mm	DIN ISO 34-1Bb	27	42
Abrasion loss	mm^3	DIN ISO 4649-A	165	39

Table 2.1: Elastollan Soft 35A and 45A material properties.

Elastollan Soft 35A and 45A are thermoplastic polyester-polyurethane materials with excellent mechanical properties and wear resistance. More information on elastollan TPU material properties is found in the technical information brochure [23]. Compared to the Sylgard 186 PDMS, which has a shore A hardness of 24 [24], the elastollan materials are a bit harder but were found soft enough for stretchable applications. Their recommended melt temperature for injection molding is 205°C, with a mold temperature of ca. 20 to 50°C [25].

The injection molding was tested on an ENGEL victory 50 press, having a clamping force of 500kN [26]. The test substrates had an LED array with 16 LEDs and 4 resistors (0603 SMD package). More information on the design is found in Section 6.1. Test substrates were made as described in the section on substrate fabrication (Section 2.3.1), but without the PI support. Figure 2.22(a) shows how the substrates were attached with double sided tape to the mold on the movable plate of the injection molding machine. Figure 2.22(b) shows the hopper and a part of the barrel of the machine.

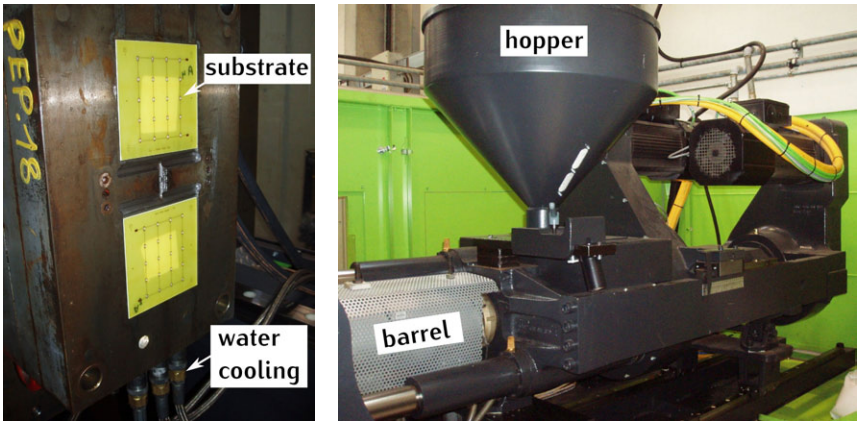

(a) Substrates attached to mold. (b) Barrel and hopper of the machine.

Figure 2.22: Thermoplastic injection molding tests on an ENGEL victory 50 press.

Both Elastollan materials were injected at a temperature of 200°C with a pressure of 577 bar into a cold mold (20°C). The used mold was not designed specially for this test, but was an existing mold available at PEP, well suited for our test. Figure 2.23 shows the substrate after injection molding.

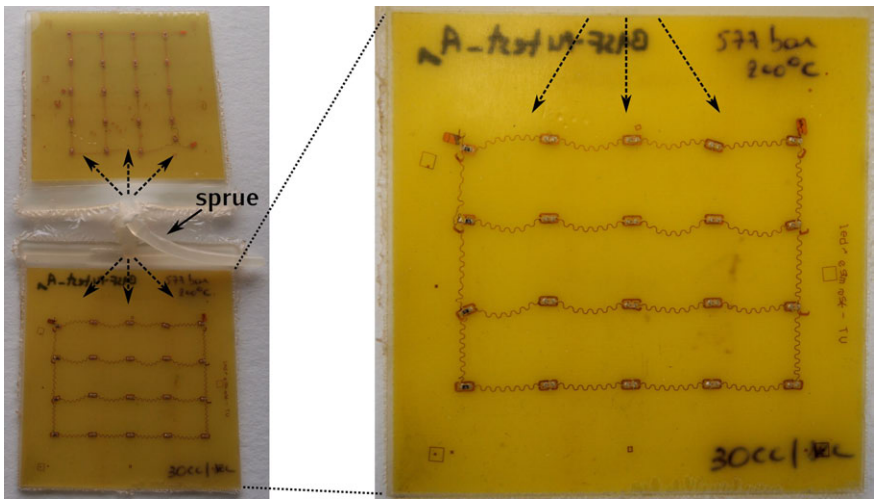

Figure 2.23: Test substrate over molded with Elastollan 35 A (200°C, 577 bar).

It was hoped that the molten material would cool down fast enough to avoid melting of the wax. From the picture it is clear this was not the case. The position where the material was injected can be recognized by the sprue.

The sprue is the passage through which a molten material is injected into the mold, refers also to the excess material which solidifies in the sprue passage. One can see that the meander positions were shifted in the direction of the injected material (indicated by the dashed arrows). In order to overcome this problem, trials at lower melt temperatures and injection pressures were performed. These parameters were lowered as low as possible to 180°C and 164 bar, but even with these test conditions the tracks shifted. Therefore we could conclude that it was possible to do thermoplastic injection molding on an industrial machine, but another temporary adhesive should be found. A good wax replacement candidate was found during this PhD while doing research on encapsulation by lamination of TPU. These developments are explained in Section 2.4.2. At the time of writing new injection molding tests are planned using this other temporary adhesive that can withstand higher temperatures.

2.4.2 Lamination

A different encapsulation method developed during this PhD is the encapsulation of the stretchable circuit by lamination of a thermoplastic elastomer. This method was developed to obtain a technology that allows encapsulation of large and thin stretchable modules or multiple smaller modules processed on large carrier panels. A typical panel size used in PCB manufacturing is 18x24 inch (45x60cm). It is expected that laminating a thin sheet onto a large stretchable circuit is an easier process compared to encapsulating the same circuit by injection molding. Figure 2.24 illustrates this encapsulation process.

In step one the upper part of the stretchable circuit is encapsulated by laminating a thermoplastic material on top. First the material is melted by increasing the heat in the lamination press. Next, pressure is applied onto the top plate, which has a 3D shape that will define the module profile. Once the material is cooled down, the top part is encapsulated and the temporary rigid carrier is removed in step two. In step three we repeat the lamination of step one to laminate a sheet of thermoplastic material at the back. The stretchable circuit is now completely embedded in the thermoplastic material. In step four the module is punched out of the laminated stack. This punching step can also be used to create openings in the stretchable module to increase the breathability and to decrease the module weight.

The implementation of this process looks straight forward because of the aimed simplicity. However one aspect introducing some difficulties is the presence of the temporary adhesive. In Section 2.3 we discussed the substrate fabrication part. This process uses wax as a temporary adhesive and was used as a starting point for this work on stretchable electronics for textiles. By making use of this process some positive and negative properties of wax were observed and are listed in Table 2.2.

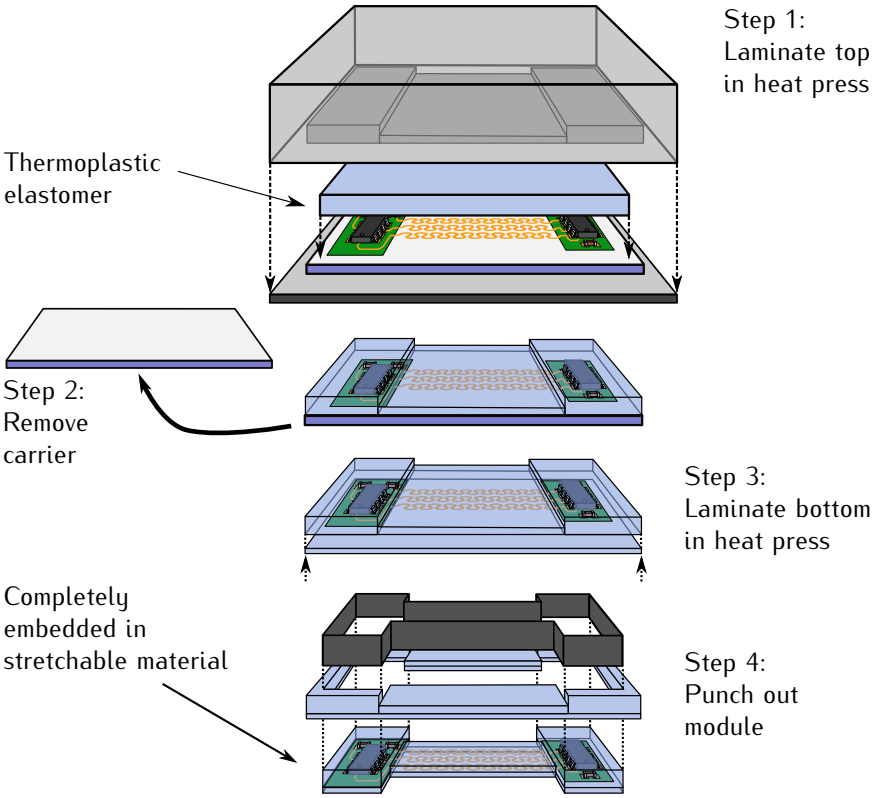

Figure 2.24: Encapsulating the electronics in a thermoplastic material by lamination.

Positive	Negative
does not stick in solid state	wax solution needs to be prepared (dilution in acetone)
removable with acetone	application by doctor blading is not straight forward
does not burn during reflow	structures are floating on the wax during reflow
resistant against development, etching and stripping chemicals	molding temperature limited to ~ 60°C
	> 90°C needed to melt wax for removing rigid carrier (can lead to PMMA mould damage)
	substrate needs to be cleaned with acetone before encapsulating the back

Table 2.2: Positive and negative properties of the Quickstick 135 wax as a temporary adhesive in the SMI technology.

The wax is well suited for the substrate fabrication part because it resists the different process steps. The main disadvantages are temperature related. Indeed the wax starts to soften around 70°C, which requires lowering of the temperature during some process steps. During reflow soldering at 260°C the wax melts completely, but does not burn. The stretchable circuit structures float onto the wax during soldering. In some cases this can cause a shift in structure positions. When a thermoplastic material is used as an encapsulation, it is not possible to use the wax as a temporary adhesive. Thermoplastic materials are applied after they are melted at an elevated temperature. If this temperature is higher than ~ 70°C, the wax starts to melt and loses its adhesion force. The picture in Figure 2.25 shows a test-sample with wax adhesive where a transparent thermoplastic polyurethane sheet (TPU, Krystalflex PE 429) was laminated on top at 90°C.

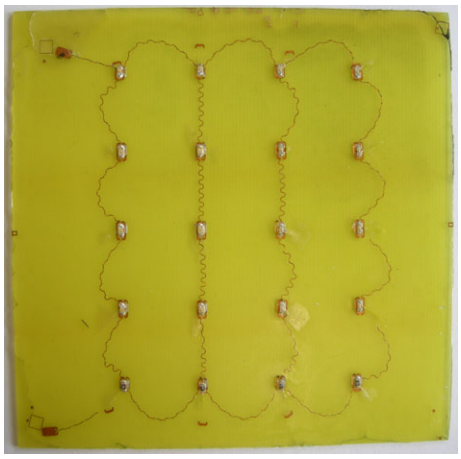

Figure 2.25: TPU lamination onto a carrier with wax adhesive.

The copper structures were floating on the heated wax and were pushed away from the center by the molten TPU during lamination. This problem was also mentioned in the case when a stretchable circuit was encapsulated in a thermoplastic material, using liquid injection molding (paragraph on industrial injection molding in Section 2.4.1). Another problem was the removal of the carrier. This was not possible without deforming the module, because the TPU starts to melt when the wax is heated up to ~ 135°C. The idea was to replace the wax with a pressure sensitive adhesive tape to overcome these problems. However the tape must meet the following conditions:

- It should be resistant against development, etching and stripping chemicals.
- The stretchable circuit should adhere to it during the whole process.

- It should be resistant to lead-free solder reflow temperatures (up to 260°C).
- The encapsulant may not adhere to the tape so that the module can be released by peeling it from the tape.

Taconic TacSil tape

The TacSil tape from Taconic was selected as a good candidate to replace the wax [27]. This tape is normally used as a carrier tape for lead-free assembly of FCBs. The build up of the tape is illustrated in Figure 2.26 and a properties overview is listed below.

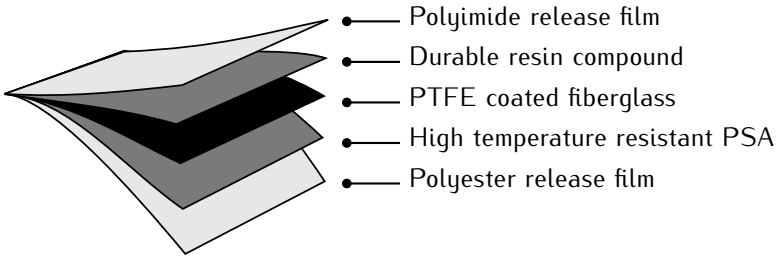

Figure 2.26: TacSil tape build up.

- PTFE (Polytetrafluoroethylene) impregnated fiberglass is used as a substrate, reinforcing materials. It offers highly credible dimensional stability at high temperatures, up to 260°C.
- The side of TacSil that is to be attached to the carrier plate is composed of a silicone adhesive specially modified for continuous use in FCB applications that leaves no adhesive residues at most lead-free surface-mount technology (SMT) temperatures.
- The other side, to be attached on a FCB, is composed of well-balanced silicone compound to maintain adhesion properties during the repeating usage. TacSil tape can be used in over 500 cycles at a normal SMT process.
- A PET (Polyethylene terephthalate) and PI film liner on both sides protects and maintains performance without any contamination and makes die-cutting easier.
- TacSil tape is available in different adhesion levels.

Due to the fact that the tape is composed of a silicone adhesive it was expected that a TPU encapsulant would not adhere to the tape. This was confirmed by laminating a Krystalflex PE 429 TPU sheet onto the tape. The laminated sheet could be peeled off without any problem.

Fabrication examples using the TacSil tape as a temporary carrier.

The same process steps as presented in the two substrate fabrication methods in Section 2.3 apply when using the TacSil tape as a wax replacement (processes are illustrated in Figures 2.6 and 2.8). But now instead of preparing a wax solution and applying it by doctor blading, the TacSil tape is roll laminated onto the temporary carrier. The copper foil with the PI support, or the FCB in the laser structuring method are attached onto the tape by roll lamination. In the case of the wax, this step was done using a heat press. The next steps, which are typical PCB steps, remain the same. But now there is no need to lower process temperatures as was the case when using the wax. An example of a test sample after etching is shown in Figure 2.27.

An 18μm BF-TZA copperfoil [28] was laminated onto a 1.2mm rigid FR4 carrier with TacSil F20 HB tape. A Riston FX 920 dry film photoresist [29] was roll laminated onto the copper and was illuminated with an etch test pattern. The result after photoresist development and spray etching was very satisfying. As can be seen in Figure 2.27, even the thinnest 30μm tracks are still adhered to the TacSil tape. Note the grid pattern visible over the whole substrate, this is the fibreglass present in the tape.

Another example of a test sample is given in Figure 2.28. The test mask had dots with different diameters (1mm, 500μm, 250μm, 125μm and 62.5 μm). Figure 2.28(b) shows a detail of 125μm and 62.5μm dots after etching and stripping. Only some of the smallest 62.5μm dots were released at some positions. The test samples with dots were used to evaluate the TPU lamination.

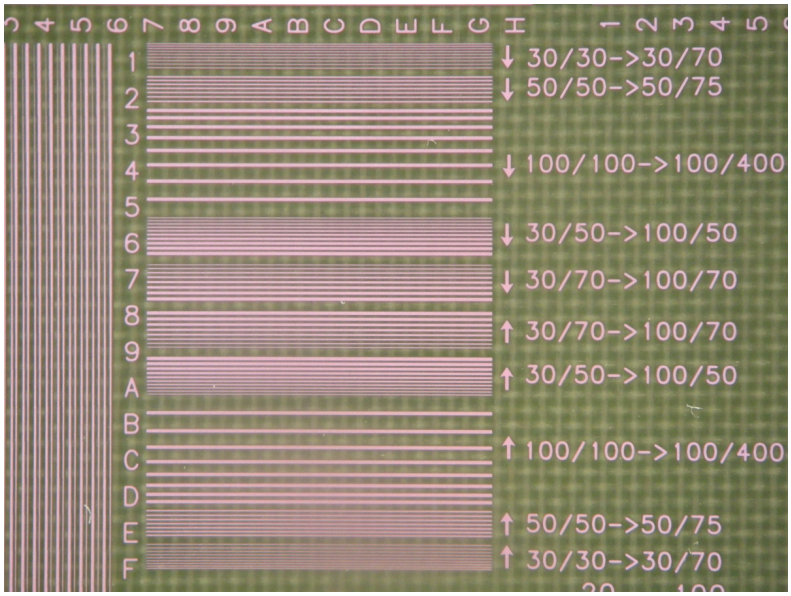

Figure 2.27: Test sample with different track widths and spacings, processed on a carrier with TacSil, after etching.

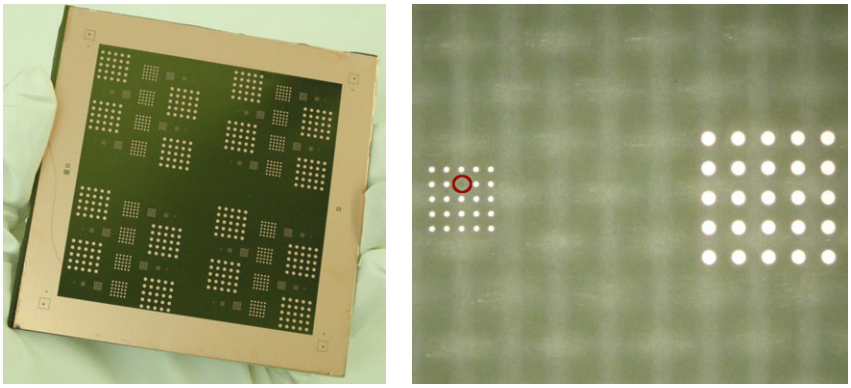

(a) 10cm x 10cm test sample after photoresist stripping.

(b) Detail of 125μ and 62.5μ dots.

Figure 2.28: 10cm x 10cm test sample, containing dots with diameters ranging from 1mm to 62.5μ*m*

A Krystalflex PE 429 TPU sheet was laminated at 110°C onto the samples. Figure 2.29(a) shows one of the laminated samples. The same lamination step was also performed on test samples with wax adhesive and one of these samples is shown in Figure 2.29(b). On the TacSil samples the dots remained in position. This was checked by placing the illumination mask on top of the sample. In the picture of Figure 2.29(c) the mask was slightly moved out of position to show the underlying copper dots. The dots on the wax samples had moved as expected. After lamination, the TPU encapsulated top part was peeled from the carrier at room temperature (see Figure 2.30). This was easy because of the low adhesion between the TPU sheet and the TacSil tape. Compared to the carrier removal in the case of wax adhesive, this step improved a lot. No elevated temperature was needed, no acetone cleaning was needed and the carriers with TacSil could be reused.

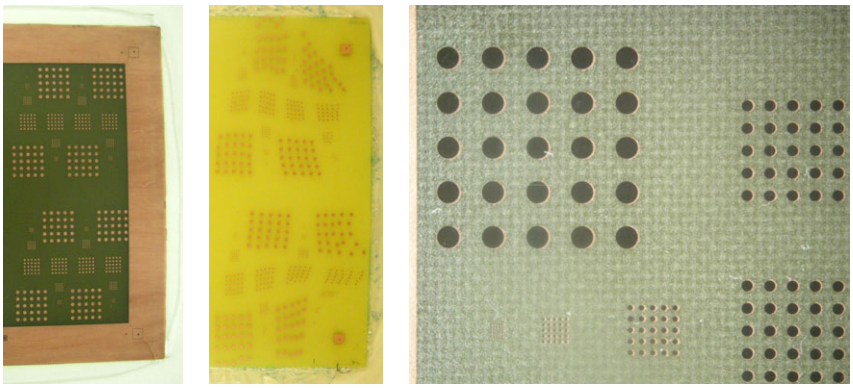

(a) TacSil adhesive (b) Wax adhesive (c) Mask on top of the TPU laminated sample

Figure 2.29: Test sample after TPU lamination.

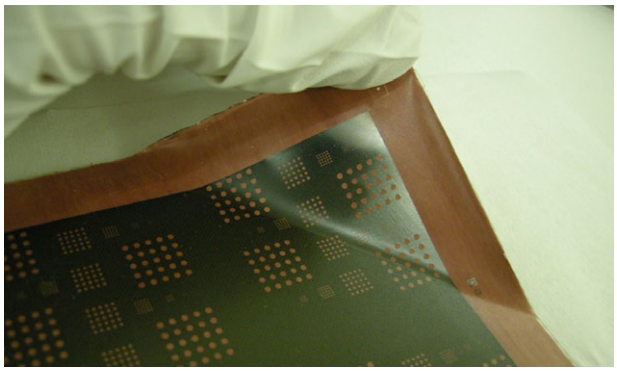

Figure 2.30: Peeling the TPU encapsulated sample from the temporary carrier.

Once the process was proved to be ok, a test design containing SMD components interconnected with meander tracks was designed (see Section 6.1 for info on the design). The sample in Figure 2.31 was made using the laser structuring method (see Section 2.3.2), with the TacSil tape as the adhesive. Note that the contact pads have a Ni/Au finish. In the case of wax adhesive it is not possible to do a Ni/Au plating because the wax starts to soften at the elevated temperatures used during the process. Lead free solder paste is manually dispensed onto the contact pads, followed by manual placement of the SMD components. Vapour phase reflow soldering with a maximum temperature of 260°C is used to solder the SMD components. No shifts in the functional islands or meander positions were observed.

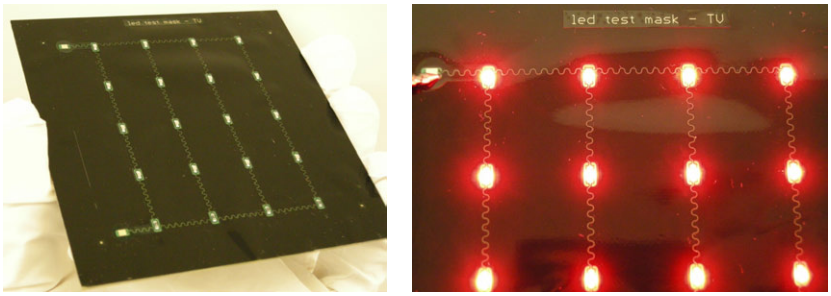

(a) Test sample with LEDs after soldering (b) Functionality check

Figure 2.31: SMD reflow soldering, using a TacSil tape carrier board.

After the assembly a Krystalflex PE 429 TPU sheet was laminated at 110°C. A 3D machined aluminum top plate was used during lamination. Figure 2.32(a)) shows the aluminum plates used in the lamination stack.

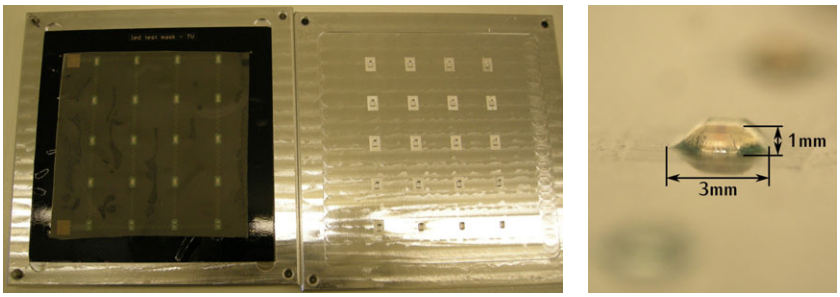

(a) 3d shaped aluminum top plate (b) Dome shape

Figure 2.32: TPU lamination onto the stretchable circuit.

It was important to achieve good alignment between the top plate with the 3D cavities for the SMD components and the assembled stretchable circuit. Therefore the alignment of the illumination mask for the copper structures was done on the outlines of the 10cm x 10cm carrier board. This plate, in turn, fitted in an opening in the lower aluminum plate. By means of registration pins, the top plate was aligned with the lower plate. Prior to lamination Poly 90 mold release form Jacobson chemicals [30] was used onto the aluminum plates to prevent the TPU from sticking. A detail of the dome shape above the SMD components after lamination is shown in Figure 2.32(b).

In Figure 2.33 the result after the punching step is visible. The punching was done using a steel rule die that was designed for this test sample. More info on steel rule die punching is described in Section 5.4.5.2, where it was used to punch FR4 stiffeners. This stretchable module was at a later stage integrated onto textile (see Section 3.3).

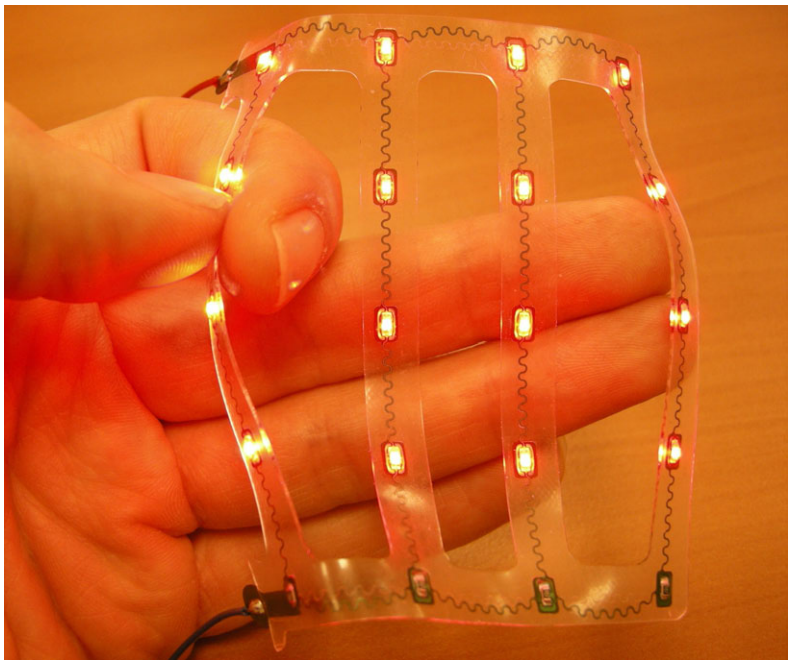

Figure 2.33: TPU encapsulated LED array after punching.

2.4.3 Adhesion between stretchable circuit and encapsulation.

An aspect we did not cover yet is the adhesion between the stretchable circuit and the encapsulation. It is important to have a good adhesion to prevent delamination of the encapsulant during product life. Adhesion was tested in accordance with the ASTM D413 standard [31]. ASTM D413 determines the adhesion strength required to separate a rubber layer from a flexible substrate such as a fabric, fiber, or sheet metal. In an adhesion test, a layer is stripped off a test specimen using an applied tensile force - this results in tearing at the bonded surfaces. The value of interest is the Adhesion Strength - defined as the average force divided by the width of the specimen. The tests were done using 180° peel test samples (Type A). The sample build up is given in Figure 2.34(a). Every peel test was done using samples with a width W of 1cm. PDMS injection molded test samples had a thickness T of 1mm. In the case of a laminated TPU encapsulation the thickness depended on the sheet thickness of the TPU and the lamination parameters. Figure 2.34(b) shows a 180° peel sample under test.

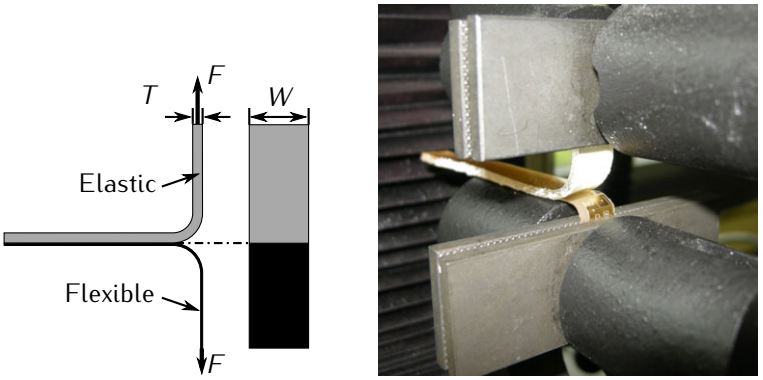

(a) Sample build up (b) Sample under test

Figure 2.34: 180° peel tests to evaluate adhesion of the encapsulation.

Sylgard 186 adhesion

A first set of peel tests was done to test the adhesion between Sylgard 186 (a PDMS) and the different materials it interfaces in the SMI technology. All test samples were produced in the same way a stretchable module would be produced (Upisel-N SE 1220 foil was used [32]). To obtain a good adhesion between the PDMS and other materials it was necessary to apply a primer prior to encapsulation. 1200 OS primer [33] from Dow Corning was used. This primer improves the adhesion and accelerates adhesion build-up of silicone

to various substrates. In Table 2.3 an overview is given of the different test samples together with the average force needed to peel the 1cm wide strips apart. In Figure 2.35 the graph for the Sylgard 186 adhesion to copper, with and without the 1200 OS primer, is given as an example. Without primer the adhesion to copper was limited and peeling started at a force of about 1N. Good adhesion was obtained with the primer and the PDMS strips in the samples broke instead of peeling apart. Graphs of the other peel tests are given in Appendix B. Also for these other materials a good adhesion was obtained with Sylgard 186 when using the primer. Without the primer there was little or no adhesion.

Material interface	primer use	Average peel force
Sylgard 186 - copper	no	1.1N
	yes	PDMS strip breaks
Sylgard 186 - polyimide	no	0.01N
	yes	PDMS strip breaks
Sylgard 186 - soldermask	no	0.3N
	yes	PDMS strip breaks
Sylgard 186 - Sylgard 186	no	2.2N - 2.8N
	yes	PDMS strip breaks

Table 2.3: PDMS peeltest sample overview (1cm wide strips, 1mm PDMS thickness).

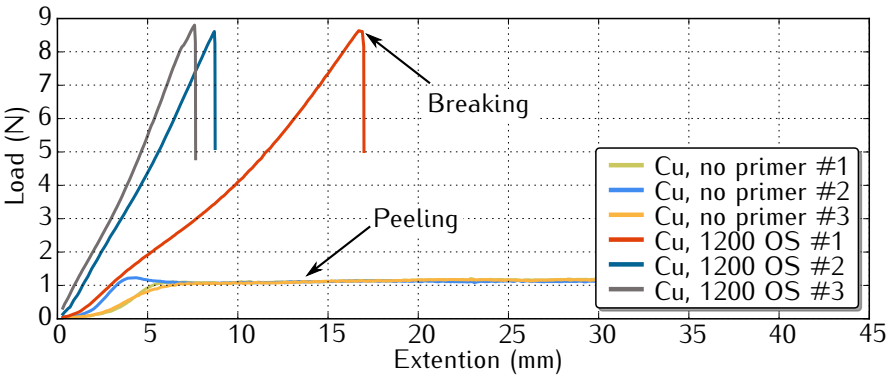

Figure 2.35: Sylgard 186 - Copper adhesion results, with and without 1200 OS primer.

Krystalflex 429 adhesion

Similar peel tests were done on test samples having a thermoplastic encapsulant applied by lamination. Different TPU materials were tested and it is not the intention to report them all. As an example the results of Krystalflex 429 are discussed. The TPU material was laminated at different temperatures onto a FCB (Upisel-N SE 1220 foil was used), to test the adhesion with copper, PI and soldermask. Table 2.4 gives an overview of the test results. For all tested lamination temperatures, there was little or no adhesion between the 429 and copper. Higher peel strengths were observed between the 429 and PI with or without solder mask. For both materials, there was better adhesion with increasing temperature. In the case of lamination at 170°C onto the solder mask, the TPU strips snapped before they could delaminate. The tests proved that sufficient adhesion could be obtained with the Krystalflex 429 TPU material as an encapsulant. The fact that no adhesion was obtained with the copper is not a problem because this situation does not occur in the material stack of the stretchable modules (the copper features are covered with solder mask).

Lamination temperature	Material interface	peak load	average load
110°C	429 - copper	0.1N	0.1N
	429 - polyimide	5.5N	3.3N
	429 - soldermask	4.3N	1.3N
130°C	429 - copper	0.1N	0.1N
	429 - polyimide	8.0N	5.7N
	429 - soldermask	6.7N	2.7N
150°C	429 - copper	0.1N	0.1N
	429 - polyimide	7.7N	6.6N
	429 - soldermask	22.8N	10.6N
170°C	429 - copper	0.1N	0.1N
	429 - polyimide	10.1N	9.3N
	429 - soldermask	31.6N	sample broken

Table 2.4: Krystalflex 429 peeltest sample overview (1cm strips, average over 3 strips).

In Figure 2.36 the graph of the Krystalflex 429 laminated at different temperatures onto PI, is given as an example. Graphs of the other peel tests are given in appendix B.

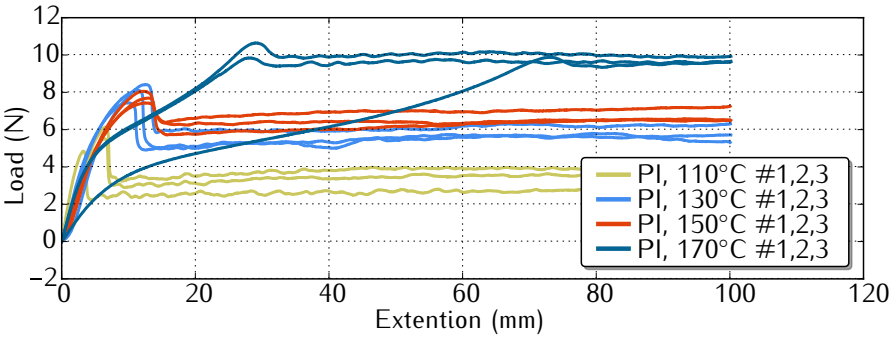

Figure 2.36: Krystalflex 429 TPU - PI adhesion results for TPU laminated at different temperatures.

2.5 Conclusions

Different stretchable technology developments to fabricate stretchable modules for textile integration were presented in this chapter. It was described how an electronic circuit is subdivided in several non-stretchable functional islands and how stretchability is obtained by interconnecting them with meanders. A simple thirteen-step implementation process is proposed, which can be used to gradually come to a well designed demonstrator or product. To simplify layouting of the meanders, a meander design tool for the EAGLE PCB software has been developed.

The stretchable module production was subdivided into a substrate fabrication part and an encapsulation part. Two different SMI substrate fabrication methods were described. The fist one used a photo definable PI as an island and meander support layer. This substrate fabrication method proved unsuitable for our purpose. The PI support was too fragile and brittle, leading to bad reliability of the stretchable module. The second fabrication method was developed to overcome this reliability problem, by producing the substrate in another way. Starting from a standard FCB, the meanders and PI islands were structured in one step by laser cutting. Most of the test samples and demonstrators realized during this PhD were made by use of this laser structuring method. Additionally we discussed some possibilities to industrialize the process.

Next to the substrate fabrication methods, the developments of two encapsulation methods were discussed; encapsulation by injection molding and by lamination. In a first phase, the injection molding of PDMS using PMMA molds was investigated. This technique was successfully used to encapsulate different test samples and demonstrators. The importance of openings in the encapsulation for breathability and contact access was addressed and it was shown how this was accomplished. Later on, also first thermoplastic injection molding tests were performed on industrial equipment. A different encapsulation method developed during this PhD was the encapsulation of stretchable circuits by lamination of a thermoplastic elastomer. Since the normally used temporary wax adhesive layer melts during lamination, the wax was not suitable for this process. Therefore, it was replaced with a pressure sensitive adhesive tape.

The last topic described the adhesion between the stretchable circuit and the encapsulation. Examples of peel test results for PDMS and TPU encapsulations were given. In case of Sylgard 186 (PDMS) encapsulation, good adhesion onto copper, PI and solder mask was obtained using a dedicated primer. For Krystalflex 429 (TPU) there was only good adhesion on PI and solder mask. Here, the lamination temperature played an important role. On copper there was no or little adhesion, but this is not considered as a problem, because this situation does not occur in the material stack of the stretchable modules (the copper features are covered with solder mask).

References

[1] (2012) The STELLA project website. [Online]. Available: http://www.stella-project.de/

[2] J. Fjelstad, *Flexible Circuit Technology*, 4th ed. BR Publishing, 2011.

[3] Institute for Interconnecting and Packaging Electronic Circuits. IPC. Bannockburn,Illinois,U.S.A. [Online]. Available: http://www.ipc.org/

[4] (1992) Guidelines for Accelerated Reliability Testing of Surface Mount Attachments. IPC. Bannockburn,Illinois,U.S.A. [Online]. Available: http://www.ipc.org/TOC/IPC-SM-785.pdf

[5] C. Coombs, *Printed circuits handbook*, 6th ed., ser. McGraw-Hill handbooks. McGraw-Hill, 2008.

[6] (2012) CadSoft's EAGLE PCB Design Software. CadSoft. [Online]. Available: http://www.cadsoftusa.com

[7] T. Loher, M. Seckel, and A. Ostmann, "Stretchable electronics manufacturing and application," in *3rd Electronic System-Integration Technology Conference (ESTC)*, Sept 2010.

[8] F. Bossuyt, *Novel Technologies for Elastic Microsystems: Development, Characterisation and Applications. PhD thesis*. Ghent University, 2011.

[9] (2012) Optec laser micromachining systems. Website. [Online]. Available: http://www.optec.be/

[10] (2012) LPKF MicroLine 6000 P. LPKF. [Online]. Available: http://www.lpkf.com/products/pcb-processing/microline-6000p.htm

[11] (2012) Vinyl Banner Making: Step by Step. Banners On Time. [Online]. Available: http://bannersontime.com/banner-making/04-vinyl-step-by-step.htm

[12] (2012) Vinyl Sign and Lettering Tutorial. TrixiePixGraphics.Com. [Online]. Available: http://www.trixiepixgraphics.com/vinyl_signs/vinyl_sign_tutorial.html

[13] (September 7, 2010) Weed Heat Transfer Vinyl Faster. Stahls' ID Direct. [Online]. Available: http://www.stahlsblog.com/weeding-vinyl-designs-faster-save-time-and-money-with-this-tip-jar/

[14] (2012) EasySIGN software. NCD Holding B.V. Hapert, Netherlands. [Online]. Available: http://www.easysign.com/mainwebv1/prdstarter.aspx

[15] "Technical datasheet - Quickstick MWH135 Mouting Wax." South Bay technologies.

[16] (2012) Sylgard 186 silicone elastomer kit. Dow Corning. [Online]. Available: http://www.dowcorning.com/applications/search/default.aspx?R=118EN

[17] (2012) Technical brocure - Altuglas. Altuglas International. [Online]. Available: http://www.altuglas.com/literature/pdf/124.pdf

[18] (2012) PEP website. Pôle Européen de Plasturgie. [Online]. Available: www.poleplasturgie.net

[19] (2012) The PASTA project website. [Online]. Available: http://www.pasta-project.eu/

[20] (2012) Plastic Injection Molding Basics. Beechmont Crest Publishing. [Online]. Available: http://www.beechmontcrest.com/plastic_injection_molding_1.htm

[21] (2012) BASF Polyurethanes Europe - Corporate website. BASF. [Online]. Available: http://www.polyurethanes.basf.de/pu/solutions/en/

[22] "Elastollan Soft 35A and 45A general product information," BASF - PU Solutions Elastogran., September 2010.

[23] (november 2011) Elastollan Material Properties - Technical information. BASF. [Online]. Available: http://www.polyurethanes.basf.de/pu/solutions/elastollan/en/function/conversions:/publish/content/group/Arbeitsgebiete_und_Produkte/Thermoplastische_Spezialelastomere/Infomaterial/elastollan_material_uk.pdf

[24] "Sylgard 186 silicone elastomer - product information," Dow Corning.

[25] "Elastollan Soft 35A and 45A processing recommendations," BASF - PU Solutions Elastogran., September 2010.

[26] (2010) Brocure ENGEL victory. ENGEL. [Online]. Available: http://www.engelglobal.com/engel_web/global/en/media/victory_en_2010.pdf

[27] (2012) TacSil - Carrier Tape for FPC Assembly. Taconic. [Online]. Available: http://www.taconic-add.com/en--products--tacsil--1.phpf

[28] (2011) BF-TZA copper foil. Data sheet. Circuit Foil. [Online]. Available: http://www.circuitfoil.com/download5.php?file=1451090214-_BF-TZA.pdf

[29] (2007) Riston FX 920 - High Performance Multi-Purpose Resist Photopolymer Film for Ultar Fine Line Applications. Data sheet and processing information. DuPont Electronic Technologies. [Online]. Available: http://www2.dupont.com/Imaging_Materials/en_US/assets/downloads/datasheets/fx900series.pdf

[30] (2003) Poly 90 Moulding release -datasheet. Jacobson Chemicals. [Online]. Available: http://www.jacobsonchemicals.co.uk/pdfs/Poly_90.pdf

[31] (2007) ASTM Standard D413, 1998 (2007), Standard Test Methods for Rubber Property - Adhesion to Flexible Substrate. ASTM International. West Conshohocken, PA. [Online]. Available: http://www.astm.org

[32] (2009) Polymide Base Copper Clad Laminate (Adhesiveless) - UPISEL-N. UBEl. Madison Avenue, New York. [Online]. Available: http://www.ube.com/content.php?pageid=82

[33] (2012) Dow Corning 1200 OS primer. Dow Corning. [Online]. Available: http://www.dowcorning.com/applications/search/default.aspx?R=8959EN

3

Integration of stretchable electronics in textiles

3.1 Introduction

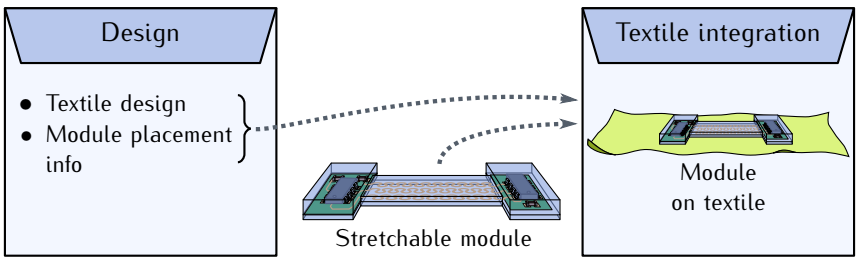

Figure 3.1: Chapter overview.

In Chapter 2 we described how the stretchable modules for textile integration were produced. The next step in our process to realize textile products which contain stretchable electronics is the textile integration. If we remember the technology toolbox (Figure 1.3), this is the point where we leave the *electronics world* and enter the *world of textiles*. The goal is to fit our stretchable modules in existing or newly designed textile products, to create a product with added value because it contains the integrated electronics. One of the questions is where to put these modules? Therefore, already during textile design, decisions need to be made on the location of the stretchable modules

in the textile product. To facilitate industrialization of the processes in a later stage, the target was to develop integration methods that are easy to adopt in the manufacturing of finished textile products like clothing, furniture, carpets, curtains, car seats,... Two different encapsulation material types were used in the SMI technology to produce the stretchable modules; thermosetting materials (e.g. PDMS) and thermoplastic materials (e.g. TPU). This has lead to two different integration methods which will be discussed in section 3.2 and 3.3. In section 3.4 the reliability of the textile integration is described. We will check the adhesion of the modules to the textile and their resistance to washing. By introducing a stretchable module we may change the properties of the textile product. In section 3.5 we take a brief look at the impact of the electronic module integration on the overall look and feel of a textile product.

3.2 PDMS adhesive layer screen printed on textile.

The selection of a technique to attach a stretchable electronic module to a textile depends on the encapsulation material of the module. In the case of a thermosetting material like PDMS, it is not possible to remelt the material in order to bond it to the textile. Instead a kind of (stretchable) glue layer is needed between the stretchable module and the textile. This was accomplished by screen printing a PDMS layer onto the textile. Screen printing is a well known process in the textile industry where it is especially used to print color patterns onto fabrics. Figure 3.2 illustrates how the screen printing technique was used in the textile integration process for PDMS encapsulated stretchable electronic modules.

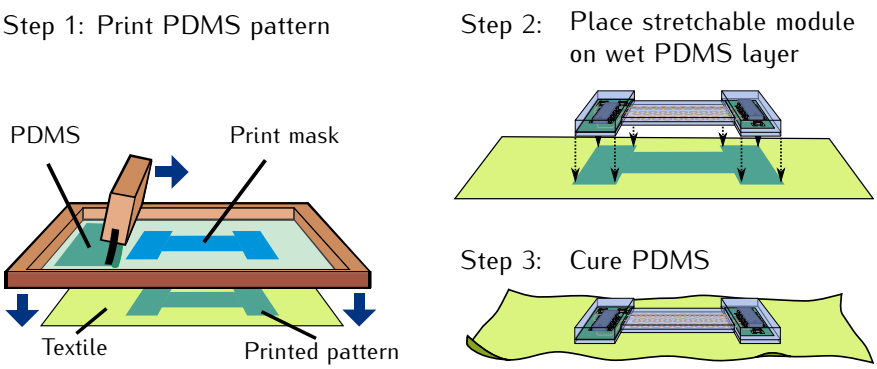

Figure 3.2: Textile bonding by screen printing PDMS.

A thin PDMS layer with a thickness of about 50μm was screen printed onto the textile. Screen printing allowed patterning such that only the spots where the electronic modules were placed, were coated. The printed PDMS layer acted as an adhesive layer between the modules and the textile. After printing, the module was manually positioned with slight pressure on the wet printed PDMS layer. Next, the PDMS was cured, which resulted in a bonding between the textile substrate and the stretchable electronic modules.

To obtain sufficient bonding between the textile and stretchable module there is the need for a thin layer of PDMS on top of the fabric. It is preferred to limit PDMS penetration through the textile because this influences (negatively) the typical textile properties like feel and wearability. This is mainly due to reduction of stretchability, because PDMS that has penetrated too deeply clogs the gaps between normally free moving textile fibers. Different parameters can influence the penetration depth. The key influence is the type of PDMS used for printing, i.e. its viscosity. A higher viscosity will result in less penetration into the fabric. Screen printing tests were performed in collaboration with Centexbel, a Belgian Textile Research Centre [1]. For performing the screen printing tests a Johannes Zimmer (mini MDI 482) apparatus was used [2]. The parameters used for optimizing the screen printing process were: the mesh properties (thickness, opening size and density), bar type (thickness, surface structure), magnetic force on the bar and velocity of the bar as it moves over the screen. After some initial trials, a mesh with 68 lines/cm and a furrowed bar of 18mm diameter was chosen as this resulted in the easiest processing. Different commercially available PDMS materials from Dow Corning were selected for screen printing: Sylgard 184, Sylgard 186 and Textile Printing Inks 9600 and 9601. Sylgard 184 and 186 were selected because these materials were also used for encapsulating the stretchable modules. The 9600 and 9601 Textile Printing Inks were selected because they are made for screen printing and it was expected that their higher viscosity would result in less penetration through the fabric. The viscosities of the examined PDMS materials are listed in Table 3.1. More detailed information on the products can be found on the suppliers web site [3].

PDMS	Viscosity (cP)
Dow Corning Sylgard 184	4575
Dow Corning Sylgard 186	99700
Dow Corning 9601 Textile printing ink	280000
Dow Corning 9600 Textile printing ink	490000

Table 3.1: Viscosity of the different PDMS materials used in screen print tests.

Sylgard 184 had too low viscosity to perform good screen printing. With Sylgard 186 it was possible to screen print onto a fabric, but it was difficult to obtain a layer on the fabric which had sufficient thickness to bond the stretchable modules. Figure 3.3 shows two cross sections of Sylgard 186 screen printed onto a woven cotton fabric. In this test no stretchable module was attached to the wet printed layer prior to curing. These pictures illustrate also the influence of the curing time onto the penetration depth of the printed layer. When slowly cured at room temperature (was done to show the principle), virtually all PDMS penetrated into the fabric structure because of the longer curing time (Figure 3.3(a)). Curing at an elevated temperature (10 minutes at 100°C, curing time not optimized) resulted in less penetration and a thin layer of PDMS was formed on top of the fabric (Figure 3.3(b)). Nevertheless, this layer was found to be too thin to provide sufficient bonding between the fabric and the modules.

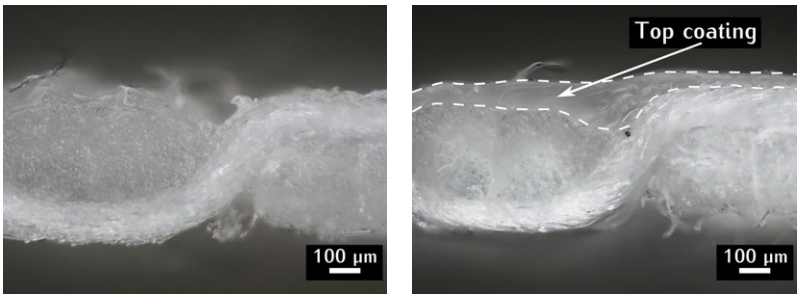

(a) Curing at room temperature. (b) Curing in oven (10min at 100°C)

Figure 3.3: Cross sections of woven cotton fabric coated with PDMS (Sylgard 186)

The 9600 and 9601 Textile Printing Inks, with a higher viscosity, are designed for screen printing color prints onto fabrics. With both materials, good printing results were obtained. During machine set up, the PDMS was printed on a PET (Polyethylene terephthalate) foil instead of on a fabric. Printing on PET foils avoids penetration of the printed layer and was therefore used to check printed layer thickness during set up. The magnetic force and bar velocity were set in order that a cured PDMS layer of around 50μm was obtained. Curing was done in an oven at 100°C for 10 minutes. Besides material viscosity and curing time, also the type of textile substrate had a strong influence on the penetration depth: the higher the density of textile fibers in the fabric, the less penetration of the printed PDMS layer into it. Typically the penetration into the fabric was less for woven fabrics, compared to knitted fabrics. Cross sections of PDMS sheets attached to a fabric with the screen printed textile printing ink are shown in Figure 3.4.

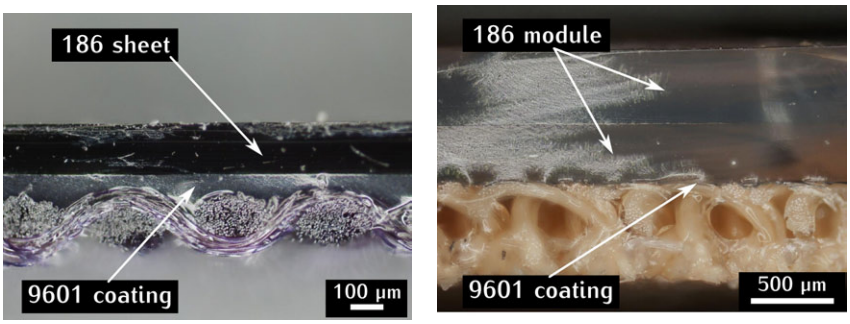

(a) Woven fabric (b) Knitted fabric

Figure 3.4: Cross sections of Sylgard 186 PDMS sheets attached to fabrics by a screen printed PDMS layer of 9601 textile printing ink.

In Figure 3.4(a) the cross section shows a woven fabric, the screen printed 9601 PDMS layer and a Sylgard 186 PDMS sheet on top. The PDMS sheet had a thickness of ca. 200μm, the thin printed layer had an average thickness of roughly 50μm. Note the smoothness of this thin layer on the side that contacts the PDMS sheet. This indicates that there were no or limited air bubbles trapped at the interface, which is important for good adhesion. Figure 3.4(b) shows a knitted fabric. In this case the Sylgard 186 PDMS sheet on top actually consists of two layers that form together the encapsulation of the stretchable electronic module. The thin screen printed layer is hardly visible because it penetrated deeper into the knitted fabric, but still provided sufficient adhesion between the knitted fabric and the PDMS module. The difference in penetration can be understood from the surface structure of the woven and knitted fabrics (see Figure 3.5): the yarns of a woven fabric typically form a tight alignment whereas the yarns of a knitted fabric typically show a more open structure (which is also represented by the voids seen in the cross section of the knitted fabric in Figure 3.4(b)). Hence, the penetration of the PDMS into the fabric is stronger. This effect becomes more pronounced because of the larger thickness (i.e. more penetration capacity) of the knitted fabric.

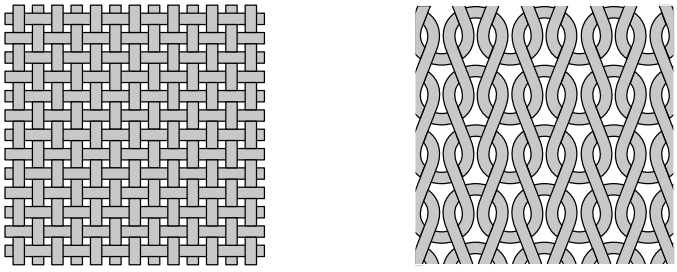

(a) Woven fabric structure (b) Knitted fabric structure

Figure 3.5: Sketches of the surface structure for woven and knitted fabrics.

Based upon the screen printing tests and reliability tests (see section 3.4) the 9601 textile printing ink was selected as the adhesive layer to attach PDMS encapsulated modules to fabrics. The developed screen printing technique was used to attach the different PDMS encapsulated test samples or demonstrators described in this PhD work. Figure 3.6 shows the PDMS encapsulated LED display module attached to a stretchable knitted fabric.

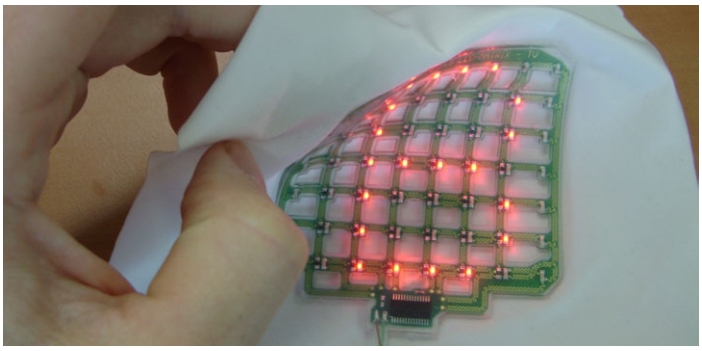

Figure 3.6: 7x8 led display on textile by screen printing a PDMS adhesive layer (9601 textile printing ink).

3.3 Lamination

In case a thermoplastic material like TPU is used as an encapsulation material for the stretchable circuit, it is possible to slightly remelt the material in order to laminate it to a fabric. Figure 3.7 illustrates the principle used.

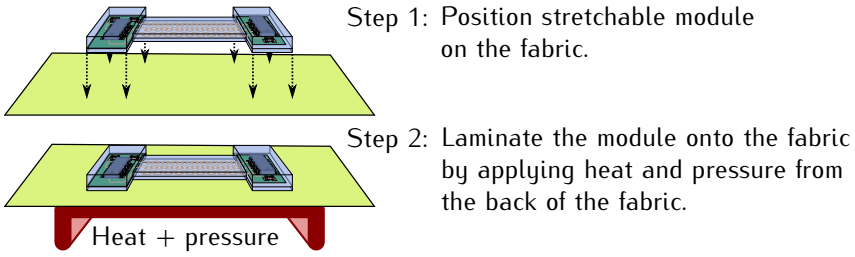

Figure 3.7: Textile bonding by lamination.

A completely encapsulated TPU module is positioned onto the fabric. By 'completely' we mean that the stretchable circuitry is surrounded by a top and bottom encapsulation, using the encapsulation method based on lamination as was presented in section 2.4.2. After positioning, the module is bonded to the fabric by slightly remelting the TPU of the bottom encapsulation at the

interface with the fabric. Light pressure is used, so the molten TPU layer can penetrate the top layer of the fabric to create the bond. This pressure was comparable with the pressure one applies when ironing. The key is to avoid complete remelting of the encapsulated module. Therefore the heat is only applied from the back for a time short enough to prevent heat transport to the top encapsulation. Dependent on the targeted application and production flow, one can also bond half encapsulated modules to the textile. This principle is illustrated in Figure 3.8.

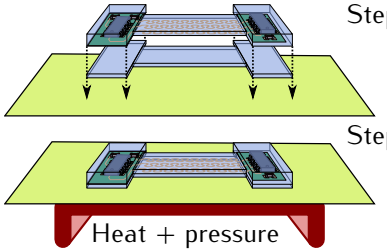

Step 1: Position top encapsulated stretchable module and bottom encapsulation on the fabric.

Step 2: Laminate the module onto the fabric by applying heat and pressure from the back of the fabric.

Figure 3.8: Textile bonding and back encapsulation in one lamination step.

In this case the stretchable module is only encapsulated at the top. To bond the module to the fabric it is aligned with the bottom encapsulation and positioned onto the fabric in step one. In step two the bottom encapsulation melts and bonds with the module and the textile in a single lamination step. Doing so can eliminate one lamination step, namely the bottom encapsulation (step 3) in the process flow that was depicted in Figure 2.24. This methodology was followed to laminate a TPU encapsulated LED array onto a stretchable knitted fabric. A picture of the result is shown in Figure 3.9.

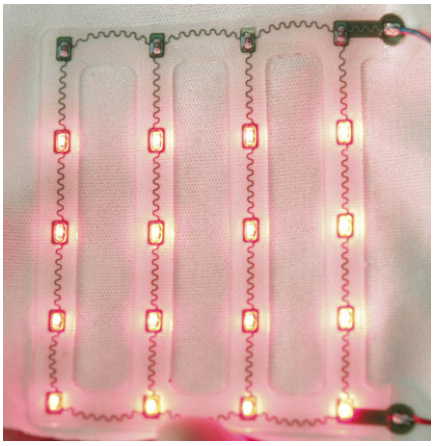

Figure 3.9: TPU encapsulated LED array, laminated onto a knitted fabric.

It is possible that the temperature required to laminate the module to the fabric is too high for the used fabric. In this case a TPU with a lower melting temperature compared to the melting temperature of the encapsulation can be used. Using a TPU which requires lower temperatures for textile lamination can also solve potential deformation of the top encapsulation. This is because lower temperatures reduce eventual softening of the TPU top encapsulation.

3.4 Reliability of the adhesive layer between the fabric and stretchable module.

An important requirement for the developed textile integration methods is their reliability during product life. Once the module is attached to the fabric it should remain attached during use and cleaning (if needed). Therefore the adhesive layer between the fabric and stretchable module should be reliable enough to survive physical deformations during use and cleaning.

When textile cleaning is required, the first step is to test whether the encapsulation is in itself sufficiently resistant against washing. This means that the encapsulation should remain intact during several washing cycles. Next, the module should not delaminate from the fabric. Textile cleaning processes can be harsh and attention should be paid that the encapsulated circuitry does not fail because of mechanical defects introduced during cleaning. This topic will be covered in Chapter 5 - Washability of textile integrated electronics. In this section we only examine the performance of the encapsulation and textile adhesive layer after several washing cycles.

PDMS encapsulation

To test the reliability in the case of a PDMS encapsulation, a module using Sylgard 186 has been attached to a knitted textile substrate, according to the screen printing procedure described in section 3.2. As textile adhesive layer the 9601 textile printing ink was used. The PDMS encapsulates a copper structure as shown in Figure 3.10. To test the adhesion between the PDMS module and the textile, a standard washing method was used: 'Textiles - Domestic washing and drying procedures for textile testing (procedure 5A) - ISO 6330:2000' [4]. More information on this washing method is given in chapter 5 in section 5.2 - Test standards.

Test samples were placed in a protective textile bag during washing. This was done to mimic the real life situation where it would be placed on the inner side of a garment or where the garment would be placed inside out. The samples were dried in open air (no tumble drying). The test sample shown in Figure 3.10(a) has been washed up to 50 times according to the standard

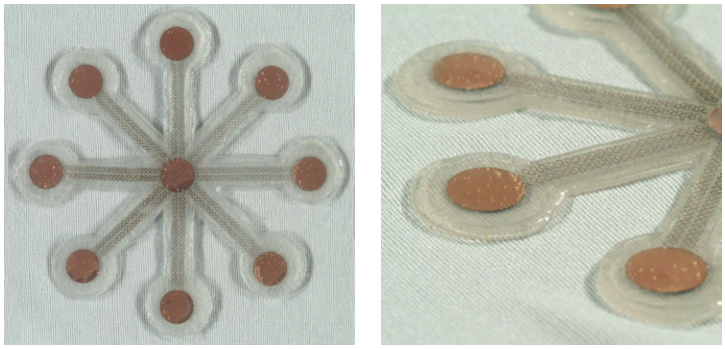

(a) overview (b) detail

Figure 3.10: PDMS test structure on a knitted fabric. The picture in part b was taken after 25 washing cycles. No damage or delamination occurred.

washing procedure. No visual damage of the washing was observed as can also be seen in Figure 3.10(b) (picture taken after 25 cycles). This test and similar ones indicated that the Sylgard 186 encapsulation was very stable. Hence, it appears to be a good choice as encapsulant for the electronics. In all cases the 9601 adhesive layer provided a good bonding between textile and module and no delamination was observed.

TPU encapsulation

The washing test was also repeated to get an indication on the feasibility of laminating a TPU encapsulated module to a fabric in terms of adhesion. Figure 3.11 shows a picture of a dummy module (encapsulation of the LED array depicted in Figure 3.9) before and after 50 washing cycles.

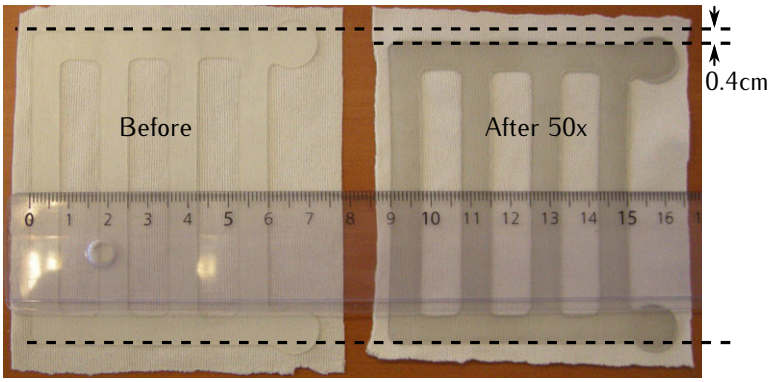

Figure 3.11: Krystalflex PE 429 encapsulated structure on a knitted fabric, before and after 50 washing cycles.

Originally they were placed on larger textiles, but were cut to smaller pieces to take the picture. It appears that this dummy module did not delaminate from the fabric after several washing cycles, indicating that there was sufficient adhesion. However after the 50 washing cycles a little shrinkage of the TPU module feature was observed. As visible in Figure 3.11, this shrinkage was mainly in one direction. New tests should be done to investigate this effect in order to determine the amount of shrinkage of this material after a number of washing cycles. This will eventually lead to the conclusion if this material is suited for applications requiring this type of cleaning process. On the other hand it is also possible that the fabric itself shrinks too much after a certain number of washing cycles. There was also a color change of the TPU after 50 washing cycles as can be seen in the pictures (Figure 3.11).

3.5 Wearability

The integration technologies for electronics in textiles presented in this PhD make use of stretchable electronic modules attached to fabrics. While it is the intention to make these modules as conformable as possible, attaching them to a fabric will always change the fabrics properties to a certain extent. How much the textile properties are allowed to change will depend on the type of application where the modules will be used. For technical textiles measurable properties like water permeability, flexibility, stretchability, drapability and weight can be of importance. While these properties are also important in the case of clothing, the perceptions of the wearer are dominant, making it more challenging to achieve a sufficient level of integration. For wearable computer systems, the term 'wearability' has been defined as the interaction between the human body and the wearable object [5]. Note that a distinction should be made between wearable technology and portable technology. In the case of wearable technology, the device is attached to the body and does not require muscular effort to remain in contact with the body (you do not have to hold it). The device remains also attached to the body while performing different tasks, also when it is not in use. With these criteria, wearable systems differ from portable technologies, such as mobile phones and PDA's, which are designed to be carried [6].

During this PhD, we did not consider all the aspects of wearability in detail. Instead, the focus was on two aspects: simple tensile testing which was performed to check if there was a significant influence of a PDMS sheet on the stretchability and an assessment of the extra add-on weight. Indeed, an important factor in wearability is the fabric thickness and its total weight (expressed in grams per square meter). The cross sections that were shown in Figure 3.10 show clearly that the attachment of the PDMS sheets can

have a large influence on the textile/garment. We can see that the total thickness easily doubles. But, when looking at the weight, the relative impact is even stronger. For a textile substrate, one can take a typical density of 100-200g/m2. For a PDMS sheet of 1.0mm thick and assuming a density of 1.12 g/cm3 (Sylgard 186 density, TPU densities are comparable), we obtain a total weight of 1120g/m2. This means that the patches where the electronic modules are attached can be ca. 10 times as heavy as the textile itself. Hence, it should be clear that such patches can only be added as relatively small areas and at strategic places. In a study by Gimperle et al. the most unobtrusive locations for placement of wearable objects were determined [5]. They are depicted in Figure 3.12.

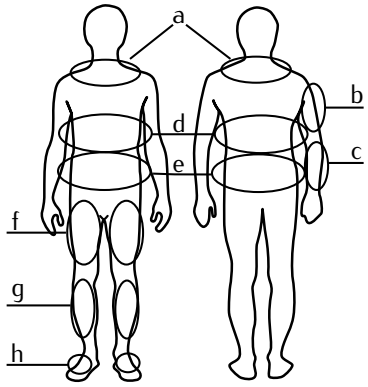

Figure 3.12: The general areas found to be the most unobstructive for wearable objects: (a) collar area, (b) rear of the upper arm, (c) forearm, (d) rear, side, and front ribcage, (e) waist and hips, (f) thigh, (g) shin, and (h) top of the foot.

Because this study was more related to larger and heavier boxed electronics, these same positions could be good candidates to position stretchable modules in case they are found to be too heavy. In order to keep the weight added by the modules to a minimum, the volume of the encapsulation needs to be minimized. This is one of the reasons for focusing on openings in the modules (see Figure 2.16 in section 2.4 on encapsulation). Also the thickness of the encapsulation should be as low as possible. In case the modules can not be made thin enough by injection molding, the developed lamination technique could provide a solution here. Of course also the electrical components will add additional weight to the fabric. Therefore components should be as small as possible and integrated circuits are preferred to reduce the number of components.

Table 3.2 gives some examples of typical module weights that were achieved with the developed technologies.

part	weight [g]
7cm x 8.5cm knitted textile patch	0.7
7cm x 8.5cm woven textile patch	1.4
LED array module (size ~7cm x 8.5cm, design in section 6.1)	2.1
7x8 LED display module (size ~7cm x 7.5cm, , design in section 6.2)	4.3
1 cent Euro coin (diameter 16.25 mm)	2.3

Table 3.2: Examples of typical module weights.

These modules add a weight that is a factor 2 to 5 times higher compared to the weight of the textile area containing them. Nevertheless this added weight can be considered as very low and unnoticeable for the wearer. Especially if you compare it for example to the weight of a 1 cent Euro coin (comparable weight on smaller surface). Feel free to tape a 1 cent Euro coin to your T-shirt to convince yourself that this added weight does not hinder during wearing.

Even though the weight can have an influence on wearability, it is also interesting to look at the stretchability. It is likely that the stretchablility of a fabric will change at the location of a stretchable module. In order to evaluate the influence of the modules on the overall stretchablility, tensile tests were performed on different test pieces. The test pieces had a width of 50mm and a length of 100mm, the effective test length between the clamps was 50mm. For woven fabrics the rate of movement of the clamps was 0.1mm/sec, for knitted fabrics it was 0.5mm/sec. Only the influence of Sylgard 186 PDMS layers with different thicknesses on different types of fabrics was tested. The same tests could be repeated for other stretchable materials on textile. Table 3.3 gives an overview of the fabrics used in the test.

Label	Fabric composition	mass[g/m^2]	Fabric type	producer + quality
K1	lycra (63% polyamide + 37% el)	160	knitted	Liebaert (2)
K2	polyester/cotton	70	knitted	Plastibert
K3	polyester	100	knitted	Seyntex Techmaflex T116W
W1	100% cotton	246	woven	-
W2	cotton DOW XLA CO/Tencel	230	woven	Alsico (3)
W3	50% cotton + 50% coolmax	185	woven	Alsico (2)

Table 3.3: Overview of the different knitted and woven fabrics used for the tensile tests.

Sylgard 186 PDMS sheets with thicknesses of 100μm, 200μm, 500μm and 1mm were bonded to the different fabrics, using the previously described screen printing technique (Section 3.2). Three test pieces were used for every fabric/PDMS layer combination. As a reference, Figures 3.13 and 3.14 depict the tensile test results of the different fabric types without the PDMS layers. Figure 3.13 contains the data of the knitted fabrics, Figure 3.14 the data of the woven fabrics.

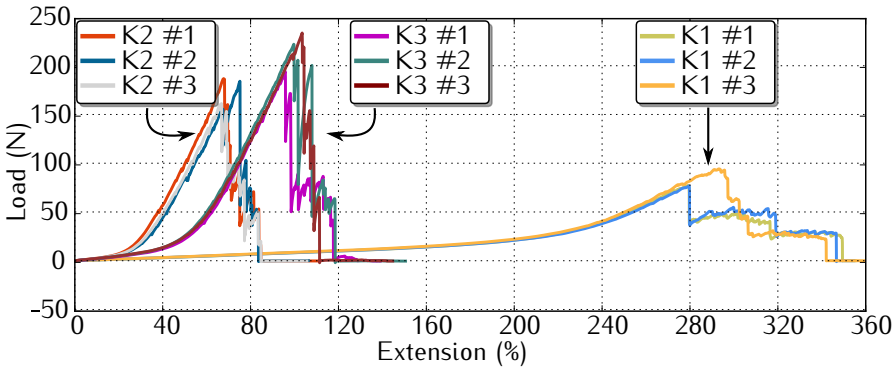

Figure 3.13: K1 - K3 tensile test.

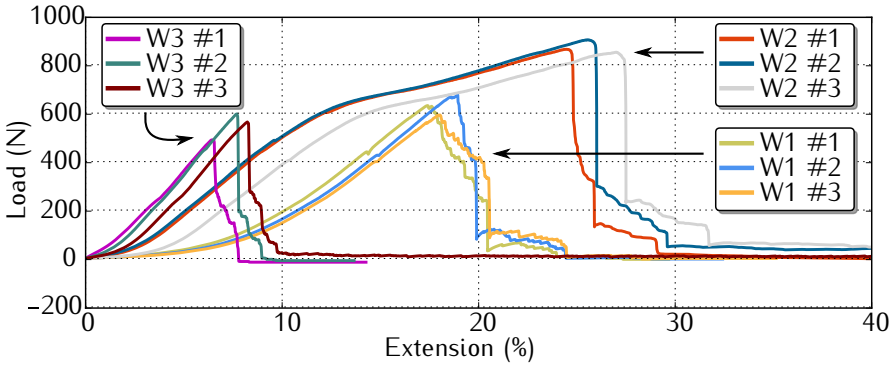

Figure 3.14: W1 - W3 tensile test.

The measurement data illustrates the great versatility in stretchability one can encounter amongst various fabrics. It is needless to say that a typical knitted fabric is more stretchable than a woven fabric because of its construction. From the tensile test data we observe that a force of about 100N results in elongations ranging from 50% to 290% in the case of knitted fabrics. For woven fabrics the elongations at the same force are a lot smaller and are in the range of 2% to 8%. There is not only a difference in stretchability between knitted and woven fabrics, but also between the different fabrics in their own category.

Because there is such a great spread in stretchability between fabrics, different textile products have a different feel when handled. This makes it difficult to speak about comfort related to stretchability in general and is thus more application dependent. Nevertheless it is possible to investigate the influence of the PDMS layers on the stretchability by comparing tensile data of fabrics with and without the PDMS. Dependent on the application the change in stretchability should be considered as acceptable or not. Tensile test data of the most stretchable knitted fabric K1 is given in Figure 3.15.

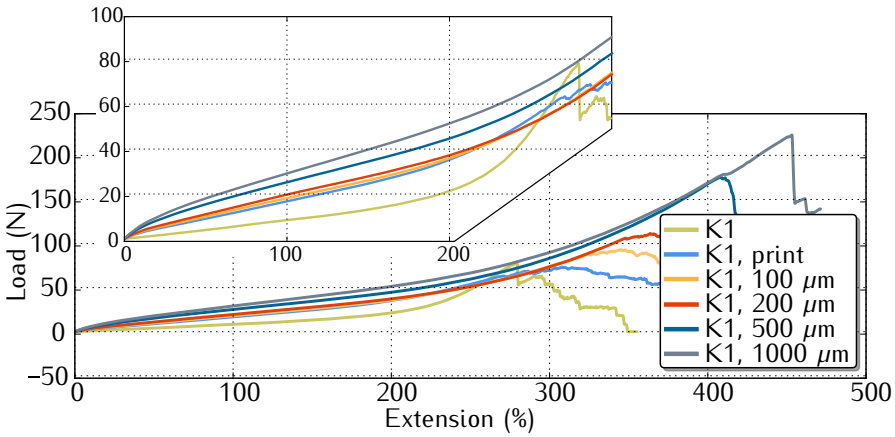

Figure 3.15: K1av tensile test.

Results are given for the reference fabric without any PDMS, for the fabric with only the screen printed glue layer and for the fabric with the PDMS layers of different thicknesses. The presented data was averaged over 3 test pieces. It is easy to see the influence of the applied PDMS. Whereas for example the reference fabric elongated more or less 195% using a force of 20N, adding only the printed glue layer reduced the elongation to approximately 120%. The elongation at 20N further decreased with increasing PDMS thicknesses to about 55% for a Sylgard 186 layer thickness of 1mm.

The K2 and K3 knitted fabrics were less stretchable compared to the K1 fabric as can be seen in Figures 3.16 and 3.17. Also for those two fabrics the influence of the PDMS was clear. Screen printing the PDMS layer reduced the elongation at 50N from 40% to approximately 20% in the case of K1 and from 60% to about 26% in the case of K2. Further reduction of the elongation due to additional PDMS layers was less pronounced. Adding a 1 mm PDMS layer decreased the elongation of the K2 fabric to 17% at a force of 50N and to 24% in the case of the K3 fabric. Given the spread on the different test pieces, these small changes can be ingnored compared to the bigger change we observed between the knitted fabrics with and without PDMS.

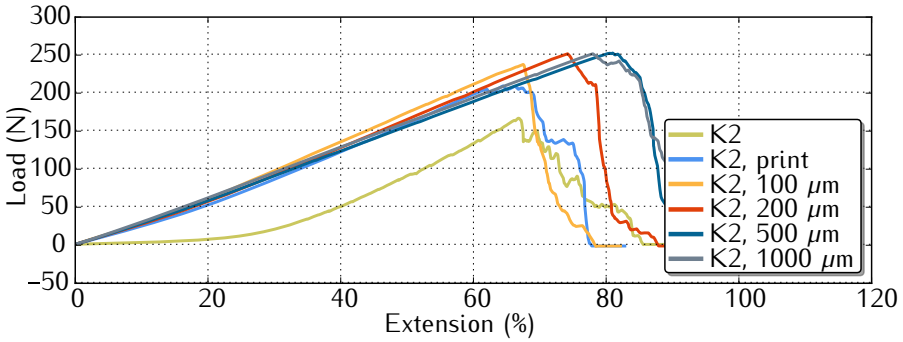

Figure 3.16: K2av tensile test.

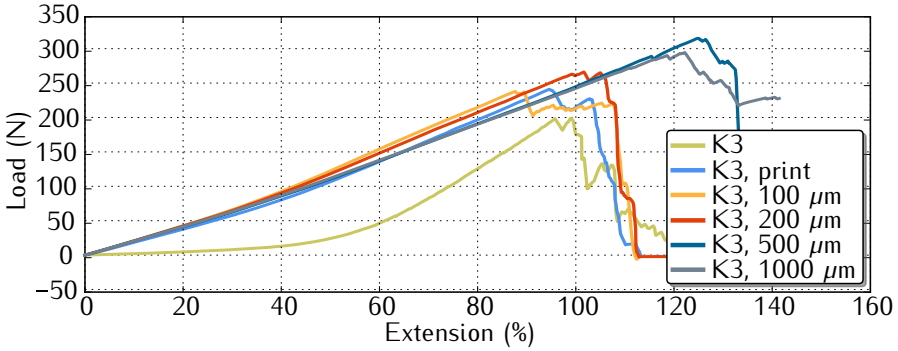

Figure 3.17: K3av tensile test.

In comparison with knitted fabrics, woven fabrics have a different construction. They are much less elastic, resulting in lower elongations. This makes that the stretchability of woven fabrics is less affected by the presence of a stretchable PDMS layer on top. Figures 3.18, 3.19 and 3.20 depict the tensile test results of the woven fabrics.

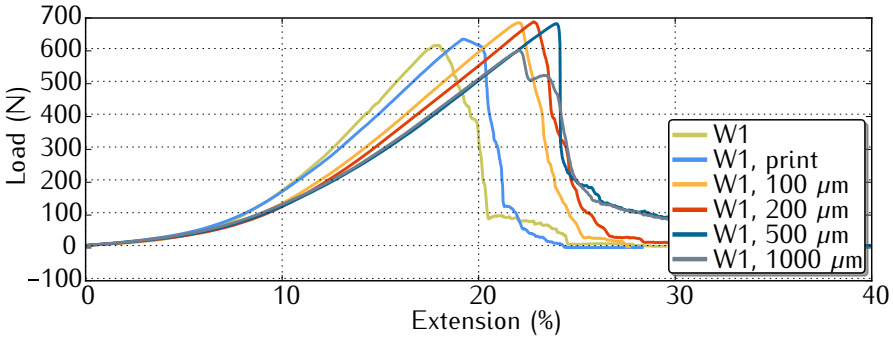

Figure 3.18: W1av tensile test.

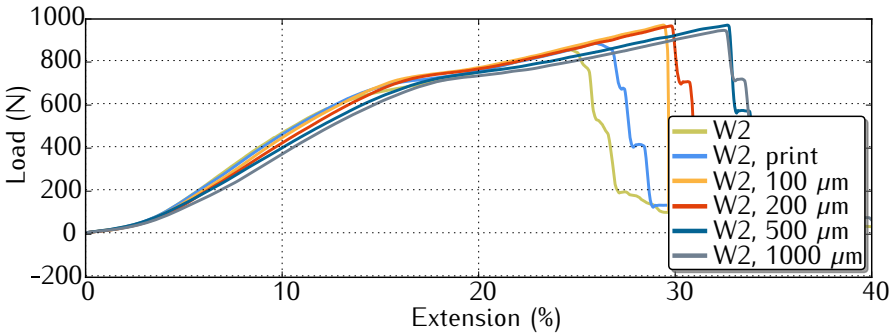

Figure 3.19: W2av tensile test.

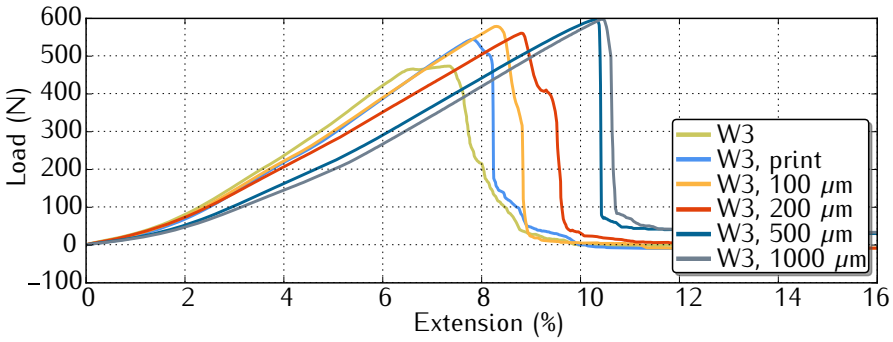

Figure 3.20: W3av tensile test.

As expected, no major influence of the PDMS layers was noticed. For W1 the elongations of the different test pieces at 100N were around 9%, for W2 around 4% and for W3 around 2.5%. On all pieces the woven fabrics broke at their maximum elongation, long before the PDMS sheets were affected. Due to the PDMS on top of the fabrics, the maximum load increased slightly. From these tensile tests, it follows that regarding the stretchability the influence of a PDMS sheet is negligible for a woven fabric but significant for a knitted structure. Nevertheless, the results might be acceptable for most applications from the viewpoint of wearability, especially because in reality more open structures are envisioned instead of plain PDMS sheets covering a large surface (see openings in encapsulation in section 2.4.1). Also the fact that the stretchable PDMS gluing layer is a printing ink, used in commercially available textile products, proves that the change in stretchability is acceptable in terms of wearability. This Dow Corning 9601 textile printing ink is used to screen print color prints on most natural and synthetic fabrics, including elastic fabrics. Typical products containing such color prints are swimsuits, hats, jackets, pants, T-shirts, sweaters, undergarments and so on. This means that in all these daily products the stretchability of the fabrics

is reduced to a certain extent by the PDMS prints, indicating that the same change of stretchability by the stretchable modules will also be acceptable. Additionally, some of the key features and benefits used in the marketing of this printing ink are its high elongation, superior wash durability, good tactility and good adhesion [7]. These same properties are also applicable for the stretchable modules, making them well suited for textile integration.

3.6 Conclusions

Two textile integration methods for the different types of stretchable electronic modules, discussed in Chapter 2, were developed. The first method used the screen printing of a PDMS glue layer to bond PDMS encapsulated stretchable modules and fabrics together. This bonding technology is easy to adopt by the textile industry, because the same printing process, with the same PDMS material is used today in color printing on fabrics. Attention was given to the penetration dept of the printed layer. By limiting the penetration into the fabric as much as possible, the stretchability of the fabric was preserved as well as possible. The second method was developed to bond TPU encapsulated stretchable modules to textiles. These modules were attached to a fabric, using a simple lamination step requiring heat and light pressure. Also this technology can easily be transfered to the industry as textile lamination is a commonly used process. This process can even be as simple as ironing the modules onto the textile.

The adhesion between Sylgard 186 (PDMS) or Krystalflex PE 429 (TPU) encapsulated modules and fabrics was found to be adequate. Fabrics containing dummy encapsulated modules were washed up to 50 times without showing delamination. Some change in color and some shrinkage were observed in the case of Krystalflex PE 429 encapsulated modules. New tests should be executed to further examine these findings.

With a focus on wearability, the achieved realizations of textile integrated stretchable electronics are doing very well. Technological developments have resulted in lightweight stretchable modules that can be used in clothing without compromising user comfort. The change in stretchability they cause are in the same range of changes introduced by typical color prints in todays textile products.

References

[1] (2012) Centexbel - Belgian Textile Research Centre. Centexbel. [Online]. Available: http://www.centexbel.be/

[2] (2012) Textile Printing machines. Johannes Zimmer Maschinenbau GmbH. Klagenfurt, Austria. [Online]. Available: http://www.zimmer-austria.com/en/products/applications/textile-printing/index.html

[3] (2012) Dow Corning - Corporate website. Dow Corning. [Online]. Available: http://www.dowcorning.com/

[4] (2000) EN ISO 6330:2000, Textiles - Domestic Washing and Drying Procedures for Textile Testing. International Organization for Standardization. Geneva, Switzerland. [Online]. Available: http://www.iso.org/

[5] F. Gemperle, C. Kasabach, J. Stivoric, M. Bauer, and R. Martin, "Design for wearability," in *Wearable Computers, 1998. Digest of Papers. Second International Symposium on Wearable Computers*, oct. 1998, pp. 116 –122.

[6] J. Knight, D. Deen-Williams, T. Arvanitis, C. Baber, S. Sotiriou, S. Anastopoulou, and M. Gargalakos, "Assessing the wearability of wearable computers," in *Wearable Computers, 2006 10th IEEE International Symposium on*, oct. 2006, pp. 75 –82.

[7] (2009) Dow Corning Textiles Ink Sell Sheet. Dow Corning. [Online]. Available: http://www.dowcorning.com/content/publishedlit/26-1446B-01.pdf

4

Interconnecting stretchable modules

4.1 Introduction

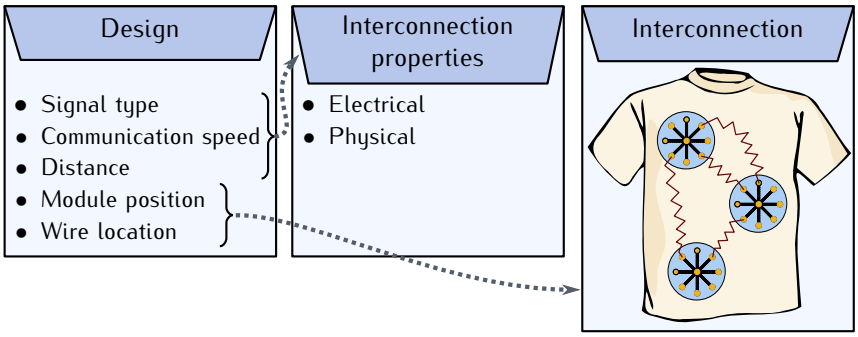

Figure 4.1: Chapter overview.

All electronic components must be interconnected and assembled to form a functional and operating system. The electrical interconnections in a system can be assigned to different levels of interconnection. At the lowest level, the interconnections are found inside the plastic packages of active and passive components. One level higher these components are interconnected with each other at board level by the copper tracks in the stretchable modules. In Chapter 2 it was explained that these interconnections are routed straight onto the flexible functional islands and have a meander shape at the stretchable

zones. It was explained how the stretchable modules can be integrated with fabrics in Chapter 3. It is possible that a certain application requires multiple stretchable modules, distributed at different positions on a textile. This ensures that interconnection at module level may be necessary. In this chapter we describe how the textile integrated electronic modules can be interconnected with each other. These same techniques can also be used to connect stretchable modules with conductive textile elements, like for example textile sensors, heating elements, antennas, etc.

4.2 Requirements for the interconnection

Interconnection requirements can differ a lot and are dictated by elements like system function and the operating parameters of the system (e.g. clock speeds, power consumption, operating environment). Table 4.1 lists the three main reasons why an interconnection to another element outside a fully encapsulated stretchable module may be needed. Without trying to be complete, some important parameters for the determination of the interconnection requirements are given for each category.

Reason for the interconnection:	**Important parameters**
Power distribution	Maximum current and voltage, allowed voltage drop, voltage stability
Signal transmission	Analog or digital, frequency (speed), rise time, impedance, noise budget
Interconnect with conductive textile element	Type of the textile element

Table 4.1: Categorization of the different reasons to establish an interconnection with a textile integrated stretchable module.

Probably the most common reason why an interconnection is required is the power distribution for the stretchable modules. In practice, this is for example the interconnection between a battery and a module. An adequate power distribution is needed to ensure an efficient, low-resistance flow of current. The resistance of the electrical conductor that provides the interconnection should be as low as possible to limit the voltage drop across the conductor. The DC resistance of the conductor depends upon the conductor's length, cross-sectional area, type of material, and temperature. The longer the conductor, the more of the voltage is 'lost' (unavailable to the load), due to the voltage drop developed across the resistance of the conductor. This implies that the overall product layout may influence the interconnection requirements. During the design phase the specific locations of the modules in the textile product are defined. Together with the provided space to route the

intermodular interconnection, this will define the length of the interconnection. The longer the interconnection becomes, the higher the constraints will be on the material type and cross-sectional area of the interconnection, in order to stay below the maximum allowed voltage drop. Also the maximum load current is an important parameter, because when this increases, the voltage drop in the supply conductor also increases.

Signal transmission between different stretchable modules will be in most cases over a digital bus, because of the modular system approach. In case the module is interconnected with for example a textile sensor or a textile antenna, the signals are more likely to be analog. As is the case for the power distribution, also in case of signal transmission, the electrical properties of the interconnects are of great importance. Careful design of the interconnection is necessary to maintain signal integrity and thus avoiding problems related to timing, noise and electromagnetic interference. To do so one needs to understand how the physical design of the interconnections might influence signal integrity. An interesting read on this topic is the book 'Signal and Power Integrity - Simplified' by Eric Bogatin [1]. This book brings together techniques for finding, fixing, and avoiding signal integrity problems in designs. It emphasizes intuitive understanding, practical tools, and engineering discipline rather than concentrating on theoretical derivation and mathematical rigor.

For analog signals, an important technical factor is the frequency of the signals. Maintaining good signal integrity becomes more challenging with increasing speed. Also here the length of the interconnection plays an important role. The signal propagation over the interconnection, the so-called time of flight, is directly proportional to the length of the conductors and must be kept short to ensure the optimal electrical performance of a system operating at high speeds. If the wavelength λ of a sinusoidal signal is in the same order as the length l of the interconnection, the energy tends to radiate off the conductor as radio waves, causing power losses. In that case the interconnections must have good transmission line characteristics to minimize signal losses and distortion. As a rule of thumb, transmission line effects should be taken into account if $l > \frac{\lambda}{10}$. For a sine wave signal of 300MHz and assuming that it travels at the speed of light, this is the case if the length becomes larger than 10cm.

For digital signals, an additional important parameter, next to the frequency of the signal, is the rise time. Signal integrity effects begin to be important when the rise time of the signal is very short compared to the time delay of the transmission line. For most electronic products, this is for rise times shorter than about 1 ns. In most digital signals, the time allocated to the rise time is about 10% of the clock period. This ensures that, when the clock frequency is 100 MHz, the rise time is roughly 1 nsec. But even if the clock frequency is low, there is still the danger of shorter rise times as a direct

consequence of the chip technology. As all fabs migrate to lower-cost, finer-feature processes, all fabricated chips will have shorter rise times. Ironically, the lowest-cost chips will always have ever-shorter rise times, even if they do not need it for the specific application.

In general, to keep signal-integrity problems at a minimum, the lowest clock frequency and longest edge rate should be used. Possible distortion of a signal traveling over an interconnect will not only depend on the properties of the signal, like frequency and rise time, but also on the electrical properties of the interconnection itself. The impedance of the interconnection, which is defined as the ratio of the voltage to the current, will determine all signal integrity effects. The instantaneous impedance a signal sees as it propagates down the line is dependent on the geometry and material properties of the interconnect. One of the goals in designing for optimized signal integrity is to design all interconnects as uniform transmission lines and to minimize the length of all non-uniform transmission lines. While this is common practice and well described for interconnects in PCB designs, the electrical characteristics for textile based interconnections might be totally different.

4.3 Textile based conductive interconnections.

Creating a list of all different interconnection possibilities, used to form a system of electronic components which are found in today's electronic products, would almost be an endless job to do. Different types of interconnections are possible, dependent on the level of interconnection. At the level of board to board interconnections or intermodular interconnections, a variety of types may be used including board-to-board and wire/cable-to-board. Subsystems may be interconnected at this level using different cable and connector configurations. While these interconnection types are robust and mature enough to be used in a wide range of existing electronic products, the story for textile based electrical interconnections is totally different. Figure 4.2 categorizes different techniques, found in literature or commercially available textile products, that could be used to establish conductive intermodular interconnections based on textile solutions. Some short comments on these conductive textile interconnections are given in this section.

Keeping overall product manufacturability in mind, it is interesting to categorize the different textile techniques by the level at which the interconnects are introduced. In principle, the introduction of the interconnects can be done at 3 levels:

- Via the intrinsic textile manufacturing process
- Via the textile finishing process
- Via the textile confection process

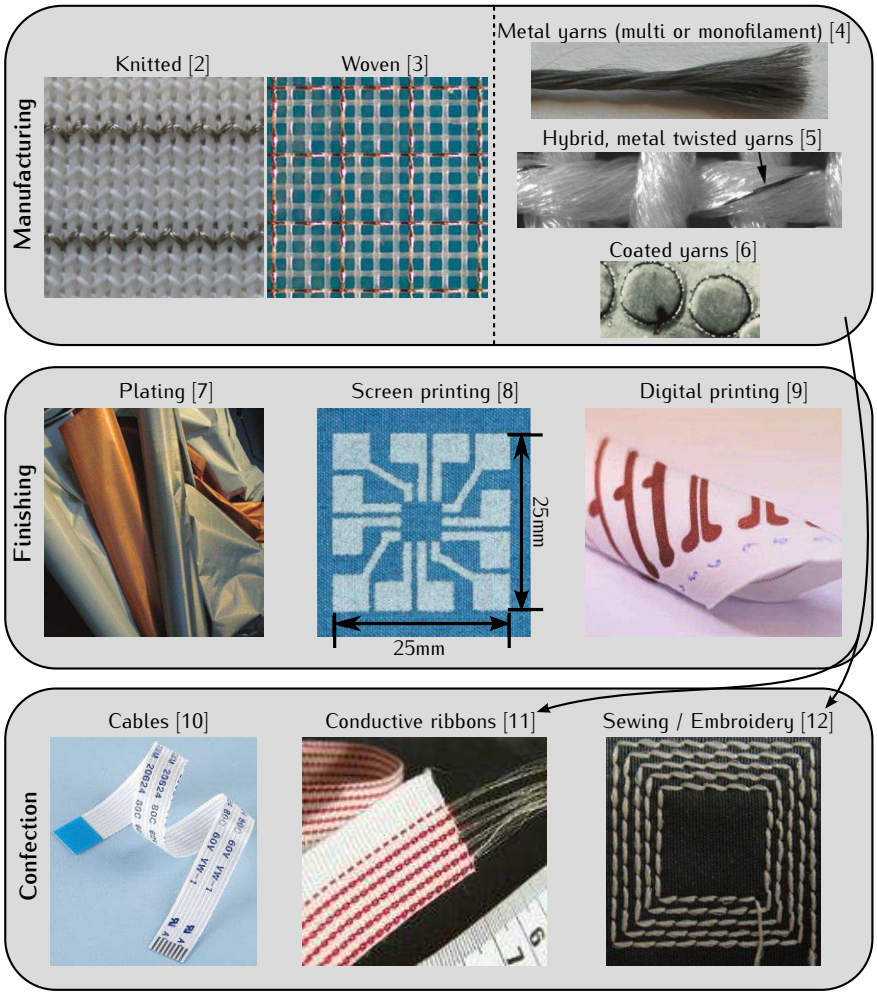

Figure 4.2: Conductive interconnections in textiles.

4.3.1 Interconnections at the intrinsic textile manufacturing process.

At this level the conductivity is already added during the manufacturing of the basic textile substrate. Typically conductive yarns are introduced while **knitting or weaving** the fabric. The number of conductive 'tracks' and their location in the fabric will depend on the used knitting or weaving process, providing different possibilities. Besides the selected process or technique, also the type of conductive yarn provides an additional degree of freedom. Conductivity can be established with different yarn types, including *metal*

yarns (100% pure metal, e.g. a pure Ag yarn), *hybrid yarns* (metal twisted yarns or for example PET fibre spun with inox fibre) or *coated yarns* (e.g. PES yarn with Ag cladding). It is important that the yarns are strong and flexible enough to withstand the weaving and knitting process and are reliable enough to ensure functionality during product life. Today, different conductive yarns are commercially available:

The *metal yarn* shown in Figure 4.2 is a multifilament conductive stainless steel yarn produced by Bekaert and sold under the trade name Bekinox. Their main application is found in the field of electromagnetic shielding textiles, where the conductive yarns provide a high level of electromagnetic shielding [4]. The knitted fabric in Figure 4.2 is a fabric produced by Heathcoat fabrics [2] and probably contains multifilament stainless steel yarns (picture was found on the do it yourself site 'How to get what you want' [13], no info was found on the yarn type). Another popular type of metal yarn, used for clothing in shielding applications, is the Textile Wire (TW) developed by Elektrisola Feindraht AG. The core of the TW is a single metal wire and is chosen from various pure metals and alloys. The outermost layer of the TW is an enamel coating, which works as an insulation for the bare wire [14]. The picture of the woven fabric in Figure 4.2 shows an example of a fabric with pure metal wires as conductors. This fabric is produced by Sefar, under the name of PowerMatrix [3]. PowerMatrix is a hybrid fabric consisting of PET, metal and marker monofilaments in warp and weft. The metal wires have a thin polymer coating to serve as insulation. This type of conductive fabric was used as a substrate to build electronic circuits as was published by Locher and Troster [15]. Their process involves: point by point selective removal of the yarn coating by laser ablation; cutting and joining (named as textile via's) of the conductive yarns to create tracks made up of yarn segments in warp and weft direction; placement of rigid interposers with electrical components onto the opened conductive yarns. Interesting is that they also evaluated electrical properties of transmission lines and interconnections using this woven fabric. The fabric allows transmission line configurations with controlled impedances around 250Ω and with flat frequency response up to 2 GHz (length of the line was 15cm). Introducing the textile via's lowered the flat frequency response to 600MHz.

The *hybrid yarn* in Figure 4.2 is a PES yarn that was twisted with one copper thread (diameter 40μm). The copper threads are insulated with a polyesterimide coating. This yarn was used in a publication by Cottet et al., in which they also presented results on the electrical characterization of textile transmission lines [5]. They achieved characteristic impedances between 120Ω and 320Ω. These transmission lines could be used for frequencies up to 1.2 GHz and 120 MHz with the maximal lengths of 10 and 100 cm, respectively. Furthermore, by using this type of yarn, the copper wire locations are not

precisely defined within the woven fabric because of their helical path around the yarn. This makes it more difficult to make interconnections with the copper wire.

A third type of conductive yarn consists of metal *coated yarns*. The picture in Figure 4.2 shows the crossection of a silver-coated nylon yarn produced by Statex under the trade name of SHIELDEX [6].

While it is currently possible to use these different types of conductive yarns at the level of manufacturing by knitting or weaving, it is important to know the limitations if they are used for interconnection technology in electronics:

- *Fixed structure:* Introducing the conductive yarns/tracks at manufacturing level implies that the conductive interconnections in the fabric have fixed positions in the fabric structure. For woven fabrics the tracks can only be parallel in vertical or horizontal direction (warp and weft). For knitted fabrics the routing of the conductors has a bit more freedom, but is still limited by the positions of the yarns in the knitted fabric structure. The predetermined yarn positions in woven and knitted fabrics puts also constraints on the achievable pitches between the conductors.
- *Tolerances:* Generally speaking, the tolerances on yarn dimensions and positions in a knitted or woven fabric are a lot larger than those found in typical technologies for electronic components and products. The variations in the fabric are caused by the deformability of textile materials and degrees of freedom during the manufacturing processes. At the level of fibers and yarns there are for example variations of diameters and densities (along a thread but also from thread to thread). At the level of fabrics, for example, the distance between yarns varies. As textile material has viscoelastic behavior, inner tensions relieve over time and geometry may change. As an example, Cottet et al. have reported wire spacing variations of $\pm 6.7\%$ on yarns with 481μm spacing ($\sigma = 32.2\mu$m) in their paper [5]. These variations must be taken into account when an interconnection is made between the conductors in the fabric and electronic interposers or modules. They also have an impact on the electrical characteristics of the textile based interconnections. Dimension variations can put limitations on transmission lines between modules, because impedance matching becomes more difficult.
- *Conductor length:* The actual length of the conductors used for the interconnections in a fabric will be longer than when a straight point to point interconnection would be used. The wires in a woven fabric follow a wavy pattern, so that the actual length increases. For knitted fabrics the effective length of the conductors will be even larger, because of the

many loops in the fabric structure. Also the yarn type will play a role here. The effective length of the conductor in a hybrid metal twisted yarn will be longer than the effective length of a straight monofilament yarn because of the helical path of the conductor in the hybrid yarn. As the DC resistance of the conductors increases with the length, this should be taken into account when designing interconnections in textiles.

- *Insulation:* Dependent on the application, the conductors used should either have insulation or not. Whenever conductors are crossing, as can be the case in woven fabrics if orthogonal tracks are used, insulation is necessary. Due to the fact the conductors are introduced at the fabrication level, a technique is required to selectively remove the insulation in order to make electrical contact with the conductive yarns.
- *Fabric to fabric connection:* If the final textile product is made from different pieces of fabric and an interconnection should run from one fabric to the other, fabric to fabric connection of the conductors becomes necessary. This can be particularly difficult because the conductor positions are fixed in the fabric and proper alignment can be a challenge.

Dependent on the application, the introduction of conductive interconnections at the intrinsic textile manufacturing process can be a good or a bad choice. In my opinion it is for example a bad idea to use the PowerMatrix as a circuit substrate as was done in the work of Locher and Troster [15]. The problem with this approach can be noticed in the graphical representation of their technology (see Figure 4.3).

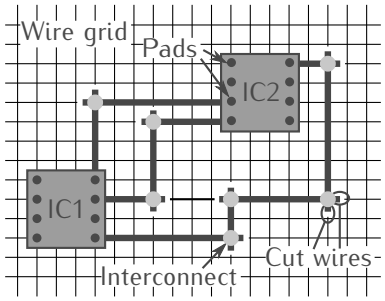

Figure 4.3: Electrical components interconnected via the wire grid in the fabric (polyester threads omitted) [15].

This approach needs a lot of wire cuts and textile interconnections if you want to do the routing of all signals in a real circuit. Even for the three routed signals in the drawing, one needs already 14 wire cuts and 7 interconnection points that require selective laser ablation to create them. The complexity of the circuit will also be limited because only orthogonal wire segments, which

are fixed in position, can be used to perform the signal routing. On the other hand, their technology developments are interesting and could be used if more modularity would be introduced into the system. This is exactly what we have tried to accomplish with the presented stretchable technology for textiles in this PhD. If an overall distributed system is designed using sub-assemblies of stretchable modules, the textile routing problems can be reduced and limited. This means that most interconnections between electrical components at board level stay within the modules. Only a small amount of intermodular interconnections are needed then among the modules to provide data exchange and power distribution. In that case the woven PowerMatrix could be used, together with the techniques described by Locher and Troster, to interconnect stretchable modules with each other. Doing so would serve a wider range of applications. A concept drawing is given in Figure 4.4. The different stretchable modules are made up of several functional islands, which are interconnected with each other by stretchable interconnections as was described before (section 2.1). Contact paths at the back of the module, which have the same spacing as the conductors in the wire grid, are then used for the textile-based interconnection. As most of the signal routing is kept inside the stretchable modules (where there is also more routing freedom), the number of textile based interconnections can be limited. As a sidenote, note that the electronic components in the SMI technology are already protected and insulated by the used encapsulant, whereas the direct mounting of electronic components onto textile may induce reliability issues if no additional mechanical protection is provided.

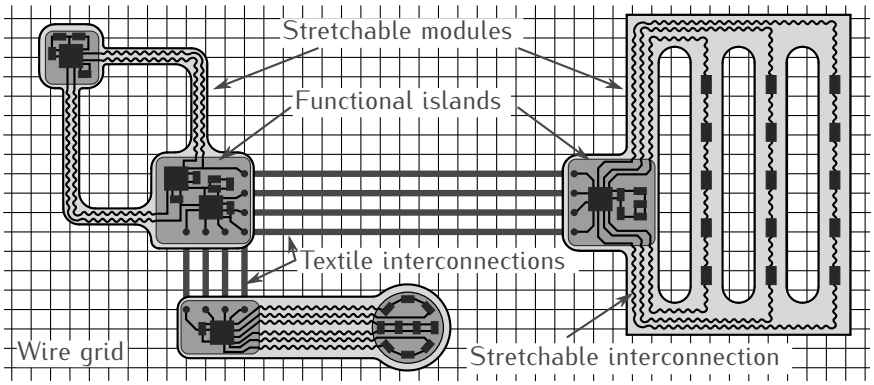

Figure 4.4: Stretchable modules interconnected via the wire grid in the fabric (concept drawing). A higher level of circuit complexity is possible using this modular approach.

4.3.2 Interconnections at the textile finishing process.

Conductivity in textiles can also be introduced during the textile finishing process. A first method is to coat/plate the entire fabric with a certain metal (e.g. silver, copper/nickel). A wide range of different metalized fabrics is commercially available and their main application field is found in EMI shielding (e.g. produced by: Statex [7, 16]; LessEmf [17]). As these fabrics are conductive over the whole surface, they are not really suited to establish interconnections. However they are used a lot in research on different types of textile based patch antennas [18, 19, 20, 21],etc. In this application field the metalized fabrics are cut into shape and used as ground plane and antenna patch in an antenna assembly. The metallic plating of fabrics could be used for textile based interconnections if the plating would be done selectively. Li et al. have published a method to construct frequency selective surfaces onto fabrics, based on selective electroless plating of PET fabrics [22]. Similar selective plating techniques could be used to pattern conductive tracks onto fabrics, which might be used as textile interconnections. Another possibility could be to start from the completely metalized fabrics and to structure them by etching, as is done in PCB manufacturing. An example of such a process was found in an online instructable of the MIT Media Lab [23]. In general, attention should be given to the preservation of conductivity of the plated metal layer during use or cleaning processes. Cho et al. did a study on the application of PU-sealing onto Cu/Ni electroless plated polyester fabrics [24]. They have shown that the electrical durability of their untreated fabrics is not enough to be used as textile conductors. Whereas the unsealed fabrics had a significant increase in resistance after a first washing cycle (5 to 9 times higher), the fabrics sealed on both sides with PU tape had a doubling of the resistance after 10 washing cycles.

A second method to create textile based interconnections at the level of textile finishing is based on screen printing. The example of a screen printed conductive pattern, depicted in Figure 4.2, was published by Kim et al. [25]. In this work they presented a healthcare monitor chip which was integrated on what they named a Planar Fashionable Circuit Board. The chip was wire bonded to the screen printed electrodes and thereafter overmolded as is illustrated in Figure 4.5. They also used the screen printed patterns for a capacitive based moisture sensor and LED-display in their system. In more recent work on this technology, Kim et al. published the electrical characterizations of these screen printed structures [8]. A silver based conductive ink was screen printed on different fabric types. Minimum track widths of 200μm, with a thickness of 10μm were obtained. Printed signal transmission lines were used to investigate DC resistance, AC impedance and maximal signal frequency. Characteristic impedances were between 180Ω and 230Ω, and

they observed a 3-dB bandthwidth of 80MHz. The feasibility of this method will mainly depend on the conductivity and mechanical properties of the used ink. They reported for example a DC resistance of 4.6Ω for a trace width of 1mm, length of 2cm and a thickness of 10μm. This resistance might be too high in case of long interconnections. Especially if it is compared to the typical DC resistance (R) of a copper trace with same dimensions, which would be about 34mΩ (R=resistivity$_{copper}$*length/(width*thickness)). With regard to the endurance of the printed tracks, they reported an increase in DC resistance up to 40 times or even loss in conductivity after washing the samples about 20 times. As was the case in the selective plating method described before, a passivation of the tracks improved the washing endurance. With the passivation material coated, the variation of the resistance values was less than 2 times that of their original value after 50 washes.

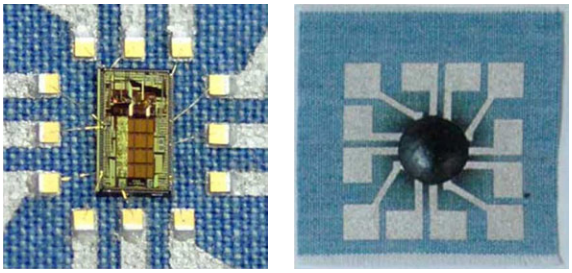

(a) (b)

Figure 4.5: Healthcare monitor chip integrated on a Planar Fashionable Circuit Board. (a) Chip wirebonded to screenprinted pattern. (b) Molded package. (Pictures from [8])

As a third method, digital printing of conductive materials could be used to make interconnections at the textile finishing level. Just like screen printing, this method can print in a selective way conductive materials onto a fabric. The difference lies in the method of applying. In digital printing a digitized pattern is directly printed to the substrate, without the need for a specially made screen as is the case in screen printing. This makes it a more flexible method, with a shorter and less expensive turn around time. The picture in Figure 4.2 is an example of the direct metal printing process developed by TNO [9]. Their process uses inkjet printing technology to print conductive copper tracks on various substrates. As is illustrated in the picture, this technology can be used to print conductive copper tracks onto fabrics. An additional advantage of this flexible method is the possibility to print on surfaces with height differences. This can be made possible by moving the printing head up and down during printing. Also for this method it is likely that the tracks should be passivated, to improve their durability under cyclic mechanical loading.

4.3.3 Interconnections at the confection process.

At last, we can consider to introduce interconnections during the textile confection process. A first method is to use electrical wiring that is standardly used in electronic products (i.e. wires, cables, ribbons). These types of interconnections can be fixed at several positions on the textile by stitches, or integrated into the textile by sewing them into a piping. The picture in Figure 4.6 illustrates the piping of electrical wires into textiles.

Figure 4.6: Electrical wires in a piping. (picture from [26])

An obvious advantage of this method is that one can rely on the well-known properties of the used electrical wiring. As a trade-off, the fabric becomes stiffer at the position of the cables (this will depend on the type of wiring). For that reason it is important to route the wires through the textile product at well thought out positions. The RGB (red green blue) color matrix that was integrated into a jacket (presented in section 6.4) made use of this method to establish the interconnection between the battery and the display. In this design, the power wires were integrated into the turquoise pipings of the jacket and were positioned such that there was no hindrance during wearing. The pipings were running from the battery pack at the back, over the shoulder, to the display at the front. The locations of the pipings are visible in Figure 4.7 as the turquoise lines in the technical drawings of the textile design.

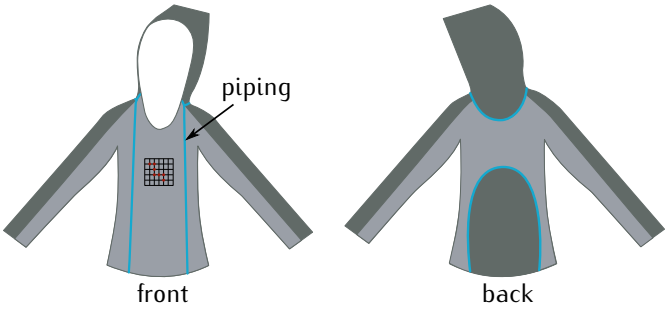

Figure 4.7: Locations of the pipings in the jacket. The pipings were used to route the electrical wiring in the jacket.

Besides traditional electrical wiring, also textile based wiring can be used. Typical wiring solutions in this second method for interconnection at the textile confection process are for example conductive textile ribbons as the one shown in Figure 4.2. These textile ribbons are well suited for sewing into garments as conductors between electronic units. They are more flexible than standard ribbons used in electronics and are a closer match to textile products because of their textile construction. Conductive yarns are integrated during weaving or knitting of the ribbons. This is similar as the introduction of conductive yarns at the intrinsic textile manufacturing level described before. The same types of conductive yarns can be used, but are in this case running in a single direction along the length of the ribbon. Instead of using the fabrics as an electronic substrate, they are used as ribbons for interconnection and are introduced at the end of the production chain when the textile product is assembled. Different types of ribbons are commercially available and produced by for example, Ohmatex [11] or Fabrick.it [27]. Figure 4.8 shows an interconnection example of the Fabrick.it ribbon to different electronic modules.

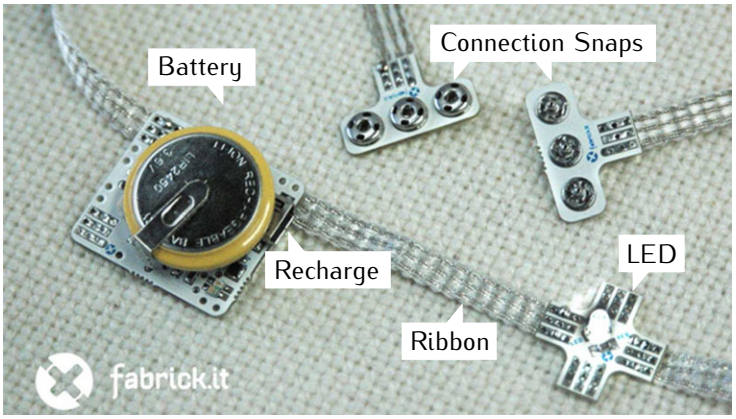

Figure 4.8: 3-wire conductive fabric ribbon from Fabrickit, connected to several electronic modules. (picture from [27])

The last interconnection method at the textile finishing process involves embroidery of conductive yarns. Interconnections between electronic modules can be formed by employing a CNC embroidery machine using conductive yarns. Also in this case different yarn types can be used. As was the case with the digital metal printing method described before, embroidery of conductive yarns on textile substrates is a very attractive approach due to the freedom of circuit design and ease of fabrication. The embroidery example given in Figure 4.2 was published by Roh et al. [12]. They realized and characterized circular and square spiral inductors that were embroidered on a textile substrate. The inductance, self-resonance frequency and quality factor were investigated

under three different environments, i.e. in free space, on a human body, and with a metal fabric ground plane. The embroidered inductors showed the same inductive behavior as general conventional inductors. Looking to the shape of the conductors, it is clear that such conductor patterns are only possible when methods with enough freedom are used. Considering the various defined categories, these methods would be the selective plating, screen printing, digital printing and embroidery. An example where embroidery of conductive yarns was used to establish interconnections between FCBs is given in Figure 4.9 and was published by Linz et al. [28].

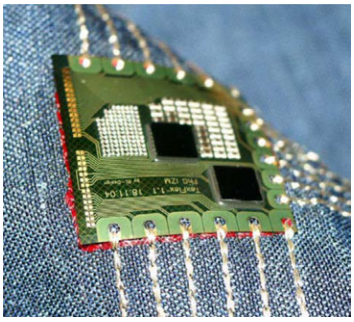

Figure 4.9: Flexible electronic module connected with conductive yarn by embroidery. (picture from [28])

An interesting feature of this embroidery technique is that the interconnection among the modules and the electrical connection between the yarn and the flexible circuit are made in one process step. The connection is made by stitching through the conductive pads on the flexible circuit boards. Linz et al. investigated the reliability of such embroidered connections and developed a theoretical model of the contact mechanism underlying embroidered contacts [29]. Based on this model, potential failure mechanisms were identified and the model was validated using embroidered test samples. They concluded that embroidered contacts are not reliable intrinsically - at least not with conductive embroidery yarns available today. To improve the reliability they encapsulated the embroidered contacts to preserve the contact during temperature cycling and washing.

4.3.4 Usability and design freedom as selection criteria of a textile based interconnection method.

Choosing an appropriate interconnection method to be used in a certain product depends a lot on the application and the interconnection requirements. Different aspects related to the design and manufacturing of the product should be taken into account in order to select the right interconnection method. The

main purpose of the interconnection is to provide an electrical path between different electrical components or modules so that signals can propagate over them with good signal integrity or a stable power network can be provided. This will determine if a certain interconnection method is usable or not. For that reason the first thing to ask in selecting a method should be: What do I need in terms of electrical characteristics for the interconnection? Based on this question a first selection of methods and materials can be made and evaluated by electrical characterization. The next decisions will be based on the overall product design. This will determine the design freedom needed to establish the different interconnections between the electrical components or modules. Together with product design, also the production chain is of great importance. This will determine at what production level the interconnections can be introduced. Dependent on the complexity of the product or circuit, a mix of different interconnection methods might be deployed to cover the different interconnection needs.

With this simple decision process in mind it is easy to understand why certain interconnection methods are more popular or more found in existing smart textile products or in application oriented research on smart textiles. In these cases all aspects of the interconnection method have to be addressed to provide a good solution. If the electrical properties of the interconnections are not sufficient, you can not build a working system and if you can not manufacture it, you have no product. Most of todays smart textile products use interconnection methods that introduce the interconnections at the end of the product chain, at what we call the textile confection level. Why? Well, because this level has the highest degree of freedom to select conductor materials and topologies to provide a working solution. We could say that the later the electronics or interconnects are introduced in the production chain, the more the design freedom increases and the overall manufacturing problems are reduced. This is summarized in Figure 4.10.

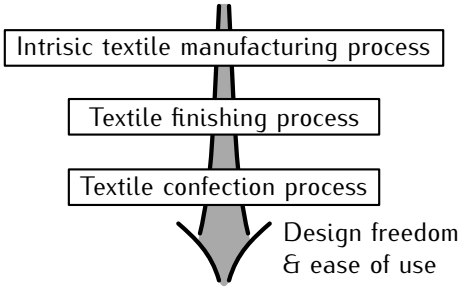

Figure 4.10: The later the interconnections are introduced in the textile product chain, the higher the design freedom.

Note that this same reasoning was used to come to the solution of the textile integrable stretchable electronic modules. It was chosen to produce the stretchable modules in a process close to PCB processing and totally decoupled from textile processes. The stretchable modules are introduced (and eventually interconnected) as late as possible in the production chain of the textile product, using simple joining methods. This avoids manufacturing difficulties as much as possible and is still able to allow a diversity of working solutions. Like Albert Einstein once said... *"Make everything as simple as possible, but not simpler"*.

4.4 Interconnection of textile integrated modules.

It would be too much work for this PhD to investigate solutions for the connection between the stretchable modules and all the previously mentioned textile based interconnection methods. Therefore a more general approach was followed. The goal was to determine the basic features needed to realize the different connection possibilities. Later on these principles can be further developed and optimized for specific cases in projects or in a PhD study on this interconnection topic. Some interconnection methods were explored already to illustrate the principles. They will be presented during this discussion. A stretchable module consists of an entirely enclosed encapsulation, so a way to access contact pads in the module is needed. The first way is to create an opening in the encapsulation in order to make contact with a pad in the module. An opening can be made at the top side of the module or at the bottom side. A second way to provide contact with the module is to let the contacts come out of the module. With these two access methods implemented, it should be possible to find solutions for the connection between the stretchable modules and all the different textile based interconnection methods. Figure 4.11 illustrates the different connection possibilities. The dots represent the connections, and can be realized by using soldering, conductive glues, embroidery, crimping, connectors, wire bonding, etc. to make the contact. An explanation of the different options is given below:

(a) Openings to contact pads are made in the top encapsulation of the module. The top side of the module is considered as the side where the components are mounted. The bottom side of the module is attached to the textile, so the contacts are facing away from the textile. This case is well suited to provide an interconnection solution for the textile based interconnection methods that were categorized as interconnections at the textile confection process.

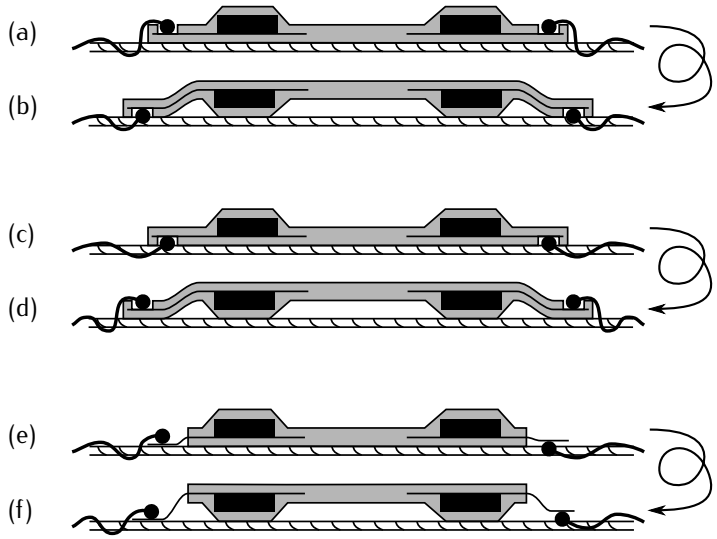

Figure 4.11: Connection possibilities from module to textile interconnections.

(b) Here the openings are also made in the top encapsulation of the module as was the case in (a). But now the module is flipped up side down and bonded to the textile with the top side. Hereby, the contacts are facing down to the textile. This case is well suited to provide an interconnection solution in case the conductors are already in or on the textile at the moment of module placement. This is true for the textile based interconnection methods at the level of textile manufacturing and textile finishing. This can also be true for the methods at the confection level when these are established prior to module placement. Note that the drawing of this connection possibility shows that by flipping the module it is possible to bond the module only locally to the textile. The idea behind this is that in general the electrical components on the functional islands will make the top encapsulation of the module locally thicker. Between the functional islands, we have stretchable interconnections with an encapsulation as thin as possible to provide good stretchability. If this part of the module is not attached to the textile it remains freestanding and can stretch freely and thus preserve the stretchability as much as possible. This same principle could also be applied when the module is bonded with the bottom side to the textile. But then thickness should be added locally at the bottom encapsulation to provide studs that bond with the textile. Alternatively the bond between a flat bottom encapsulation and the textile could also be made at selective positions.

(c) Instead of creating openings to contact pads in the top encapsulation, openings can also be made in the bottom encapsulation. To do so, the functional islands of the module should have contact pads at the bottom side. This can be realized by using a double sided flex in the laser structuring process that was presented in section 2.3.2. When the module is bonded with the bottom side to the textile, the contact pads are facing down to the textile, which is similar to possibility (b).

(d) Here the module with the openings at the bottom side of the encapsulation is flipped upside down to bond to the textile. In this case the contact pads are facing away from the textile, which is similar to possibility (a).

(e) The stretchable module can be encapsulated in a way that the contacts stick out of the module. A flexible functional island can be extended so that it comes out of the encapsulation. When double sided islands are considered, the contact pads can be at the top or bottom side of the flex.

(f) This interconnection possibility is the same as the one in (e), but here the module is flipped and bonded with the side of the top encapsulation to the textile. Again, the interconnection pads can be at both sides.

4.4.1 Implementation of connection possibilities

cases (e) and (f)

The implementation of cases (e) and (f) is straight forward. When the encapsulation is done *by liquid injection molding*, a flexible island (or e.g. wires or a ribbon) should extend the mold cavity, so it ends up out of the encapsulation. For example, the power wires coming out of the encapsulation of the 7x8 LED matrix (see section 6.2) are an implementation of interconnection possibility (e). Figure 4.12 shows a picture of this implementation.

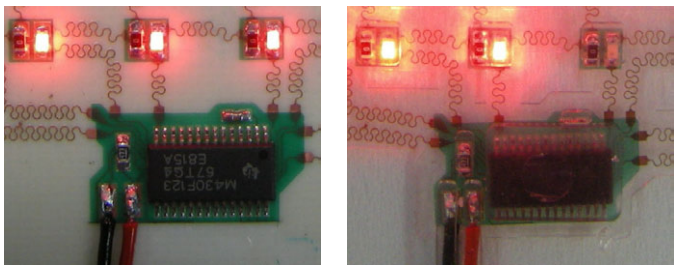

(a) (b)

Figure 4.12: Power interconnecion of the 7x8 LED matrix: (a) power wires soldered prior to encapsulation. (b) result after encapsulation.

Wires were soldered to the contact pads on the functional island, prior to injection molding. Slots in the mold were foreseen so the wires extended the mold cavity. A connector was added to the power wires. After textile integration the connection was made to electric wires that were routed in the textile (at confection level).

Similar techniques could be used in case of encapsulation *by lamination*. It is also possible to mask contact pads with a tape, prior to lamination. After lamination the encapsulant sticks to the tape, which can be peeled from the contact pads to free them up. This was done to solder the power wires to the stretchable LED array (see section 6.1) that was encapsulated by TPU lamination (see Figure 4.13). This is also an implementation of possibility (e), in which the flex with connection pads protrudes out of the encapsulation.

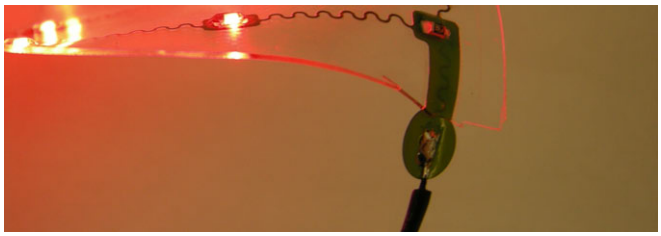

Figure 4.13: Power interconnection of the LED array: Contact pads are coming out of the TPU encapsulation.

cases (a) to (d)

The implementation of cases (a) to (d) requires openings in the encapsulation, making their implementation equal in that sense. One possibility to create these openings could be to laser ablate holes in the encapsulation at the location of the contact pads. An ablation method like this was not investigated in this PhD as it is dependent on properties like the encapsulation material and its thickness above the pads. Instead it was attempted to create the openings during the encapsulation step, so that a process to create openings after the encapsulation is not necessary. The method used to create the openings is different depending on the type of encapsulation process, i.e. by liquid injection molding or by lamination. In the case of *liquid injection molding*, the creation of the openings at the encapsulation step was discussed in section 2.4. Enough clamping force of the mold onto the contact pads was required to keep the pads free from encapsulant. This was made possible in a lab environment, using two PMMA mold halves which were held together using screws at the side and additional clamps in the middle. In order to illustrate the possibilities of making openings in the encapsulation during the molding step, the blinking LED modules were designed (see Figure 4.14). The shape of the opening to the contact pad is determined by the mold shape.

The different shapes that were included in the design are highlighted in Figure 4.14. Cable slots with different shapes were used to demonstrate the possibilities of this molding technique.

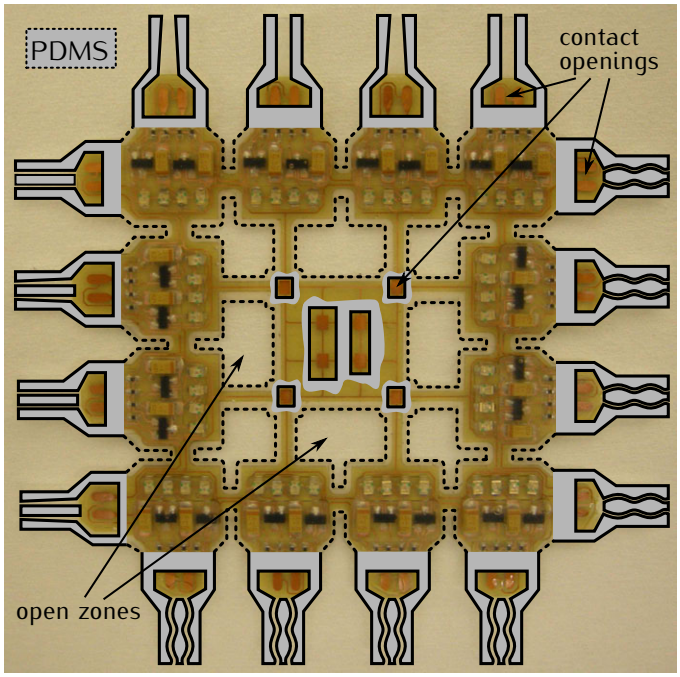

Figure 4.14: Indication of the different types of openings in the PDMS encapsulation of the blinking LED modules. Openings were created to access contact pads and to realize open zones in the center of the module at locations without functionality.

The pictures in Figure 4.15 are details of some of the openings in the realization of the blinking LED modules.

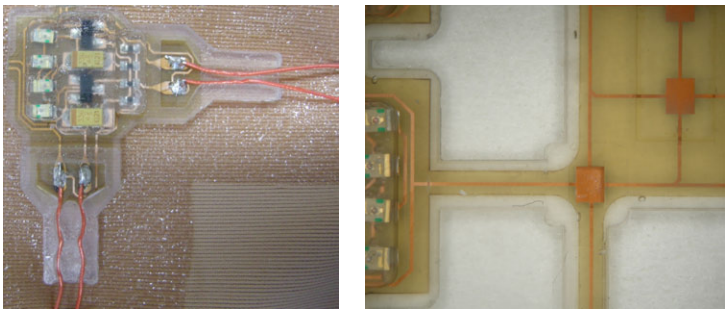

Figure 4.15: Blinking LED openings to the contact pads.

The power wires in the left picture of Figure 4.15 were placed and soldered to the contact pads of the module after the module was placed onto the fabric. The right picture shows openings to contact pads and open zones in the molded encapsulation that were included in the design for testing purposes. Because the openings were made in the top encapsulation and are facing away from the textile, this is an implementation of connection possibility (a).

Another implementation of possibility (a) was used to examine the feasibility of interconnecting stretchable modules with an embroidered conductive yarn. A general view of the test circuit is depicted in Figure 4.16 and a detail of the center pad is shown in Figure 4.17 (left).

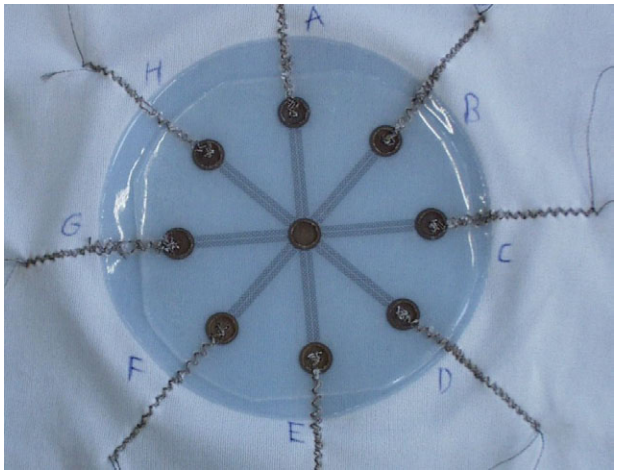

Figure 4.16: Embroidered conductive yarn, connected to pads in a stretchable module.

Figure 4.17: Detail of the center pad opening (left) and an embroidered contact (right).

Openings in the PDMS top encapsulation were foreseen to provide access to the contact pad surface onto which an embroidered connection could be made. The diameter of the star-formed structure was about 100mm and the circular copper pads were 10mm in diameter. The detailed photograph also clearly shows the meander shaped stretchable interconnections between the

pads. In this way the center pad is connected to each of the 8 'satellite' pads. After stitching this provided an easy way to check continuity of the interconnections. This test vehicle was attached onto a knitted fabric with the contact pads facing away from the textile.

The embroidered connection was realized by Centexbel, a Belgian Textile Research Centre [30]. A silver coated polyamide yarn (Shieldex 235 f34 dtex 2 ply) was sewn forward in the direction of the pad, then through the pad and finally continuing away from the pad. Zig zag sewing was used to prevent the reduction of stretchability of the knitted fabric as much as possible. A detail of the connection is shown in Figure 4.17 (right). Several stitches through the contact pad were made to have sufficient contact area between the conductive yarn and the copper pad. Note that it was possible to stitch through the PDMS encapsulation, from the side of the module to the contact pad, located about a centimeter away from the border.

To protect the connections, they could be encapsulated. The goal of contact encapsulation is then to increase the reliability of the connection. Figure 4.18 depicts how the openings in the modules were filled with PDMS for protection.

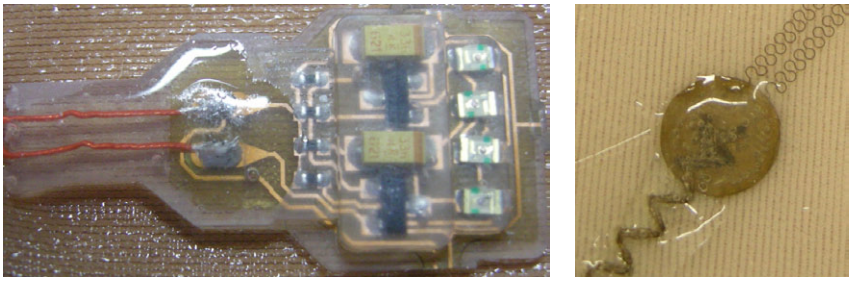

Figure 4.18: Contact openings in the modules filled with PDMS to protect the contacts.

The creation of openings, using encapsulation by *lamination*, was not investigated in this PhD. However, Figure 4.19 illustrates how this could be made possible. The encapsulation step would start from a sheet of the thermoplastic material, using the same lamination steps as presented in Figure 2.24 in section 2.4.2. But now openings would be punched in the sheet at the locations where openings to the contacts are desired. The picture illustrates how the sheet and the stretchable circuit are placed in the lamination stack. Note that this stack is drawn 'up side down' compared to what was presented in Figure 2.24. The thermoplastic sheet is placed at the bottom because the lamination requires preheating of the thermoplastic material, prior to pressing it onto the stretchable circuit. This is done in order to soften the material so that it can deform around the components. If the sheet would be placed at the top, it could come down because of gravity and possibly flow onto the

contact pads. The key to create the openings in the encapsulated module is to design the surface of the lamination plate so that the encapsulant does not flow onto the pads during lamination. To do so, the plate should stick through the punched openings in the sheet so that it closes on the contact pads. As said before, this was not tested yet, but could be a feasible way to implement the creation of contact openings in modules encapsulated by lamination.

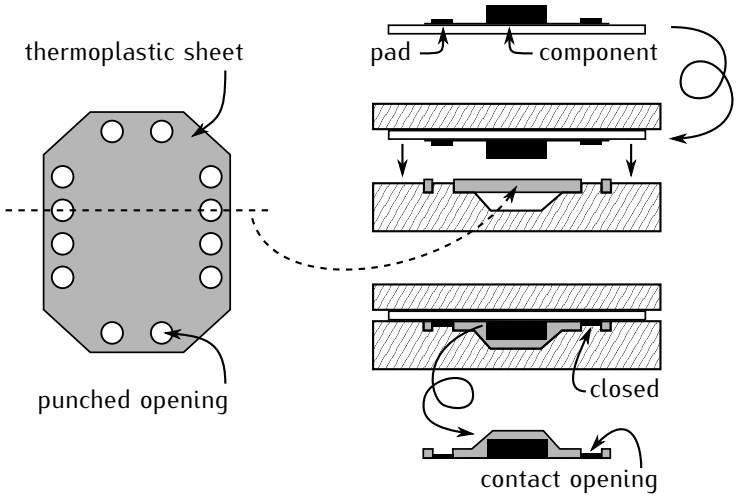

Figure 4.19: Concept to create contact openings in a thermoplastic encapsulated stretchable module during the lamination step.

In preceding sections, only examples of connection possibilities were shown with contact pads facing away from the textile. The main reason is that it was sufficient to connect the modules designed in this PhD with standard soldered wires that were integrated in textiles. In all demonstrators these connections were needed to provide power to the used modules. Soldering and the embroidery of conductive yarns were used to make the connections in the presented examples. The implementation of this was easy, by using modules on textile with opened contact pads facing away from the textile. Implementing connection possibilities (b) and (c) of Figure 4.11, with contact pads facing down to the textile, requires the same encapsulation techniques to realize the modules containing the openings. However, the connection itself between the contact pad in the module and the textile based interconnection can be a greater challenge. This is because the connection is hidden underneath the module. The realization of this type of interconnection is at the time of writing under investigation in the frame of the Pasta [31] and Place-it [32] projects.

4.5 Conclusions

Various reasons can imply that interconnections with stretchable modules are required. Probably the most common reason is the power distribution for the stretchable modules. Other reasons include the signal transmission between different modules and the interconnection of modules with conductive textile elements (e.g. textile sensor, textile antenna). In all cases the interconnection provides an electrical path between different electrical elements. Therefore the electrical characteristics of the interconnection are of major importance.

Different textile based interconnection methods exist or are currently under development. We have categorized them according to the level at which they are introduced during textile manufacturing: Via the intrinsic textile manufacturing process, via the textile finishing process, via the textile confection process. The later the electronics or interconnects are introduced into the production chain, the more the design freedom increases and the overall manufacturing problems are reduced. In most of the cases this is at the cost of a lowered integration level.

In order to connect the stretchable modules with a certain textile based interconnection method, one should be able to make contact with contact pads of the module. We discussed the different connection possibilities from module to textile interconnections. These possibilities are all based on the creation of openings in the modules or on contacts that protrude out of the module. Different implementations of some of the proposed connection possibilities were presented.

References

[1] E. Bogatin, *Signal Integrity - Simplified*, 2nd ed. Prentice Hall Professional Technical Reference, 2009.

[2] (2012) Knitted fabric with conductive yarns from heathcoat. heathcoat fabrics. [Online]. Available: http://www.heathcoat.co.uk/

[3] (2012) Power matrix. SEFAR. [Online]. Available: http://www.sefar.com/data/docs/download/1229/en/SF-PDF-Smart-Fabrics-CI-13-PowerMatrix-EN.pdf

[4] (2012) Stainless steel fibres for shielding textiles - bekinox. Bekaert. [Online]. Available: http://www.bekaert.com/en/productcatalog/products/b/stainlesssteelfibresforshieldingtextiles-bekinox.aspx

[5] D. Cottet, J. Grzyb, T. Kirstein, and G. Troster, "Electrical characterization of textile transmission lines," *Advanced Packaging, IEEE Transactions on*, vol. 26, no. 2, pp. 182 – 190, may 2003.

[6] (2012) Shieldex yarns. Statex. [Online]. Available: http://www.statex.biz/?page_id=245&lang=en

[7] (2012) Shieldex fabrics. Statex. [Online]. Available: http://www.statex.biz/?page_id=247&lang=en

[8] Y. Kim, H. Kim, and H.-J. Yoo, "Electrical characterization of screen-printed circuits on the fabric," *Advanced Packaging, IEEE Transactions on*, vol. 33, no. 1, pp. 196 –205, feb. 2010.

[9] (2012) Digital printing of conductive tracks. - flyer. TNO. [Online]. Available: http://www.tno.nl/downloads/TNO_Digital_printing_conductive_of_tracks1.pdf

[10] (2012) FFC - Flexible Flat cable. Tung Hing Electric Wire Co Ltd. [Online]. Available: http://www.tunghingwire.com/En_Product_FlexibleFlatCable.html

[11] (2012) Conductive ribbon. Ohmatex ApS. [Online]. Available: http://www.ohmatex.dk/

[12] J.-S. Roh, Y.-S. Chi, J.-H. Lee, S. Nam, and T. J. Kang, "Characterization of embroidered inductors," *Smart Materials and Structures*, vol. 19, no. 11, p. 12pp, sept. 2010.

[13] How to get what you want - conductive fabrics. [Online]. Available: http://www.kobakant.at/DIY/?p=376

[14] (2012) Textile Wire - a product from Elektrisola Feindraht AG. Elektrisola Feindraht AGl. Escholzmatt, Switzerland. [Online]. Available: http://www.textile-wire.ch

[15] I. Locher and G. Troster, "Fundamental building blocks for circuits on textiles," *Advanced Packaging, IEEE Transactions on*, vol. 30, no. 3, pp. 541 –550, aug. 2007.

[16] (2012) SHIELDEX Metalized Fabrics & Conductive Fabric Tapes. Statex. [Online]. Available: http://www.fine-silver-productsnet.com/shmefayaandf.html

[17] (2012) EMF Shielding & Conductive Fabrics. LessEmf. [Online]. Available: http://www.lessemf.com/fabric.html

[18] I. Locher, M. Klemm, T. Kirstein, and G. Troster, "Design and characterization of purely textile patch antennas," *Advanced Packaging, IEEE Transactions on*, vol. 29, no. 4, pp. 777 –788, nov. 2006.

[19] C. Hertleer, A. Tronquo, H. Rogier, L. Vallozzi, and L. Van Langenhove, "Aperture-coupled patch antenna for integration into wearable textile systems," *Antennas and Wireless Propagation Letters, IEEE*, vol. 6, pp. 392 –395, 2007.

[20] L. Vallozzi, H. Rogier, and C. Hertleer, "Dual polarized textile patch antenna for integration into protective garments," *Antennas and Wireless Propagation Letters, IEEE*, vol. 7, pp. 440 –443, 2008.

[21] H. Giddens, D. L. Paul, G. S. Hilton, and J. P. McGeehan, "Influence of body proximity on the efficiency of a wearable textile patch antenna," in *Antennas and Propagation (EUCAP), 2012 6th European Conference on*, march 2012, pp. 1353 –1357.

[22] C. Li, Q. Wang, Z. Tang, J. Han, M. Shi, and M. Li, "Fabrication and testing of frequency selective surface based on fabrics," *Modelling and Computation in Engineering*, pp. 177 – 180, Oct 2010. [Online]. Available: http://dx.doi.org/10.1201/b10025-33

[23] (2012) Salt and Vinegar Etching of conductive fabrics. High-Low Tech Group - MIT Media Lab. [Online]. Available: http://hlt.media.mit.edu/?p=1370l

[24] J. Cho, J. Moon, K. Jeong, and G. Cho, "Application of pu-sealing into cu/ni electroless plated polyester fabrics for e-textiles," *Fibers and Polymers*, vol. 8, pp. 330–334, 2007. [Online]. Available: http://dx.doi.org/10.1007/BF02877279

[25] H. Kim, Y. Kim, Y.-S. Kwon, and H.-J. Yoo, "A 1.12mw continuous healthcare monitor chip integrated on a planar fashionable circuit board," in *Solid-State Circuits Conference, 2008. ISSCC 2008. Digest of Technical Papers. IEEE International*, feb. 2008, pp. 150 –603.

[26] T. Barranti. (2012) Wired piping. [Online]. Available: http://taborbarranti.com/tutorials/wired-piping/

[27] (2012) Conductive ribbon. Fabrickit. [Online]. Available: http://www.fabrick.it/

[28] T. Linz, C. Kallmayer, R. Aschenbrenner, and H. Reichl, "Embroidering electrical interconnects with conductive yarn for the integration of flexible electronic modules into fabric," in *Wearable Computers, 2005. Proceedings. Ninth IEEE International Symposium on*, oct. 2005, pp. 86 – 89.

[29] T. Linz, E. P. Simon, and H. Walter, "Modeling embroidered contacts for electronics in textiles," *Journal of the Textile Institute*, vol. 103, no. 6, pp. 644–653, 2012. [Online]. Available: http://www.tandfonline.com/doi/abs/10.1080/00405000.2011.597568

[30] (2012) Centexbel - Belgian Textile Research Centre. Centexbel. [Online]. Available: http://www.centexbel.be/

[31] (2012) The PASTA project website. [Online]. Available: http://www.pasta-project.eu/

[32] (2012) The Place-it project website. [Online]. Available: http://www.place-it-project.eu/

5 Washability of textile integrated electronics

5.1 Introduction

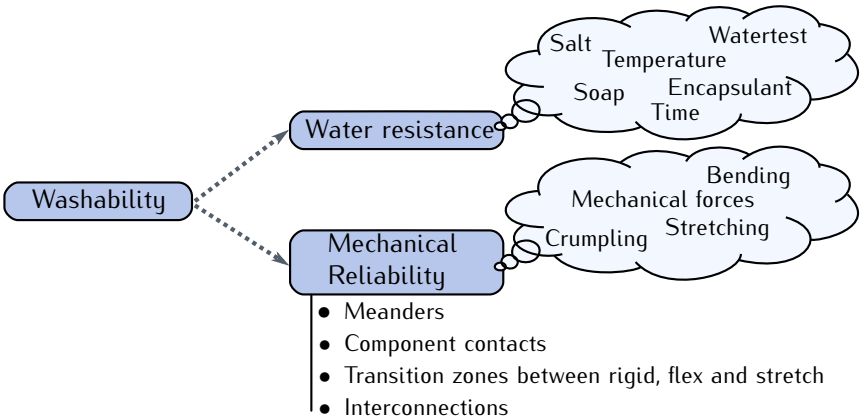

Figure 5.1: Chapter overview.

Previous chapters explained how stretchable modules can be designed, produced, integrated in textile and if required interconnected with other textile integrated modules. Dependent on the final application it is likely that the textile product needs cleaning during product life. In case the electronic cir-

cuits are textile integrated in an irreversible way, all the electronic components should be well protected in order to wash or clean the product. One property of the stretchable modules is that they are encapsulated in a (stretchable) polymer. It is this property that opens the potential for washability, because the encapsulant acts as a conformal coating to protect the electronics against moisture and mechanical forces that are introduced during typical cleaning processes. In general, it can be stated that there are two major challenges to obtain washability for stretchable electronics: Sufficient water resistance and good mechanical reliability. This is illustrated in Figure 5.1. In this chapter we will discuss both these washability aspects.

An encapsulant should protect the electronics from water during the cleaning process. This water resistance will depend on factors such as the temperature of the water, the type of cleaning agent that is used and the immersion/cleaning time. The encapsulant needs to be chemically resistant to the cleaning agent and also the adhesive layer between the fabric and the stretchable module should survive the several cleaning cycles. Next to being water resistant, the stretchable modules should be reliable enough to survive the physical deformations during the cleaning process. This cleaning process might induce other deformations than those present during normal product use. Note that, for example, the meanders are subjected to other movements than the uniaxial elongation, typically evaluated in cyclic stretch tests. During cleaning in a washing machine they are stressed due to a combination of stretching, twisting, bending, crumpling... Not only the reliability of the meanders itself but also the reliability of the contacts of the rigid SMD components on the islands in the stretchable circuit are important. Mechanical failure of these interconnections needs to be avoided to ensure proper functioning of the device. Other fragile zones in the stretchable circuits are the transitions between rigid, flexible and stretchable elements in the design, together with the interconnections between different stretchable modules. This diversity of mechanically critical subparts in a stretchable module leads to the expectation that different mechanical failure modes might be encountered when investigating the cleaning of textile integrated stretchable modules. In this chapter we will focus on some of these mechanical failures.

5.2 Test standards

First question to be asked is: How will we test/evaluate the washability of the stretchable modules? At the time of writing there are no real standards available for testing the washability of (stretchable, conformable) electronic circuits. In (reliability) testing, the test should be designed in such a way that it mimics reality as closely as possible. Therefore, a well suited test is

to evaluate the modules after they are cleaned in the same way as would be done with the actual product. The eventual cleaning process and the targeted number of cleaning cycles will depend on the final product and its requirements. It is obvious that there will be differences in cleaning processes between, for example, an industrial or a medical device or a device for the consumer market. Typically a textile cleaning standard will be selected to evaluate whether the fabrics that are used in the textile product meet the requirements. This same cleaning standard should be a good candidate to test the washability of the stretchable modules that are used in the product for which the standard applies. Using these standard textile cleaning procedures in an early phase of the research or product development, will reveal the different failure mechanisms. Given the hostile environment for the electronics, it might be a challenging task to meet the requirements of existing textile cleaning methods. As a general rule in the textile industry, clothing textiles should be able to endure at least 30 washing cycles to be commercially viable [1]. But again, specific requirements will depend on the targeted application.

In this chapter on washability we focus on common water-based laundry. The ISO 6330:2000 standard [2] was selected as it is representative for domestic laundry conditions. This standard describes several common washing tests (it even includes a procedure for hand wash, see Table 5.1) at several different temperatures.

More specifically, procedure 5A of ISO 6330:2000 was selected because it seemed to be a good compromise between the cleaning requirements and the technical challenges for the development of embedded, stretchable electronics. The details of procedure 5A are:

- The use of a front-loading washing machine (type A) which is most common in Europe (90%)
- A washing test at 40° C.
- Normal agitation during heating, washing and rinsing.
- Standard detergents (IEC or ECE which are slightly alkaline (pH $\sim$ 10)).

Next to domestic washing, also some industrial washing tests were performed. These industrial washing tests are considered as more severe tests as the washing temperature is higher and the washing machine is filled with a higher loading ballast. For industrial washing, procedure ISO 15797:2002 was used [3]. This is a standard with industrial washing and finishing procedures for testing of workwear. All standardized cleaning tests, performed during this PhD, were done at Centexbel (Belgian Textile Research Centre)[4]. These cleaning tests were used to evaluate the washing reliability of the stretchable modules as is described in section 5.4.

Table 5.1: Washing procedures for horizontal rotating drum machine - Type A

Procedure No.	Agitation during heating, washing and rinsing	Total load (dry mass)	Washing				Rinse 1		Rinse 2			Rinse 3			Rinse 4		
			Temp	Liquor level	Wash time	Cool down	Liquor level	Rinse time	Liquor level	Rinse time	Spin time	Liquor level	Rinse time	Spin time	Liquor level	Rinse time	Spin time
		kg	°C	cm	min		cm	min	cm	min	min	cm	min	min	cm	min	min
1A	Normal	2±0.1	92±3	10	15	Yes	13	3	13	3	-	13	2	-	13	2	5
2A	Normal	2±0.1	60±3	10	15	No	13	3	13	3	-	13	2	-	13	2	5
3A	Normal	2±0.1	60±3	10	15	No	13	3	13	2	-	13	2	2	-	-	-
4A	Normal	2±0.1	50±3	10	15	No	13	3	13	2	-	13	2	2	-	-	-
5A	Normal	2±0.1	40±3	10	15	No	13	3	13	3	-	13	2	-	13	2	5
6A	Normal	2±0.1	40±3	10	15	No	13	3	13	2	-	13	2	2	-	-	-
7A	Gentle	2±0.1	40±3	13	3	No	13	3	13	3	1	13	2	6	-	-	-
8A	Gentle	2±0.1	30±3	13	3	No	13	3	13	3	-	13	2	2	-	-	-
9A	Gentle	2	92±3	10	12	Yes	13	3	13	3	-	13	2	2	-	-	-
Simulated Hand wash	Gentle	2	40±3	13	1	No	13	2	13	2	2	-	-	-	-	-	-

5.3 Water resistance

5.3.1 Introduction

As explained in the introduction of this chapter, washability can be split up into water resistance and mechanical reliability. In this section we will discuss water resistance and the next section (5.4) will be on the mechanical reliability.

During washing the stretchable modules are in a mixture of water and soap. The encapsulant should protect the electronics from this mixture to prevent short circuits and electrical failure of the device. It should be noted that the level of encapsulation is also determined by the type of application: Should the device be functional in wet environments? (rain, sweat, underwater, ...) Should the device function during washing or is it only powered up after washing? In this Phd the water resistance of the worst case scenario where the stretchable modules are functional during immersion in a water/soap mixture was investigated.

Evaluating the functionality of an encapsulated electronic circuit that is under water is not as easy as it seems. It is the goal of this section to inform the reader on problems that may occur when determining water resistance. A measurement method to investigate the water resistance is described and evaluated. The measurement results are used to formulate conclusions on the water resistance of stretchable electronic modules.

5.3.2 Basic concept of the Water Effect Test (WET).

In order to understand the principle behind the water effect test we first spend a few words on what is called an electrochemical cell (Figure 5.2). **Electrical conductivity** is the ability of a material to conduct electric current. An electric current results from the motion of electrically charged particles in response to forces that act on them from an applied electric field. Within most solid materials a current arises from the flow of electrons, which is called **electronic conduction**. In all conductors, semiconductors, and many insulated materials only electronic conduction exists, and the electrical conductivity is strongly dependent on the number of electrons available to participate in the conduction process. Most metals are extremely good conductors of electricity, because of the large number of free electrons that can be excited in an empty and available energy state. In water and ionic materials or fluids a net motion of charged ions can occur. This phenomenon produces an electric current and is called **ionic conduction** [5].

Electrochemistry studies chemical reactions which take place in a solution at the interface of an electron conductor or **electrode** (a metal or a semiconductor) and an ionic conductor (the **electrolyte**), and which involve electron

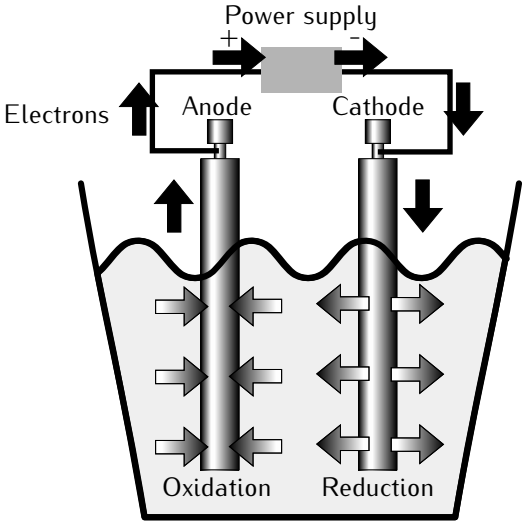

Figure 5.2: In an electrolytic cell, electrons are forced through the circuit by an external source.

transfer between the electrode and the electrolyte or species in solution. By definition an **electrochemical cell** consists of two electrodes (in our case copper) in contact with an electrolyte (in our case water+soap). And finally we come to the **electrolytic cell** which is an electrochemical cell in which a non-spontaneous reaction is driven by an external source (Figure 5.2). It will be familiar from introductory chemistry courses that **oxidation** is the removal of electrons from a species and **reduction** is the addition of electrons to a species. The electrode at which oxidation occurs is called the **anode**; the electrode at which the reduction occurs is called the **cathode**. In an electrolytic cell electrons have to be withdrawn from the anode because oxidation does not occur spontaneously, and at the cathode there must be a supply of electrons to drive the reduction. Therefore, in an electrolytic cell the anode is relatively positive to the cathode. More information on this matter can be found in Atkins book on physical chemistry [6].

In this writing we are not interested in the exact reactions that take place when one puts a stretchable electronic module in an electrolyte like water+soap. But we will use this concept of the electrolytic cell to design a measurement setup that provides us some information on the level of protection of the encapsulant used around the modules. Two electrically isolated copper tracks with a different potential (e.g., a power line) can be considered as the electrodes of an electrochemical cell.

Figure 5.3 shows a detail of the Water Effect Test sample design (WET sample). The WET sample has two closely spaced copper tracks that are

routed across the sample surface. Total track length is about 1 meter and the pitch is 200 μm (100 μm width, 100 μm spacing). In the ideal case, when these tracks are unprotected and not placed in water, no current can flow between the two tracks when a voltage is applied. In a real situation, however, there will always flow a small current between the tracks through some alternate path. In an electronic circuit this **leakage current** should be small enough to ensure proper circuit operation. The threshold to consider the leakage current as acceptable will depend on the circuit itself. When we place these unprotected tracks in a water/soap mixture a measurable current will flow through the circuit, which is the sum of the leakage currents and the current flow created by the reactions that take place in the electrochemical cell. It is likely that the portion of the total current attributed to the ionic conduction through the water will be significantly larger than the original leakage current observed before immersion in water. Encapsulating the tracks (like is done in the stretchable modules) should create a physical barrier for the water to avoid the unacceptable increase in current between the tracks.

To mimic a stretchable module, the test structure was made on a FCB (18 μm copper on 50 μm polyimide). The copper tracks were covered with OSP (Organic Surface Protection) to provide corrosion protection. This FCB was then encapsulated with a certain stretchable polymer to evaluate its protection. Evaluation was done by measuring the (leakage) current while the test sample was immersed in a water soap mixture at a certain temperature.

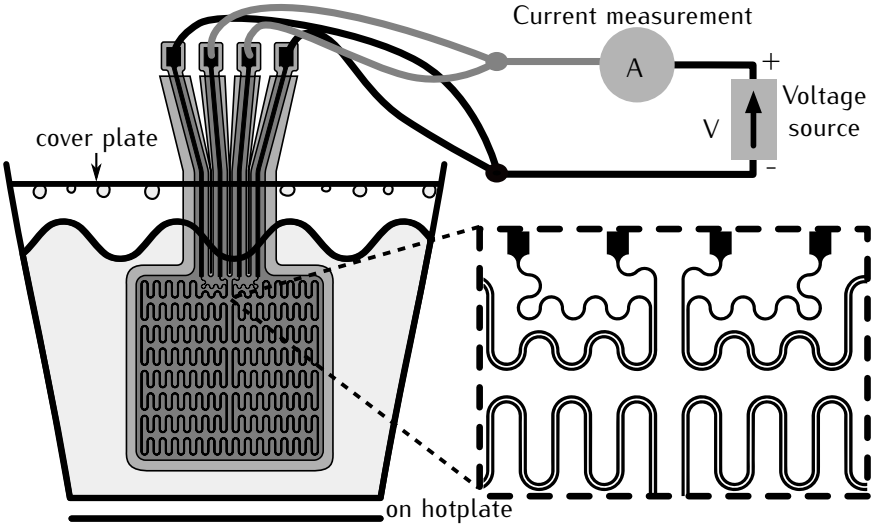

Figure 5.3: WET sample.

5.3.3 Measurement setup.

A schematic drawing of the measurement setup is shown in Figure 5.3. A dish with the water/soap mixture was placed on a hotplate. In order to prevent evaporation of the water during the test, a cover plate was used. The WET samples were placed in the water through slits in the cover plate. By doing this, the contact pads of the WET sample are positioned at the other side of the cover plate, preventing water condensation onto the contact pads. Figure 5.4 shows a picture of eight WET samples hanging in the dish.

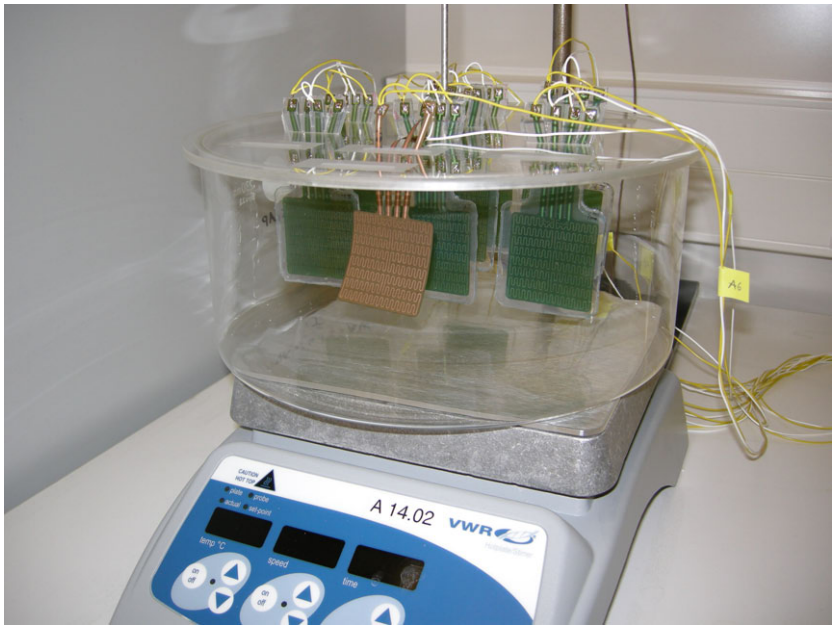

Figure 5.4: Water Effect Test setup.

The setup to measure the leakage current was built around a Keithley 2400 source meter (SMU) [7]. The SMU sources the voltage and measures the current. A Keithley 7001 switch system [8] with a 7011C quad 1x10 multiplexer card [9] was used to measure multiple samples. Only one of the 4 available banks was used to multiplex up to ten WET-samples. The interconnection scheme between the SMU and the switch system is illustrated in Figure 5.5. A Lab Windows [10] program was written to automate the measurements and to log the data in an excel file. This program was named WET-program. Communication with the equipment was done using GPIB (General Purpose Interface Bus) [11]. A National Instruments GPIB-ENET/100 Ethernet-to-GPIB controller [12] was used to allow communication between the PC and the measurement setup on an Ethernet-based TCP/IP network.

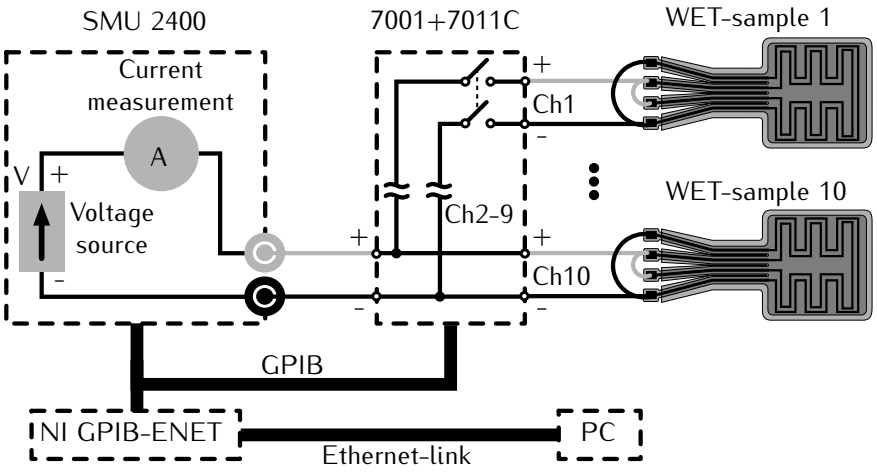

Figure 5.5: Schematic drawing of the measurement topology.

A typical WET-measurement cycle contains the following steps:

- The WET-samples are placed through the slits in the cover plate.
- The contacts from the WET-samples to the switch system are soldered.
- The different parameters (see Table 5.2) for the WET-measurement are configured in the WET-program.
- The measurement is started and the measured data is displayed and logged in real time by the WET-program.

In a WET-measurement we want to monitor the leakage current between the tracks of different WET-samples over a certain amount of time. A few parameters need to be defined before starting a measurement. These parameters are listed in Table 5.2.

Parameter [unit]	
Voltage[Volt]	5
Number of channels	8
Measure delay [sec.]	1
Time between measurements [sec.]	300 (=5min)
Number of measurements	not fixed

Table 5.2: Measurement parameters of the WET-tests.

The **voltage (V)** defines the voltage between the tracks of the WET-samples, applied by the voltage source. The **number of channels (N)** is equal to the amount of WET-samples we want to measure. In the current setup this

number was limited to ten because only one of the four banks of the multiplexer card was used. A measurement of the WET-samples was done at a predefined interval. The parameter for this interval was named the **time between measurements (TBM)**. During a measurement of the leakage current of N WET-samples, the voltage source is switched from sample to sample. This creates transition effects and therefore we allow the system to settle before taking the measurement. The waiting time between switching and measuring was named the **measurement delay (MD)**. At last we have the **number of measurements (Mnbr)** that are done during the water effect test. A tool was included in the WET-program to calculate this number based upon the total measurement time and the TBM and MD. The different parameters are shown on the diagram of Figure 5.6. This diagram shows the voltages on the different channels over time. The WET-measurement starts with applying the voltage on channel 1. After a time equal to MD the current is measured and logged. Next the voltage is switched to channel 2. Again we wait MD seconds before performing the current measurement. This continues till we have measured the current on the last channel N. After this sequence, we measured the leakage current of the WET-samples on the different channels for the first time. Now we wait for the time determined by parameter TBM before we repeat the sequence to measure the samples for a second time. During the waiting time TBM the voltage stays on the last channel N, making this channel different from the other N-1 channels. When the sequence ends for the second time we wait again TBM seconds. This is repeated till we reach Mnbr measurement sequences.

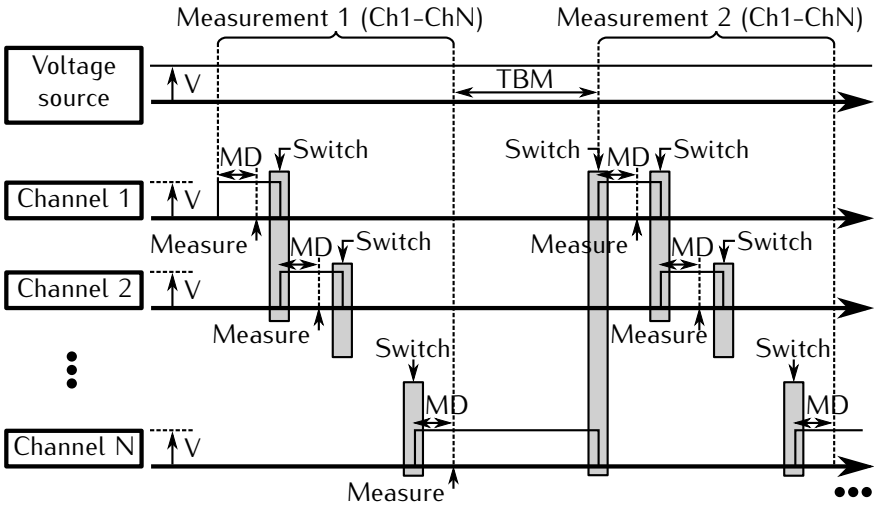

Figure 5.6: Timing diagram of a WET-measurement.

5.3.4 Overview of the different WET-measurements.

First trials

The WET-sample described and illustrated in section 5.3.2, Figure 5.3 was not the version that was designed and realized at the beginning of the WET-study. Also the WET-setup described in section 5.3.3 evolved from measurements on a single sample to the measurement of more samples simultaneously. First versions of the WET-samples were made without the polyimide support, thus starting from a copper foil in stead of a FCB. This resulted in broken copper tracks in the straight segments of the test structure, proving again the importance of the polyimide support. A next version with polyimide support was robust enough, but another problem came up during the measurements. Figure 5.7 shows the current measured between the tracks on eight PDMS WET-samples hanging in the air. These samples were not immersed in water but even then we can observe an increase in leakage current over time. Note also the difference between the WET-sample on channel 8 and the other seven WET-samples. Channel 8 is the last channel in the measurement sequence and differentiates itself from the other channels because the voltage stays on this last channel between the measurements (see section 5.3.3). This means that there is more time for electrochemical reactions on channel 8 in comparison to the other channels.

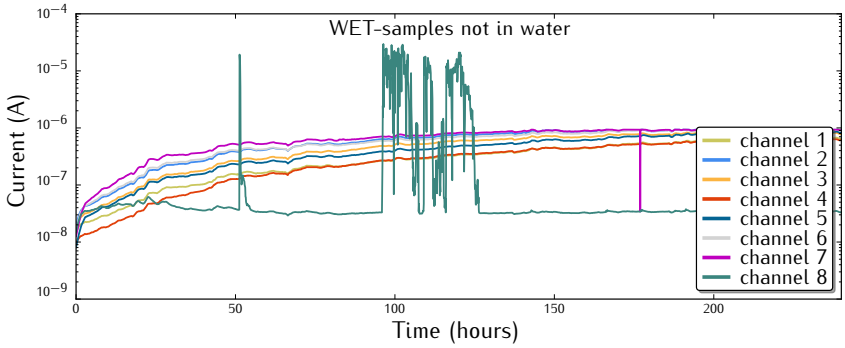

Figure 5.7: One of the first measurement with WET-samples hanging in the air.

The reason for the increase in leakage current over time can be found in the way the samples were interconnected to the switching card of the measurement setup. Figure 5.8(a) shows the soldered interconnections of the WET sample. Two problem zones are indicated on the picture. In these zones an (unwanted) additional leakage pad is created between the two tracks at a different potential. The reason for this leakage pad is contamination between the contact pads. One of these contaminants are flux residues from the solder.

Therefore the design was changed as is shown in Figure 5.8(b). By separating the contact pads physically from each other, we eliminate the possible creation of an additional leakage pad between the contact pads. Doing so has resulted in much lower, stable leakage currents when the samples were hanging in the air prior to placing them in the water (see section 5.3.5)

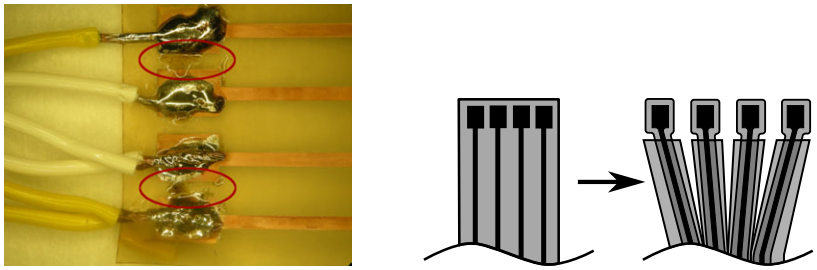

(a) Problem zones in the first layout. (b) Difference between the old and the newer version.

Figure 5.8: Change in the contact layout of the WET-samples because of leakage currents at the interconnection.

Final WET-tests

It took several iterations in changing/making WET-samples and optimizing the measurement setup to achieve the measurement results that will be described in this writing. The FCB design of the WET-samples was the one with the separated contact pads that was shown in Figure 5.3. The measurement setup that was used to measure the leakage current was the one described in section 5.3.3. Different types of encapsulation were tested. Table 5.3 gives an overview of the different tests.

WET A was a first test where the WET-samples were not protected with an encapsulation. It is obvious that this is the worst case which resulted in the highest leakage currents. In **WET B** the WET-samples were encapsulated with PDMS. This was done by casting PDMS onto the flexes. The 1200 OS primer from Dow Corning was used prior to encapsulation. The casting plates had a thickness of 1mm to achieve an encapsulation of about that thickness. TPU was used as an encapsulation in the **WET C** test. A 0.6mm thick sheet was laminated on each side of the FCB. This was done in a vacuum lamination press at 110°C using a light 'kiss pressure' to limit the flow of the TPU. The difference in the next three tests **WET D, E and F** is the additional protection of the copper tracks with a solder mask. This solder mask should act as an additional barrier to shield the tracks from water. An ELPEMER SD 2463 FLEX-HF [13] solder mask was applied by screen printing with a thickness

Test name	Description	Used samples
WET A	Flexfoil (with test structure) without any encapsulation. (type A)	4 of type A
WET B	Flexfoil encapsulated by casting 1mm sylgard 186 (PDMS) on each side. (type B)	7 of type B, 1 of type A as a reference
WET C	Flexfoil encapsulated by laminating 0.6mm PE 429 (TPU) on each side. (type C)	7 of type C, 1 of type A as a reference
WET D	Flexfoil covered with soldermask and without any encapsulation (type D)	7 of type D, 1 of type A as a reference
WET E	Flexfoil with soldermask, encapsulated by casting 1mm sylgard 186 (PDMS) on each side. (type E)	7 of type E, 1 of type A as a reference
WET F	Flexfoil with soldermask, encapsulated by laminating 0.6mm PE 429 (TPU) on each side. (type F)	7 of type F, 1 of type A as a reference

Table 5.3: Parameters of the WET-measurement.

of 20μm. In order to compare the leakage currents of the encapsulated WET-samples in tests B to F with a sample without this protection, an additional 'reference sample' of type A was added to the test batch. Pictures of a WET C and a WET F sample are shown in Figure 5.9.

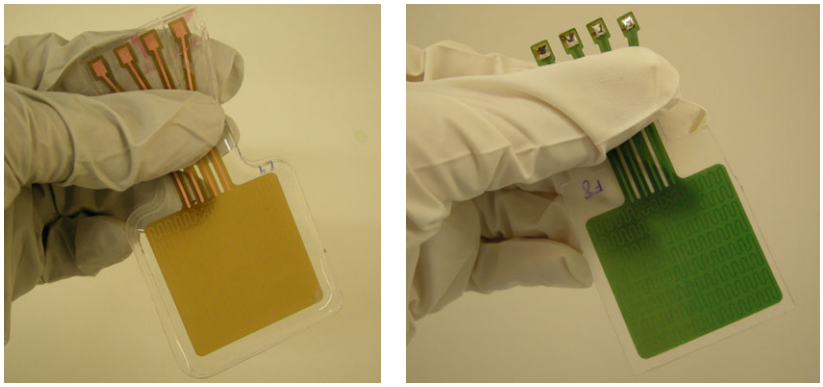

(a) WET C sample (b) WET F sample

Figure 5.9: (a) Picture of a WET-sample with PDMS encapsulation. (b) A WET-sample with solder mask and TPU encapsulation.

In every test the samples were placed in a water/soap mixture at 40°C in a dish on a hotplate. The mixture was prepared in the same way as a mixture in a washing machine in accordance with the ISO 6330:2000 standard for water-based cleaning (see section 5.2). A ratio of 2.5 g/l of the ECE soap was added to soft water with a ppm (parts per million) lower than 3. The

mixture was gently stirred during the measurement. A fresh mixture was used for every test. The parameters of the measurement configuration were the same for every test and are listed in Table 5.4

Parameter [unit]	
Voltage [Volt]	5
Number of channels	8
Measure delay [sec.]	1
Time between measurements [sec.]	300 (=5min)
Number of measurements	not fixed

Table 5.4: Measurement parameters of the WET-tests.

A voltage of 5 volt was chosen because this is more or less the expected voltage for battery powered electronics in textiles. Every 5 minutes the leakage current between the tracks of each WET-sample was logged. The number of measurements was not fixed. This was because the total measurement time was depending on the time that the used equipment was available in the lab and on the measurement itself (measurement was stopped if no significant changes in the data were observed).

5.3.5 Measurement results.

WET A results: no encapsulation.

Four WET A samples without encapsulation were tested. The measured current is shown on the graph in Figure 5.10. In the first part of the measurement, indicated with **(1)**, the samples were hanging in the air and a low leakage current of about $10^{-11}A$ was measured. From the moment the samples were put into the water **(2)**, the measured current value shoots up to about $100mA$ because of the ionic conduction through the water. A drop in the current of about a factor of ten was observed immediately after the samples were taken out of the water. During the rest of the drying period **(3)** there was only a small reduction of the current. It has to be noted that the samples were hanging in a dish without water during the drying period. At the end of the test the samples were still wet, probably because of the humid atmosphere inside the dish, which was closed with the cover plate. In the next tests the samples were dried in the air, outside the dish. Finally we observe the difference between channel 4 and the rest. Channel 4 is the last measured channel in the sequence. The voltage stays on this last channel between the measurements (see section 5.3.3). This means that there is more time for electrochemical reactions on channel 4 in comparison to the other channels.

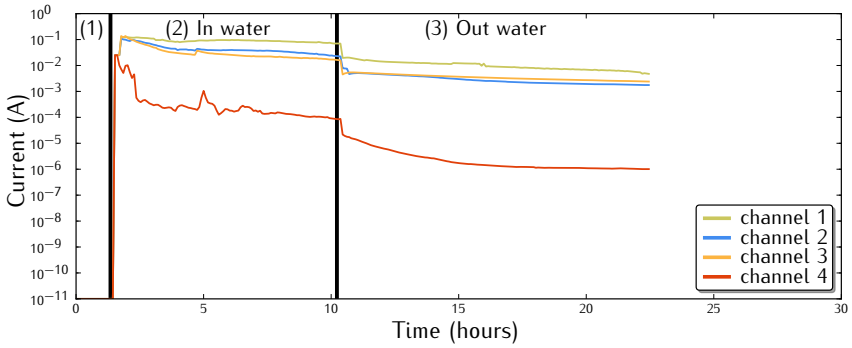

Figure 5.10: WET A.

A picture of the samples after the test can be seen in Figure 5.11. Copper oxidation took place on the 'inner track' which was at a higher potential than the other track. This is in line with the theory of the electrolytic cell explained in section 5.3.2; oxidation took place at the anode, reduction at the cathode. Also the difference between the WET-sample on channel 4 and the others was visible. The sample on channel 4 (Figure 5.11(b)), where the voltage was also applied in between the measurements, was oxidized much more aggressively than for example the one on channel 3 (Figure 5.11(a)).

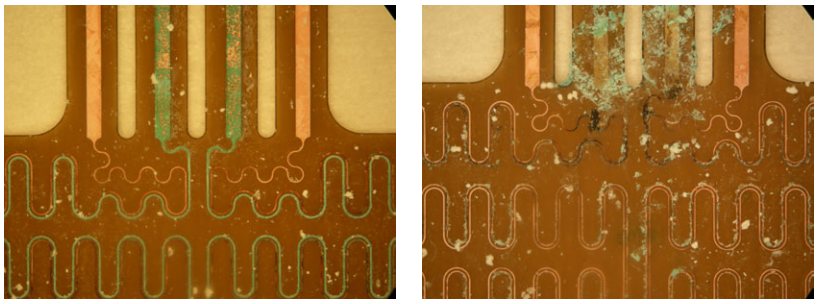

(a) After WET A on channel3 (b) After WET A on channel4

Figure 5.11: Copper oxidation at the anode (+) of the unprotected WET A samples.

WET B measurement: PDMS encapsulation.

In this test, 7 type B samples with PDMS encapsulation were used together with one reference sample of type A. The reference sample was measured on channel 7 of the measurement setup. The data is plotted in Figure 5.12.

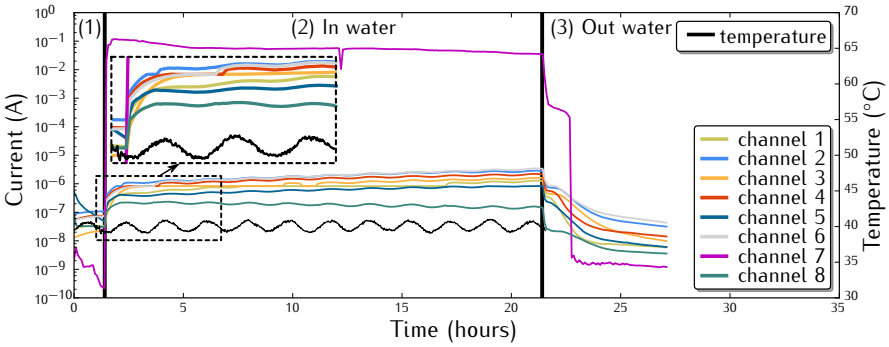

Figure 5.12: WET B.

In the first part of the measurement **(1)**, when the samples were hanging in the air, the leakage currents were in the order of $10^{-7}A$. Compared to the other five WET-measurements this initial leakage current is a factor 100 to 1000 higher. One of the reasons for this higher value can be that the primer + the PDMS lowers the electrical isolation between the copper tracks. An other possible explanation is the fact that the PDMS encapsulation was done outside the cleanroom, thus increasing the risk of contamination and dust collection prior to encapsulation. Immediately after the samples were put in the water **(2)**, the current of the reference sample on channel 7 increased to a value of $\sim 100mA$. On the other hand, the rise in current for encapsulated samples was a lot smaller. Here the current rise was also immediately visible (after the first measurement in water). Then the current increased further with a factor 10 in about an hour. From then on the current remains more or less stable in the order of $10^{-6}A$. A sudden drop in the leakage current was observed when the WET-samples were taken out of the water **(3)**. The current dropped further during the drying time of the sample.

Looking back to the current data measured during the time that the WET-samples were in the water **(2)**, we observe a ripple on the data. This ripple has a constant period of $\sim$1 hour and 55 minutes and is in phase on all samples. It is believed that this was a temperature effect caused by the temperature regulation of the hotplate. Therefore, the temperature of the water/soap mixture was measured in the next WET C measurement. This measurement was done with a type K thermocouple and the data was logged with a laptop next to the measurement setup. The measured temperature was mapped onto the graph in Figure 5.12. The temperature difference between the maxima and minima was around 1.6°C and the period was in line with the ripple in the current measurements. If we can observe these small temperature deviations in our current measurement, then it is for sure that we should also

observe the big temperature difference of $\sim$ 20°C when the WET-samples go from ambient temperature to a temperature of 40°C in the water bath and visa versa. This can explain the sudden changes in current when the samples were put in or taken out of the water.

WET C measurement: TPU encapsulation.

The difference between this test and WET B was the use of TPU encapsulation instead of a PDMS encapsulation. Again a reference sample of type A was added to the 7 WET C samples. The measured data is plotted in Figure 5.13.

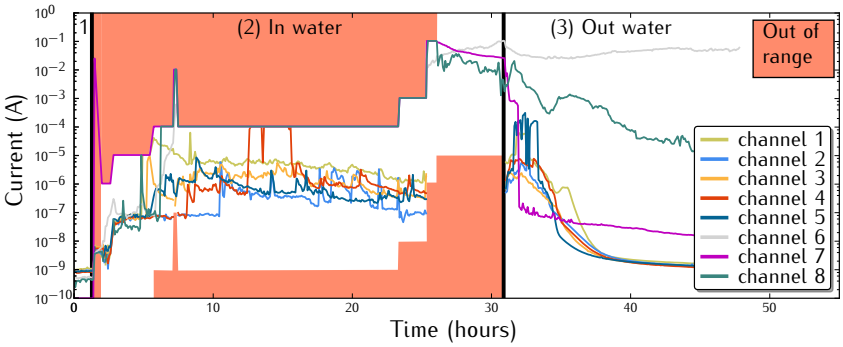

Figure 5.13: WET C.

The leakage currents during the first phase of the measurement **(1)** were in the order of $10^{-9}A$ which is a lower initial value compared to WET B. From the moment the samples were put in the water the measurement blocked. The current values were not stable enough for the SMU to perform the measurements using the AUTO RANGE function of the equipment. This function was used to span the large range of current values that were expected; from the low leakage currents to the high currents of the reference sample. This worked fine in the previous WET A and B measurements. The reason for the problem was found later during the WET E measurement (see further). It was the additional laptop for the water temperature measurement that caused too much noise. During the WET C measurement the problem was solved by fixing the range instead of letting the SMU search for the right range. This implies that the range is limited now to five decades. The measurement range is indicated on the graph. It was manually changed from time to time to check channels with currents limited by the upper boundary of the measurement range.

We observe large current peaks in the period when the WET C samples were immersed in water **(2)**. Especially on channel 6 and 8, where the measured current was as high as the current in the reference sample on channel 7. The reason for the bad result can be seen on the pictures of Figure 5.14.

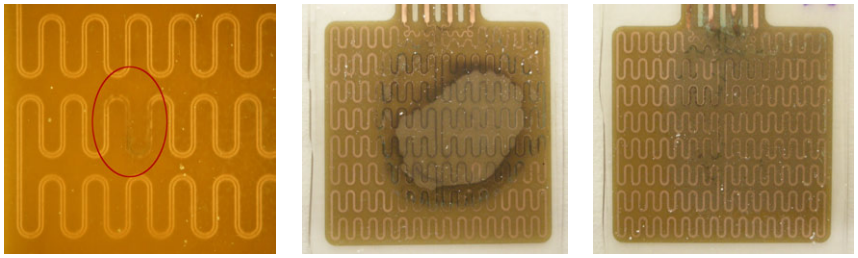

(a) After WET C on channel1. (b) After WET C on channel6. (c) After WET C on channel8.

Figure 5.14: Oxidation of copper tracks because of delamination of the TPU

Apparently there was bad adhesion between the FCB and the TPU, causing the TPU to delaminate during the measurement. The reason for the bad adhesion can be the low 'kiss pressure' used during the lamination or a too low lamination temperature. The delamination made it possible for the water to diffuse through the TPU and to create a water film between the copper tracks and the TPU. This entrapped water was detected by an increase in leakage current, proving the effectiveness of the measurement. During the drying period **(3)** the current decreased again. Except on channel 6 where water was still trapped in the sample after the drying period.

WET D measurement: solder mask.

In this test the flexfoils in the WET-samples were completely covered with solder mask, so too were the copper tracks. No other additional encapsulation was applied. The measurement data is plotted in Figure 5.15.

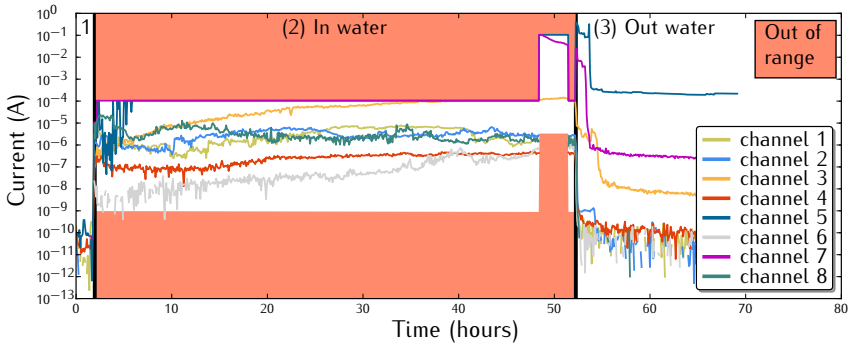

Figure 5.15: WET D.

Also during this measurement the water temperature was monitored, causing the AUTO RANGE function of the SMU to fail. Therefore, the measurement range was fixed again from the moment the samples were in the water. There was a very quick increase in the leakage current when the samples were put into the water. This rapid response is probably due to the small thickness of the solder mask ($\sim 20\mu$m). Overall we can say that the currents of the samples on channels 1,2,4,6 and 8 are more or less in the same range as the best samples of the WET C test (range $10^{-7}A$ to $10^{-5}A$). This should mean that there was water leakage through the solder mask at some spots but not everywhere. The larger currents measured on channels 3 and 5 indicate that there was a lot more water leakage on these WET-samples. The pictures in Figure 5.16 and Figure 5.17 confirm these findings, based upon visual inspection.

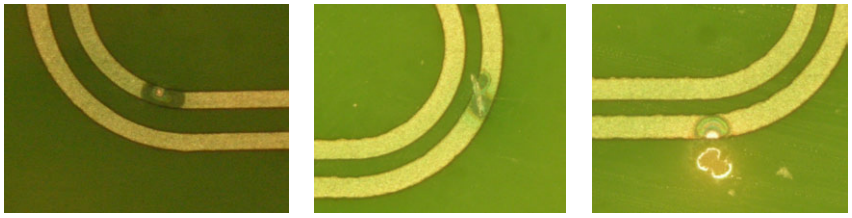

(a) Pinhole on channel1. (b) Crack on channel2. (c) Pinhole on channel2.

Figure 5.16: Pinholes and cracks in the solder mask causing an increase in leakage currents.

In the pictures of Figure 5.16 we see two types of small defects in the solder mask; pinholes and a scratch or crack. Because of these defects we observe an increase in current, which is larger if more defects are present. The pinholes are present due to bad solder mask printing. The WET-samples were made on 9*12 inch (228*305mm) substrates. The solder mask printing on this substrate size appeared not to be ideal in our lab. During printing the boards were fixed in the screen printer on a vacuum table. This vacuum was not strong enough to hold the boards during screen release. Therefore tape was used at the corners of the board to improve the fixing. However the board was still able to bend up during release, which resulted in uneven prints and pinholes. Some zones on the board were printed better than others and the best printed WET-samples were selected for the WET-measurements. These badly printed samples were still very useful because they showed the effects of the water in case of a bad solder mask print. Solder mask printing is a mature and well know process step in the industry, where even prints are a must. In our lab we need some changes to the machine and additional optimization to achieve good solder mask printing on the 9*12 inch substrates.

Figure 5.17 shows pictures of the WET-samples on channel 3 and 5, where the largest leakage currents were observed. The sample on channel 3 shown in Figure 5.17(a) had a very bad, uneven solder mask print. The copper tracks were affected by the water over the whole WET-sample surface. A detail is shown in Figure 5.17(b). The sample on channel 5 had a badly etched spot as can be seen on Figure 5.17(c).

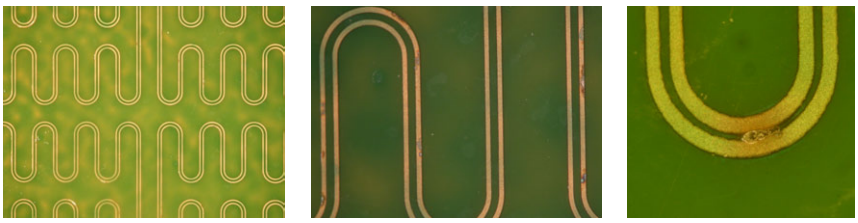

(a) Uneven solder mask on channel3.

(b) detail on channel3.

(c) Bad etched on channel5.

Figure 5.17: Samples on channels 3 and 5 were showing highest leakage currents due to bad solder mask printing and a bad etched spot.

WET E measurement: solder mask and PDMS encapsulation.

The WET E samples were made in the same way as the WET B samples, but with an additional solder mask. Solder mask printing was done in the same way as with the WET D samples resulting in a print which was acceptable but not perfect. The leakage currents are plotted in Figure 5.18

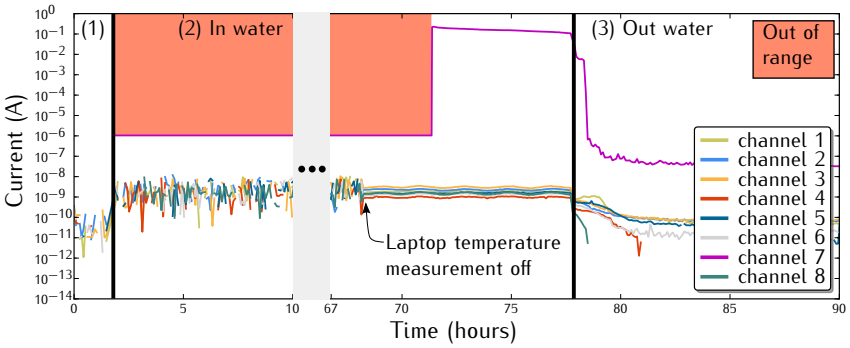

Figure 5.18: WET E.

Also during this measurement the water temperature was monitored, causing the AUTO RANGE function of the SMU to fail. But this time the temperature measurement was stopped before the end of the measurement and the

laptop was removed from the setup. After removing, the measurements were more stable than before. Later on the range was set again to the auto range without any problem. This taught us that it was the presence of the laptop that was causing the additional noise on the measurements. After laptop removal the temperature effect of the hotplate regulation was again visible in the leakage current data.

If we compare the graph of the WET E measurement with the one of the WET B measurements (Figure 5.13), the following observations are made:

- The initial leakage current before immersing the WET E samples was a factor 100 to 1000 lower compared to the WET B samples.
- The leakage current measured during the period the WET E samples were in the water was around $10^{-9}A$. In the case of the WET B samples this was around $10^{-6}A$.
- In both measurements the leakage currents remained stable when the samples were in the water.

From this we can conclude that the leakage current of PDMS encapsulated WET samples was lowered by adding the solder mask. This is not related to the additional protection from water due to the solder mask, but because the leakage currents were also lower prior to water immersion. A possible reason for the higher leakage currents of the WET B samples was already given. Nevertheless, we can assume that the solder mask will also give an additional protection in case the PDMS encapsulation would have a defect.

WET F measurement: solder mask and TPU encapsulation.

In the last of six WET measurements, the WET F samples were protected by a solder mask and a TPU encapsulation. No water temperature measurement was performed, avoiding the problem with the auto range function. The data is plotted in Figure 5.19.

These leakage currents were comparable with the good result of the previous WET E measurement, but compared to the WET C measurement this was a big improvement. Without the solder mask there were delamination problems with the TPU encapsulation. With the soldermask the TPU adhesion was better. This ensured that the solder mask + TPU provided a good protection for the copper tracks, resulting in low leakage currents when immersed in water.

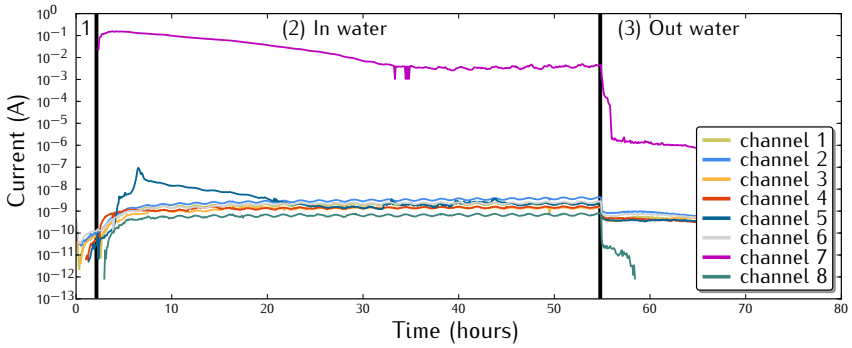

Figure 5.19: WET F.

5.3.6 Conclusions.

The water resistance of stretchable modules was investigated by tests based on leakage current measurements. Six different WET-sample types were tested; without encapsulation, with PDMS and TPU encapsulation and the same but with an additional solder mask. These samples mimic a stretchable module because they were made in the same way, with the same materials. Attention was given to the importance of the test sample design to avoid faulty current measurements caused by leakage currents at the contact pads. Increases in leakage current, indicating bad water resistance, could be related to visual damage of the sample in all cases. This proves the effectiveness of the developed test method. The following conclusions can be drawn:

- The test sample design is very sensitive for leakage currents. Without encapsulation currents up to 100 mA were reached during water immersion. With encapsulation the temperature regulation of the hotplate was visible in the current measurement.
- Overall we can say that all encapsulation types have the potential of being a good encapsulation with respect to water resistance. In all cases the leakage currents were lowered significantly compared to the reference sample without encapsulation.
- The WET B samples with a PDMS encapsulation had a higher initial leakage current compared to the others. One of the reasons for this higher value can be that the primer + the PDMS lowers the electrical isolation between the copper tracks. Another possible explanation is the fact that the PDMS encapsulation was done outside the cleanroom, thus increasing the risk of contamination and dust collection prior to encapsulation. Besides that, the leakage currents during the water immersion remained stable, indicating good protection of the PDMS encapsulation.

- Bad adhesion of the TPU to the FCB was found to be the problem of increased leakage currents on the WET C samples. Some of the samples showed better adhesion than others, leading to less increase in leakage current. However this adhesion problem should be solved first, prior to formulating a conclusion on the protection of the TPU encapsulation.
- The solder mask on its own has proven to be an additional protection for the water during the WET D measurements. However, uneven printing and pinholes caused increases in leakage currents, proving the importance of an even solder mask print.
- Best results were obtained with either PDMS or TPU encapsulation in combination with the solder mask. In both cases the leakage currents remained stable around $10^{-9}A$. This proves good water resistance during water immersion, measured up to 55 hours.

5.4 Mechanical reliability during washing

5.4.1 Introduction

In the previous sections, water resistance of stretchable electronic modules was analyzed. Next to water resistant, these modules should be robust enough to survive the mechanical 'abuse' they encounter during typical textile cleaning processes. The mechanical reliability of the stretchable modules during washing will be referred to as 'washing reliability'. During this PhD, different water-based cleaning processes were used with different test sample designs. All cleaning procedures were performed at Centexbel, in accordance to an appropriate textile cleaning standard. We will discuss the washing reliability of textile integrated blinking LED modules and of a test sample for SMD contact reliability assessment.

5.4.2 Blinking LED test sample

5.4.2.1 Test sample description.

The blinking LED module presented here was originally designed as a technology demonstrator to illustrate the concept of interconnecting different PDMS encapsulated modules with a textile integrated electric wire. In a later phase these blinking LED modules were also used to conduct a first number of washing tests which are described in the next section (5.4.2.2). Every blinking LED module is a flexible island with four LEDs that are blinking two by two. Information on the design is found in section 6.3). Figure 5.20 shows a test sample with two blinking LED modules on a knitted fabric. The substrates were fabricated using the laser structuring method described in section 2.3.2, starting

from a 25μm thick PI FCB with 9μm Cu. The components were soldered with lead free solder in a vapour phase reflow oven. Encapsulation of the circuit was done with Sylgard 186 using the process described in section 2.4.1. After module placement on textile, the electric wires were soldered and the contact openings in the PDMS were sealed with PDMS (3-4241 dielectric gel, Dow Corning). The LED module with the corner shape of Figure 5.20 has two places for interconnecting the power. At one side the power arrives and at the other side the power is further distributed to another module.

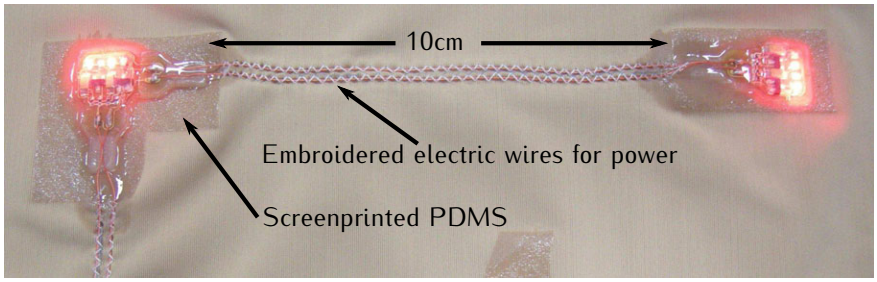

Figure 5.20: Blinking LED test sample on knitted fabric.

5.4.2.2 Washing procedure.

Three blinking LED samples of the type shown in Figure 5.20 were used for washing tests. They are referred to as L1, L2 and L3. Given the fact that these were the first washing tests with PDMS encapsulated electronics on textile, these three samples were used to explore different washing tests. The wash test history of each sample is given in Table 5.5.

Test sample	Washing tests
L1 and L2	Immersion in hard water, 3 hours, 60°C
	Immersion in hard water + soap, 3 hours, 60°C
	Gyro wash, 30 min, 60°C
L1	5x domestic washing, protective bag, open air drying
	5x industrial washing at 40°C, tumble drying
	1x industrial washing at 65°C, tumble drying -> L1 broken
L2	5x domestic washing, without protective bag, open air drying -> L2 broken after the sixth time
L3	1x domestic washing, protective bag, tumble drying -> L3 broken after 2nd time

Table 5.5: Overview of the different washing tests each test samples went through.

Immersion tests of blinking LED samples.

- Step 1: immersion in water.

  In a first step, two samples (L1 and L2) were immersed in hard water at 60°C. The recipient with samples was horizontally shaken (ca. 25 cycles per minute - amplitude of 2cm). After 3 hours, the samples were removed from the liquid and dried overnight. When testing the dried samples it appeared that all LEDs on both samples were still working.

- Step 2: immersion in water-soap mixture

  Based on the positive results of Step 1, the same procedure was repeated using again L1 and L2 but this time soap was added to the water. The soap was of the type used for standardized textile washing (so called ECE Soap), the concentration was 2.5g/l as this is also the concentration used in the actual machine washing tests (see further). Again the samples were removed from the liquid after 3 hours and subsequently dried overnight. When testing the dried samples it appeared that all LEDs were still working.

Gyro washing tests of blinking LED samples.

In the next step, samples L1 and L2 were subjected to a gyro washing instead of immersion. The term 'gyro washing' refers to a simplified washing method, used for evaluation of e.g. color fastness of textile materials. The equipment consists of several separate vessels, per vessel only one sample was put in together with the water-soap mixture (800ml hard water, 2g ECE soap). The sample was positioned around a plastic tube that fitted in the vessel in order to limit the mechanical action on the sample. The vessels were swung around and kept at the washing temperature of 60°C via the 'au-bain-marie' method. This washing was performed during 30 minutes. After this gyro washing, the samples were dried overnight. Again all LEDs on both L1 and L2 remained functional.

Standardized domestic washing of blinking LED samples.

Given the encouraging results obtained with the immersion and gyro washing, domestic washing was performed according to the standard ISO 6330 - method 5A. This means washing at 40°C, together with other items. Two more parameters were varied: (i) the samples were added to the washing load with or without a protective bag and (ii) the drying method was varied: open air or tumble drying. During tumble drying, the temperature goes up to a maximum of 50°C.

The results for the different tests:

- With a protective bag and with open air drying: Sample L1 was washed and dried this way, it was still functional after repeating five times the washing and drying procedure. Then, the test was stopped and sample L1 was used for a different type of testing (see further).
- Without protective bag and with open air drying: Sample L2 was washed and dried this way. It was still functional after repeating the washing and drying procedure for five times. But after the 6th washing and drying cycle, the sample was no longer functioning.
- With a protective bag and with tumble drying: Sample L3 was tested this way, after the 1st time the sample was still fine but already after the 2nd washing and drying cycle, the sample was no longer functioning.

Standardized industrial washing on blinking LED samples.

Next to the domestic washing, the goal was also to perform industrial washing. This was performed according to the standard 'Textiles - Industrial washing and finishing procedures for testing of workwear' - ISO15797. The temperature during washing was either 40°C or 65°C. However, compared to the domestic washing, the total load in the washing machine is larger, implying that stronger mechanical forces are working on the sample. In this case only tumble drying was performed, with temperatures reaching up to 80°C. To do the test, sample L1 was simply added to another washing load. After repeating the industrial washing at 40°C and drying for five times the outcome of the test was that both LED groups of L1 were still functioning. Given this good and somewhat unexpected result, a washing test was performed at 65°C. After the first washing, one group of LEDs did not function anymore. Between the 2nd and 5th time washing, the other group of LEDs was also affected: instead of blinking, the LEDs of that group were now burning continuously. This indicates a serious defect in the circuitry, so a decision was made to stop the testing on sample L1.

5.4.2.3 Analysis and evaluation of blinking LED samples after failure.

After the LED modules were not blinking anymore, the samples were subjected to failure analysis. At first the conductivity of the interconnections to the power module were tested. This was done by putting needles through the PDMS to make contact with the pads. When powered up, all the LEDs were blinking again, indicating that the samples suffered damage only at the

interconnections. X-ray imaging revealed that some of the electrical wires at the interconnection were broken. Optical and X-ray images of a broken wire at the interconnection are shown in Figure 5.21.

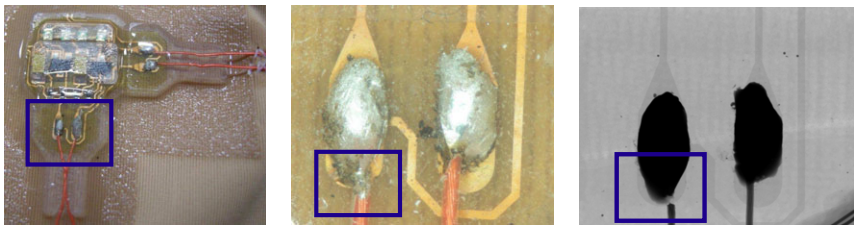

(a) Module interconnection. (b) Detail (c) X-ray of the broken wire.

Figure 5.21: Images of the broken contact.

This result teaches us that the electronic circuit is still functional after washing and that the failure arises at the interconnection. It is not the solder ball that releases from the copper pad, but the wire that breaks at the solder ball. One of the causes of a broken wire at this position can be bad stripping of the insulation around the wire. The insulation stripping was done manually and if the wire was cut to deep, this can induce a weaker zone in the wire at the position of the cut. If the wire is placed in a static application this is less of a problem, but when the wire is bent multiple times it can crack. Nevertheless, this means that the forces on this weak spot should be lowered to prevent failure. This can be done by using a PDMS (or other material) with a higher hardness as a sealant or by creating a stiffer zone at the transition. Also a small SMD connector can be used to make a more reliable connection.

5.4.2.4 Conclusions on washing tests of blinking LED modules.

Different washing tests were performed on textile integrated blinking LED modules. During the immersion in water or gyro washing no or limited mechanical forces are applied to the test sample. After these gentle tests no damage was observed on test samples L1 and L2. The other tests have shown that the PDMS encapsulated LED modules can withstand up to a certain degree standard domestic or industrial textile washing. However there were differences in sample lifetime: sample L2 survived 5 domestic washing cycles whereas sample L1 also survived 5 additional industrial washing cycles. Tumble drying on the other hand seems, not surprisingly, a harder process than the washing itself and sample L3 was broken after the second cycle. Still, one sample (L1) managed to survive five cycles. Reasons for these differences

in lifetime can be found in the random nature of a washing or tumble drying cycle, but also in the observed failure mechanism. On all test samples the failure was found at the interconnection between the blinking LED module and the electric wire for powering the modules. The wire was broken at the interface with the solderball, which is the weakest point when bending the wire. Keeping in mind that the LED modules themselves were still functional, we can conclude that these first washing tests are very promising with respect to the washing of PDMS encapsulated modules.

5.4.3 Washing reliability of component contacts

After the evaluation of the first washing test with the blinking LED test sample, it became clear that more dedicated tests where needed. This section includes the different tests that were designed and evaluated to test washing reliability. These tests are used to detect the different (mechanical) failure modes when washing textile integrated stretchable electronics. Test samples are named using the following naming convention: WR1_R2S4 which stands for washing reliability test number 1, run 2, sample 4.

5.4.3.1 Test sample description.

The purpose of the WR tests is to evaluate the solder contacts of SMD components on a flexible island when a molded module is washed several times in a standard washing machine.

In order to avoid problems with broken wire interconnections the sample was designed with measurement pads that can be accessed through openings in the PDMS. Figure 5.22 shows the names of the measurement pads.

Four different types of SMD component packages which are often used in electronic circuits are tested: 0402, 0603, TSSOP28 and QFN32. One test sample contains 50 SMD resistors and four dummy IC's. In total there are 220 contacts that can cause failure during washing. It makes no sense to measure all contacts on each sample individually. Therefore the contacts were grouped in daisy chains to reduce the number of measurement pads. The 0402 (R1-R25) and 0603 (R26-R50) components are 0 Ohm resistors which are interconnected in series. Between every 5 resistors there is a measurement pad to detect if there are discontinuities in the chain. These pads are named P1 to P11. The TSSOP28 (Dummy 1 and 3) and QFN32 (Dummy 2 and 4) components are dummy IC's from Practical Components (A-TSSOP28T-4.4mm-DC-Sn and A-MLF32-5mm-.5mm-DC-Sn). The pins of these IC's are internally interconnected in groups of 2. A daisy chain with measurement pads is created to detect broken contacts. Figure 5.23 shows the layout of the daisy chains in the dummy IC's.

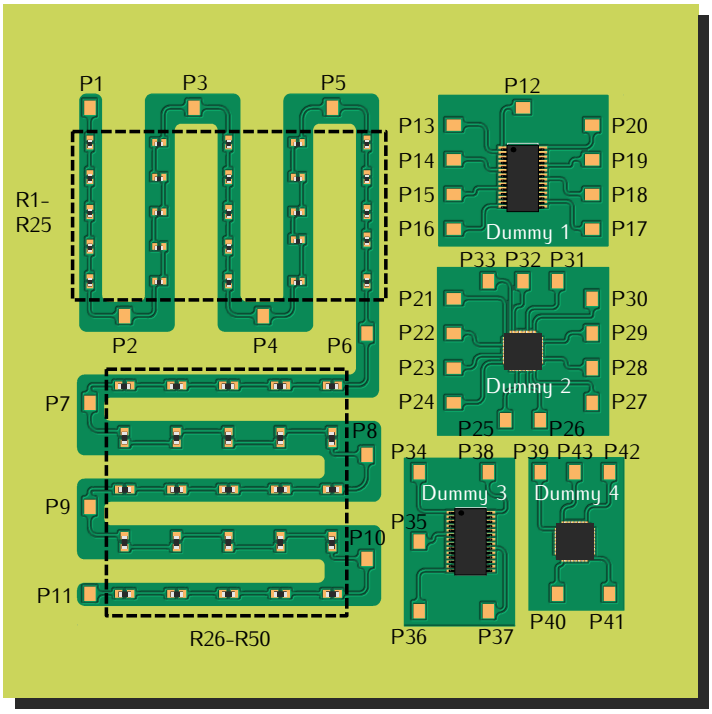

Figure 5.22: Measurement pads of the wash test sample.

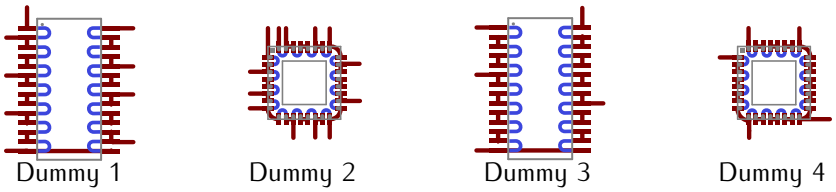

Figure 5.23: Daisy chains in the different dummy IC's

The samples were made using the laser structuring method described in section 2.3.2. A FCB with the test pattern was laminated with wax on a rigid carrier board. This FCB was laser cut to define flexible islands. The components were soldered with lead free solder in a vapour phase reflow oven. The component islands were encapsulated using sylgard 186 PDMS. Finally the modules were attached to a fabric using the screen printing technique described in section 3.2. Figure 5.24 shows a picture of a WR1 test sample.

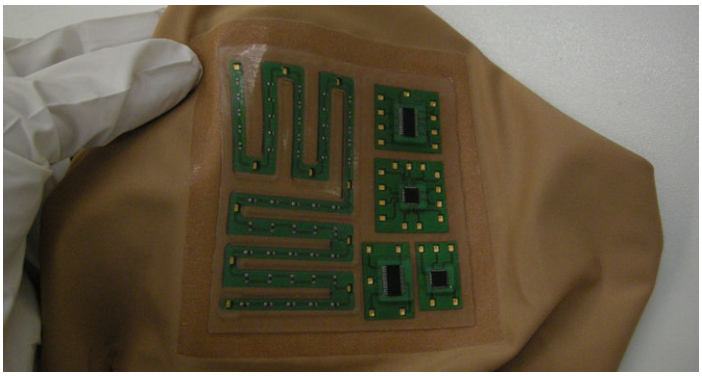

Figure 5.24: Wash test sample (WR1) on a knitted fabric.

5.4.4 WR1

WR1 represents the first of two wash tests with different test designs that were developed during this PhD. The differences between these designs are explained in section WR2 5.4.5.

5.4.4.1 WR1 assembly information

In the washing reliability tests the SMD solder contacts are evaluated. Therefore it is important to know how the solder joints were established. An overview of the assembly information of the WR1 test samples is given in Table 5.6. The test samples were processed individually on 10cmx10cm FR4 carriers. Solder paste dispensing was done manually, followed by manual placement of the different SMD's. Reflow of the solder paste took place in a vapour phase oven at the cleanroom facilities of CMST.

Board size	10cm x 10cm (=one WR1 sample)
Solderpaste dispensing	Manual
Component placement	Manual
Soldering	Vapour phase @ CMST

Table 5.6: Assembly info for WR1 samples.

5.4.4.2 WR1 test information

Ten WR1 test samples were used in the first wash tests. The molded test modules were attached on a knitted or woven fabric. These two types of fabrics were used to make a difference between stretchable (knitted) and less

stretchable (woven) fabrics. The test samples were subjected to an industrial or domestic washing cycle, followed by a tumble drying cycle. These samples were not put in a protective bag. An overview is given in Table 5.7.

Test sample	Fabric	Wash test
WR1_R2S1 to S3	Knitted	Industrial washing - 65°C - ISO15797 (no bag)
		Tumble drying (up to 80°C)
WR1_R2S4,S5,S12	Knitted	Domestic washing - 40°C - ISO 6330 (method 5A, no bag)
		Tumble drying (up to 50°C)
WR1_R2S8 to S11	Woven	Domestic washing - 40°C - ISO 6330 (method 5A, no bag)
		Tumble drying (up to 50°C)

Table 5.7: Wash test information for WR1 samples.

5.4.4.3 Wash test results

The test patterns on the wash test sample (see Figure 5.22) are grouped in different daisy chain types. Table 5.8 gives an overview of the different types. Type A and B are the chains with SMD resistors. There are 5 resistors between each pair of measurements points, resulting in 10 contacts in the chain. Type C,D,G and H are chains on the contact pads of the TSSOP dummy IC's, type E,F and I representing the chains of the QFN dummy IC's. Differences in these chain types are based on the number of IC contacts in the chain.

Chain Type	Package	Contacts in chain	Measurement points
A	0402	10	P1-P2, P2-P3, P3-P4, P4-P5, P5-P6
B	0603	10	P6-P7, P7-P8, P8-P9, P9-P10, P10-P11
C	TSSOP	2	P12-P13, P6-P17
D	TSSOP	4	P13-P14, P14-P15, P15-P16, P17-P18, P18-P19, P19-P20
E	QFN	2	P21-P22, P23-P24, P24-P25, P26-P27, P27-P28, P29-P30, P30-P31, P32-P33
F	QFN	4	P22-P23, P25-P26, P28-P29, P31-P32
G	TSSOP	6	P34-P35, P36-P37
H	TSSOP	8	P35-P36, P37-P38
I	QFN	4	P39-P40, P40-P41, P41-P42, P42-P43

Table 5.8: Different daisy chain types in the WR sample.

Figure 5.25 gives an overview of the chain status of 3 samples (S1 to S3) with the WR1 design on a knitted fabric after one industrial washing cycle followed by a tumble drying cycle. For each chain type it is shown how many of the chains are still conducting and how many are broken due to a mechanical failure. Averages in percent of the number of conducting chains for each chain type are placed in labels onto the graph. All resistor chains are open (type A and B). There is little difference between the results for QFN and TSSOP packages. Contacts in the chains of the QFN IC's (E,F,I) survived the test better than the contacts in the chains of the TSSOP IC's (C,D,G,H).

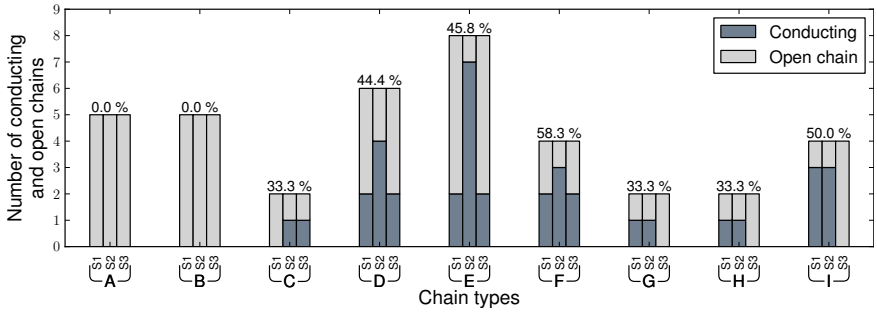

Figure 5.25: Chain status after one washing and tumble drying cycle (WR1, industrial, knitted).

Figure 5.26 gives an overview of the chain status of 3 test samples with the WR1 design on a knitted fabric after one domestic washing cycle followed by a tumble drying cycle. Only one resistor chain survived the first washing and tumble drying cycle. In this test the difference between the QFN and TSSOP packages is more visible. Less of the chains of the QFN IC's (E,F,I) were open in comparison with the contacts in the chains of the TSSOP IC's (C,D,G,H). The overall results for the QFN and TSSOP packages are better than the results of the industrial washing shown in Figure 5.25.

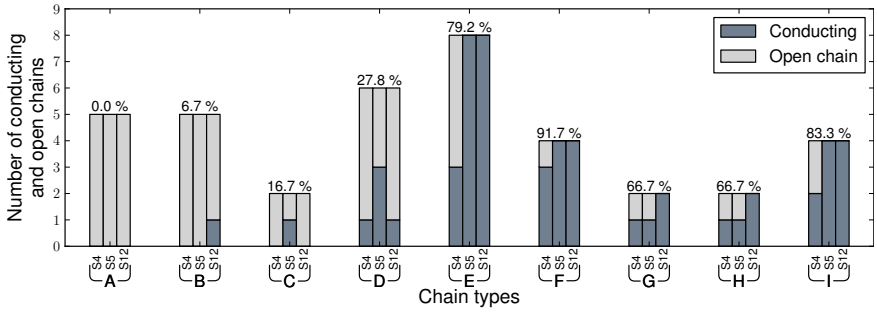

Figure 5.26: Chain status after one washing and tumble drying cycle (WR1, domestic, knitted).

Figure 5.27 gives an overview of the chain status of 4 test samples with the WR1 design on a woven fabric after one domestic washing cycle followed by a tumble drying cycle. The woven fabric gives more strength to the encapsulated test modules, which leads to less broken chains in comparison with the results of the test modules on knitted fabrics. Looking to the different chain types, the resistor chains are again most prone to failure. Almost all resistor chains are open (type A and B). Also in this test the QFN IC's (E,F,I) are scoring better than the TSSOP IC's (C,D,G,H).

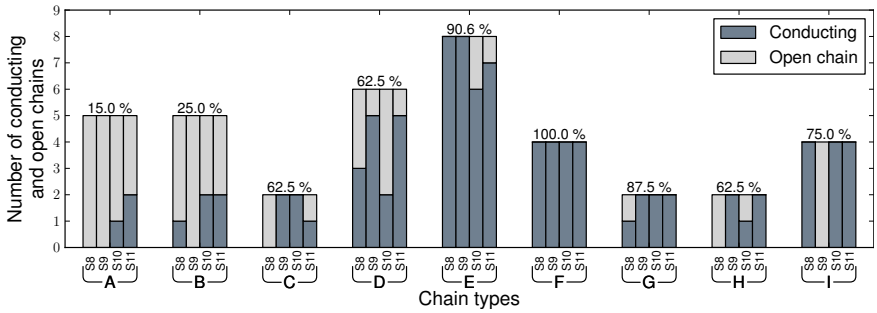

Figure 5.27: Chain status after one washing and tumble drying cycle (WR1, domestic, woven)

Test samples WR1_R2S8 to S11 are showing the best results (Figure 5.27) and were subjected to two more domestic washing and tumble drying cycles. As an example Figure 5.28 shows the chain status of sample S8 after each cycle. The graph shows that it is not only during the first washing and drying cycle that the weak connections are broken. The trend observed is that the number of broken connections increases with the number of washings, indicating a progressive destruction of the sample. The same trend was found for the other test samples after multiple washing cycles.

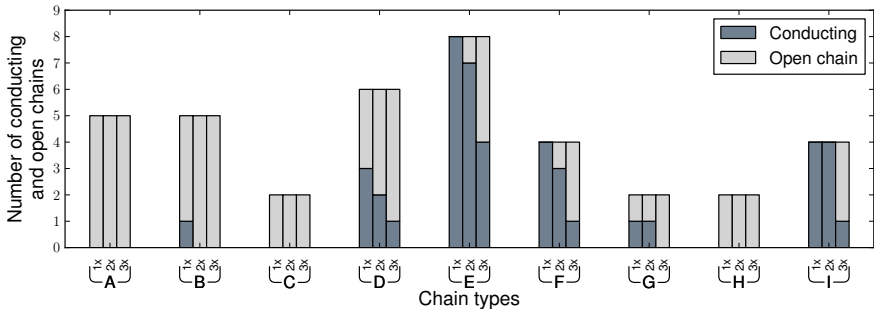

Figure 5.28: Chain status of S8 after multiple washing and tumble drying cycles (WR1, domestic, woven)

5.4.4.4 Test sample failure analysis

First we consider the chains with the 0 Ohm resistors (chains A and B). The conductivity was lost here between almost all measurement pads. Analysis showed that failure occurred near the contact pads of the SMD resistors, at the transition between pad and track. A crack in the copper track led to a loss in conductivity. The crack arises when the substrate bends too much during washing (Figure 5.29(a)). The SMD resistor together with the thicker part of the solder creates a rigid zone. Next to it, on the track, the solder is thinner. Because the solder is brittle and this zone tries to bend, a crack propagates through the solder and the underlying copper track. In Figure 5.29(b) one can also see that the (rigid) pad lifts from the polyimide when the sample is bent.

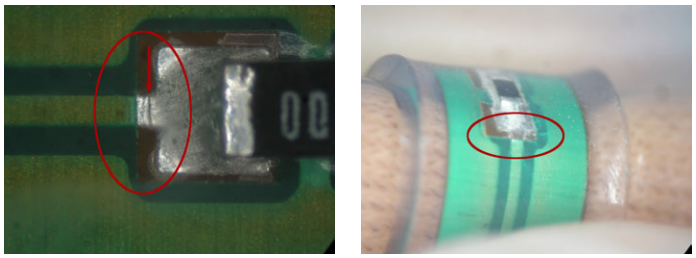

(a) Crack in solder and copper track. (b) Copper pad lifting from polyimide.

Figure 5.29: Failures at SMD resistors

Secondly, when we look to the interconnections of the TSSOP package, another problem becomes visible (see Figure 5.30). The leads, together with the solder and copper pad, are pulled from the FCB, starting at the corner of the package. At the moment the sample is bent, there is too much force on the leads because the large rigid TSSOP package cannot bend. Also the QFN packages have broken contacts due to this bending.

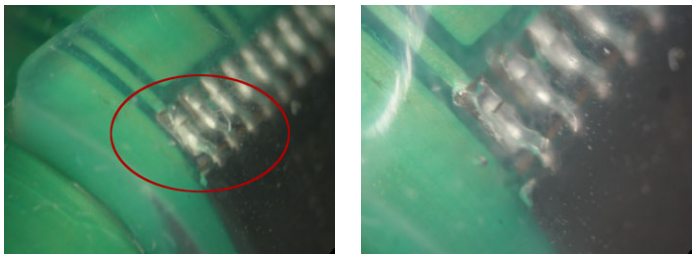

(a) Lifted pad at the TSSOP lead. (b) Detail of the lifted pad.

Figure 5.30: Failures at the TSSOP leads

5.4.4.5 Conclusions on the WR1 tests

Several washability tests using the WR1 design on textile substrates were performed. Briefly summarized, the following main conclusions can be deduced:

- Most of the connections with the SMD components in the WR1 design failed already after one washing and tumble drying cycle.
- The resistor chains are most prone to failure. No difference was observed between the 0603 and the smaller 0402 package.
- The pad layout of the SMD resistors should be redesigned to prevent the cracking and pad lifting.
- The contacts in the chains of the QFN IC's survived the tests better than the contacts in the chains of the TSSOP IC's.
- The TSSOP and QFN contacts need additional reinforcement to lower and shift the stresses on the contact pads when bending.
- WR1 test structures on a woven fabric are better suited to cope with the cleaning process than structures on knitted fabrics. The woven fabric gives more strength to the encapsulated test modules.
- Domestic washing shows better results than industrial washing because it is a milder washing cycle, inducing less forces on the solder contacts.
- Electrical contacts are gradually destroyed by the mechanical action during washing, i.e. the effect becomes worse per washing cycle.
- Tumble drying is a step with a severe impact and should be replaced by line drying in the next washing tests.

5.4.5 WR2

The purpose of the WR2 test was to improve the WR1 test design. Changes were made to the 0402 and 0603 pad layout and FR4 stiffeners were used to reinforce the TSSOP and QFN contacts. The samples were processed on a 9inchx12inch (22.8cmx30.5cm) board instead of a 10cmx10cm board. Components were placed automatically instead of manually.

Figure 5.31 shows the 9x12 inch FCB. The FCB was made at Electronic Apparatus using DuPont AP8515 (= 25um PI + 18um Cu). Each FCB contained 6 wash test samples. The one in the lower right corner served as a reference sample and had the same design as the WR1 test samples. The other 5 contained the improved design.

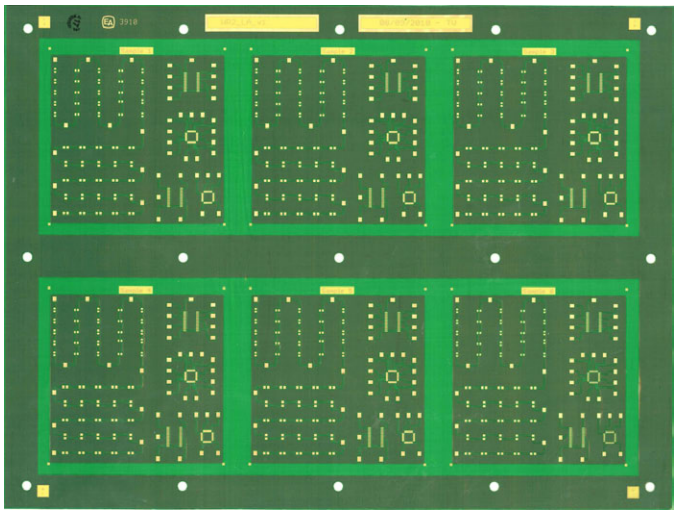

Figure 5.31: 6 wash test samples on a 9inchx12inch FCB (22.8cmx30.5cm).

5.4.5.1 Changes in the design.

The aim was to change the pad layout to avoid fragile zones where a crack could be formed. In the WR1 design, the solder mask opening was bigger than the size of the copper pad (see Figure 5.32(a)). This is to create some margin for aligning the solder mask. But because of this bigger opening size, the solder flowed onto the track (visible in Figure 5.29(a)). This created the fragile zone where the crack was formed. To solve this, the solder mask was reduced to the original pad size. The pad size itself was increased in the new design (see Figure 5.32(b)). This resulted in a smaller solder mask opening compared to the copper area. This is called a solder mask defined pad. This way the solder did not flow onto the thinner track any more. Also the width from the copper track to the pad was changed gradually to distribute the stresses.

5.4.5.2 FR4 stiffeners

The solder contacts of the TSSOP and QFN packages were reinforced by making the board substrate stiffer. A thin FR4 board was placed underneath the components. This should support the contacts and shift the bending zone further away from the contact pads. The difference is illustrated in Figure 5.33. The FCB bends now at the edge of the FR4 stiffener. Because everything is encapsulated in PDMS the bending radius of the FCB is limited and avoids folding around the stiffener edge.

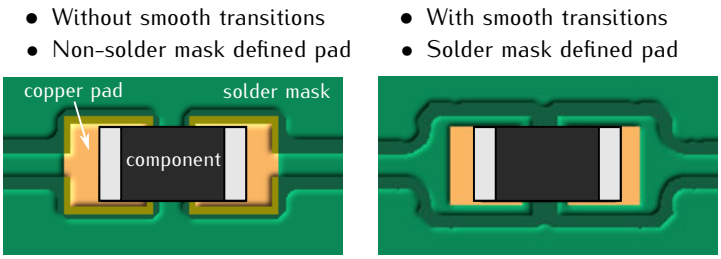

(a) Reference design (WR1). (b) Improved design (WR2).

Figure 5.32: Difference between the WR1 and WR2 designs.

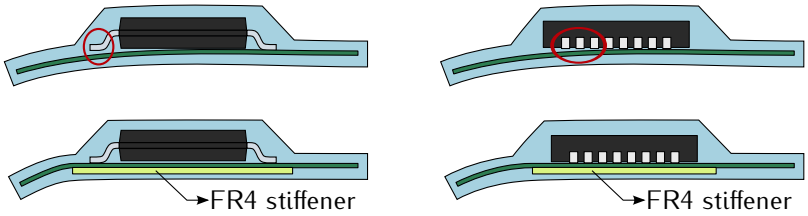

(a) TSSOP (b) QFN

Figure 5.33: FR4 stiffeners underneath TSSOP and QFN components.

In this WR2 test an FR4 stiffener of 200um thickness was used. Double sided Nitto Denko tape (No.585) was laminated manually with a roller. The FR4 + tape stack was cut to the desired shapes with a steel rule die. A picture of the steel rule die is shown in Figure 5.34.

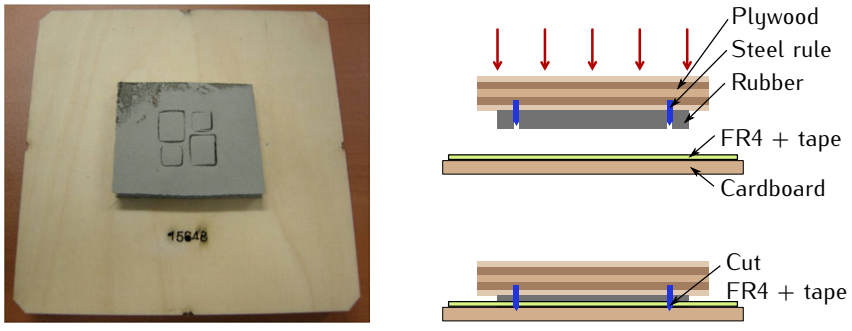

(a) Picture of the steel rule die. (b) Steel rule die build up.

Figure 5.34: Steel rule die for punching out FR4 stiffeners.

Steel rule die cutting is a process used to cut sheet materials including paper, cardboard, rubber and plastic. Most standard cardboard boxes and packages are made using this technique. This cutting process was used to cut the FR4+adhesive tape laminate. Milling was tried but did not show satisfying results. The FR4 was milled out fine, but the tape laminated on it was not. The die is constructed out of a substrate which is made of high-grade and high-density plywood. The steel rule itself is essentially an elongated razor blade made out of hardened steel. The steel rule is bended to position it into slits in the substrate. Rubber pads are adhered to the substrate to help eject the material after it is cut. Without the inclusion of ejection rubber, the material may tend to get stuck amongst the steel rules. Figure 5.35 shows pictures of the FR4 stiffeners that were used in the WR2 test. The stiffeners were placed underneath the TSSOP and QFN packages after molding the top part of the samples. Placement and alignment of these stiffeners was done manually.

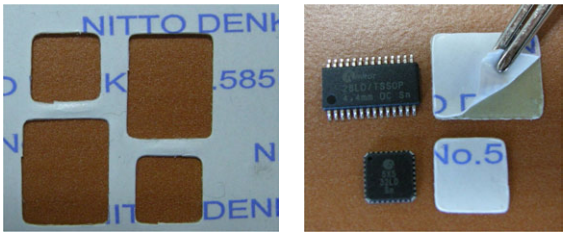

(a) Stiffeners punched out.

(b) Stiffeners for TSSOP and QFN support.

Figure 5.35: Stiffeners punched out of FR4 + tape stack.

5.4.5.3 Assembly information

The first board (sample 1 to 6) was assembled manually. The next four boards (samples 7 to 30) were assembled at Page Electronics. Details of the automatic assembly are given in Table 5.9.

Board size	9inch x 12inch (=6 samples)
Solderpaste dispensing	Mydata MY500 pasta-jetter
Component placement	Juki KE-2050 chip shooter
Soldering	Reflow, max temp 241°C

Table 5.9: Assembly info for WR2 samples.

5.4.5.4 Problems when molding the WR2 test samples.

To create contact openings in the PDMS it was necessary to close the mold tightly onto the pads. The mold was closed with screws and bolts making it difficult to obtain a uniform clamping force. In case the clamping force onto the pads becomes to low, PDMS can flow onto the pads. With the WR1 test samples this problem was avoided by using additional clamping on the center of the mold. This was possible because the mold was only 10cmx10cm. The mold for the 6 WR2 samples had a larger size of 22.5cmx30.5cm, which made it difficult to use the additional clamping. Eventually, the molding of the WR2 samples was done without additional clamping, resulting in PDMS migrating onto the contact pads. Figure 5.36(a) shows a worst case scenario where the PDMS layer on the pad is rather thick. The excess PDMS was scratched away to reopen the contact opening as shown in Figure 5.36(b).

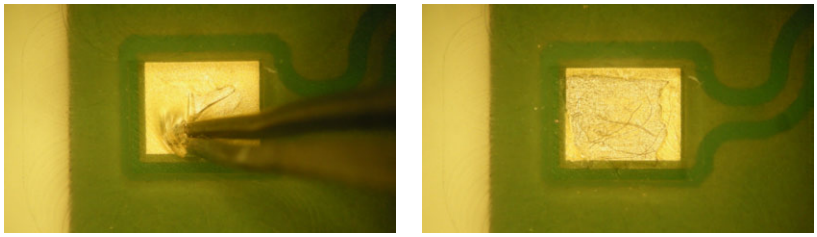

(a) PDMS on contact pad after molding. (b) PDMS scratched away.

Figure 5.36: Contact pads covered with PDMS.

5.4.5.5 WR2 test information

30 WR2 test samples were made for the WR2 tests. As was done in the WR1 test, the test modules were attached to a knitted or woven fabric. WR2 test samples were subjected to domestic washing, followed by drying on a line. Distinction was made between washing with and without a protective bag. The samples were washed in batches of six where each batch contained one reference sample with the previous WR1 design. Test conditions for the first and third batch were identical to check the reproducibility of the test. An overview is given in Table 5.10.

Test sample	Fabric	Wash test
WR2_R1S1 to S6 (S6=reference)	Woven	Domestic washing - 40°C - ISO 6330 (method 5A, in protective bag)
		Open air line drying
WR2_R1S7 to S12 (S12=reference)	Woven	Domestic washing - 40°C - ISO 6330 (method 5A, without protective bag)
		Open air line drying
WR2_R1S13 to S18 (S18=reference)	Woven	Domestic washing - 40°C - ISO 6330 (method 5A, in protective bag)
		Open air line drying
WR2_R1S19 to S24 (S24=reference)	Knitted	Domestic washing - 40°C - ISO 6330 (method 5A, in protective bag)
		Open air line drying
WR2_R1S25 to S30 (S30=reference)	Knitted	Domestic washing - 40°C - ISO 6330 (method 5A, without protective bag)
		Open air line drying

Table 5.10: Wash test info for WR2 samples.

5.4.5.6 WR2 wash test results

Each WR2 test sample contained the same components at the same position as in the WR1 samples. Therefore the same names for the chain types previously presented in Table 5.8 were used.

Figures 5.37 and 5.38 give an overview of the chain status of the first batch of six test samples on a woven fabric after every multiple of five domestic washing cycles. The samples were dried on a line between subsequent cycles. Washing was continued up to 25 washing cycles. Test samples S1 to S5 were samples with the new WR2 design including stiffeners to support the IC's. Test sample S6 had the previous WR1 design and was used as a reference.

In Figure 5.37 the data of the 5 improved WR2 test samples is plotted, thus excluding the reference sample. Each vertical bar, in a group of five, shows for each sample (S1 to S5 from left to right) the number of conducting and open chains. Averages in percent of the number of conducting chains for each chain type are placed in labels onto the graph. Only the differences between the subsequent multiple of five cycles are plotted. After the maximum tested amount of 25 cycles, the status of all chains is plotted. Most of the changes in number of conducting chains took place for chain types A and B (SMD resistors). The percentage of conducting chains went down from 100% to 68% and 88% for type A and B respectively. In this test the chains with the larger 0603 SMD resistors (type B) showed less failures compared to the chains with the smaller 0402 SMD resistors (type A). Sample 5 showed an early failure

after the first washing cycle on one chain of type D (TSSOP contact). Besides this broken chain no other chains on TSSOP packages (C,D,G,H) were broken after 25 cycles. For the QFN packages (E,F,I) only two chains of type E were broken on sample S2 after 15 cycles.

Figure 5.38 contains the results of the wash test for reference sample S6. As expected these results are far worse and after 25 washing cycles only a few chains maintained conductivity. Comparing the percentages with those of Figure 5.37, it is clear that the WR2 design is a major improvement. Because sample 6 is a reference sample, having the previous WR1 design, it should follow the trend of the results of the WR1 tests. Indeed also here all SMD resistor chains (A,B) are broken in an early phase and the contacts in the chains of the QFN IC's (E,F,I) survived the tests better than the contacts in the chains of the TSSOP IC's (C,D,G,H).

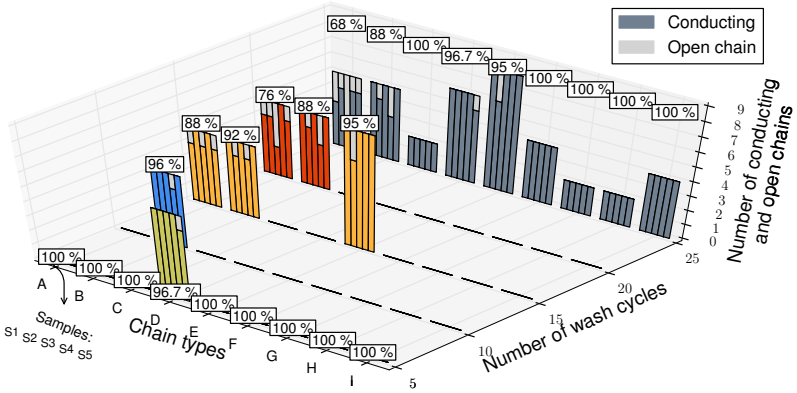

Figure 5.37: Chain status after every multiple of five washing cycles (WR2, woven, domestic, line drying, in bag).

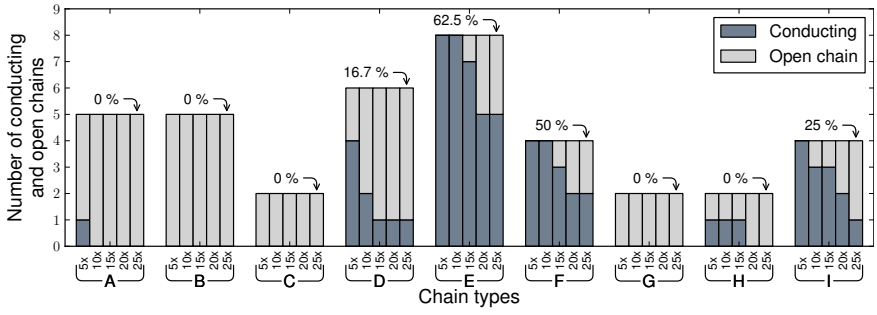

Figure 5.38: Chain status of reference S6 after multiple washing cycles (WR2, woven, domestic, line drying, in bag).

Wash test results of the second batch of six samples are given in Figures 5.39 and 5.40. These samples were identical as those in the first batch, but were washed without a protective bag. The data in Figure 5.39 indicates that domestic washing without protective bag is more severe. More changes in the number of conducting chains can be observed as compared with washing using a protective bag. Also the percentages of the number of conducting chains for each chain type are lower than the ones of the first batch in Figure 5.37. Resistor chains of type A are showing more broken chains than chains of type B. A result which was also observed in the test data of the first batch.

Figure 5.40 shows the results of the wash test for reference sample S12. Looking to this graph it is again clear that the WR1 design of the reference sample scored a lot worse than the improved WR2 design. Also this reference sample S12 has a lower number of conducting chains after 25 washing cycles as compared with reference sample S6 which was washed in a protective bag.

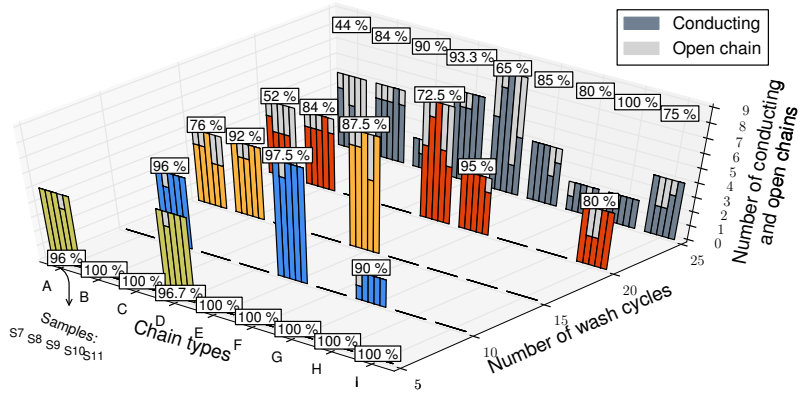

Figure 5.39: Chain status after every multiple of five washing cycles (WR2, woven, domestic, line drying, no bag).

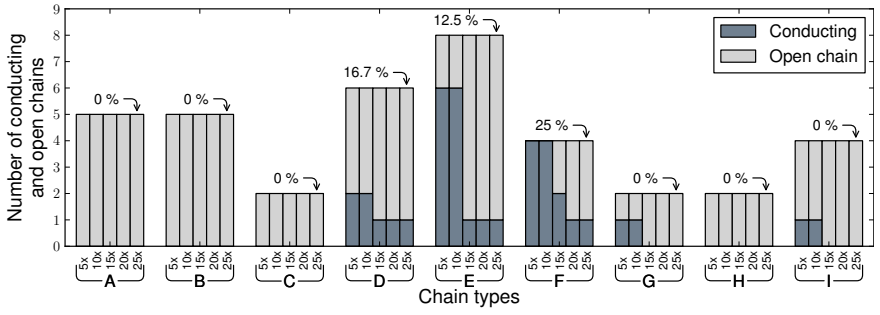

Figure 5.40: Chain status of reference S12 after multiple washing cycles (WR2, woven, domestic, line drying, no bag).

The third batch was used to evaluate the reproducibility of the wash test performed on the first batch. This was to determine if domestic washing in a protective bag indeed leads to less broken chains compared to washing without a protective bag. Therefore test samples S13 to S18 were washed using the same conditions as samples S1 to S6.

The data plotted in Figures 5.41 and 5.42 is very similar to the data in the plots of the first batch (Figures 5.37 and 5.38). Most changes in number of conducting chains are again seen in types A and B, with type A showing the most broken chains. Only a few chains are broken on the QFN packages and no chains were broken on the TSSOP packages. Also the percentages are again higher than those of batch 2 where no protective bag was used. Therefore it can be concluded that for woven fabrics the use of a protective bag had a positive result on the contact reliability of the WR2 test samples.

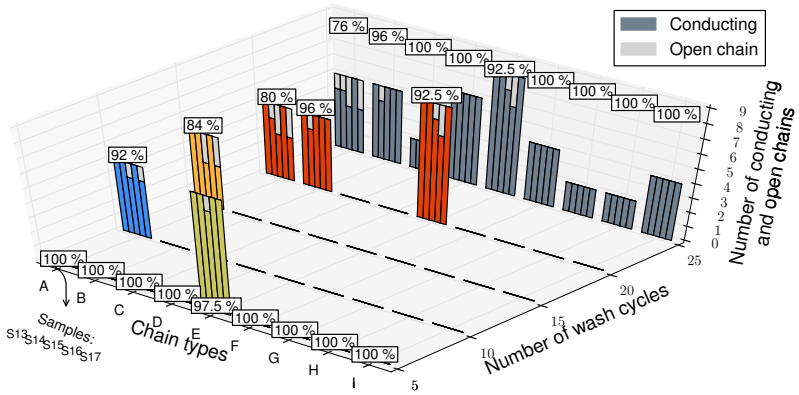

Figure 5.41: Chain status after every multiple of five washing cycles (WR2, woven, domestic, line drying, in bag).

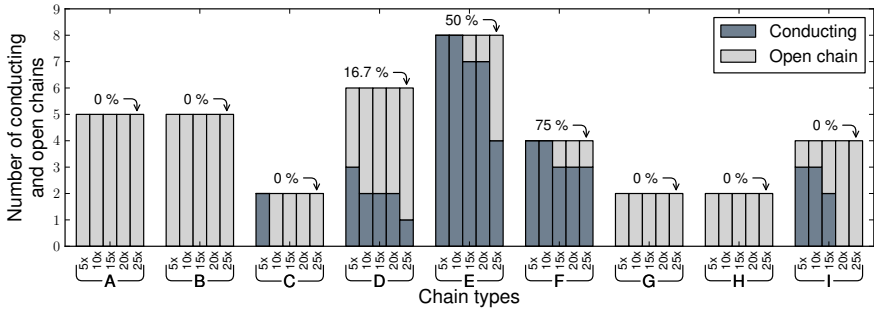

Figure 5.42: Chain status of reference S18 after multiple washing cycles (WR2, woven, domestic, line drying, in bag).

The test modules of the fourth batch were placed on a stretchable knitted fabric instead of the less stretchable woven fabric. These samples were again subjected to domestic washing, using a protective bag. The test results are presented in Figures 5.43 and 5.44. The graph of Figure 5.43 indicates that after 25 washing cycles the 5 test samples in this batch were only showing 3 broken chains out of a total of 190 chains. Important to mention is the fact that these 3 defects were present prior to the washing test and were caused by poorly soldered contacts. This means that not a single defect was introduced during the 25 washing cycles.

Figure 5.44 shows the chain status of reference sample S24 which was a member of the fourth batch. We see a progressive destruction on all chain types after the different washing cycles. Comparison of the graphs in Figures 5.43 and 5.44 illustrates again the big improvement the WR2 design introduces.

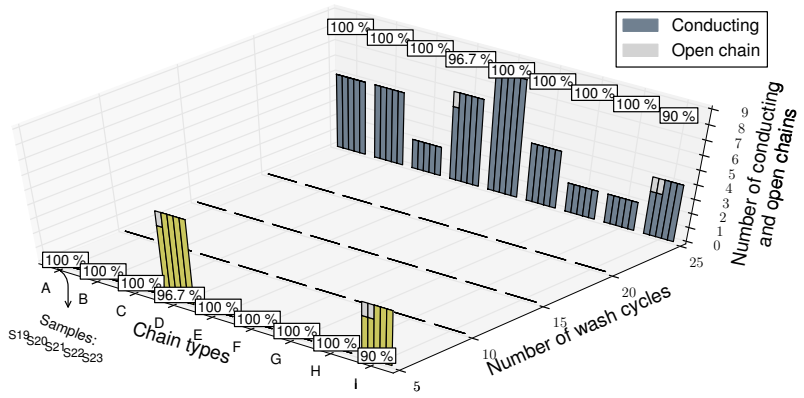

Figure 5.43: Chain status after every multiple of five washing cycles (WR2, knitted, domestic, line drying, in bag).

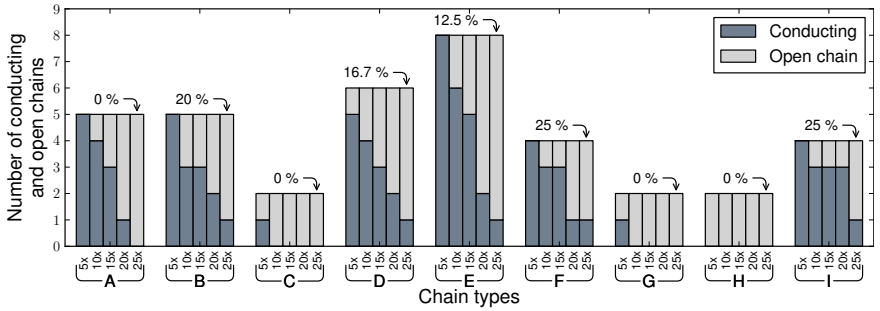

Figure 5.44: Chain status of reference S24 after multiple washing cycles (WR2, knitted, domestic, line drying, in bag).

The test samples in the fifth and last batch in the WR2 test were identical to the samples of the fourth batch (on a knitted fabric). But now the samples were washed without a protective bag to investigate if this would induce more broken chains. The data in Figure 5.45 shows that this was *not* the case. Again there were some defects prior to the washing test (4 defects). Washing up to 25 cycles did not introduce more defects, similar to the results obtained with batch four.

Figure 5.46 shows the chain status of reference sample S30 of the last batch. There were a lot more broken chains in comparison with the results of sample S24 (Figure 5.44). This indicates that washing without a protective bag is more severe, but did not seem to have influence on the samples containing the improved WR2 design.

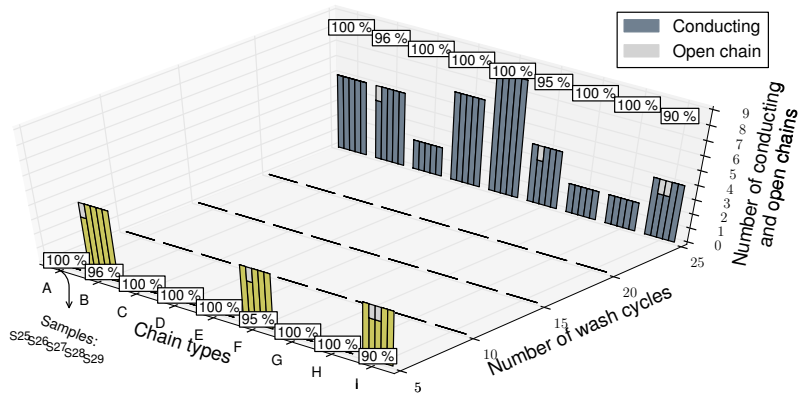

Figure 5.45: Chain status after every multiple of five washing cycles (WR2, knitted, domestic, line drying, no bag).

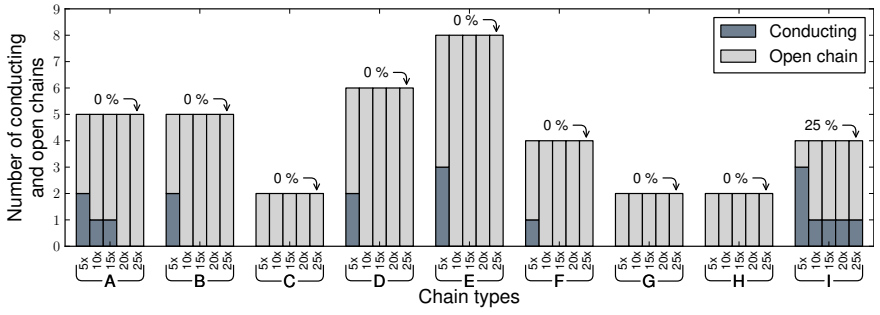

Figure 5.46: Chain status of reference S30 after multiple washing cycles (WR2, knitted, domestic, line drying, no bag).

5.4.5.7 Test sample failure analysis

The data of the WR2 test series presented in the previous section 5.4.5.6 has shown that, compared to the WR1 design, there were less broken chains even after 25 washing cycles. Nevertheless, every failure should be considered as unwanted. Therefore the WR2 test samples were visually inspected after the 25 washing cycles to detect the different failure mechanisms. There was a clear difference in the amount of broken chains between test samples with modules on a woven fabric and test samples with modules on a knitted fabric. In the case of a knitted fabric (batch 4 and 5), no defects were introduced during washing. For samples with a woven fabric (batch 1, 2 and 3), the most broken chains were detected on chain types A and B, where type A showed the highest failure rate. Figure 5.47(a) shows that this conductivity loss in the resistor chains is due to cracks in the FCB. No defects were found on the solder contacts of the SMD resistors. Also the smooth transitions from copper track to copper pad were free from cracks. Some of the measurement pads had also cracks in the middle of the pad as can be seen in Figure 5.47(b). These cracks do not contribute to the loss of chain conductivity between two measurement pads, but are of course unwanted if such a pad is needed in a real application.

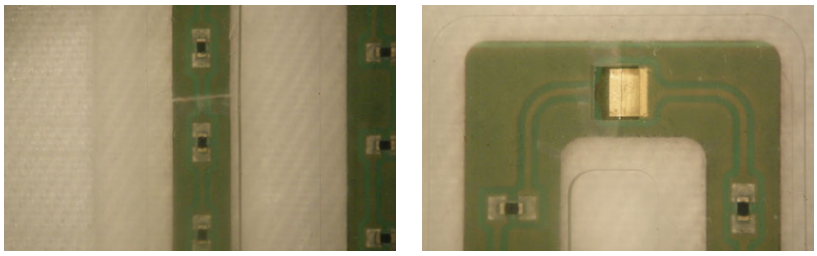

(a) Cracks in the FCB of the resistor chains. (b) Cracks in the measurement pads.

Figure 5.47: Failures in the SMD resistor chain types A and B.

In the data analysis of the WR2 modules on a woven fabric it was noticed that type A was more susceptible to breakage than type B. It was expected that visual inspection would reveal more broken contacts on the smaller SMD resistor packages compared to the larger packages in the type B chains. But as mentioned before no evidence of broken contacts were found and failure in chain conductivity was caused by cracks in the FCB. Therefore the difference between A and B should be found somewhere else. The data in Table 5.11 shows the percentage of broken chains for each chain of types A and B, averaged over all the tested samples with a woven fabric, excluding the reference samples. This means that this average was taken over $3x5 = 15$ samples.

Type	A					B				
Chain	P1-P2	P2-P3	P3-P4	P4-P5	P5-P6	P6-P7	P7-P8	P8-P9	P9-P10	P10-P11
% broken	93.3	20	13.3	13.3	46.6	13.3	0	0	6.6	33.3

Table 5.11: Overview of the percentage of broken chains of type A and B for each chain after 25 washing cycles (15 samples, reference excluded).

It can be seen that chains of type A were indeed more often broken than the chains of type B. The P1-P2 chains had the highest failure rate. Only on one out of 15 samples did the P1-P2 chain survive, resulting in 93.3 % of broken P1-P2 chains. Also the P5-P6 and P10-P11 chains had a higher failure rate compared to the rest. The positions of these chains are highlighted in Figure 5.48.

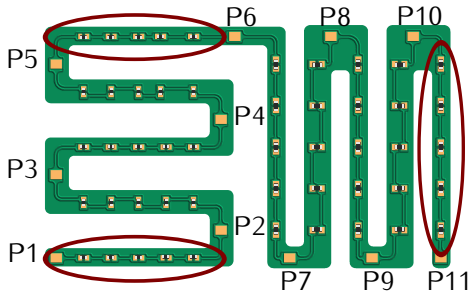

Figure 5.48: Positions of the chains of type A and B.

The three chains with the highest failure rate are located at the outer boundaries of the 'snake' between P1 and P11. It is believed that these outer boundaries are more likely to deform during washing than the 'more protected' inner chains. Bending, twisting, stretching these outer chains more often than the rest of the chains could be the reason for the differences seen in failure rate. It is remarkable that the P1-P2 chain was broken on almost all test samples. This chain is one of the ends of the snake. Compared to the other end of the snake (P10-P11), the P1-P2 chain is positioned further away from its neighboring chain P2-P3. This could lead to a higher degree of movement of freedom compared to the P10-P11 chain and could be the reason for the difference in failure rate. The same reasoning can be used to explain why the P7-P8 and P8-P9 chains have a much lower failure rate. They are better protected by their close neighbors than the other chains.

Chain types other than A and B are located on the TSSOP and QFN IC islands. The dummy IC's are supported with stiffeners to prevent bending at the solder contacts. No clear evidence of broken solder contacts like those

seen on the WR1 samples (Figure 5.30) were found on the WR2 samples. Instead the flexes showed folds, causing cracks in the copper tracks because of the small bending radius. An example of such a fold is shown in Figure 5.49(a). On the sample visible in Figure 5.49(b) such a fold eventually lead to rupture of the FCB.

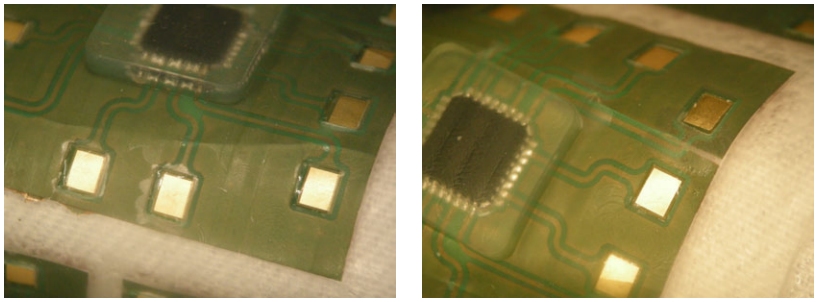

(a) Fold across multiple copper tracks. (b) Fold in the FCB which resulted in a crack.

Figure 5.49: Folding of the FCB on the dummy IC islands.

The folds could only be created if the FCB was bent to a very small bending radius. Normally this is not possible because the FCB is encapsulated with a ~0.4mm PDMS encapsulation on each side. Only if the FCB delaminates from the PDMS it is possible to achieve a bending radius small enough to create a fold. This is illustrated in Figure 5.50.

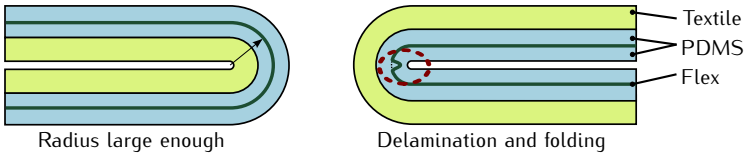

Figure 5.50: Left: Bending radius is large enough to prevent folding. Right: When the FCB delaminates the FCB can bend in the opposite direction and create a fold.

Bending a sample with the textile on the inner side keeps the bending radius of the FCB large enough to prevent folding. When the encapsulated module is located on the inner side, the radius of the FCB becomes smaller but is still not small enough to create a fold. Because the FCB is on the inner side of the bended sample it is under compression. The compression force can lead to delamination of the FCB from the PDMS encapsulation and the FCB can bend in the opposite direction with a bending radius small enough to create a fold.

In the pictures of Figure 5.49 the sample was slightly bent with the encapsulated modules on the outer side of the sample. In Figure 5.51 the sample was bent with the encapsulated modules on the inner side, showing the delamination of the FCB and formation of the fold.

Besides the cracks and the folds another failure mechanism was observed. After about 15 washing cycles some of the FCB corners protruded through the PDMS encapsulation (Figure 5.52(a)). Once these corners come out of the PDMS encapsulation, further washing can cause more damage (Figure 5.52(b)). The sharp FCB corners should be rounded to overcome this problem.

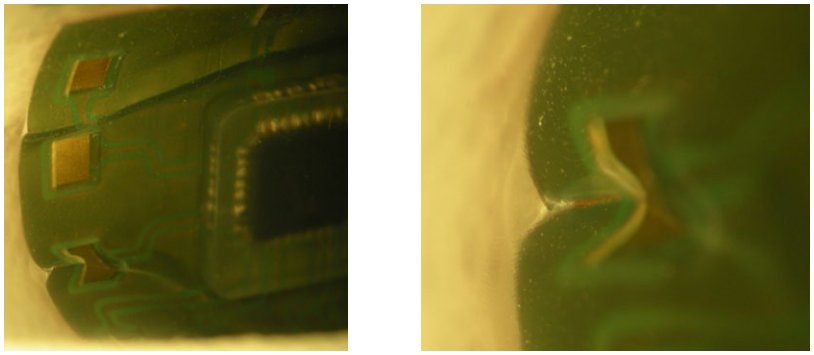

(a) Fold due to inward bending. (b) Detail of the fold.

Figure 5.51: Local delamination resulting in a fold.

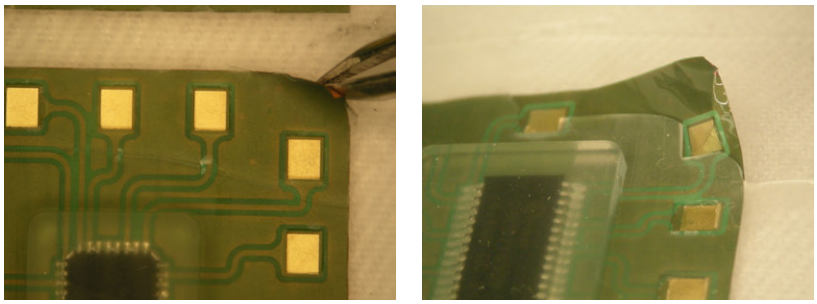

(a) Corner of the FCB sticking out of the PDMS encapsulation. (b) Complete destruction of the PDMS top layer at a FCB corner.

Figure 5.52: PDMS rupture at some of the FCB corners.

Finally the reference samples underwent examination to determine whether the same failure mechanisms of the WR1 test run were present. Indeed the reference samples had again cracks at the solder contacts and measurement pads as can be seen in Figure 5.53.

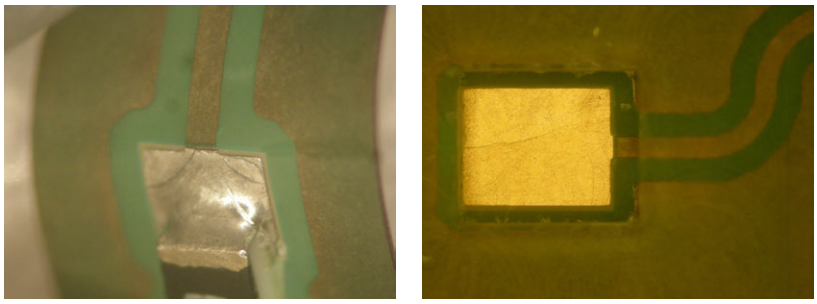

(a) Crack at the weak transition between copper pad and copper track.

(b) Crack at the weak transition between measurement pad and copper track.

Figure 5.53: Typical cracks in the copper on reference samples.

Measurement data showed that the washing reliability of the WR2 test modules on the knitted fabric was better than when the same modules were placed onto the woven fabric. For the modules on the woven fabric, cracks in the FCB were the cause of conductivity loss in the chains. In the case of modules that were placed on a knitted fabric, no conductivity loss was measured even after 25 washing cycles. Also the visual inspection of these samples revealed no cracks or other defects. The difference is found in the different stress levels that were present in the modules when they were bent using a certain force. The picture in Figure 5.54 illustrates this in a visual way.

Figure 5.54: Illustration of the different resistance to bending in WR2 test samples. From left to right: knitted fabric and outward bending, knitted and inward, woven and outward, woven and inward.

The modules shown in Figure 5.54 were cut out of a larger 30x30cm fabric and a rubber band was used to hold them during bending. It is clear that the highest stress level is present in the module on the woven fabric when

bended inwards. This has led to the folding and eventually cracking of the FCB as described before. Replacing the woven fabric with the knitted fabric changes the composition of module and fabric stack. The knitted fabric is able to stretch when the module is bent inwards, allowing the stack neutral axis to run closer to the electrical layer, and thus relieving the stress on the FCB. As a result, it requires less force to bend the module & knitted fabric combination as is seen in Figure 5.54.

5.4.5.8 Conclusions on the WR2 tests

The purpose of the WR2 test was to improve the WR1 test design. This was done with success by changing the 0402 and 0603 pad layout and by introducing FR4 stiffeners to reinforce the TSSOP and QFN contacts. Out of the WR2 wash tests the following conclusions could be made:

- It was clear that the WR2 test samples were a major improvement compared to the WR1 samples. While most of the chains of the WR1 samples had broken contacts after one washing cycle, most of the WR2 chains survived up to 25 cycles.
- The conductivity loss in the different chains of the WR2 samples was related to folds and cracks in the FCB and not because of broken contacts. The defects were only found on samples where the modules were placed on a woven fabric. This was due to stresses in the module when bending inwards.
- WR2 test samples with the modules on a knitted fabric were showing the best results. No defects were introduced during the 25 washing cycles.
- Domestic washing without a protective bag was more severe than washing with a bag. For samples with a woven fabric the use of a protective bag had a positive result on the reliability. For samples on a knitted fabric there was no influence, because no defects were introduced by the washing procedure.

References

[1] " Personal communication with Guy Buyle, Research scientist and European project co-ordinator at Centexbel, Belgium," 2009.

[2] ISO 6330:2000 - Textiles - Domestic washing and drying procedures for textile testing. International Organisation for Standardisation, norm 2000. [Online]. Available: http://www.iso.org/

[3] ISO 15797:2002 - Textiles - Industrial washing and finishing procedures for testing of workwear. International Organisation for Standardisation, norm 2002. [Online]. Available: http://www.iso.org/

[4] (2012) Centexbel - Belgian Textile Research Centre. Centexbel. [Online]. Available: http://www.centexbel.be/

[5] (2011) Water Conductivity. Lenntech BV. Delft, The Netherlands. [Online]. Available: http://www.lenntech.com/applications/ultrapure/conductivity/water-conductivity.htm

[6] P. Atkins and J. de Paula, *Atkins' Physical Chemistry*, 7th ed. Oxford, 2002.

[7] (2011) Model 2400 General-Purpose Sourcemeter. Keithley. Cleaveland, Ohio, U.S.A. [Online]. Available: http://www.keithley.com/products/dcac/voltagesource/broadpurpose/?mn=2400

[8] (2011) Model 7001 80 Ch - 2 Slot Half Rack Switch Mainframe. Keithley. Cleaveland, Ohio, U.S.A. [Online]. Available: http://www.keithley.com/products/switch/multi/?mn=7001

[9] (2011) Model 7011-C Quad 1x10 Mux. Keithley. Cleaveland, Ohio, U.S.A. [Online]. Available: http://www.keithley.com/products/dcac/currentsource/broadpurpose/?mn=7011-C

[10] (2011) NI LabWindows/CVI. National Instruments. Austin, Texas, U.S.A. [Online]. Available: http://www.ni.com/lwcvi/

[11] (2009) GPIB 101, A Tutorial of the GPIB Bus. ICS Electronics. Pleasantont, CA. [Online]. Available: http://www.icselect.com/ab_note.html#anchor338658

[12] (2011) NI GPIB-ENET/100. National Instruments. Austin, Texas, U.S.A. [Online]. Available: http://sine.ni.com/nips/cds/view/p/lang/en/nid/10622

[13] (2011) ELPEMER SD 2463 FLEX-HF. Lackwerke Peters GmbH. Kempen, Germany. [Online]. Available: http://http://www.peters.de/en/products/circuit-printing-lacquers/solder-resists/elpemer/446-elpemer-sd-2463-flex-hf-vsd-series

6

Technology demonstrators

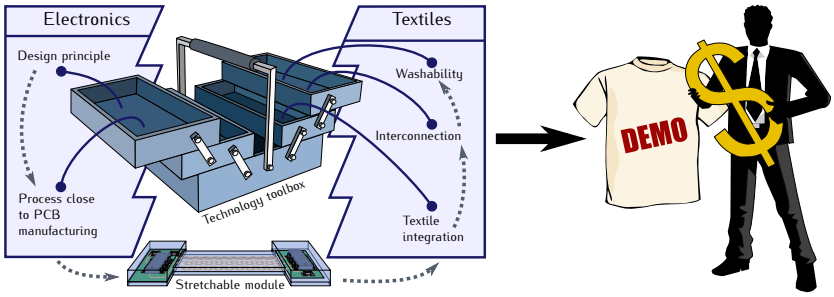

Figure 6.1: Chapter overview.

In previous chapters the main focus was on technology developments to realize textile integrated stretchable electronics. These developments were done to create a kind of 'toolbox' to support the creation of stretchable and washable electronics for textile products (Figure 1.3). By 'filling' this toolbox with design principles, processes for stretchable modules, integration methods, interconnection technologies and test methods, it becomes possible to actually design and realize textile applications with integrated stretchable circuitry. Some technology demonstrators were already shown in previous chapters as examples for technology steps (LED array, 7x8 LED display, blinking LED modules). These demonstrators were mainly used to test and improve the new

technology developments. In this chapter we will give more information on their design. In the period of this PhD also other demonstrators were designed and realized in projects and master theses related to the PhD subject. Some of these applications of the technology will be shown in this chapter; an RGB color display, a party shirt and a wireless battery charger. The electronic circuitry of the different demonstrators presented here, was designed using the meander design tool described in section 2.2.2.

6.1 LED array

The LED array of which the design is shown in Figure 6.2, served as a simple test vehicle for different tests. It was mainly used for encapsulation tests by means of TPU lamination or industrial injection molding (see section 2.4). All LEDs in the 4x4 array are lighting up together when powered.

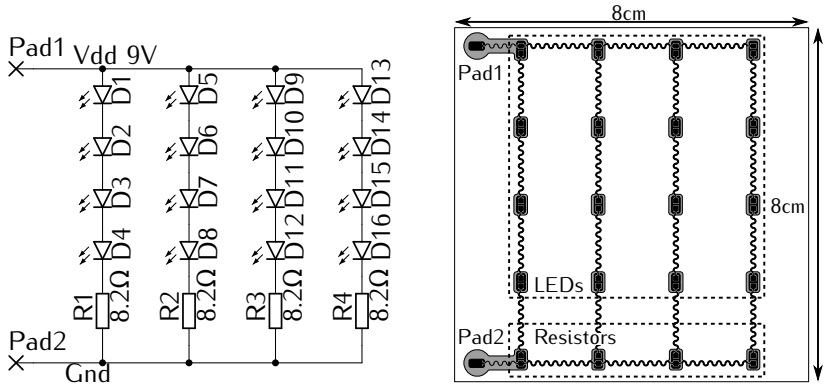

(a) Scematic (b) Layout

Figure 6.2: LED array design.

The design has 16 SMD LEDs and 4 SMD resistors on flexible islands, interconnected with each other via copper meanders. Meander width (W) is 100μm, their horseshoe angle (α) is 0° and they have a radius (R) of 500μm (for info on meander parameters see Figures A.14 and A.15). Component information is given in Table 6.1. The circuit is powered by a 9V source.

Component name	Package	Description
D1 - D5	0603	Red SMD LED (Avago HSMZ-C190)
R1 - R4	0603	8.2Ω current limiting resistor

Table 6.1: Components for the LED array.

The design fits on a 10cm x 10cm carrier board and six of them fit on a 9inch x 12inch carrier (Figure 6.3(a)). Figure 6.3 depicts realizations of this design.

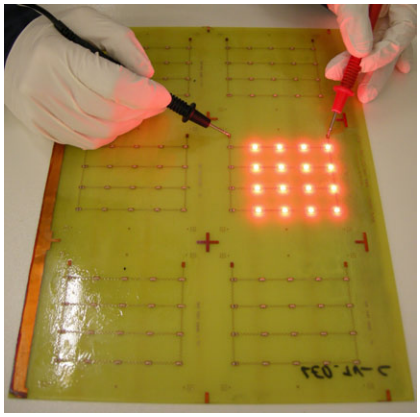

(a) Functionality check after substrate fabrication.

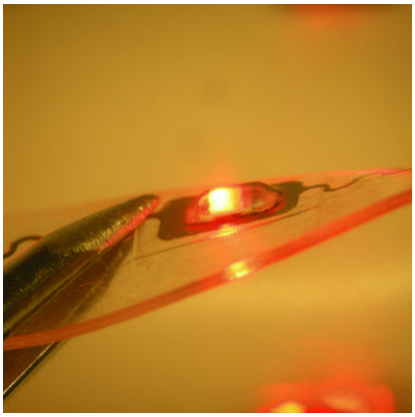

(b) Detail of the LED dome.

(c) Stretching

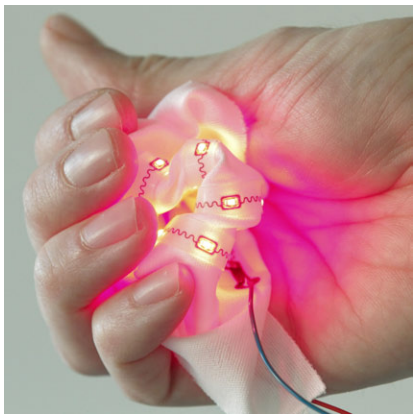

(d) Crumpling

Figure 6.3: LED array pictures.

6.2 7x8 LED display

To evaluate the different process developments on an actual electronic design, a simple but attractive demonstrator was designed in this PhD. This technology demonstrator shows a stretchable 7x8 single color LED-matrix, which can be used for example in wearable signage applications. The use of LEDs provides a visual feedback in case of circuit malfunction. The electronic circuit was built up around a MSP430F123 low power microcontroller from Texas Instruments [1]. The microcontroller was programmed to show a scrolling text message on the 7x8 LED-matrix.

It was the aim to design a single color LED matrix of which the LEDs can be turned on and off individually. There are several electronic designs possible to accomplish this. The aim was to realize the design with the minimum of electrical components to drive the LEDs. In a more traditional way this can be done by multiplexing. In Figure 6.4(a) one can see a simple representation of multiplexing with LEDs. The anodes (+) of the LEDs in one column are interconnected with each other to define the columns. The rows are defined by interconnecting the cathodes (-). As an example LED2 and LED3 are turned on by putting a high voltage (logic 1) on the signal line of the first column and on the signal lines of the second and third row. The appropriate LEDs are turned on one column at a time. When going fast enough, it appears to the eye that every LED is lit at the same time. The number of signal lines is determined by the sum of the number of columns and the number of rows. In the case of a 7x8 LED matrix 15 interconnections are needed from the LED matrix to an island with the driving electronics when using this multiplexing scheme.

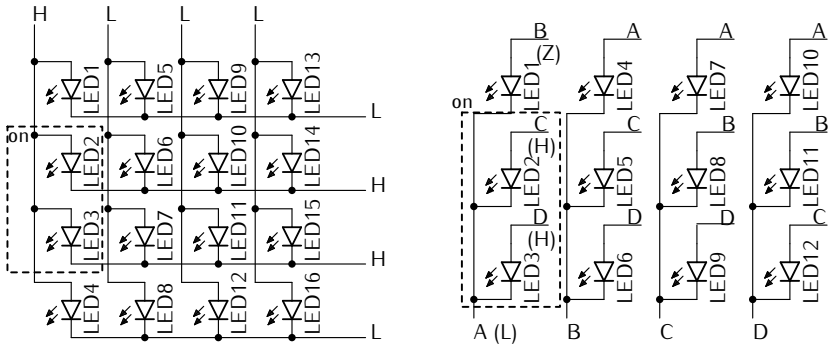

(a) Multiplexing a 4x4 matrix with 8 signals. (b) Charlieplexing a 3x4 matrix with 4 signals.

Figure 6.4: Multiplexing and Charlieplexing schemes for LED matrices.

In order to further reduce the number of interconnections, a more unusual multiplexing technique called 'Charlieplexing' was used [2]. Figure 6.4(b) illustrates how Charlieplexing was used to drive an LED matrix. A name has been given to each column (A to D). This are also the names for the used signal lines. For driving the LEDs of column A, the signal line which interconnects the cathodes of the LEDs is pulled low to ground (L). The other signal lines B, C and D are used to turn the LEDs in the column on or off. In the example LED2 and 3 are turned on by putting a high voltage (H) on lines C and D. Signal line B is connected to high impedance (Z) to turn LED1 off. The other LEDs in columns B, C and D are off. LED7 for example is off because its reverse biased (A low, C high). LED5 is off because line B is at a high impedance so no current can flow through LED5. To display a complete image the columns are selected in sequence by pulling the corresponding signal line to ground. The remaining lines are used to turn the column LEDs on or off. By alternating the function of the signal lines between selecting a column and driving the LED's on or off, the number of signal lines is reduced with respect to the more traditional multiplexing. With this Charlieplexing scheme, n signal lines can be used to drive $n(n-1)$ LEDs. In the case of a 7x8 LED matrix this means 8 interconnections instead of 15. This makes it possible to drive the 56 LEDs with one 8 bit I/O port of the microcontroller. A driving algorithm was developed and programmed in C to drive the 7x8 LED matrix. This algorithm was used to program the microcontroller in order to show a scrolling text on the display. The interconnection scheme of the circuit for the 7x8 LED display is shown in Figure 6.5. An overview of the used components is listed in Table 6.2.

Component name	Package	Description
LED1 - LED56	0603	Red SMD LED (Avago HSMZ-C190)
R1 - R36	0603	0Ω resistor used as a jumpers
R37	0603	$47k\Omega$ pull-up resistor on the reset pin
C1	0402	100nF decoupling capacitor
IC1	TSSOP28	MSP430F123IPW microcontroller
Molex	1mm/8way	Molex FFC/FPC socket for JTAG programming

Table 6.2: Components for the 7x8 LED display.

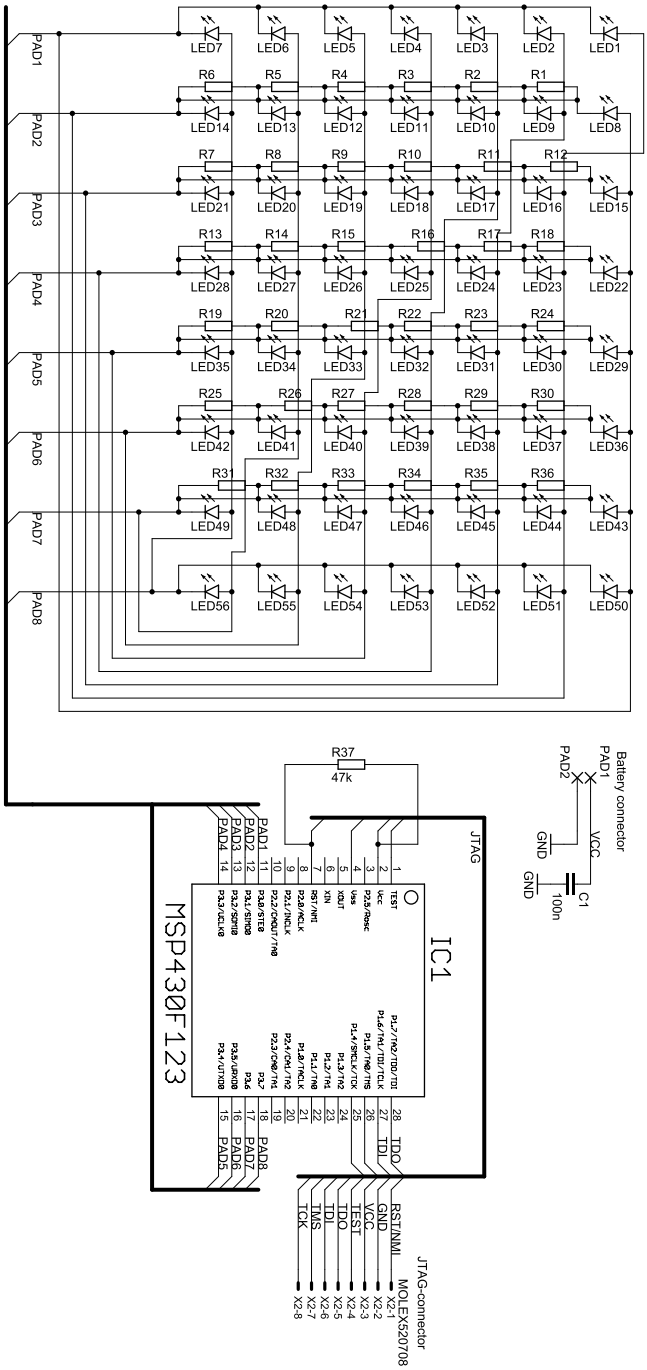

Figure 6.5: 7x8 LED display design.

One can see 2 parts in the schematic of Figure 6.5. The part with the LEDs was layouted in a stretchable matrix and the part with the microcontroller was placed on a flexible island. Figure 6.6 shows the actual layout of the stretchable circuit. The LED islands are interconnected with meander shaped conductors to achieve stretchability. Meander width (W) is 100μm, their horseshoe angle (α) is 45° and they have a radius (R) of 300μm (for info on meander parameters see Figures A.14 and A.15). Every LED island contains a 0Ω resistor, used as a jumper, so all tracks could be routed in a single layer. The interconnections between the microcontroller and JTAG connector at the bottom were routed in such a way that the connector could be cut off after programming, to size down the controller island.

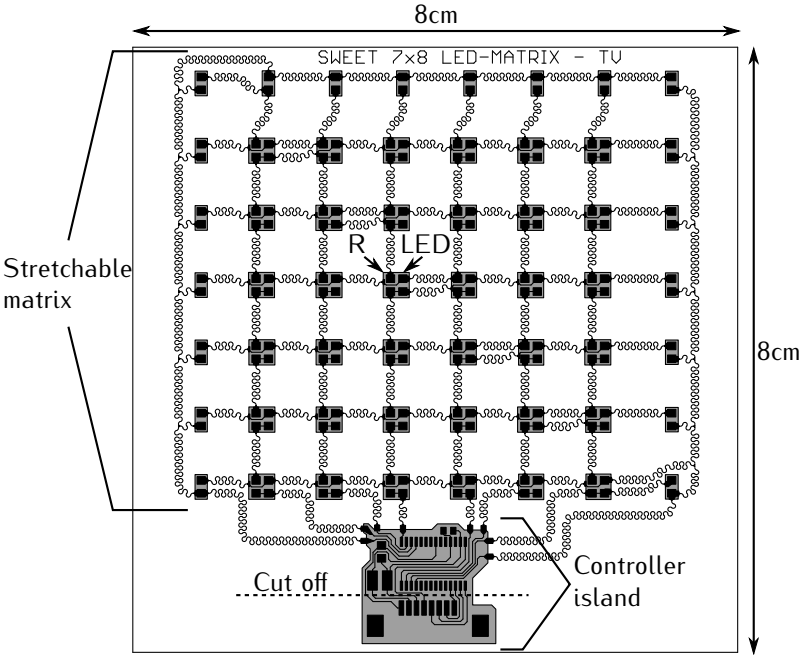

Figure 6.6: 7x8 LED display layout.

Figure 6.7 shows some pictures of realisations of this technology demonstrator.

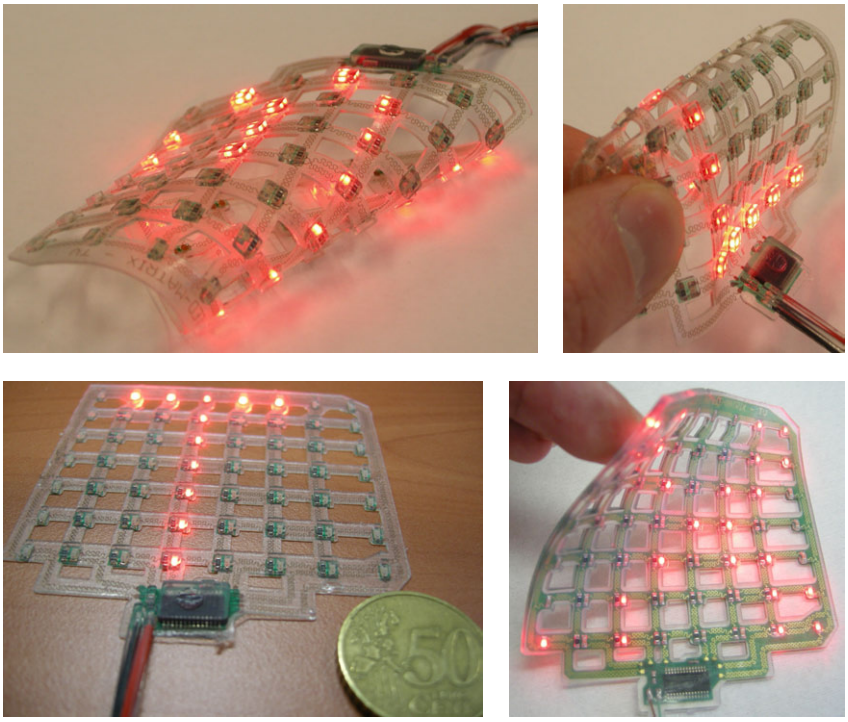

Figure 6.7: Pictures of the 7x8 LED display.

6.3 Blinking LED modules

The blinking LED module design was made to test the creation of openings in the encapsulation to access contact pads and to show the principle of interconnecting modules with embroidered and soldered electric wires. Eventually the samples were also used to carry out a first series of washing experiments (see section 5.4.2). Different blinking led modules were grouped on one design as can be seen in Figure 6.9. Every blinking LED module was layouted on a flexible island with four LEDs that are blinking two by two. The electronic circuit on each island was based on an astable multivibrator circuit to obtain the oscillation required for turning on and off the LEDs, which lead to the blinking. The basic working principle of the astable multivibrator can be found on the internet [3]. The schematic of a single blinking LED module is shown in Figure 6.8. Besides the four LEDs this circuit has only two transistors, two capacitors and four resistors. The components are listed in Table 6.3.

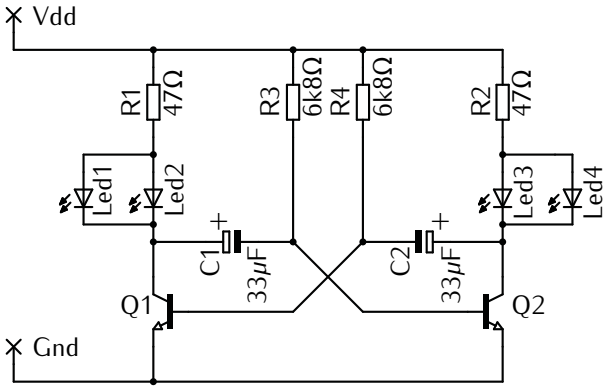

Figure 6.8: Blinking LED module schematic (astable multivibrator).

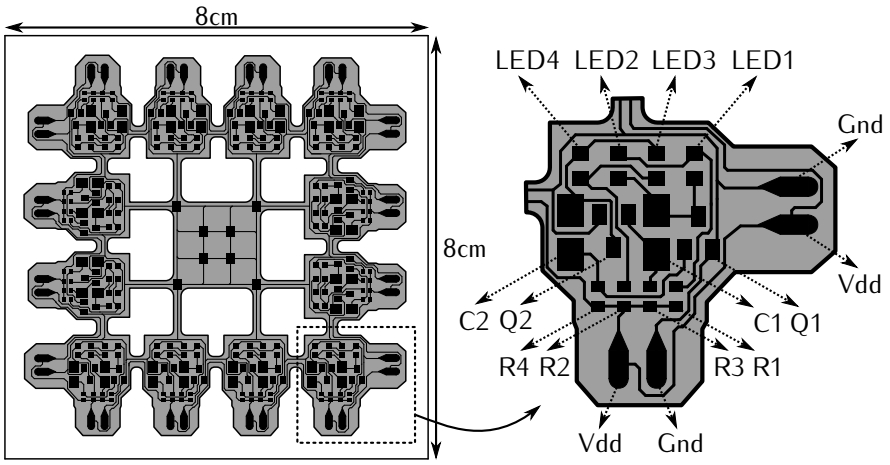

Figure 6.9: Blinking LED module layout.

Component name	Package	Description
Led1 - Led4	0603	Red SMD LED (Avago HSMZ-C190)
Q1,Q2	SOT-23	Transistor BC847B
R1,R2	0402	47Ω resistor
R3,R4	0402	6k8Ω resistor
C1,C2	Case A	33µF capacitor

Table 6.3: Components for a blinking LED module.

Figure 6.10(a) shows the blinking LED modules after PDMS encapsulation. The design was made in such a way that powering one module also powered the other modules, providing a fast and easy way to check functionality of all modules at once. Figure 6.10(b) shows the modules after separating them from each other with a knife.

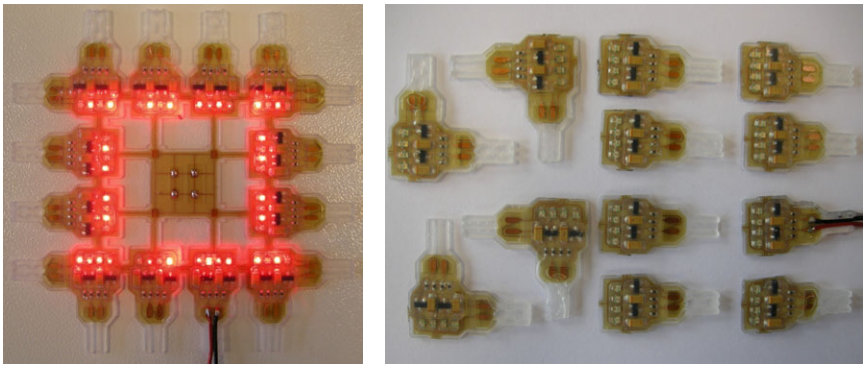

(a) All modules powered together. (b) Modules after separation.

Figure 6.10: Blinking LED modules.

Two different types of blinking LED modules were included in the design; 'corner modules' and 'end modules'. The corner modules had two interconnection points for power, while the end modules had only one. These two types could be used together to make a chain of interconnected blinking LED modules. Figure 6.11 shows the combination of a corner and an end module on a knitted fabric.

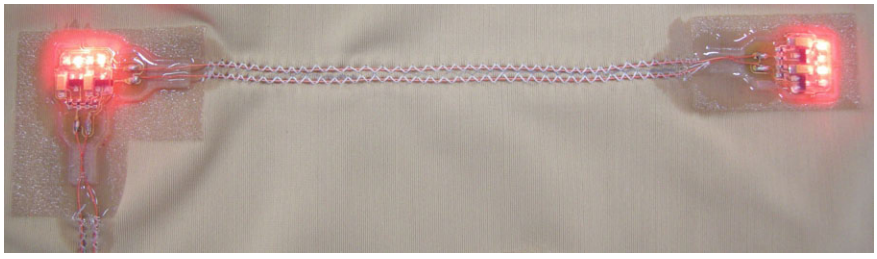

Figure 6.11: Blinking LED corner and end module interconnected on a knitted fabric.

6.4 RGB color display

First technology demonstrators, showing textile integrated stretchable electronics, like the 7x8 LED display were a great success. They triggered the interest from people not only active in textile research but also from other domains. As an example the textile mobile project was born [4]. The project aimed at creating a mobile set-up to demonstrate the on-going research at Ghent University that focuses on the production of Intelligent Textile. The project combined work in microelectronics with textile development, and music applications. Results were demonstrated at various public events. In this project a flexible 8x8 RGB LED display module, produced by CMST, was integrated in a vest. The design contained a wireless module to send images from a computer to the display. PDMS encapsulation and textile integration was done using the methods developed and described in this PhD. In a thesis to obtain her bachelors degree in fashion technology, Nikky Vlaemynck designed a vest to integrate the display [5]. Pictures of the final result are shown in Figures 6.12 and 6.13.

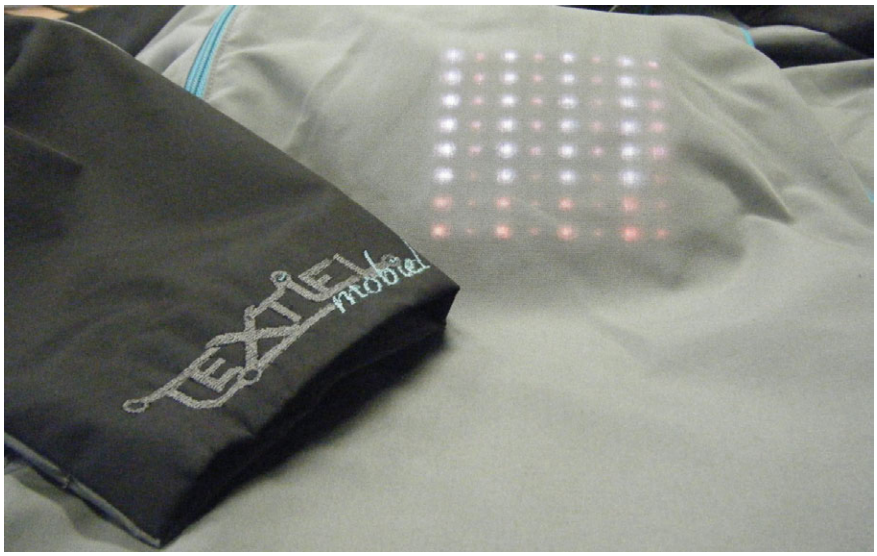

Figure 6.12: Textile Mobile demonstrator: RGB color display integrated in a vest.

Figure 6.13: Textile Mobile demonstrator: RGB color display integrated in a vest.

6.5 Party Shirt

The party shirt was developed in the frame of a multidisciplinair master thesis cluster, which received financial support from BiR&D [6]. The aim was to develop a social game, in which music was played to two teams. During this game the team members danced according to the music. The movements of the participants were registered using wireless movement sensor nodes. The level of synchronisation of the participants to the music and between the members of the same team were calculated in real-time and a proper visual feedback was generated, wirelessly sent, and shown on the wearable stretchable and textile integrated LED display, worn by each of the participants. The movement sensor information was also used off-line to analyse the interaction (co-operation and competition) between the participants, as well as the influence of the game settings (especially the LED display) on this interaction.

This Master Thesis was a co-operation between the electronic engineering research group CMST (Centre for Microsystems Technology) from Ghent University Faculty of Engineering and the human sciences research group

IPEM (Institute of Psychoacoustics and Electronic Music) from Ghent University Faculty of Arts and Philosophy. The work was split up into two master theses:

- Thesis at CMST: Development of a stretchable multifunctional LED matrix for integration in textile [7].
- Thesis at IPEM: The Social Gaming Partyshirt - An Interactive Application using Music, Movement and Luminescent Textile in a Social Gaming Context [8].

Here we will discus briefly the realization of the Party Shirt which is shown in Figure 6.14.

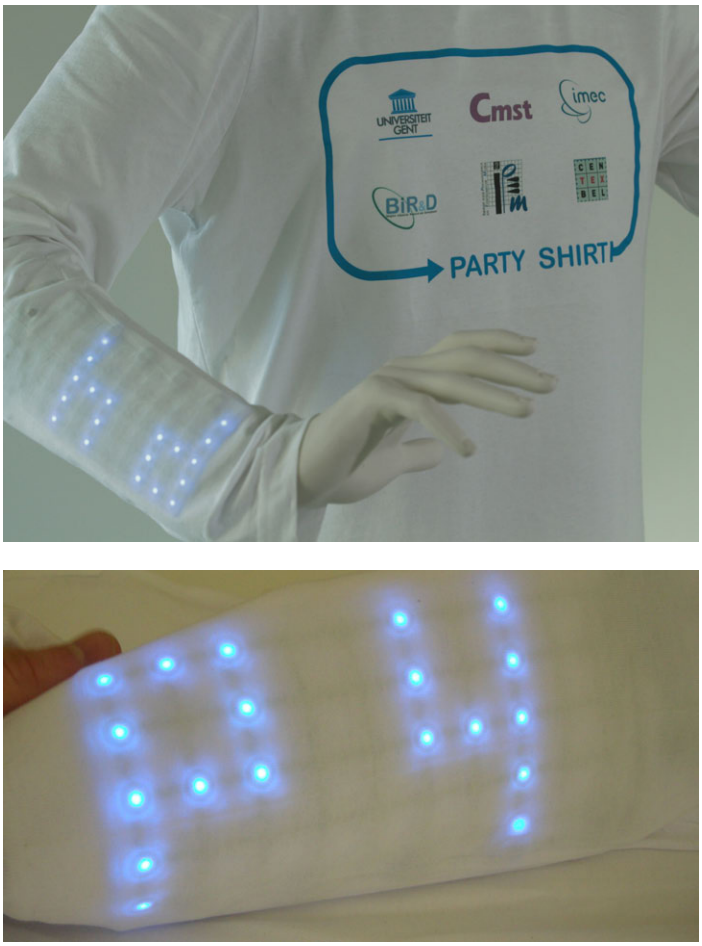

Figure 6.14: Pictures of the Party Shirt (P4 on the display means 'Player 4').

The Party Shirt has a stretchable 5x10 RGB LED display (Figure 6.15(b)) which is integrated into the sleeve of a T-shirt. Stretchable substrate fabrication was done using the laser structuring method described in section 2.3.2. PDMS injection molding was done, using a PMMA mold to encapsulate the stretchable circuit (Figure 6.15(a)). After encapsulation the stretchable display module was attached to a 10cm x 20cm knitted fabric, using the screen printing integration method described in section 3.2. The fabric, containing the display, was sewn into the sleeve of a T-shirt.

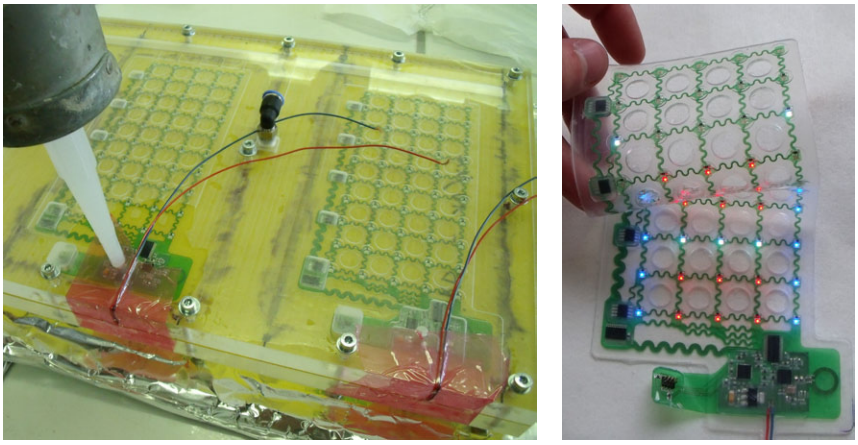

(a) PDMS encapsulation, using a PMMA mold. (b) stretchable display module.

Figure 6.15: Stretchable 5x10 RGB LED display.

The 50 RGB LEDs in the display were multiplexed column by column. A PWM LED driver was used to drive the 5 color LEDs in one column. Column switching was done using p-mos transistors at the common anodes of the LEDs. The display circuit contained an RF chip and a loop antenna for wireless communication with a PC. The different ICs in the circuit were controlled by a microcontroller, programmed in C. Prior to the start of this master thesis a microcontroller test board, containing the RF circuit together with other features, was designed and realized to assist the students in circuit and system developments. This test board was also helpful for other developments using a microcontoller during this PhD and is still used in other projects. More information on this test board is found in appendix C. The layout of the Party Shirt display is shown in Figure 6.16. The meander design tool, described in section 2.2.2, was used to route the different meanders in the design. For more information on the design of the stretchable display module in the Party Shirt, we refer to the master thesis [7].

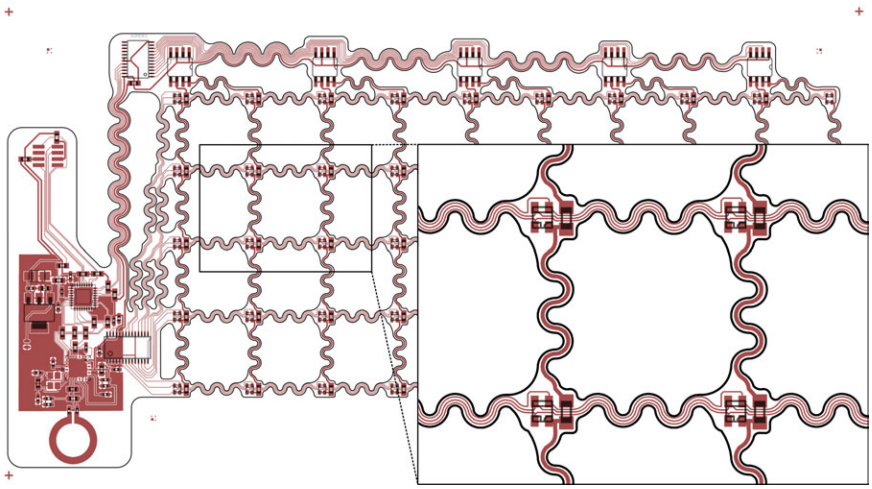

Figure 6.16: Circuit layout of the stretchable RGB led matrix used in the Party Shirt.

Four Party Shirts were made and used to demonstrate the dance game developed during the master thesis at IPEM. The social game adopted the name BeatLED and more information is found in Nies et al. [9]. From the six financially supported projects in the Call MSc2009, BiR&D selected two projects receiving a student-award of which this thesis cluster was one.

6.6 Wireless battery charger.

An important part in every textile integrated electronic system is its power supply. It was not the intention to provide a fixed solution for textile integrated batteries during this PhD study. However, the subject received some attention during research, as a power source was needed in the different technology demonstrators we described before. For these demonstrators, stand alone battery packs were used. These packs could be attached to or detached from the stretchable circuits with a connector. No special attention was given to the textile integration as they were simply sewn into a pocket on the garment. While this solution could be acceptable in some cases, a solution with a higher degree of textile integration could be needed in others. The type of battery and the integration level is application dependent. Questions related to the selection are:

- What is the amount of power the circuit needs? What is the maximal voltage and current?

- Should the battery be rechargeable or only replaceable?
- How long should the battery last before recharging or replacing?
- Should/can the battery be rigid, flexible or stretchable?
- Should the battery be permanently integrated in the textile product or should it be detachable?
- Is there need for a waterproof or even a washable battery?
- What types of battery packs are currently available on the market that could fit the needs?

It is clear that depending on the targeted product requirements, the search for a suited power solution can become a real quest. An example of a challenging case is a conformable, permanently integrated power solution. A first attempt to tackle this case was done during the SWEET project. In collaboration with the ESAT-MICAS group at KU Leuven, a wireless battery charger which supplies power and supports bidirectional data transfer during recharge was realized [10]. The concept underlying the design is shown in Figure 6.17.

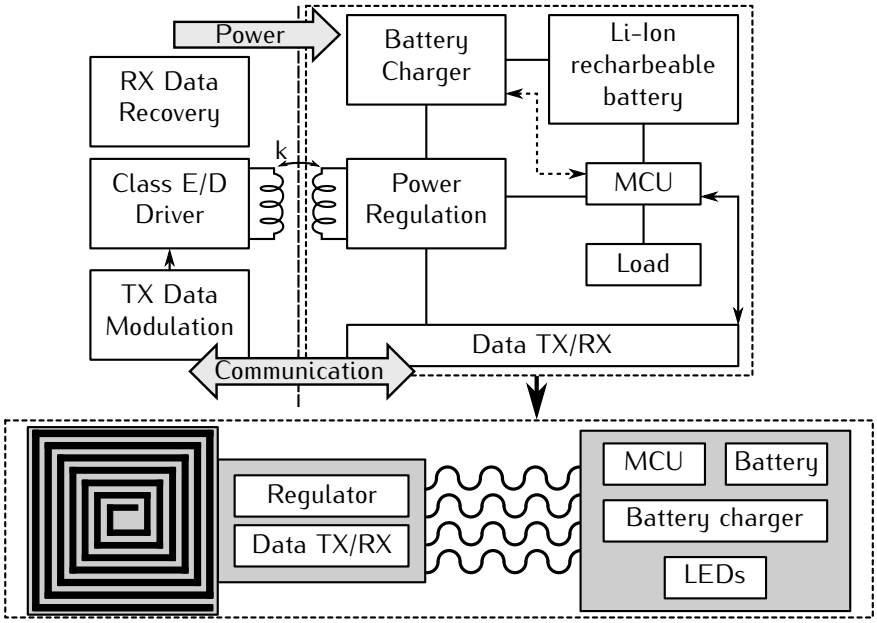

Figure 6.17: Block level schematic of the wireless battery charging system (top) and its subdivision in functional islands for implementation in the SMI technology (bottom).

On the top, a block level schematic of the developed system is depicted. The left (primary side) and right (secondary side) parts are respectively the external base and the embedded battery charger which are connected by an inductive link. A microcontroller (MCU) monitors the battery status, manages

the communication process and drives the load. For demonstration purposes, the load consists of a LED array.

The circuitry of the secondary side was implemented in the SMI technology using the techniques described in this PhD. The circuit was split up in two flexible islands, interconnected with each other by four meanders (Figure 6.17 bottom). The first island contains a planar coil, together with the power regulation and data communication sub-modules. A second island contains a thin flexible rechargeable battery, a microcontroller, a battery charger and the load. Stretchable substrate fabrication was done using the laser structuring method described in section 2.3.2. Encapsulation was done by liquid injection molding, using Sylgard 186 PDMS (info in section 2.4.1). Figure 6.18 depicts the conformable, wireless chargeable battery module. This module was later on integrated in a suit using the screen printing technique described in section 3.2. More information on the design and performance of this demonstrator is found in Carta et al. [10].

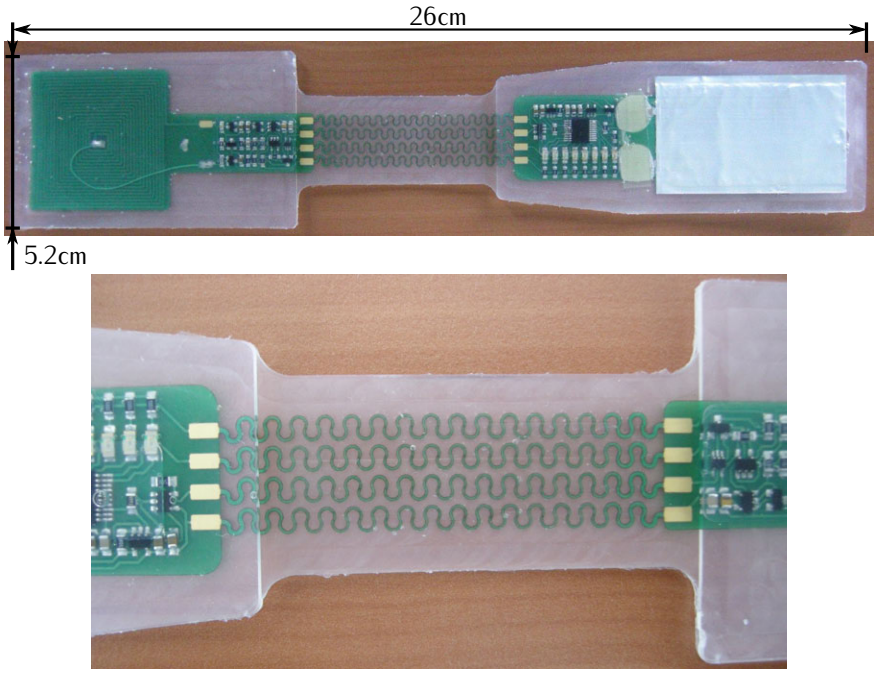

Figure 6.18: PDMS encapsulated conformable, wireless chargeable battery module.

With a module size off 26cm x 5cm it is clear that this solution is too big to implement in a real application. The main reason for this oversized design is the fact that the charging module was built for research and demonstration purposes. Research was done on the inductive charging and bidirectional data

transfer by the ESAT-MICAS group. Later on the design was used by CMST to demonstrate the textile integration possibilities of the SMI technology.

In a real product design the inductive charging circuitry should be implemented using a more integrated solution. This would reduce the number of components and consequently also the overall circuit dimensions. In the end this would lead to a design containing only the coil and the battery, together with a small island holding the additional circuitry.

A good starting point for the design would be to use the Qi 1.0 standard, developed by the Wireless Power Consortium (WPC)[11]. In this standard, similar principles as those for the stretchable, inductive chargeable module are used. Established in 2008, the WPC is a group of Asian, European, and American companies in diverse industries, including electronics manufacturers and original equipment manufacturers (OEMs). More than 100 companies are currently member of the consortium (e.g. ConvenientPower, Powermat, Texas Instruments, ST Ericsson, Philips, Energizer, Sony, Samsung, Panasonic, Nokia). The WPC standard defines the type of inductive coupling (coil configuration) and the communications protocol to be used for low-power wireless devices. Any device operating under this standard will be able to pair with any other WPC-compliant device. Under the WPC standard, 'low power' for wireless transfer means a draw of 0 to 5 W. Systems that fall within the scope of this standard are those that use inductive coupling between two planar coils to transfer power from the power transmitter to the power receiver. The distance between the two coils is typically 5 mm. Regulation of the output voltage is provided by a digital control loop where the power receiver communicates with the power transmitter and requests more or less power. Communication is unidirectional from the power receiver to the power transmitter via backscatter modulation [12].

As one of the founding members, Texas Instruments develops controller ICs for transmitters and receivers, which are WPC compliant. Figure 6.19 illustrates how their components can be used in a typical inductive charging topology. If we look to the receiver side, the system is integrated in an advanced receiver IC for wireless power transfer (e.g. bq51013 and bq51011). This makes it the only IC required between Rx coil and 5V DC output voltage. The device provides the AC/DC power conversion while integrating the digital control required to comply with the Qi v1.0 communication protocol. The device integrates a low-impedance full synchronous rectifier, low-dropout regulator, digital control, and accurate voltage and current loops. The entire power stage (rectifier and LDO) utilizes low resistive NMOS FETs to ensures high efficiency and low power dissipation [13]. Only a small amount of additional SMD passives are needed next to the IC to complete the circuitry at the receiver side. Figure 6.20 depicts how all receiver side circuitry fits on a 5 mm x 15 mm PCB [14].

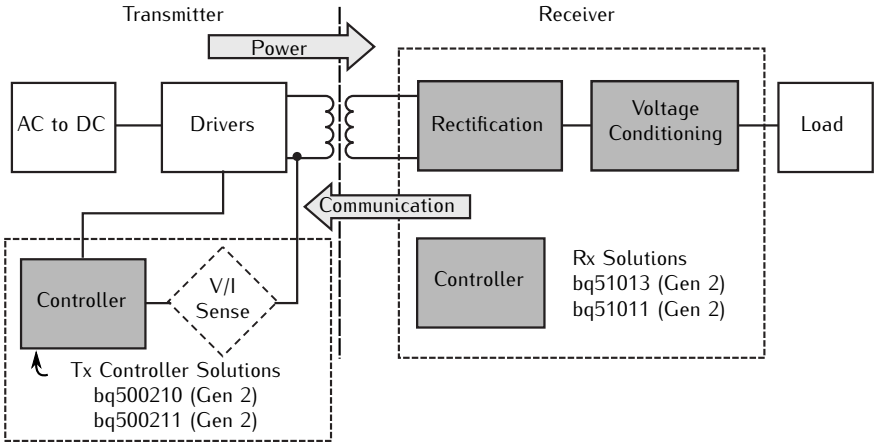

Figure 6.19: Typical wireless-power functional diagram, using TI controller IC's.

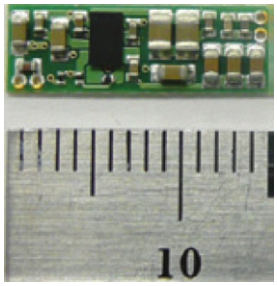

Figure 6.20: 5mm x 15mm PCB with all receiver side circuitry.

6.7 Conclusions

The different demonstrators presented in this chapter illustrate the use of the developed stretchable technology for textile integration. In the design phase, the meander design tool was used to route the meanders. The laser structuring method was used to fabricate the stretchable substrates, which were encapsulated by liquid injection molding or lamination. Both the textile screen printing technique and the textile lamination technique were used to integrate the encapsulated modules with fabrics. The successful realizations have led to the demonstration of a stretchable LED array, a 7x8 LED display, blinking LED modules, an RGB color display, a party shirt and a wireless battery charger. These demonstrators can be considered as building blocks, possibly leading to some first real applications in the future...

References

[1] (2004) MSP430x12x Mixed Signal Microcontroller (Rev. C). Texas Instruments. [Online]. Available: http://www.ti.com/product/msp430f123

[2] (February 10, 2003) Charlieplexing-reduced pin count LED display multiplexing. Maxim Application Note 1880. Maxim. [Online]. Available: http://pdfserv.maxim-ic.com/en/an/AN1880.pdf

[3] (2012) Multivibrator. Wikipedia. [Online]. Available: http://en.wikipedia.org/wiki/Multivibrator

[4] "UGent Textiel Mobiel, Projecten Wetenschap en Maatschappij," Call 2008.

[5] N. Vlaemynck, *Intelligent clothing: Dance for light. Bachelor thesis*. University College Ghent, 2010.

[6] (2012) Belgian industrial Research and Development. BiR&D. [Online]. Available: http://www.birdbelgium.com/

[7] W. Bothuyne, *Development of a stretchable multifunctional LED matrix for integration in textile. Master thesis*. Ghent University, 2010.

[8] T. De Nies, *The Social Gaming Partyshirt - An Interactive Application using Music, Movement and Luminescent Textile in a Social Gaming Context. Master thesis*. Ghent University, 2010.

[9] T. D. Nies, R. van de Walle, T. Vervust, J. Vanfleteren, M. Demey, and M. Leman, "BeatLED - the social gaming partyshirt," in *SMC*, 2010.

[10] R. Carta, P. Jourand, B. Hermans, J. Thoné, D. Brosteaux, T. Vervust, F. Bossuyt, F. Axisa, J. Vanfleteren, and R. Puers, "Design and implementation of advanced systems in a flexible-stretchable technology for biomedical applications," *Sensors and Actuators A: Physical*, vol. 156, no. 1, pp. 79 – 87, 2009.

[11] (2012) WPC - Wireless Power Consortium. Website. [Online]. Available: http://www.wirelesspowerconsortium.com/

[12] (2011) An introduction to the Wireless Power Consortium standard and TI's compliant solutions. Texas Instruments. [Online]. Available: http://www.ti.com/lit/an/slyt401/slyt401.pdf

[13] (August, 2011) Integrated wireless power supply receiver, Qi (Wireless Power Consortium) compliant. Texas Instruments. [Online]. Available: http://www.ti.com/lit/ds/symlink/bq51011.pdf

[14] (2012) Battery Management Solutions. Texas Instruments. [Online]. Available: www.ti.com

7 Conclusion and outlook

This final chapter discusses the main achievements obtained during this PhD study, together with some suggestions for future work.

7.1 Main achievements

In this thesis it was the objective to provide solutions that contribute in today's efforts on the creation of products with textile integrated electronics. It was noticed, that the missing link in most research on smart textile products could be attributed to the absence of a well suited integration method for electronics in textiles. Most electronic based research projects for smart textile products are application driven. While they provide new electronic systems, they often neglect the proper integration of these systems, which is usually limited to sewing rigid modules into the textile. Textile driven research projects on the other hand create fabrics with added functionality. Typical examples include textile based sensor elements or antennas. However, these projects often neglect the fact that also the interfacing electronics should be designed and integrated to achieve a practical solution. In order to bridge the gap between the electronic and textile industries, the concept of a technology toolbox for textile integrated electronics was created. This toolbox should contain solutions for the electronic industry, allowing them to design and manufacture electronic circuits that are well suited for textile integration. Additionally, this toolbox should provide solutions for the textile industry, so these electronic circuits can be easily integrated in textile products. The main topics

that defined the toolbox structure were described: design principles, circuit manufacturing processes, textile integration processes, interconnection methods and washability testing. Washability was a target that was set especially for this PhD, but will not always be required. Generally, the toolbox should contain a set of tests that evaluate the reliability of the textile product and the developed washablility tests are an example of that.

During this PhD work, the toolbox was filled with different solutions, of which the developments were based on technologies for stretchable electronics. The characteristics of these type of circuits allowed textile integration of electronics in such a way that the typical flexible/stretchable of typical textile products is preserved. At the beginning of this work, these stretchable technologies were still in an early development phase. Realizations were limited to encapsulated meandering copper tracks, which was still far away from a complete functional circuit. With the challenge of creating a technology for robust and washable textile integrated electronics as a driving force, the laser structuring fabrication method was developed. This stretchable substrate fabrication method makes use of standard flexible circuit boards and should be easy to adopt by printed circuit board manufactures. Next to the development of this new stretchable substrate, also advances were made in the encapsulation part of the stretchable technology. In this part, the stretchable circuit is encapsulated in an elastomer, to obtain a stretchable module, which is later on used for textile integration. Liquid injection molding techniques have made it possible to create openings in the encapsulation of stretchable modules. These openings are important to improve the conformability and breathability of the modules and make it possible to access contact pads. Additionally, a new encapsulation method that is based on TPU lamination was developed. Normally, there is a wax adhesive layer on the temporary carrier that is used during the stretchable substrate fabrication step. Since this layer melts because of the heat during lamination, the wax was replaced with a pressure sensitive adhesive tape to bring this new encapsulation method to a success.

The developed fabrication methods make the realization of functional stretchable modules possible. The next goal of this PhD was the integration of these modules into textiles. To facilitate industrialization of the processes in a later stage, the target was to develop integration methods that are easy to adopt in textile manufacturing. The use of two different encapsulation material types (thermosetting and thermoplastic) have led to two different integration methods. The first method uses the screen printing of a PDMS glue layer to bond PDMS encapsulated stretchable modules and fabrics together. A lamination step is used in the second method to bond TPU encapsulated stretchable modules to fabrics. While the developments resulted in lightweight stretchable modules, attaching them to a fabric will always change the fabrics properties to a certain extent. This aspect was investigated and it was was found that

the change in stretchability they cause, is in the same range of changes introduced by typical color prints in todays textile products. Therefore, it can be concluded that the developed technology makes it possible to integrate electronics in textiles without compromising user comfort.

It is possible that applications require different textile integrated stretchable modules, which are interconnected with each other. The creation of openings in the encapsulation makes it possible to access contact pads. This allows the interconnection of textile integrated stretchable modules, by using one of the many textile based interconnection methods. Different realizations were given as examples. These included the interconnection of blinking LED modules with a textile integrated electrical wire and the interconnection of a stretchable module with an embroidered conductive yarn.

Besides technology developments, also a large part of this PhD was devoted to the washability assessment of the textile integrated stretchable modules. It was stated that there are two major challenges to obtain washability for stretchable electronics: sufficient water resistance and good mechanical reliability. Research on the first aspect has led to the development of the Water Effect Test. This test is based on the measurement of leakage currents between encapsulated copper tracks, while they are immersed in a hot water/soap mixture. It was proven that a soldermask in combination with a PDMS or TPU encapsulation provide protection for the copper tracks during 55 hours. Washing reliability of the textile integrated modules is the second aspect that was investigated. The developed Washing Reliability test (WR test) evaluates the solder contacts of SMD components on a flexible island when an encapsulated module is washed several times in a standard washing machine. Two different WR designs were used in the tests. It was shown that the WR2 design, which is an improved version of the WR1 design, was able to survive the maximum tested amount of 25 domestic washing cycles. There was conductivity loss in some of the chains, but only in the case that these WR2 modules were attached to a woven fabric instead of a knitted fabric. The defects were related to folds and cracks in the flexible board and were not caused by broken contacts.

The different technology developments have led to various functional demonstrators in projects and were also used to produce the different test samples described in this dissertation. These successful realizations include a stretchable LED array, a 7x8 LED display, blinking LED modules, an RGB color display, a party shirt and a wireless battery charger. To come to the realization of a demonstrator, it should be designed first. The layout of a stretchable circuit contains meander shaped stretchable tracks. This implies that PCB CAD design software should contain a toolset to route these meandering tracks. A meander design tool for the EAGLE PCB design software was developed for this purpose.

7.2 Future work

A large number of technical innovations were made during this PhD research. With the new developed technologies, it is now possible to actually realize textile integrated stretchable electronic circuits, which was not possible at the beginning of this work. However, the multidisciplinarity that makes the integration of electronics into clothing so challenging, ensures that there is still much research needed to achieve a technology mature enough for industrial production and to manufacture fully characterized and reliable products. As a result, new solutions should be added to the technology toolbox and existing items must be developed further. This section lists some recommendations for future work.

A first topic that requires further research is the use of the wax adhesive on a temporary carrier. The use of this wax was introduced in the work of Bossuyt F. (PhD) and is good to use in a lab environment, but can introduce problems when used on an industrial scale. The main problem with this wax can be found at the carrier release step. After the injection molding of the top part of the module, this carrier is removed by heating up the wax. This step should be fast in order to be feasible in an industrial injection molding process. This means a fast heating up of the wax, peeling off the carrier and removal of wax residues that are left on the module. In the current process, the heating up of the wax before removal takes 3 to 5 minutes at a hotplate temperature of 150°C, which might be too long. The removal of wax residues can only be done with acetone. A solution should be found to remove this residue while the module stays in the injection molding machine or a method should be foreseen to take the half encapsulated module out of the mold and replace it after residue removal. These problems are not existing when the solution with the pressure sensitive adhesive, that was developed in this dissertation, is used. Peeling off the carrier is fast because it does not require an additional step like heating and no residue removal is needed. However, this new method is only a solution for encapsulation materials that do not adhere to the tape. Up to now this has proven to be possible for TPU and other thermoplastic materials that can be injection molded or laminated, but not for PDMS materials. So for PDMS materials the use of the wax is still the only possibility.

The developed textile integration methods have proven to be good solutions. Currently, the stretchable modules are aligned and placed manually onto the fabrics. It would be worthwhile to investigate if this step could be automated.

For some applications, the interconnection of stretchable modules with textile based interconnection methods might be important. While this was not

the main goal of this work, some advances in a good direction were made and advice was given. The development of the connection techniques itself is still open for future research.

Different results related to washability were shown, but also here much remains to be tested. The washing reliability of soldered SMD contacts on functional islands was evaluated, but the combination of functional islands and stretchable meanders has not yet been subjected to washing tests. It is also important to mention that the washability of a certain module will depend a lot on several design aspects, like the shape and size of the module, the location of the functional islands and the density of the electrical components. We can assume that the textile integrated module design should result in a device that is as conformable as possible, without the introduction of high stresses in the module during deformation. However, more experience is needed to translate this assumption into a set of practical design rules.

An interesting challenge for the future is to find applications that can really benefit from textile integrated stretchable electronic modules. From the moment that the circuitry can be designed as a single and small circuit, there is probably no need for stretchability and a flexible or even rigid module can be sufficient. Nevertheless, the developed encapsulation and textile integration methods can also be used for these type of modules. In order to benefit from stretchability, the application should contain electronic circuitry that is distributed over a large surface. Examples of such a circuit are the LED displays presented in this work. These circuits really need the stretchability, so that user comfort is preserved when integrated in textile. Another interesting feature that the developed stretchable technology can bring, is found in devices that can be shaped by thermoforming. The developed method with the pressure sensitive adhesive on the carrier plate can be used to encapsulate a stretchable circuit in a rigid thermoplastic material, instead of in an elastic material. It might be possible to do a one time deformation of such a module, where at the positions at which the module is deformed, the stretchable interconnections would be subjected to a one time stretch. Research on this topic might lead to a new set of applications.

A

Meander tool for Eagle PCB design software.

A.1 Getting started with the tool

To launch the tool:

- Startup Eagle
- Type 'run meandertool' in the command line of the board window.
- Hit enter.
- The meander tool will pop up.

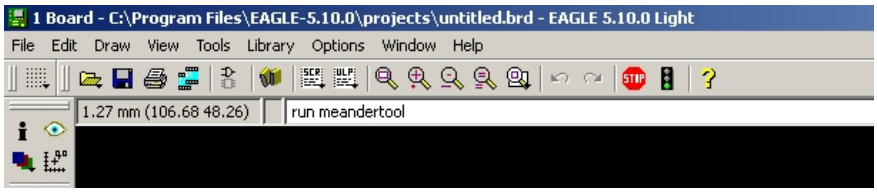

Figure A.1: Launching the meander tool.

A.1.1 Draw meanders

Meanders can be drawn directly into the board layout. The shape of the meander is defined by the number of turns (n), the width (w), the radius (r)

and the angle (a) (see Figure A.2). The angle between the meander and the x-axis is set with the direction (d) parameter. Angles are given in degree measurement. The drawing layer can be chosen by changing the layer number (e.g. 1=Top, 16=Bottom). Every track in Eagle has a signal name. Change the signal name for the meander you want to draw, to add it to the right signal in the netlist. The begin point of the meander is defined by its x-y coordinate. This begin point is automatically updated with the endpoint of the last drawn meander (or other structure).

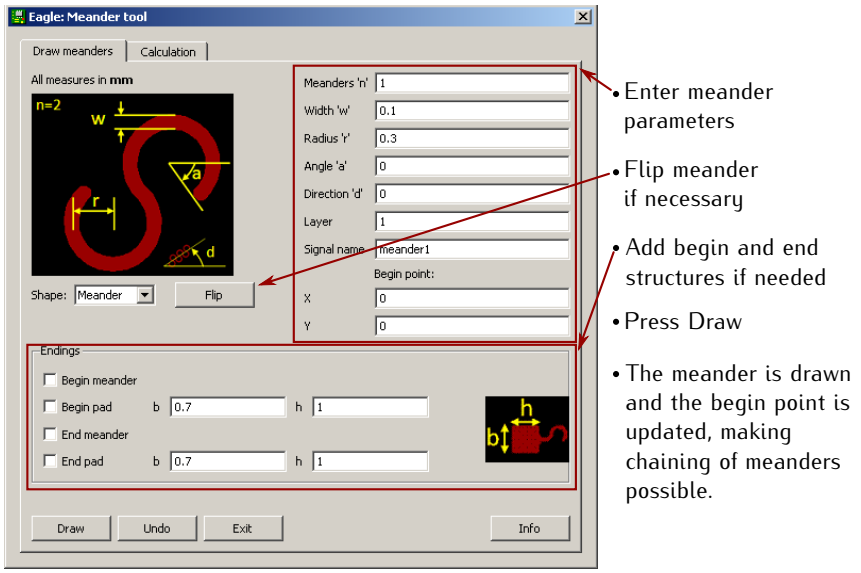

Figure A.2: Steps to follow for meander drawing.

Begin and end shapes can be added to the meander if necessary. These shapes are commented in Figure A.3.

(a) Begin pad. (b) Begin meander (c) begin pad + begin meander

Figure A.3: Illustration of the begin shapes that can be added to the meander.

A.1.2 Draw other shapes

The other shapes one can draw are illustrated in the Figures A.4, A.5 and A.6.

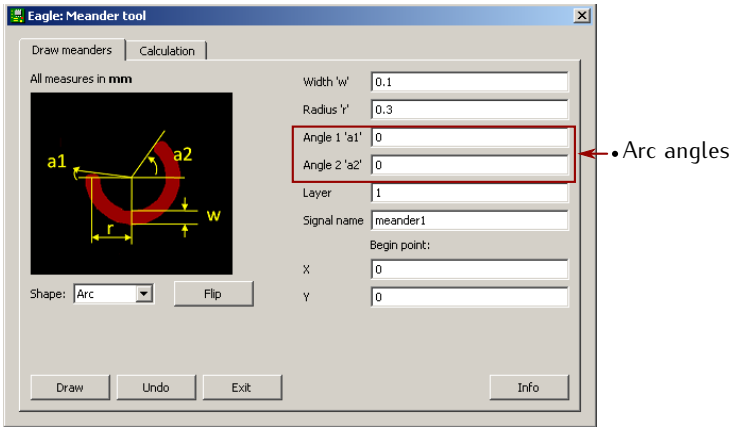

Figure A.4: ***Arc:*** *Draw one turn of a meander, defined by two different angles.*

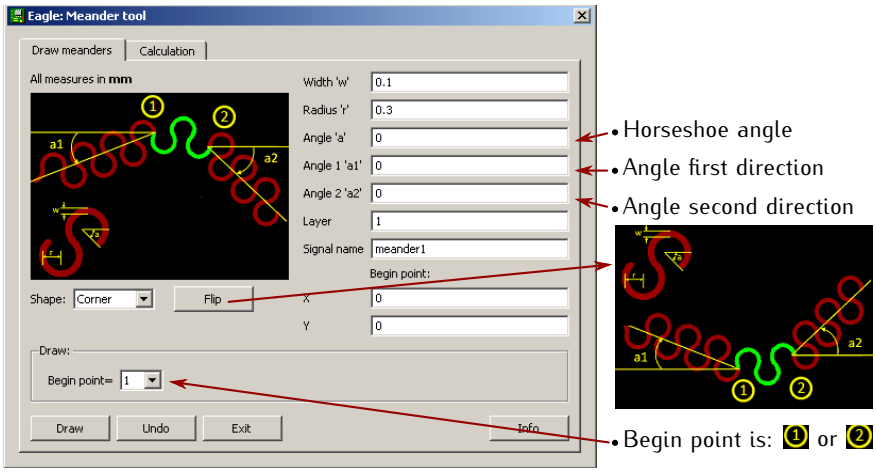

Figure A.5: ***Corner:*** *Draw a corner to go from one direction to another.*

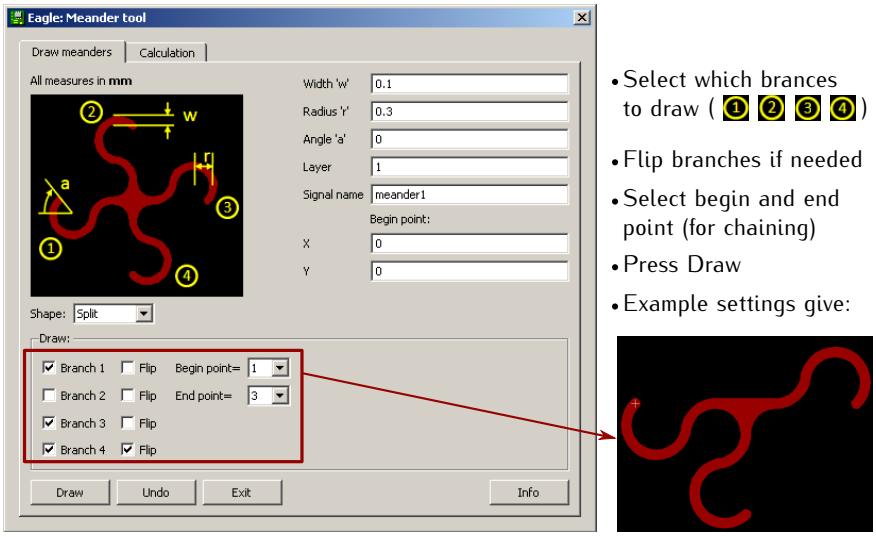

Figure A.6: ***Split:*** *Draw a split with two, three or four branches.*

A.1.3 Calculations tab, how to use...

The use of the meander tool will be explained using a simple design example. The first thing to do, is draw the schematic and create the board from this schematic (example in Figure A.7).

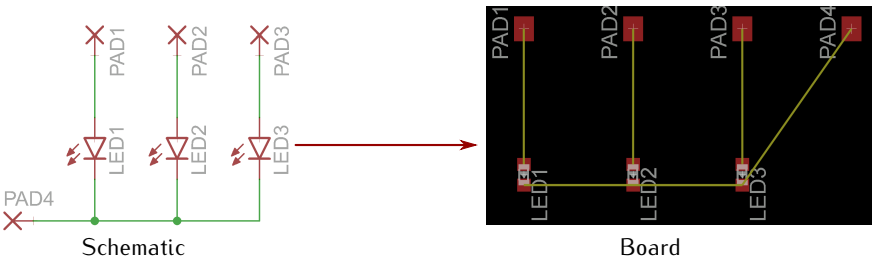

Figure A.7: Example of a schematic and board layout.

The yellow lines in the board layout are 'air wires' which are unrouted. It is the intention to route these wires with meanders. Without the meander calculations section in the meander tool this would be a hard job to do. This is because we need to determine the number of meander turns and the meander radius to exactly fit the length between the components. In the calculations tab of the meander tool one can see the list of unrouted signals, together with the x-y coordinates of the begin and end points. It is advised to give proper names to signals in the schematic editor, making it easier to recognize unrouted signals.

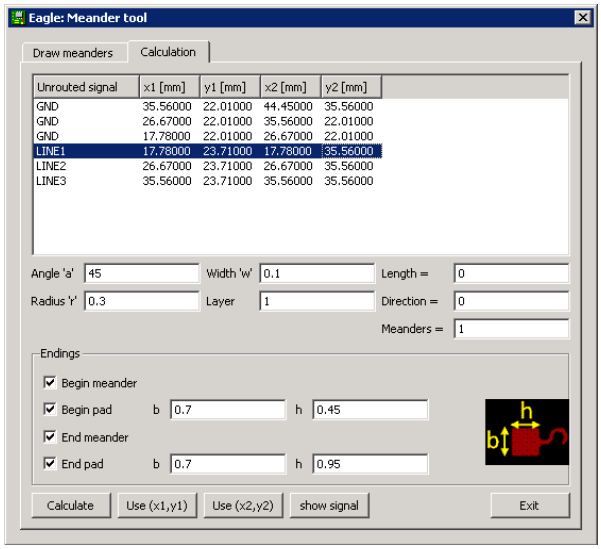

Figure A.8: Meander calculations for signal LINE1.

- Select the signal you want to route. If you're not sure if it is the correct signal, press 'show signal'. This highlights the selected signal in the board editor.
- Set up the parameters for the meander you want to draw between the begin and end point of the unrouted signal (angle, radius and width).
- Check the boxes if you need begin or end shapes attached to the meander.
- Press calculate. After calculation the window is updated (Figure A.9).

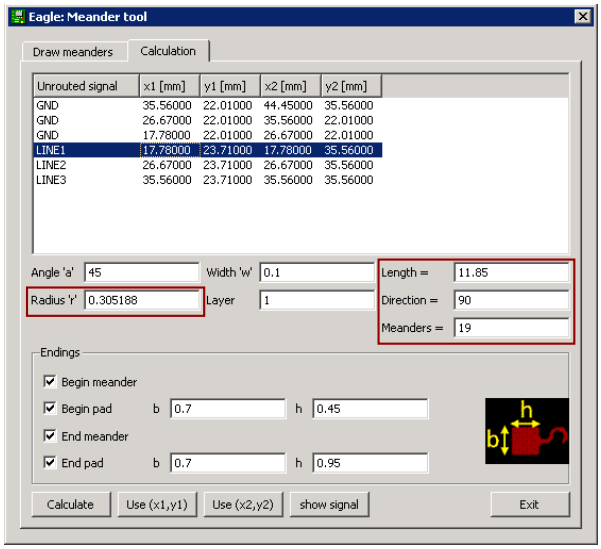

Figure A.9: Calculated values for the LINE1 meander.

The tool calculated:

- The total length of the meander (+ endings).
- The direction of the meander.
- The number of meander turns.
- The adaptation of the radius to have a perfect fit between begin and end point of the unrouted signal.

Go back to the 'draw meanders' tab. The calculated parameters are automatically filled in (Figure A.10).

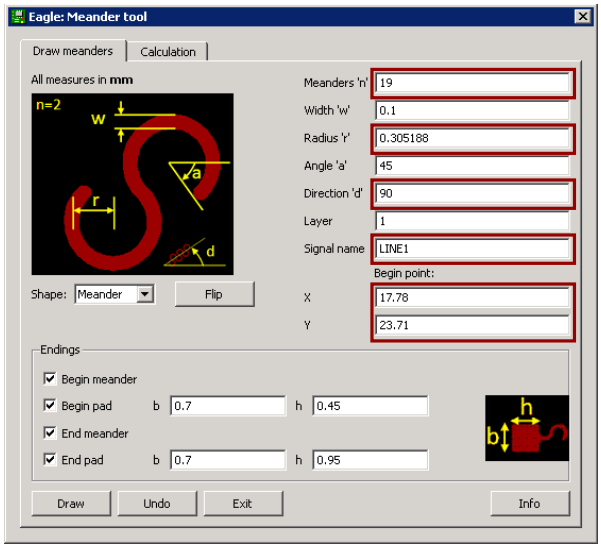

Figure A.10: Calculated values are automatically filled in.

Once you press the draw button, the meander is drawn (Figure A.11(a)). This can be repeated for the other signals (Figure A.11(b)). During this process, the unrouted signal list is updated every time.

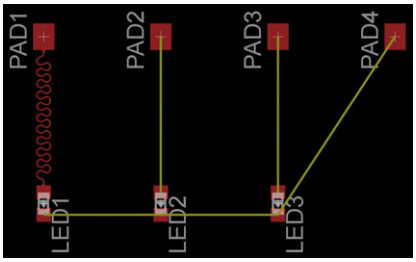

(a) First meander routed.

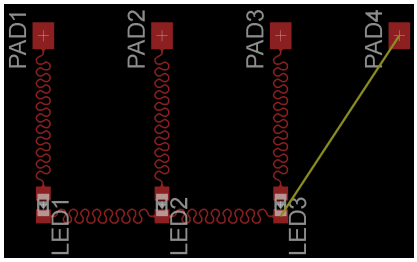

(b) Using the same process for other meanders.

Figure A.11: Drawing meanders using the calculator option of the meander tool.

In case you have to make a turn (here from LED3 to PAD4) you can perform the following actions:

- First draw a corner with the same signal name.
- New airwires will be created.
- Exit the meander tool and move the corner to the desired position.
- Press the Rastnest button in the board layout to let eagle recalculate the airwires.

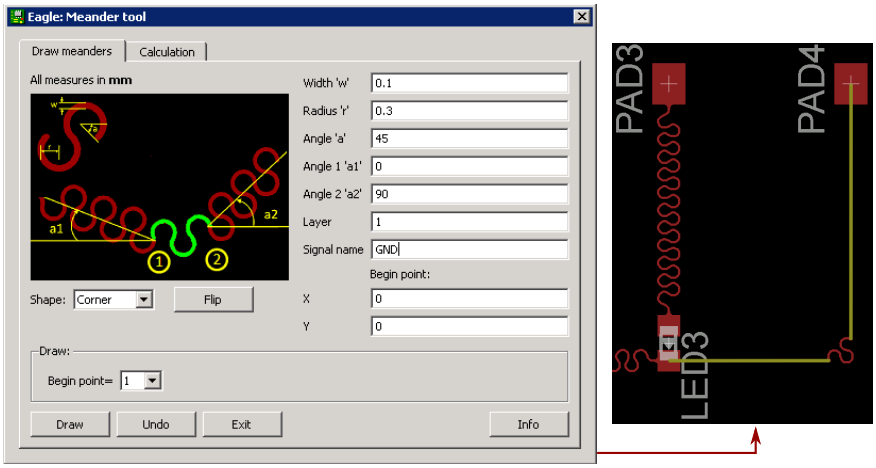

Figure A.12: Making a turn.

Now you can run the meander tool again to calculate the meanders in order to route the unrouted signals (Figure A.13).

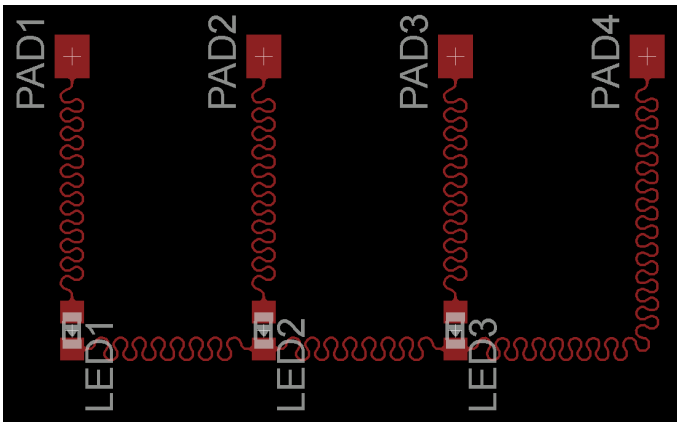

Figure A.13: Routing the last signals completes this layout design.

A.2 Goniometric calculations

This section gives an overview of the goniometric calculations used in the meander tool to draw the different shapes.

Meander

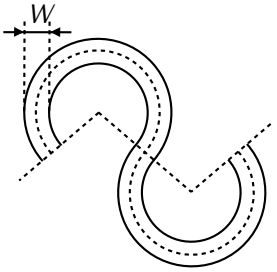

Figure A.14: Meander width W.

The drawing in Figure A.14 shows the definition of the width (W) of the meander. In the rest of the drawings in this section, only the centerline of the meander is drawn. Figure A.15 shows the coordinates of one meander turn with (x, y) the coordinates of the begin point p.

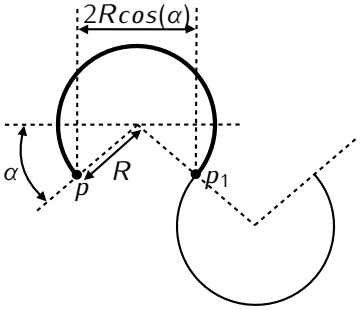

α = horseshoe angle
R = radius

$p_1$coordinate :

$x_1 = x + 2R\cos(\alpha)$

$y_1 = y$

Figure A.15: Coordinates of one meander turn.

Pad

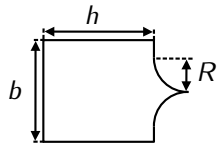

Figure A.16: Pad dimensions.

Figure A.16 illustrates the begin and end pad dimensions. Note that the height (h) and the width (b) are defined here on the centerline. In the end these dimensions are increased by the meander width (W).

Begin meander

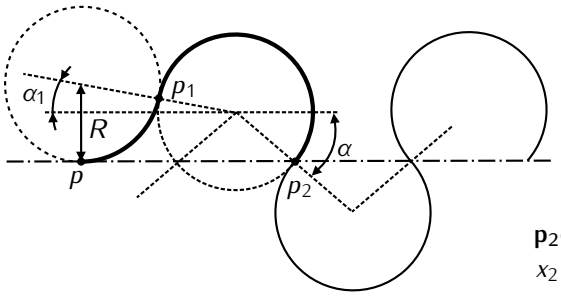

α_1 angle :

$$R = 2R\sin(\alpha_1) + R\sin(\alpha)$$

$$\alpha_1 = \arcsin\left(\frac{1-\sin\alpha}{2}\right)$$

p_1 coordinate :

$$x_1 = x + R\cos(\alpha_1)$$

$$y_1 = y + R(1-\sin(\alpha_1))$$

p_2 coordinate :

$$x_2 = x_1 + R(\cos(\alpha_1) + \cos(\alpha))$$

$$y_2 = y_1 + R(\sin(\alpha_1) - 1)$$

Figure A.17: Coordinates of a begin meander.

Figure A.17 shows how the begin meander is defined. The begin point p has (x, y) as coordinates. Calculation of the coordinates is done step by step because there is also a rotation implemented in the meander tool. This rotation is done in the 'locale coordination system' with the start point of the arc as the orgin:

$$x_{rotated} = x\cos(\alpha_{rot}) - y\sin(\alpha_{rot})$$

$$y_{rotated} = x\sin(\alpha_{rot}) + y\cos(\alpha_{rot})$$

So first we calculate the end coordinate of the arc without a translation. Then we do the rotation and next the translation.
Example:

$$x_1 = R\cos(\alpha_1)$$

$$y_1 = R(1-\sin(\alpha_1))$$

$$x_{rotated+translated} = x_1\cos(\alpha_{rot}) - y_1\sin(\alpha_{rot}) + x$$

$$y_{rotated+translated} = x_1\sin(\alpha_{rot}) + y_1\cos(\alpha_{rot}) + y$$

Meander turn

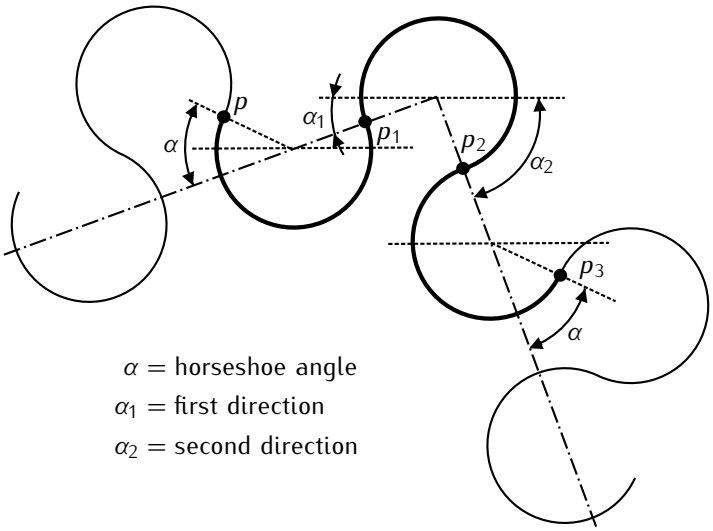

Figure A.18: Meander turn

Figure A.18 illustrates how a meander turn is used to go from one meander direction (α_1) to another (α_2). A turn can be drawn starting from two different starting points (p or p_3).

Calculations beginning from $p(x, y)$:

p_1 coordinate

$$x_1 = x + R(\cos(\alpha - \alpha_1) + \cos(\alpha_1))$$
$$y_1 = y - R(\sin(\alpha - \alpha_1) - \sin(\alpha_1))$$

p_2 coordinate

$$x_2 = x_1 + R(\cos(\alpha_1) + \cos(\alpha_2))$$
$$y_2 = y_1 + R(\sin(\alpha_1) - \sin(\alpha_2))$$

p_3 coordinate

$$x_3 = x_2 + R(\cos(\alpha_2) + \cos(\alpha - \alpha_2))$$
$$y_3 = y_2 - R(\sin(\alpha_2) - \sin(\alpha - \alpha_2))$$

Calculations beginning from $p_3(x_3, y_3)$:

p_2 coordinate

$$x_2 = x_3 - R(\cos(\alpha_2) + \cos(\alpha - \alpha_2))$$
$$y_2 = y_3 - R(\sin(\alpha - \alpha_2) - \sin(\alpha_2))$$

p_1 coordinate

$$x_1 = x_2 - R(\cos(\alpha_1) + \cos(\alpha_2))$$
$$y_1 = y_2 - R(\sin(\alpha_1) - \sin(\alpha_2))$$

p coordinate

$$x = x_1 - R(\cos(\alpha - \alpha_1) + \cos(\alpha_1))$$
$$y = y_1 - R(\sin(\alpha_1) - \sin(\alpha - \alpha_1))$$

Meander calculations

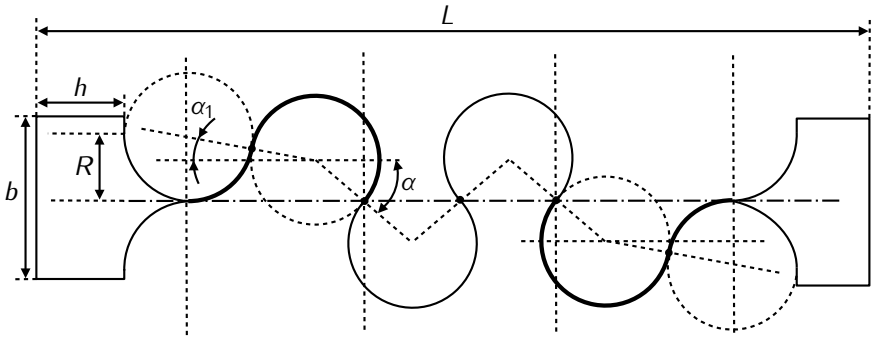

Figure A.19: Total meander, including begin and end structures.

Algorithm used in the meander calculations:

- Calculate length (L) of the unrouted air wire.
- Calculate number of meander turns (N) (function of L, radius (R) and horseshoe angle (α)).
- Calculate the correct value of R (because N is rounded to nearest integer).

α= horseshoe angle; E=number of endings (0,1 or 2); E_p=number of end pads (0,1 or 2); N=number of turns

α_1 angle:

$$\alpha_1 = \arcsin\left(\frac{1-\sin\alpha}{2}\right)$$

Number of meander turns (N):

$$L = ER(\cos(\alpha) + 2\cos(\alpha_1)) + 2NR\cos(\alpha) + E_p(h+R)$$
$$=> N = round\left(\frac{L - ER(\cos(\alpha) + 2\cos(\alpha_1)) - E_p(h+R)}{2R\cos(\alpha)}\right)$$

Radius (R) in function of L, N and α:

$$R = \frac{L - E_p h}{E(\cos(\alpha) + 2\cos(\alpha_1)) + 2N\cos(\alpha) + E_p}$$

Remark: In the meander program E_p and h are split up (begin-pad, end-pad, h_1, h_2).

B

Peel test graphs

B.1 PDMS adhesion

Graphs of the Sylgard 186 peel test results.

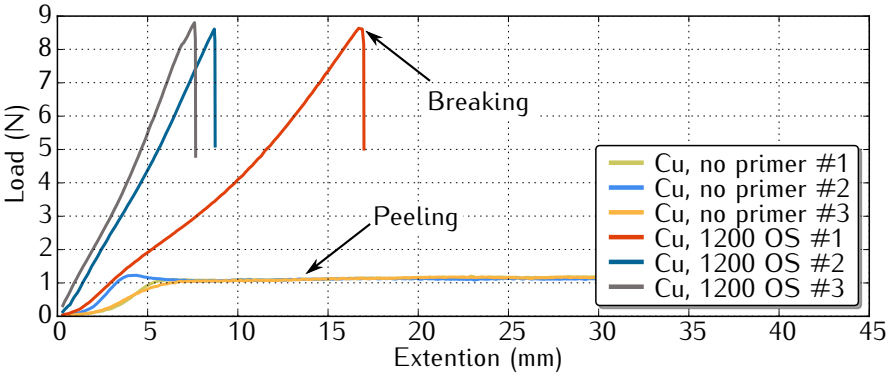

Figure B.1: Sylgard 186 - Copper adhesion results, with and without 1200 OS primer.

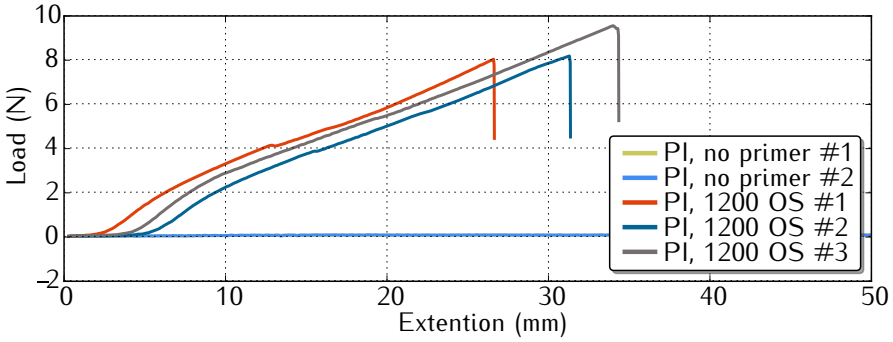

Figure B.2: Sylgard 186 - Polyimide adhesion results, with and without 1200 OS primer.

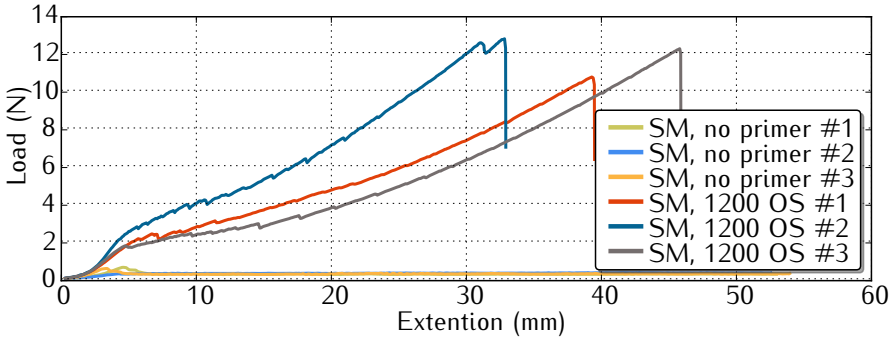

Figure B.3: Sylgard 186 - Soldermask adhesion results, with and without 1200 OS primer.

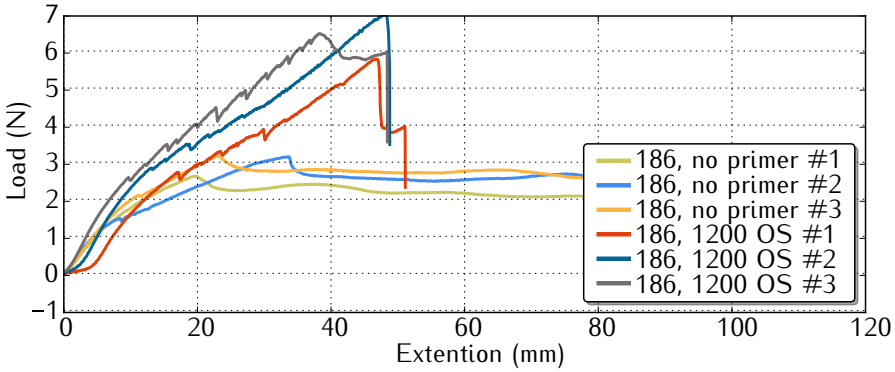

Figure B.4: Sylgard 186 - Sylgard186 adhesion results, with and without 1200 OS primer.

B.2 TPU adhesion

Graphs of the Krystalflex 429 peel test results.

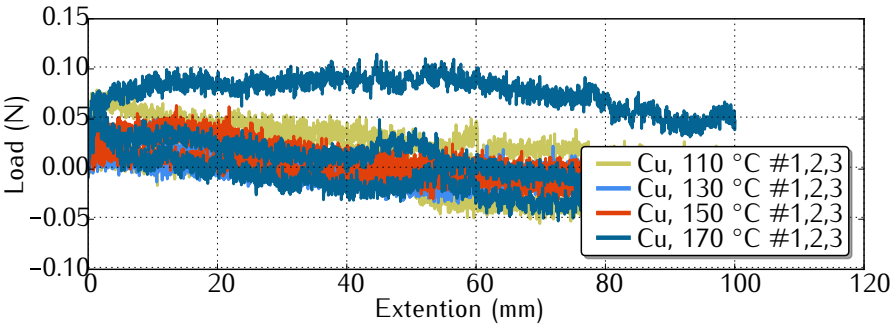

Figure B.5: Krystalflex 429 TPU - copper adhesion results for TPU laminated at different temperatures.

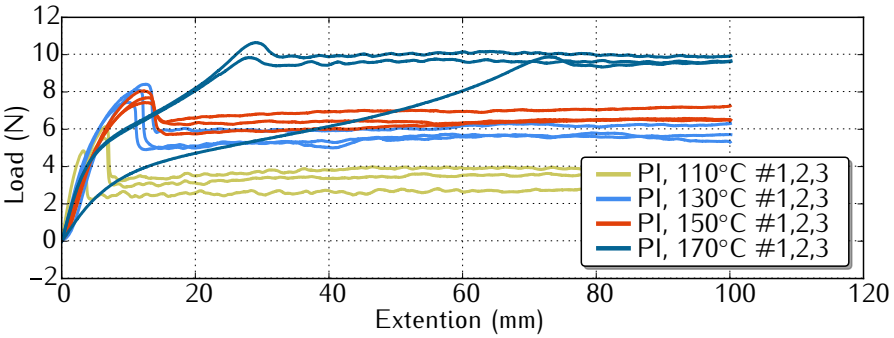

Figure B.6: Krystalflex 429 TPU - polyimide adhesion results for TPU laminated at different temperatures.

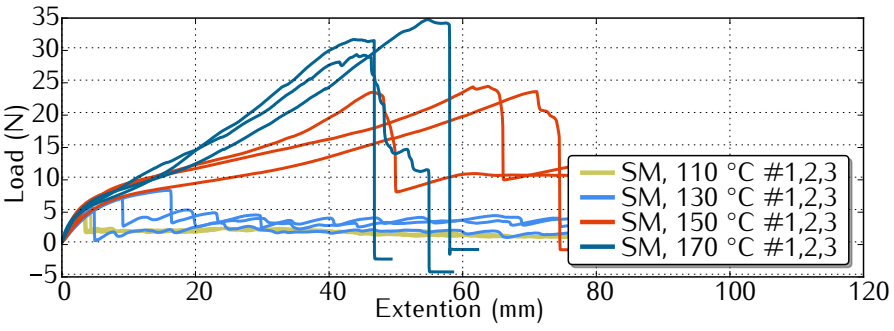

Figure B.7: Krystalflex 429 TPU - soldermask adhesion results for TPU laminated at different temperatures.

C

MSP430F2132 Development Board Manual

Thomas Vervust, Benoît Huyghe - 3 March, 2009

C.1 Introduction

The development board has been designed to allow quick prototyping and testing of a new application using a Texas Instruments MSP430f2132 microcontroller. Several frequently used components, such as a USB controller and wireless module, are incorporated on the board and can easily be connected to the microcontroller using switches. Pin headers provide easy access to all pins and external functions of the microcontroller. Several LEDs and push buttons are present to allow visual feedback and testing of interrupts while debugging microcontroller code. The board can be powered through various sources: USB, battery, DC adapter or external power supply.

C.2 Microcontroller

The MSP430f2132 is an ultra-low-power 16-bit microcontroller from Texas Instruments [1]. It features two built-in 16-bit timers, a 10-bit A/D converter with integrated reference and a data transfer controller (DTC), a comparator, built-in communication capability using the universal serial communication interface, and 24 I/O pins [2].

C.2.1 Programming

Loading code into the microcontroller can be executed via a JTAG-interface [3]. A 14 pins JTAG connector can be connected to the board using the JTAG pin header, located on the upper left side of the board. Make sure the board is powered on, as the design does not allow for the JTAG to power the microcontroller.

Writing code for the MSP430 microcontroller family can easily be done with a software tool called *IAR embedded workbench*. This program also supports realtime debugging of code, which can greatly reduce the amount of time for implementing an application. A kickstart version of this program can freely be downloaded from the Texas Instruments website [4]. Example code which demonstrates the use of several of the functions of the microcontroller is also available online.

Figure C.1 lists the connections between the JTAG pin header and the microcontroller.

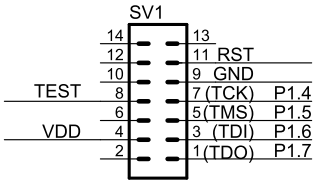

Figure C.1: Connections between JTAG pin header and microcontroller.

C.2.2 Reset

The development board is equipped with a manual reset circuit for the microcontroller, illustrated in Figure C.2. Whenever the reset-pin of the microcontroller is pulled low, a reset is executed. This can be manually forced by pressing the reset-button. In normal operation, the RC-circuit will slowly pull the reset-pin high, allowing the microcontroller to start all its functions in a controlled way.

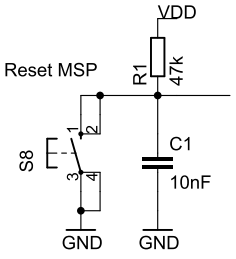

Figure C.2: Microcontroller reset circuit.

C.2.3 Pin headers

All of the microcontroller pins can easily be accessed through the two 34-way pin headers on the lower left side of the board. The connections between the pin headers and the microcontroller are listed in Figure C.3.

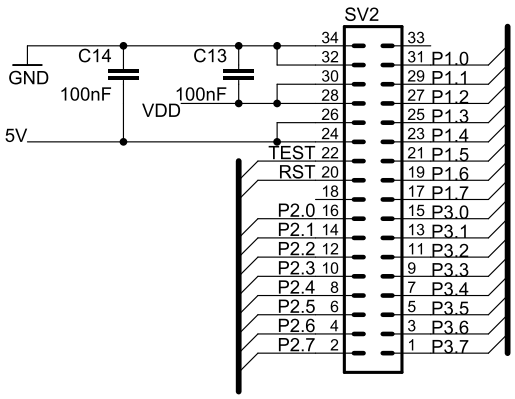

Figure C.3: Connections between the pin headers and microcontroller.

C.2.4 Crystal

The development board is equipped with a high precision watch crystal operating at 32.768 kHz with a ± 20 ppm accuracy. The user can choose to enable or disable this crystal by sliding the switch as is illustrated in Figure C.4. Optionnally, a different crystal can be used by disabling the watch crystal and connecting the other crystal via the pin headers to the microcontroller.

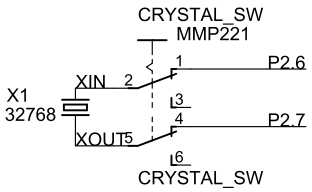

Figure C.4: Microcontroller crystal circuit.

C.2.5 LEDs

Eight LEDs have been placed on the development board that can individually be connected to one of the port 1 pins of the microcontroller by setting the appropriate switch as indicated in Figure C.5. To light up a LED, the appropriate

switch must be set in the on position and the corresponding microcontroller pin must be set high. The LEDs can be used for visualization or debugging purposes.

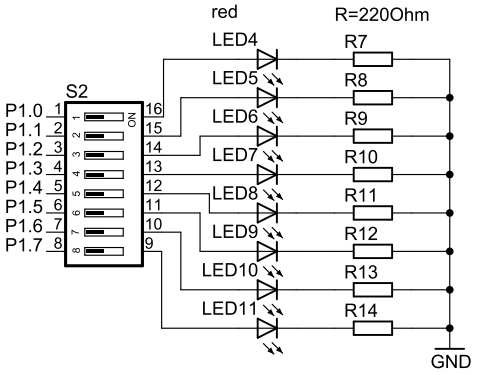

Figure C.5: Available LEDs for debugging or visualisation.

C.2.6 Push buttons

Four push buttons have also been incorporated in the development board design. These buttons are connected to several pins of the microcontroller, which support interrupts, as indicated on Figure C.6. The buttons allow for the user to manually pull one of the pins of the microcontroller low. By activating the internal pull-up resistor of the microcontroller for the appropriate pin, a high-to-low transition could then trigger an interrupt on the corresponding pin. This way, the buttons can be used for testing and debugging purposes.

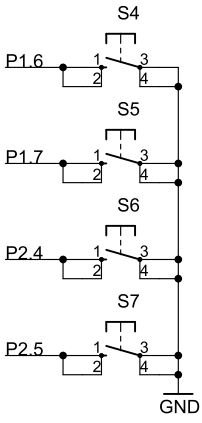

Figure C.6: Available push buttons for debugging or interrupt.

C.3 Communication

The microcontroller is equipped with two Universial Serial Communication Interfaces (USCI), which support a number of standard communication protocols. The USCI A supports SPI and UART while USCI B supports SPI and I^2C.

C.3.1 SPI

Both USCIs support the SPI protocol in two forms: 3-wire and 4-wire. The latter is used when multiple masters are present on the bus to ensure none of them transmit data at the same time. All pins that are required for 4-wire SPI, including the supply voltage and the ground, are available at the top of the board via two pin headers. The connections to these pin headers are displayed in Figure C.7. This allows to easily connect a device to the board using the SPI protocol via one or both USCIs. Take care however, that none of the pins is in multiple use, as some pins of the SPI interfaces are shared between USCIs and different communication modes.

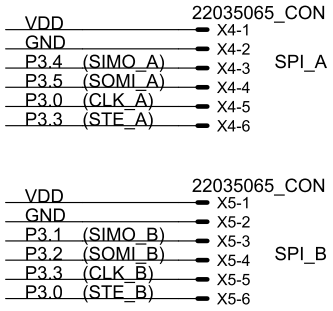

Figure C.7: Connections to the SPI pin header.

General information on the SPI protocol can be found in several places on the internet [5]. More specific information on the bytes that should be send via SPI to achieve a variety of functions can be found in the datasheet of components that are used.

C.3.2 I^2C

The USCI B supports the I^2C protocol. A pin header is present at the top of the board, which is connected to the necessary pins for I^2C communication (data line SDA and clock line SCL), the power supply and ground. The connections are illustrated in Figure C.8. Note that before the interface can be used, the pin header must be enabled by sliding the switch in the correct position.

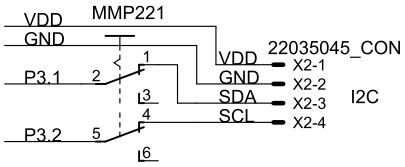

Figure C.8: Connections to the I²C pin header.

The I²C protocol requires both communication lines (SDA and SCL) to be connected via a pull-up resistor to the voltage supply. Some components have these pull-up resistors build-in their circuits, yet sometimes, these resistors have to be added externally. Therefore, pull-up resistors are present on the board which can individually be enabled or disabled with a switch. Figure C.9 shows the circuit around these pull-up resistors.

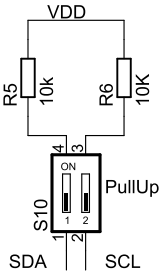

Figure C.9: Circuit around the I²C pull-up resistors.

The basic working principle of the I²C protocol can be found on the internet [6], as well as the official I²C bus specification [7]. More specific information, as for example device slave address and register addresses, can be found in the device specific datasheets.

C.3.3 UART

The USCI A supports the UART protocol. The pins for this communication bus are available at the top of the board, together with the voltage supply and the ground. The schematic with the connections is displayed in Figure C.10.

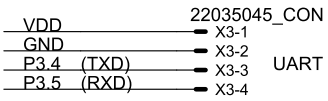

Figure C.10: Connections to the UART pin header.

The UART protocol is the most simple protocol to connect two devices with each other. This two-wire interface is the basis for various standards as for example the RS232 standard, also known as the serial port of a computer. More information on the UART protocol can be found on the internet [8]. For more specific information concerning the actual data format of the transmitted information, check the datasheet of the used component.

C.4 Interfaces

The development board is equipped with two independent interfaces, a USB and a wireless RF interface, which can be used to communicate with the board.

C.4.1 USB

The USB connection is implemented using a USB to UART bridge IC by FTDI. This IC will translate incoming USB signals to standard UART signals and vice versa. The circuit that is used is displayed in Figure C.11 and is mainly built around the FT232R from FTDI [9].

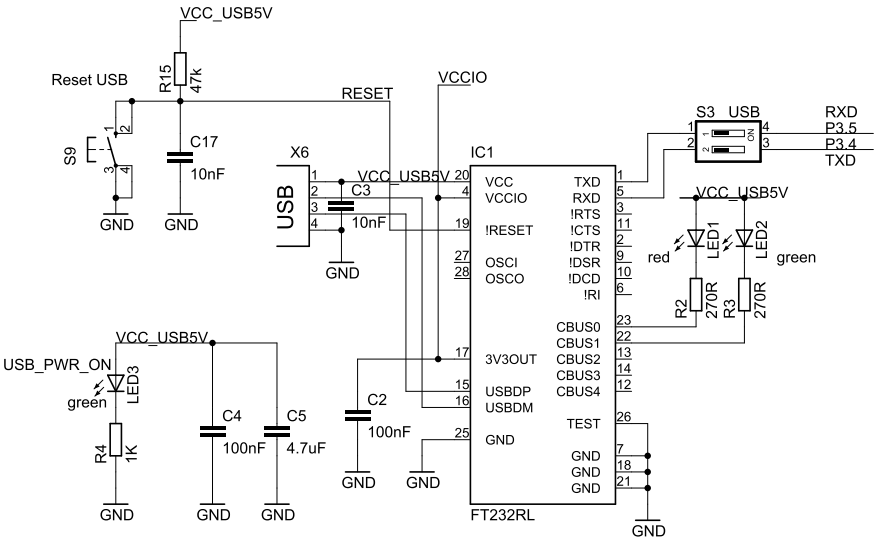

Figure C.11: FTDI USB to UART bridge circuit.

Reset

As with the microcontroller, this chip has a reset pin which must be pulled high in normal operation. A similar circuit as in Figure C.2 allows for a manual reset of the chip by pressing a button, while an RC circuit will slowly pull the reset pin high when the button is released.

LEDs

Three different LEDs are present in this part of the circuit. A green LED, located very closely to the USB socket, will illuminate as soon as the board is connected to a pc via USB. The other two LEDs indicate if data is being received (CBUS1, green LED) or transmitted (CBUS0, red LED) via USB.

UART

The communication with the microcontroller is executed using UART communication. This protocol is supported by the microcontrollers USCI A and a connection can be realized by setting the switches in the on position. Make sure however, that no other device is using one or both of the required pins for the UART communication, as this might result in malfunction.

C.4.2 RF Wireless

A wireless interface is implemented on the board using an nRF2401 RF radio chip from Nordic Semiconductor [10]. This radio chip communicates via SPI with the microcontroller and is able to transmit or receive information using Gaussian Frequency Shift Keying (GFSK) in the 2.4 GHz ISM frequency band. Figure C.12 illustrates the circuit around the radio chip. The *ANT1M* and *ANT2M* terminals are connected to a PCB antenna which is designed to match to the impedance of the RF chip.

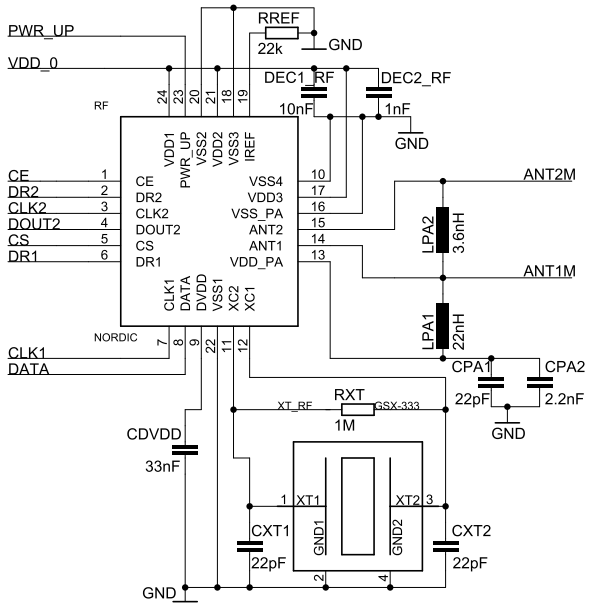

Figure C.12: RF interface circuit.

SPI

The communication between the microcontroller and the RF chip is implemented as an SPI interface. It is however a modified version of the standard protocol, as only one pin is present on the radio chip for data communication, combining both the *SIMO* and *SOMI* lines from SPI. Therefore, care must be taken in programming the communication between both devices, as both pins of the microcontroller are actually shorted in the design. Example code for the communication is available within CMST.

The selection circuit for the SPI communication is displayed in Figure C.13 and can be found on the board within the area bounded by the dotted line and marked *Wireless Select*. The RF chip is actually a dual receiver and thus features two SPI interfaces. The selection circuit allows the user to connect either of these interfaces with either of the USCIs of the microcontroller. The two dip switches allow individual enabling of each of the pins of the RF chip, by connecting them to the microcontroller. The other big switch allows choice to connect the first SPI interface with USCI A and the second with USCI B or vice versa.

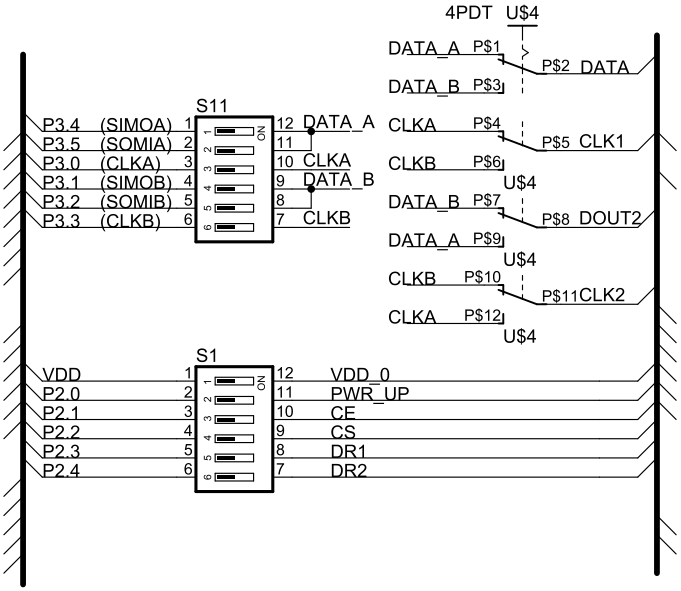

Figure C.13: RF-chip SPI interface selection circuit with switches.

C.5 Power Supply

The development board is equipped with separate circuits for 3.3 and 5 V. Each circuit can be powered from a variety of sources.

C.5.1 DC adapter

On the upper right side of the board, a connector for a DC adapter is present. Once a DC adapter is connected, the LED close to the socket should light up. It is assumed that the output voltage of the adapter is 5 V. Figure C.14 shows the regulator circuit using an LD1117AV33 from ST Microelectronics, which supplies a 3.3 V source with a maximum output current of 1 A [11].

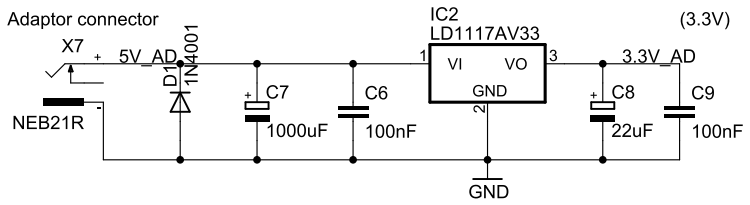

Figure C.14: DC adapter 3.3 V regulator circuit.

C.5.2 USB

Below the DC connector, a USB type B socket is present. A 5 V power supply can directly be accessed from this USB connector when it is plugged into a computer. When a cable is correctly attached to the socket, the LED close to the socket should light up to show power is present. When using this supply for power, check the maximal amount of current the USB port can deliver, as this depends on the port configuration. A 3.3 V power supply is also available through the FTDI chip, as can be seen on Figure C.11. The internal regulator of the FTDI allows for a maximal output current of 50 mA [9].

C.5.3 Battery

Below the USB socket, a two pin header is present, which allows for connecting a battery to the board. The output voltage of the battery connected to this pin header is regultated by a Micel MIC5209 3.3 V LDO with a maximum output current of 0.5 A [12]. The circuit around this LDO is illustrated in Figure C.15.

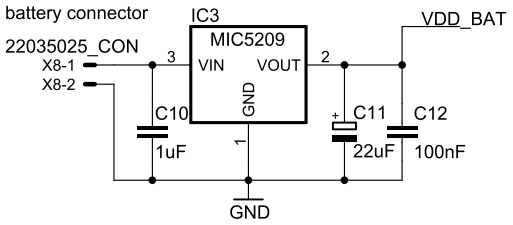

Figure C.15: DC adapter 3.3 V regulator circuit.

C.5.4 External power supply

Below the battery pin header, a 3-way pin header is present to allow connection for an external power supply. Both the 3.3 and 5 V circuits may be powered by an external power supply.

C.5.5 Selection

The selection of the source for each of the circuits is possible through switches. The circuit of the switches is displayed in Figure C.16. The left switch allows choice between the DC adapter and the USB interface. This switch will assign both the 5 V and the 3.3 V power circuit to one of the sources. The second switch allows to choose between the selected source from the first switch or a battery as a power source for the 3.3 V power circuit. The 5 V circuit can not be powered from the battery as a lithium polymer battery is assumed, which only delivers voltages around 3.7 V. When powering the board through an external power supply, make sure that no other power source conflicts with this external supply.

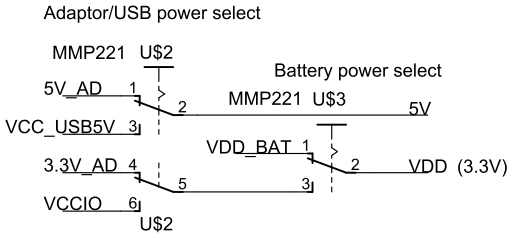

Figure C.16: Switch circuit for source selection.

C.6 Full schematic

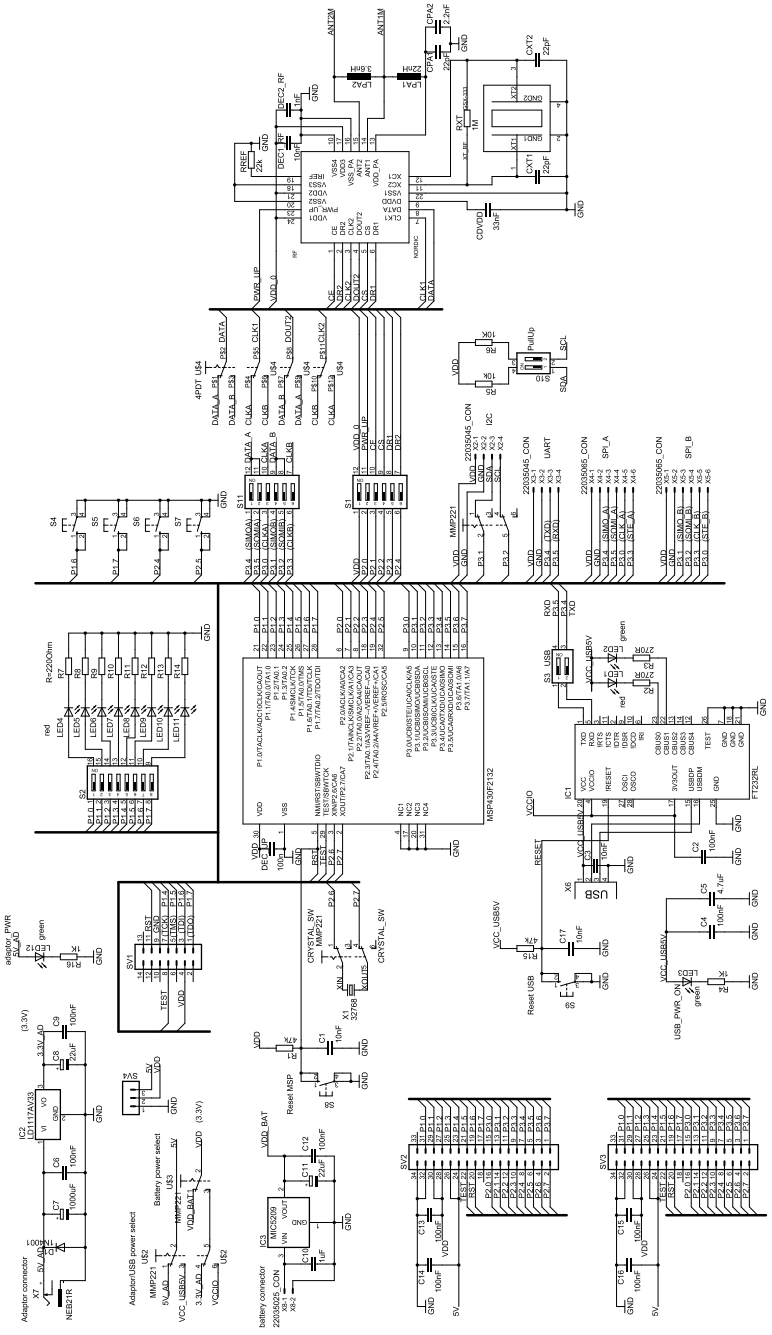

Figure C.17: Full circuit schematic (best viewed in digital format of the dissertation).

C.7 Board layout

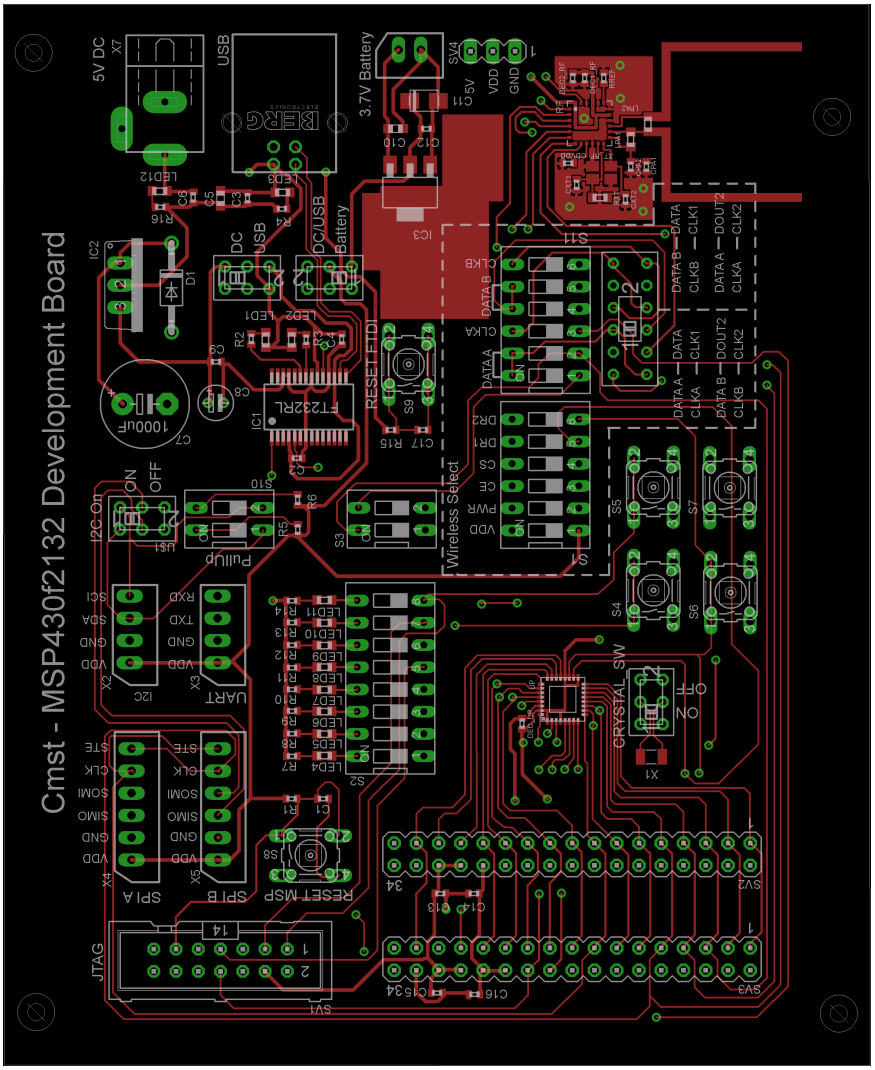

Figure C.18: Top board design.

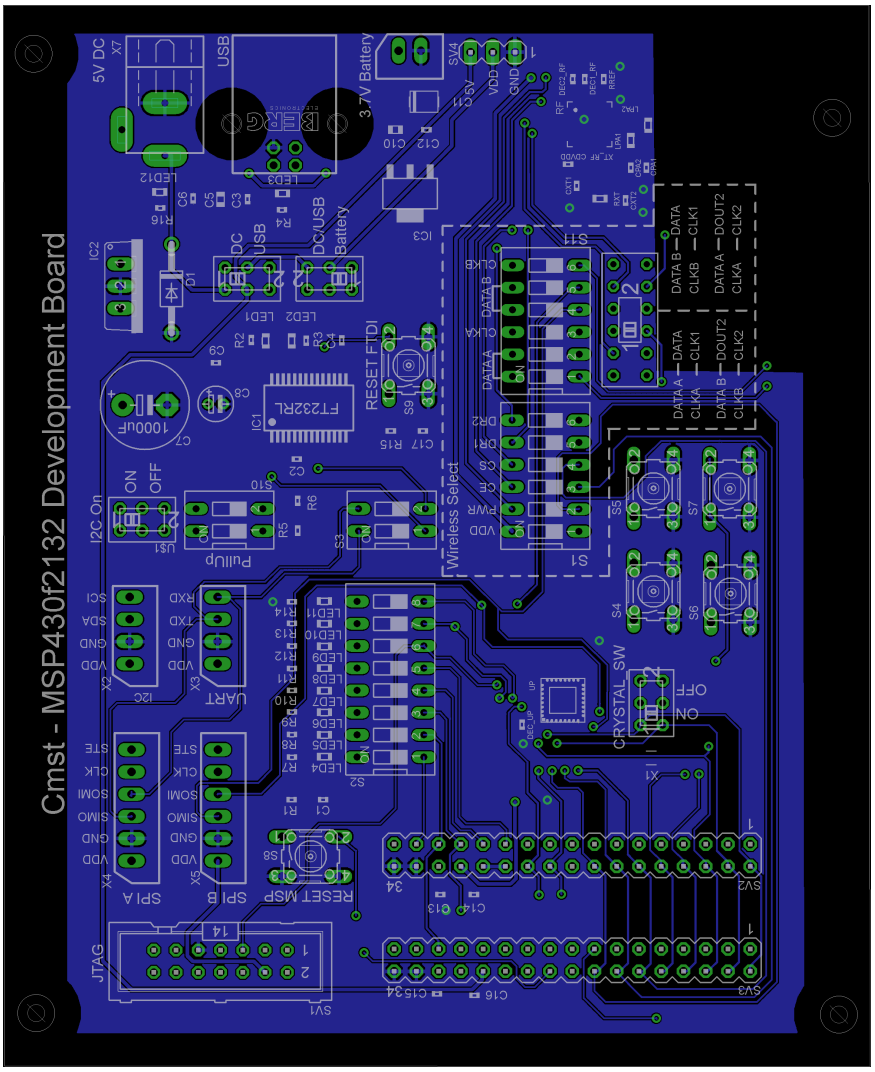

Figure C.19: Bottom board design.

References

[1] "MSP430f21x2 mixed signal microcontroller - Component datasheet," Texas Instruments, May 2008.

[2] "MSP430x2xx family user guide - Component user guide," Texas Instruments, 2008.

[3] (2009) Joint Test Action Group (JTAG). Wikipedia. [Online]. Available: http://en.wikipedia.org/wiki/Joint_Test_Action_Group

[4] (2009) MSP430F2132 product website. Texas Instruments. [Online]. Available: http://focus.ti.com/docs/prod/folders/print/msp430f2132.html

[5] (2009) Serial Peripheral Interface Bus. Wikipedia. [Online]. Available: http://en.wikipedia.org/wiki/Serial_Peripheral_Interface_Bus

[6] (2009) I^2C. Wikipedia. [Online]. Available: http://en.wikipedia.org/wiki/I%C2%B2C

[7] "The I^2C-bus specification, Version 2.1," Philips Semiconductors, January 2000.

[8] (2009) Universal asynchronous receiver/transmitter. Wikipedia. [Online]. Available: http://en.wikipedia.org/wiki/UART

[9] "FT232R USB UART I.C. - Component datasheet," Future Technology Devices International, 2005.

[10] "Single chip 2.4 GHz transciever, nRF2401 - Component datasheet," Nordic Semiconductor, June 2004.

[11] "LD1117A Series - Component datasheet," ST Microelectronics, July 2005.

[12] "MIC5209 - Component datasheet," Micrel, June 2006.

D
Publication list

Journal papers

[1] T. Vervust, G. Buyle, F. Bossuyt, M. Jablonski, and J. Vanfleteren, "Washing reliability of textile integrated stretchable electronic modules," *Mirocroelectronics Reliability, submitted*, 2012.

[2] T. De Nies, T. Vervust, M. Demey, M. Leman, J. Vanfleteren, and R. Van de Walle, "Synchronizing Music and Movement with BeatLED: an Interactive Social Game," *J. New Music Research, accepted*, 2012.

[3] J. Vanfleteren, T. Loeher, M. Gonzalez, F. Bossuyt, T. Vervust, I. De Wolf, and M. Jablonski, "SCB and SMI : Two stretchable circuit technologies, based on standard printed circuit board processes," *Circuit World, accepted*, 2012.

[4] M. Jablonski, F. Bossuyt, J. Vanfleteren, T. Vervust, and H. de Vries, "Reliability of a stretchable interconnect utilizing terminated, in-plane meandered copper conductor," *Mirocroelectronics Reliability, submitted*, 2012.

[5] F. Bossuyt, T. Vervust, and J. Vanfleteren, "Stretchable Electronics Technology for Large Area Applications: Fabrication and Mechanical Characterisation," *IEEE Trans. on Components, Packaging and Manufacturing Technology, in press*, 2012.

[6] T. Vervust, G. Buyle, F. Bossuyt, and J. Vanfleteren, "Integration of stretchable and washable electronic modules for smart textile applications,"

Journal of the Textile Institute, pp. 1–12, March 2012. [Online]. Available: http://www.tandfonline.com/doi/abs/10.1080/00405000.2012.664866

[7] J. Vanfleteren, M. Gonzalez, F. Bossuyt, Y. Y. Hsu, T. Vervust, I. De Wolf, and M. Jablonski, "Printed circuit board technology inspired stretchable circuits," *MRS Bulletin*, vol. 37, no. 3, pp. 254–260, March 2012. [Online]. Available: http://dx.doi.org/10.1557/mrs.2012.48

[8] R. Carta, P. Jourand, B. Hermans, J. Thoné, D. Brosteaux, T. Vervust, F. Bossuyt, F. Axisa, J. Vanfleteren, and R. Puers, "Design and implementation of advanced systems in a flexible-stretchable technology for biomedical applications," *Sensors and Actuators A-Physical*, vol. 156, no. 1, pp. 79–87, 2009. [Online]. Available: http://dx.doi.org/10.1016/j.sna.2009.03.012

Proceedings of International Conferences

[1] T. De Nies, T. Vervust, M. Demey, R. Van de Walle, J. Vanfleteren, and M. Leman, "beatLED : the social gaming partyshirt," in *Sound and music computing conference, proceedings*, Venetië, Italië, 2011, pp. 526–532. [Online]. Available: http://smcnetwork.org/smc_papers-2011219

[2] T. Vervust, F. Bossuyt, F. Axisa, and J. Vanfleteren, "Stretchable and washable electronics for embedding in textiles," in *MRS Proceedings*, vol. 1271. San Francisco, CA, USA: Materials Research Society (MRS), April 2010, pp. 1–6. [Online]. Available: http://dx.doi.org/10.1557/PROC-1271-JJ04-03

[3] F. Bossuyt, T. Vervust, F. Axisa, and J. Vanfleteren, "Improved stretchable electronics technology for large area applications," in *MRS Proceedings*, vol. 1271. San Francisco, CA, USA: Materials Research Society (MRS), April 2010, pp. 1–7. [Online]. Available: http://dx.doi.org/10.1557/PROC-1271-JJ08-03

[4] F. Bossuyt, T. Vervust, F. Axisa, and J. Vanfleteren, "From single conductive layer to double conductive layer stretchable electronics," in *MRS Spring Meeting, Abstracts*. San Francisco, CA, USA: Materials Research Society (MRS), 2010.

[5] T. Sterken, F. Bossuyt, R. Verplancke, T. Vervust, F. Axisa, and J. Vanfleteren, "Lifetime of stretchable meander-shaped copper conductors in PDMS subjected to cyclic elongation," in *MRS Spring Meeting, Abstracts*. San Francisco, CA, USA: Materials Research Society (MRS), 2010.

[6] T. Vervust, F. Bossuyt, F. Axisa, and J. Vanfleteren, "Stretchable and washable electronics for integration in textiles," in *China International Forum for Technical Textiles and Nonwovens, Proceedings*, Shanghai, China, October 2009, pp. 1–6.

[7] F. Bossuyt, T. Vervust, F. Axisa, and J. Vanfleteren, "A new low cost, elastic and conformable electronics technology for soft and stretchable electronic devices by use of a stretchable substrate," in *Microelectronics and Packaging Conference, 2009. EMPC 2009. European*. IEEE, June 2009, pp. 697–702.

[8] D. Brosteaux, E. Lippens, R. Cornelissen, E. Schacht, R. Carta, P. Jourand, R. Puers, F. Axisa, T. Vervust, F. Bossuyt, and J. Vanfleteren, "In vitro cytotoxicity testing and the application of elastic interconnection technology for short-term implantable electronics," in *Engineering in Medicine and Biology Society, 2009. EMBC 2009. Annual International Conference of the IEEE*. Minneapolis, MN, USA: IEEE, September 2009, pp. 4880 –4883. [Online]. Available: http://dx.doi.org/10.1109/IEMBS.2009.5332457

[9] F. Axisa, F. Bossuyt, T. Vervust, and J. Vanfleteren, "Laser based fast prototyping methodology of producing stretchable and conformable electronic systems," in *Electronics System-Integration Technology Conference, 2008. ESTC 2008. 2nd*, Greenwich, UK, September 2008, pp. 1387 –1390. [Online]. Available: http://dx.doi.org/10.1109/ESTC.2008.4684558

[10] F. Axisa, F. Bossuyt, J. Missine, R. Verplancke, T. Vervust, and J. Vanfleteren, "Stretchable engineering technologies for the development of advanced stretchable polymeric systems," in *Portable Information Devices, 2008 and the 2008 7th IEEE Conference on Polymers and Adhesives in Microelectronics and Photonics. PORTABLE-POLYTRONIC 2008. 2nd IEEE International Interdisciplinary Conference on*, August 2008, pp. 1 –8. [Online]. Available: http://dx.doi.org/10.1109/PORTABLE-POLYTRONIC.2008.4681277

[11] J. Vanfleteren, F. Axisa, D. Brosteaux, F. Bossuyt, E. De Leersnyder, T. Vervust, B. t. Huyghe, J. Missinne, R. Verplancke, and M. Gonzalez, "Elastic electronic circuits and systems using Moulded Interconnect Device (MID) technology," in *MRS Spring Meeting, Abstracts*. San Francisco, CA, USA: Materials Research Society (MRS), 2008.

Presentations

[1] T. Sterken, J. Vanfleteren, F. Bossuyt, S. Brebels, W. Christiaens, T. Vervust, M. Jablonski, S. Dunphy, F. Vermeiren, Y.-y. Hsu, T. Torfs, and M. Opdebeeck, "A reliable and comfortable package for wearable medical devices," in *Microelectronic packaging for medical and Hi-Rel devices, Abstracts*. Minneapolis, MN, USA: International Microelectronics And Packaging Society (IMAPS), June 2011.

[2] G. Buyle, T. Vervust, J. Leonard, and J. Vanfleteren, "SWEET - Stretchable and washable electronics," in *Presented at Avantex-Symposium*, Frankfurt/Main, Germany, May 2011.

[3] F. Bossuyt, J. Vanfleteren, J. De Baets, T. Vervust, M. Jablonski, and D. S., "Stretchable Moulded Interconnect Technology," in *3rd Flexible and Stretchable Electronics Workshop*, Berlin, Germany, November 2011.

[4] T. Vervust, G. Buyle, F. Bossuyt, F. Axisa, and J. Vanfleteren, "Development of stretchable and washable electronics for wearable signage," in *2nd Flexible and Stretchable Electronics Workshop*, Ghent, Belgium, November 2009.

[5] F. Bossuyt, T. Vervust, F. Axisa, and J. Vanfleteren, "Stretchable electronics for ambient applications," in *8th Belgian Day on Biomedical Engineering*, Brussels, Belgium, Oktober 2009.

[6] T. Vervust, G. Buyle, F. Bossuyt, F. Axisa, and J. Vanfleteren, "Development of stretchable and washable electronics for wearable signage," in *Smart Textiles Salon*, Ghent, Belgium, September 2009.

Patents

[1] F. Axisa, J. Vanfleteren, and T. Vervust, "Method for manufacturing a stretchable electronic device," U.S. Patent Application 2009/0 317 639A1, December 24, 2009.